The role of the haemodynamic Palladin protein within the Vasculature

Ciaran McGinn, B.Sc

Thesis Submitted to Dublin City University (DCU) for the Degree of Doctor of Philosophy (Ph.D)

Research was carried out in the School of Health and Human Performance, DCU, under the supervision of Doctor Ronan P. Murphy.

Declaration

I hereby certify that this material, which I now submit for assessment on the programme of study leading to the award of Doctor of Philosophy is entirely my own work, that I have exercised reasonable care to ensure that the work is original, and does not to the best of my knowledge breach any law of copyright, and has not been taken from the work of others save and to the extent that such work has been cited and acknowledged within the text of my work.

Signed: _____   ID No.: __58116753__

Date: _____

Acknowledgements

You know, there are so many people that I have to thank for helping me get this far. I would like to first thank Dr. Ronan Murphy for allowing me to work in his lab. I don't think that I'd be in any way successful at this postgrad degree without his help and all of that great knowledge he imparted on us. I'd also like to thank Dr. Phil Cummins. His pursuing of results from the lab also helped push us in the right direction. It was also a pleasure working alongside a great bunch: Brian, Shan, Fiona and Keith – my fellow PhD buddies! Wouldn't be half as much fun inside this lab without you all! Honestly can say it has been an amazing, life-changing experience. I'd say it's absolutely going to be downhill from here! I'd also like to thank the other laboratory folk who added to the fun: Paul, Mishan, Ger, Andrew, Laura, Rob, Anthony, Tony, Colin, Alisha & Hannah.

It also falls on me to thank the rest who made the last 5 years great. I always think this is like the end credits to a great TV series; you get a near-complete list of those who had some influence on the story! Thanks to Maja, Laura, Fiona, Paul and Joey for all the T3 times, along with the other guys! That first year was incredibly busy; it was nice having a similar group around that could also go out for an evening or two when we felt that pain of too much work! Thanks to all the amazing people who joined up when we went in to the next years; Mark, Paul K., Amy, Sam, Mary, Ciara, Alan, Claire, Andrew, Tom (the future world president), Colm, Norah, Stefano, Mari, Aoife, Sarah-Jane and the whole sport science lot, Gemma, Sarah, Kathy, Iza, Moira, Bianca, Roisin and the rest! But special thanks go to the postgrad mascots – the inanimate Red Ball and Nessy!

Also I suppose I better thank the other important people – Barry and Michael (My dad)! It's great that they put up with me for all this time! Thanks also to Sheila, the most amazing person I've ever known; wouldn't have made it this far without her! RIP Mam. And also thanks to the various aunts, uncles and cousins who've supported me! It's also worth acknowledging the other great female in my life – Grainne - thank you so much. It was phenomenal how you put up with me in the last few months – in good times and in the not good times. You've all been so very amazing!! Thanks to all else I've met in the epic story of how I made it this far to get my doctorate! Hope this isn't the absolute end, but the beginning of fantastic times!

Abstract

Physiological mechanotransduction experienced by the vasculature affects the expression of many actin-binding proteins that play an important role in endothelial cell function and the patho-physiology of cardiovascular disease (CVD). The expression of one such protein - Palladin – plays an important role in cell cytoskeletal regulation, acting as a mediator for the regulation of vascular homeostasis through its unique protein-actin and protein-protein interactions. This study aims to elucidate the role for Palladin within the actin dynamics of the vasculature.

Models mimicking the haemodynamic forces of cyclic strain and shear stress, acting on Human Aortic Endothelial Cells (HAECs) reveal that Palladin expression and localisation is mechanically altered within the vasculature. Protein expression increases especially as a result of both acute and chronic shear stress stimulation of the cell. Cellular fractionations of HAECs document the translocation of Palladin from the membrane to the cytoskeleton under laminar shear. Investigation of Palladin expression following culture of cells with extracellular matrices also suggest an integrin-mediated signalling of the protein.

Following the shear stress-induced inflammatory response, the endothelial cells appear to export excess protein within secreted microparticles, complex structures which have been previously implicated in playing a role in inflammation and coagulation leading to impaired vascular function in CVDs. The presence of Palladin and two other proteins - LASP-1 and Drebrin- within these shear-induced microparticles is investigated here.

Palladin appears to show an interaction with Drebrin (developmentally regulated brain protein), an actin-binding protein which itself is characterised in HAECs. Furthermore, the actin-binding, haemodynamically regulated protein - LASP-1 (Lim and Sh3 domain protein) was also investigated. Palladin is previously known to mediate the binding of LASP-1 to actin stress fibres. Here, we discuss the interactions between the three proteins, and also investigate the response of LASP-1 and Drebrin to haemodynamic force, namely shear stress.

Table of Contents

List of Figures

List of Tables

Abbreviations

ADF   Actin Depolymerisation Factor

ADP   Adenosine Di-phosphate

AM   Acetoxymethylester

APC   Allophycocyanin

APS   Ammonium Persulfate

ATP   Adenosine Triphosphate

BBB   Blood Brain Barrier

BCA   Bicinchoninic Acid

BSA   Bovine Serum Albumin

cAMP   Cyclic Adenosine Monophosphate

cDNA   Complimentary Deoxyribonucleic Acid

cGMP   Cyclic Guanosine Monophosphate

CKAP4   Cytoskeleton-associated Protein

ChIP   Chromatin Immunoprecipitation

Co-IP   Co-immunoprecipitation

Coll   Collagen – Type IV

CRIP2   Cysteine-rich Protein 2

Ct   Cycle Threshold

C-Terminal   Carboxyl Terminal

CVD   Cardiovascular disease

DAPI   4',6-Diamidino-2-Phenylindole

dH$_2$O   Distilled Water

DMEM	Dulbecco's Modified Eagle Medium
DMSO	Dimethlysulphoxide
DNA	Deoxyribonucleic Acid
dNTP	Deoxy Nucleotide Triphosphate
DTT	Dithiothreitol
ECGS	Endothelial Cell Growth Supplement
ECM	Extracellular Matrix
EDTA	Ethylenediaminetetraacetic Acid
EGF	Epidermal Growth Factor
EGFR	Epidermal Growth Factor Receptor
ELISA	Enzyme-Linked Immunosorbent Assay
EMPs	Endothelial Microparticles
eNOS	Endothelial Nitric Oxide Synthase
ERM	Ezrin/Radixin/Moesin
EVL	Ena/VASP-like
F-Actin	Filamentous Actin
FACS	Fluorescence Activated Cell Sorting
FAK	Focal Adhesion Kinase
FCS	Fetal Calf Serum
FG	Fibrinogen
FITC	Fluorescein Isothiocyanate
FLK-1	Fetal Liver Kinase 1
FN	Fibronectin
FOXO1A	Forkhead Box Protein O1A

FUS	Fused in Sarcoma
G-Actin	Globular Actin
GAPDH	Glyceraldehyde 3-phosphate Dehydrogenase
GFP	Green Fluorescent Protein
GTP	Guanosine-5'-triphosphate
HAEC	Human Aortic Endothelial Cell
HaoSMC	Human Aortic Smooth Muscle Cell
HBMVEC	Human Brain Microvascular Endothelial Cell
HCl	Hydrochloric Acid
HEK	Human Embryonic Kidney
HRP	Horseradish Peroxidase
HSP	Heat Shock Protein
HUVEC	Human Umbilical Vein Endothelial Cells
ICAM-1	Intercellular Adhesion Molecule 1
Ig	Immunoglobulin
IMS	Industrial Methylated Spirits
IP	Immunoprecipitation
KEGG	Kyoto Encyclopaedia of Genes and Genomes
LAMP1	Lysosomal-Associated Membrane Protein 1
LASP-1	LIM and SH3 Domain Protein 1
LB	Lysogeny Broth
LIM	Lin-II, isl-I, mec-3
LSS	Laminar Shear Stress
MALDI-TOF	Matrix Assisted Laser Desorption/Ionisation-Time of Flight

MAP	Mitogen-activated Protein
MgCl2	Magnesium Chloride
MHC	Major Histocompatibility Complex
miRNA	Micro Ribonucleic Acid
MLCK	Myosin Light Chain Kinase
MOPS	3-(N-morpholino)propanesulfonic Acid
MP	Microparticle
mRNA	Messenger Ribonucleic Acid
MVB	Multi-Vesicular Bodies
MVP	Major Vault Protein
NaCl	Sodium Chloride
NaOH	Sodium Hydroxide
NC1	Non-collagenous domain
NF-κB	Nuclear Factor kappa-B
NO	Nitric Oxide
PAGE	Polyacrylamide Gel Electrophoresis
PARP-1	Poly [ADP-ribose] polymerase 1
PBS	Phosphate Buffered Saline
PCR	Polymerase Chain Reaction
PECAM-1	Platelet Endothelial Cell Adhesion Molecule 1
PI3-K	Phosphoinositide-3-Kinase
PKA	Protein Kinase A
PKC	Protein Kinase C
PKG	Protein Kinase G

POZ	Pox Virus and Zinc Finger
PS	Phosphatidylserine
P/S	Penicillin/Streptomycin
PTEN	Phosphatase and Tensin Homolog
qRT-PCR	Quantitative Reverse Transcriptase Polymerase Chain Reaction
RaoSMC	Rat Aortic Smooth Muscle Cell
RIPA	Radioimmunoprecipitation Assay
RNA	Ribonucleic Acid
ROCK	Rho-associated Protein Kinase
ROS	Reactive Oxygen Species
RPM	Rotations per Minute
RT-PCR	Reverse Transcriptase Polymerase Chain Reaction
SDS	Sodium Dodecyl Sulphate
SDS-PAGE	Sodium Dodecyl Sulphate Polyacrylamide Gel Electrophoresis
SEM	Scanning Electron Microscopy
SFM	Serum Free Medium
SH3	Src Homology Region 3
shRNA	Short Hairpin Ribonucleic Acid
siRNA	Small Interfering Ribonucleic Acid
SOC	Super Optimal Broth with Catabolite Repression
SPIN90	SH3 Protein Interacting with Nck, 90kDa
Src	Sarcoma
SSB	Sample Solubilisation Buffer
STRING	Search Tool for the Retrieval of Interacting Genes

TAE	Tris Acetate Ethylenediaminetetraacetic Acid
TBS	Tris Buffered Saline
TE	Tris – Ethylenediaminetetraacetic Acid
TEMED	N,N,N', N'-Tetramethylethlylenediamine
TGF-β1	Transforming Growth Factor β1
TNF	Tumour Necrosis Factor
tRNA	Transfer Ribonucleic Acid
uPAR	Urokinase-type Plasminogen Activator Receptor
VASP	Vasodilator-stimulated Phosphoprotein
VCAM-1	Vascular Cell Adhesion Molecule 1
VE-cadherin	Vascular Endothelial Cadherin
VEGF	Vascular Endothelial Growth Factor
VWF	Von Willebrand Factor

Units

bp	Base Pairs
cm	Centimetre
^{o}C	Degree Celsius
g	Grams
hr	Hour
kb	Kilobase pairs
kDa	KiloDaltons
kg	Kilogram
L	Litre
μg	Microgram
μl	Microlitre
μm	Micrometre
μM	Micromolar
mA	Milliamperes
mbar	Millibars
mg	Milligrams
ml	Millilitres
mM	Millimolar
ms	Milliseconds
min	Minutes
M	Molar
ng	Nanograms

nm	Nanometres
nM	NanoMolar
N/m^2	Newton per Metre squared
Pa	Pascal
pmol	Picomolar
px	Pixels
U	Units
V	Volts
v/v	Volume per Volume Concentration
w/v	Weight per Volume Concentration

Presentations of Research: Posters

8th International Symposium on Biomechanics in Vascular Biology and Cardiovascular Disease. April 2013. **Investigation of the Protein Interactions of the Shear Responsive Proteins Palladin, LASP-1 & Drebrin, and their Presence in Endothelial Derived Microparticles**

McGinn, Ciaran; Fitzpatrick, Paul; Shan, Chunxu; MacDonnell, Brian; Dowling, Paul; Cummins, Philip; Murphy, Ronan.

Arteriosclerosis, Thrombosis and Vascular Biology (ATVB) Scientific Session. April 2012. **Investigation of the Protein Interactions of the Shear Responsive Protein, Palladin, and Its Presence in Endothelial-Derived Microparticles**

McGinn, Ciaran; Fitzpatrick, Paul; Shan, Chunxu; Murphy, Andrew; MacDonnell, Brian; Dowling, Paul; Cummins, Philip; Murphy, Ronan.

North American Vascular Biology Organisation (NAVBO) Workshops in Vascular Biology. October 2011. **Palladin, a Shear Responsive Cytoskeletal Adaptor Protein, is Present in Endothelial Derived Microparticles**

McGinn, Ciaran; Fitzpatrick, Paul; Shan, Chunxu; Murphy, Andrew; MacDonnell, Brian; Dowling, Paul; Cummins, Philip; Murphy, Ronan.

Dublin City University School of Biotechnology Research Day. January 2011. **Characterisation of the Actin-Binding Protein, Palladin, Under Haemodynamic Conditions in Human Aortic Endothelial Cells**

McGinn, Ciaran; Murphy, Andrew; Fitzpatrick, Paul; Shan, Chunxu; Otey, Carol; Cummins, Philip; Murphy, Ronan.

(Bio)pharmaceutical & Pharmacological Sciences Research Day. January 2010. **Characterisation of the Palladin Protein in Human Aortic Endothelial Cells**

McGinn, Ciaran; Murphy, Andrew; Fitzpatrick, Paul; Shan, Chunxu; Otey, Carol; Cummins, Philip; Murphy, Ronan.

Presentations of Research: Oral Presentations

Dublin City University School of Biotechnology Research Day. January 2012.

Palladin, a Shear Responsive Cytoskeletal Adaptor Protein, is Present in Endothelial Derived Microparticles

Dublin City University Biological Research Society Postgraduate Research Talk Series. April 2011.

Palladin - A Structural Protein in Endothelial Cells

<u>Publications</u>

McGinn, C.M., MacDonnell, B.F., Shan, C.X., Cummins, P.M., Murphy, R.P. (2014). Microparticles: A Pivotal Nexus in Vascular Homeostasis and Disease. *Curr Clin Pharm.* In Print.

CHAPTER ONE

INTRODUCTION

1.1 THE CARDIOVASCULAR SYSTEM

The human body is dependent on the circulatory system to allow for the constant flow of blood, which in turn facilitates the cellular exchange of essential nutrients and gases, and disposal of wastes. This circulatory system can be divided into two subsystems: lymphatic and cardiovascular. The lymphatic system has many roles, including the transport of interstitial fluid and antigen presenting cells around the body. The other system - the cardiovascular system – is arguably the more important, as it facilitates the distribution of blood around the human body. The cardiovascular system is also responsible for many other functions such as maintaining homeostasis, e.g. temperature, pH, and in the immune response to diseases and infections (Aird, 2011). This system consists of the heart, blood vessels, and the approximately 5 litres of blood that the blood vessels constantly transport around the body.

1.1.1 Cardiovascular disease

Cardiovascular disease (CVD) is a general term to characterise dysfunction of the heart or circulatory system (Kelly, 2010) and is widely regarded as one of the leading causes of death in developed countries (Gaziano *et al.*, 2006) (Table 1.1). A 2010 study on mortality rates in the US (the most recent complete study available) showed that over 2150 Americans die of CVD-related illnesses daily – one death every 40 seconds (Go *et al.*, 2013), with 34% of these deaths occurring before the age of 75. Within the countries of the EU, the latest available statistics from 2012 indicate how CVD-related illnesses claimed the lives of over 4 million people annually, almost half of which are people in the EU member countries. Overall in Europe, CVD causes 47% of all deaths (Nichols *et al.*, 2013). Moreover, in highly populated countries such as China and India, CVD is also a leading cause of death (Joshi *et al.*, 2008) - highlighting how CVD affects all the major population groups in the world.

CVD itself can encompass a broad spectrum of disorders that includes arteriosclerosis, heart failure, hypertension and stroke. Many lifestyle-dependent risk factors exist that can exacerbate this condition, including smoking, lack of physical activity or poor diet. Healthy diet and regular exercise have long been observed to aid in reducing incidents of CVD events (Hellenius *et al.*, 1993), as they help reduce resting heart rate (Green *et al.*, 2008). Furthermore, a healthy lifestyle is commonly known to slow down the

progression of atherosclerosis (Zagura *et al.*, 2012). Exercise can also lower the resting blood pressure in patients with hypertension (Pal *et al.*, 2013) and help improve health in patients with peripheral vascular diseases (Haas *et al.*, 2012). Several *in vivo* studies suggest that the exercise-induced haemodynamic forces alter the endothelium blood vessel tone and reactivity in a healthy and beneficial manner (Johnson *et al.*, 2011; Laughlin *et al.*, 2011; Tinken *et al.*, 2010).

Although some of these risk factors show increasing trends in high income countries, the rate of increase in risk factor prevalence is higher still in developing countries (Celermajer *et al.*, 2012). Cigarette smoking in particular is a well-established risk factor for CVD, exacerbating endothelial dysfunction and haemostatic imbalance (Virdis *et al.*, 2010). Many studies have proven a link between these factors and CVD with respect to the endothelium (Reriani *et al.*, 2010; Hadi *et al.*, 2005).

The imbalance of vascular homeostasis that leads to dysfunction, and subsequent development of CVD, can arise due to dysregulation of the endothelium. This ultimately leads to impairment of endothelial function and adverse tissue remodelling (Endemann and Schiffrin, 2004). Importantly, certain regions of the vasculature are more prone to endothelial dysfunction than others (Cicha *et al.*, 2008), namely areas of low shear and/or flow disturbances at arterial bifurcations and curvatures (illustrated in further detail in Chapter 1.2). Studies also demonstrate that this aberrant shear stress and disturbed flow pattern modulate not only the clinical manifestations of disease but also enhances the progression of atherosclerotic lesions (Chiu and Chien, 2011). The altered morphology and function of endothelial cells under these varied haemodynamic conditions are mediated by a number of well, and not so well, characterised cellular and molecular mechanisms, including signalling GTPases signalling cascades involving Rac and Rho (Hirase and Node, 2012; Mazzag *et al.*, 2003; Wojciak-Stothard and Ridley, 2003).

Table 1.1: Total cause of deaths worldwide for the year 2011. The table documents the estimates of mortality throughout the world in 2011 – the most recent full statistics available. Mortality estimates are based on analysis of latest available national information on levels and causes of mortality grouped together with the latest available information from the World Health Organisation WHOSIS database. Cardiovascular disease accounts for approximately 11% of total deaths for the year – the largest individual cause of death (World Health Statistics, 2013).

Cause of Death	Death Toll (In Millions)
Heart Disease	7
Stroke	6.2
Lower Respiratory Infection	3.2
Chronic Obstructive Pulmonary Disease	3
Diarrhoeal Diseases	1.9
HIV/Aids	1.6
Trachea, Bronchus, Lung Cancers	1.5
Diabetes	1.4
Road Injury	1.3
Prematurity	1.2

1.1.2 The Vasculature

The cardiovascular system consists of the heart pumping blood along a vast network of vessels (Hahn and Schwartz, 2009). The classification of these vessels, based on the direction that the blood flows relative to the heart, shows the convergence of several vessels (the veins) into one vein, the vena cava, that returns blood to the heart. In contrast, the outgoing vessel, the aorta, diverges into several vessels carrying oxygenated blood away from the heart. The points of such divergence are known as arterial bifurcations (Hahn and Schwartz, 2009; Lusis, 2000).

The vasculature refers to the arrangement of blood vessels in the body which itself can be sub-divided into microvasculature and the macrovasculature. Microvasculature refers to the arrangement of smaller vessels of the circulatory system, such as capillaries, arterioles and venules. Macrovasculature refers to the larger blood vessels, such as veins and arteries, containing an internal diameter greater than 100 microns. All blood vessels of the vasculature share a common three-layered structure (Figure 1.1). These three layers are:

(i)   Tunica Externa

The tunica externa, also known as the tunica adventitia, is the outer layer covering of the blood vessel, mostly consisting of elastic and collagen fibres. The collagen serves to anchor blood vessels to nearby organs. The elastic fibres separate the tunica externa and the tunica media. The tunica externa also contains nerves and tiny blood vessels to supply tissues of the vessel wall. These blood vessels are called *vasa vasorum*, which translates as "vessels to the vessels".

(ii)   Tunica Media

The tunica media is the middle layer of the blood vessel. It is made up of more elastic fibres, and smooth muscle cells. The smooth muscle cells are spindle shaped, and have a circular arrangement around the vessel which is perpendicular to the direction of the blood flow. Here, the lumen is regulated, and as a direct result, so is the blood pressure of the vessel.

(iii)   Tunica intima

The tunica intima refers to the innermost layer of a vessel. It is made up of a 0.2-4 µm thick monolayer of endothelial cells which is in direct contact with the blood flow as it passes through the vessel. It plays an important role with regards to exchange of materials. The tunica intima also possesses a framework of collagen fibres which give the basal lamina significant tensile strength, while also providing resilience for pulsatile stretching and recoil.
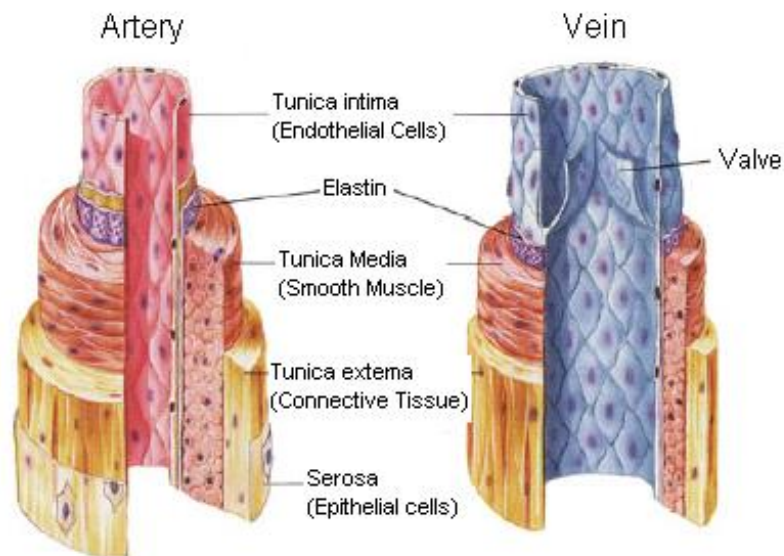
Figure 1.1: The Human Blood Vessel. This illustrates the three main layers of the blood vessel - Tunica intima, Tunica Media and Tunica Externa. © Fox, Stuart I. Human physiology 4th edition, Brown Publishers.

1.1.3 The Endothelium

The endothelial cell layer of the tunica intima appears as a cobblestone morphology that elongates and aligns in the direction of the flow of blood. However, at arterial bifurcations and veins, they appear to show a cuboidal, or plump, morphology. Research has shown how the endothelial cell layer is vital in regards to its multiple functions within the vascular blood vessel (Tao *et al.*, 2012). These functions include growth regulation, coagulation, production of extracellular matrix (ECM) components, the immune response and modulation of blood flow and blood vessel tone (Sasaki and Toyoda, 2013; Sumpio *et al.*, 2002). Normal endothelial function is pivotal in vascular homeostasis and cell functions that limit development of atherosclerosis (Lusis, 2000).

During embryonic development, a common precursor cell called the angioblast is derived from the mesoderm. These angioblast cells differentiate into endothelial cells and, depending on their interactions with surrounding cell areas, acquire organ-specific properties. Such interactions may occur through cell-cell or cell-matrix signalling. Palladin (as discussed in greater detail in Chapter 1.5) is a protein encoded by the PALLD gene, and is responsible for cell structure, adhesion and migration (Goicoechea *et al.*, 2010) as well as playing a vital role in embryonic development (Luo *et al.*, 2005). Palladin has been identified within endothelial cell nuclei in human coronary vessels with atherosclerosis (Jin *et al.*, 2010). The work presented here in this thesis aims to

characterise the Palladin protein in greater depth through investigating its expression within Human Aortic Endothelial Cells. As it is an actin-binding protein responsible for cell adhesion and migration, and considering it localises to different areas within the cell (Jin *et al.*, 2010; Rachlin and Otey, 2006; Goicoechea *et al.*, 2010) it was hypothesised that this protein displays differential expression levels in response to the haemodynamic forces that the endothelial cell layer is subjected to. A notable binding partner of Palladin is the LASP-1 protein (Rachlin and Otey, 2006), a crucial protein involved in cell motility which itself is described in detail in Chapter 1.5.4. A further objective of the work presented here is the investigation of the expression of this and other binding partner proteins of Palladin in response to haemodynamic force. It was hypothesised that the force-induced patterns of expression may be characterised as being similar to that of Palladin. Later, the release of protein in Endothelial Microparticles is also investigated. As discussed in Chapter 1.6, these particles are released from cells following the onset of haemodynamic force. A hypothesis for reduction in protein expression after later time points of haemodynamic force was the expulsion of excess protein encapsulated in the microparticles. Further investigation lead to observing the release of binding protein partners of Palladin through these particles.

The healthy endothelial cell layer can respond to the wide variety of both biomechanical/ haemodynamic forces (cyclic strain and shear stress) and biochemical (e.g. growth factors, hormones, cytokines, and oxygen) forces in order to regulate the functions of the endothelium. These functions include the regulation of vascular tone, regulation of the endothelial cell barrier and permeability, regulation of vascular growth and vessel formation, and regulation of inflammatory and immune reactions (DeCaterina and Libby, 2007). As discussed further in the next section, the deregulation of these functions has severe consequences for many cell fates and functions including aberrant migration, proliferation and adhesion. The dysfunction of these endothelial processes can also signal the start of atherosclerosis (Lehoux *et al.*, 2006)

1.1.4   Endothelial Dysfunction

Endothelial dysfunction is a systemic pathological state of the endothelium, which can be defined as an imbalance between the dilating and constricting nature of the endothelium (Aird, 2007; DeCaterina and Libby, 2007). It occurs as a result of certain "stimulation" of the endothelium, be it biochemical or biomechanical. This can

encompass injury to the endothelium, the action of blood-borne constituents, altered haemodynamics, etc. It can also result from and/or contribute to several disease processes such as hypertension, hypercholesterolaemia or diabetes (Münzel *et al.*, 2008). Endothelial function has been observed to be inversely associated with the number of risk factors (Balbarini *et al.*, 2007) and therefore global cardiovascular risk (Versari *et al.*, 2009).

Within a short time frame of the endothelium being stimulated, normal physiological conditions will prevail. However over a longer time frame, endothelial function becomes impaired, which leads to endothelial cell dysfunction. Such alterations of the endothelial cell morphology and phenotype are considered to be early and crucial steps within the development and progression of cardiovascular disease (Deanfield *et al.*, 2007; Suwaidi *et al.*, 2010).

Because of the morphology of the vascular system, certain areas are more prone to endothelial dysfunction than others, namely areas of low shear (such as the shear patterns of atherosclerotic sites) and/or flow disturbances at curvatures in the vessel, or at arterial bifurcations – the point where the aorta divides into two smaller arteries (Hahn and Schwartz, 2009). This low shear stress and the disturbed flow pattern are observed to modulate clinical manifestations of disease and also enhance the progression of atherosclerotic lesions (Chiu and Chien, 2011). As stated previously, the morphology of endothelial cells under these varied haemodynamic conditions are mediated by a number of signalling GTPases such as Rac and Rho (Mazzag *et al.*, 2003; Wojciak-Stothard and Ridley, 2003). Dysfunction is associated with an increased expression of adhesion molecules, altered vascular tone, and release of chemokines, cytokines and reactive oxygen species from the endothelium. This results in inflammation within the vessel (Endemann and Schiffrin, 2004).

There are three endothelial responses to dysfunction or injury (Pasyk and Jakobczak, 2004). First is the immediate transient response, which begins immediately following mild injury and lasts about 30 minutes, causing increased vascular permeability. The second response, the immediate-sustained response, occurs after severe injury and is associated with cell necrosis. The vascular leakage which results from this necrosis can last for a long period of time (several days). The third response is the delayed-prolonged response, where a delayed but long lasting vascular leakage occurs from direct injury of

cells, caused by mild-to-moderate exposure to heat, x-rays or UV radiation (Kumar *et al.,* 2009).

One of the key features of endothelial dysfunction is the impairment of arterial dilation prohibiting proper blood flow. The endothelium can release many vasodilators such as Nitric Oxide (NO) to allow for dilation. Other vasodilators include prostacyclin and bradykinin (Giannotti and Landmesser, 2007). Changes in the ability to release such vasodilators are linked to the development and progression of CVD. Many of the vasoprotective responses of the endothelium are mediated by NO. Moreover, NO is responsible for regulation of vascular permeability, platelet aggregation, monocyte adhesion, cytokine expression and tissue oxidation (Esper *et al.*, 2006). It is formed from endothelial cells from the endothelial NO synthase enzyme (eNOS) acting on L-arginine precursor. The eNOS is found in the caveolae of the cell membrane; there, the protein caveolin-1 is displaced by the binding of calcium to calmodulin, which activates the eNOS and leads to NO production (Davignon and Ganz, 2004).

NO can also be released into the bloodstream where it is inactivated by oxyhemoglobin. However, before inactivation can occur, it may remain close to the endothelial surface where it can inhibit leukocyte and platelet adhesion and activation (Hossain et al., 2012). Haemodynamic forces within the vasculature are very important in the regulation of NO. For example, healthy atheroprotective laminar blood flow is capable of stimulating NO production (Harrison *et al.*, 2006).
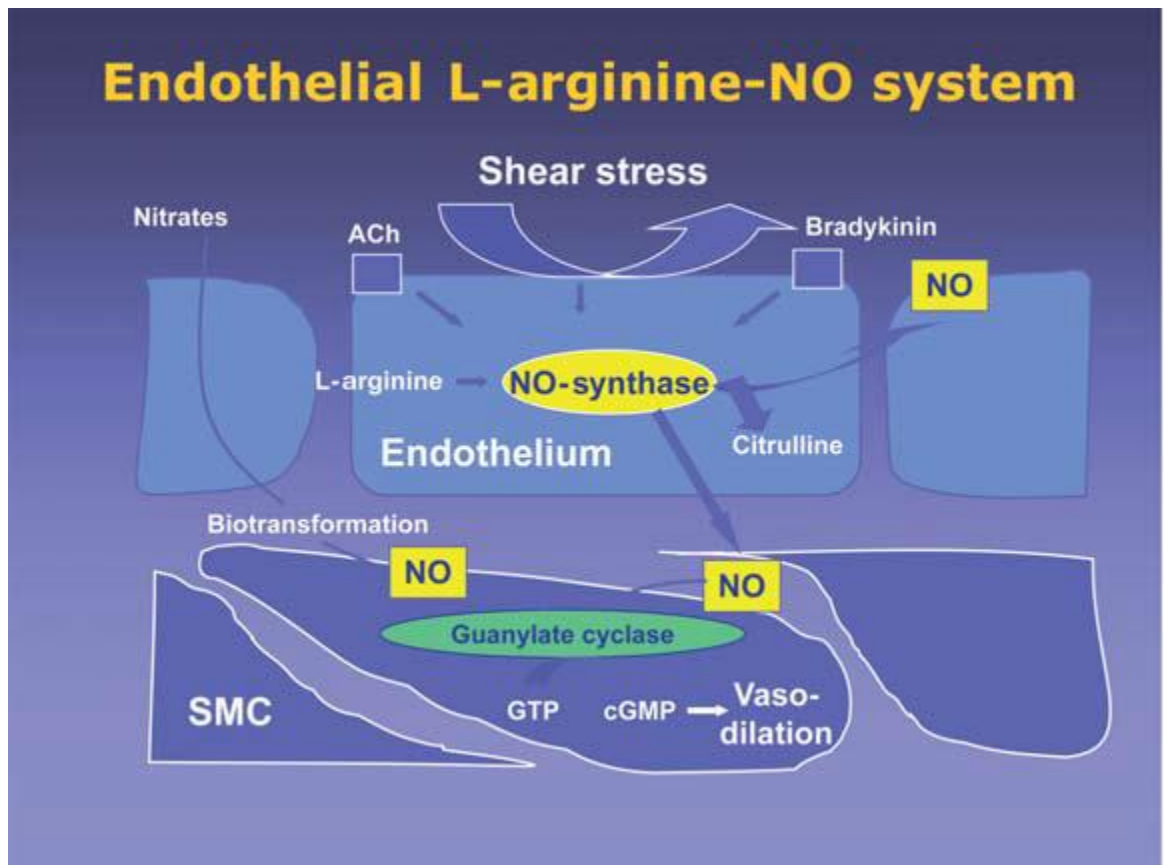
Figure 1.2: The Endothelial L-arginine-Nitric Oxide System. This illustrates the pathway that leads to vasodilation. Shear stress from blood flow stimulates the activation of Endothelial Nitric Oxide Synthase (eNOS). eNOS uses the L-arginine amino acid to produce Nitric Oxide, which in turn activates Guanylate Cyclase and leads to vasodilation. Pathological shear stress can result in an imbalance of Nitric Oxide, which results in altered vasodilation and subsequent endothelial dysfunction (Giannotti and Landmesser, 2007).

1.2 HAEMODYNAMIC REGULATION

With regards to stimuli regulating endothelial function, haemodynamic forces are highly important and dramatically influence the endothelial cells. Haemodynamic forces within the vasculature are among the various stimuli which can determine vessel distribution and diameter. They are able to do this on a cellular level, while mediating regulatory events within the vessels themselves (Gimbrone Jr and Garcia-Cardena, 2013). It is through the ability of components in the vessel structure responding to biochemical and biomechanical stimuli which make the regulation of blood flow possible.

These forces are essential to development of the physiology of the vasculature, but the de-regulation of them plays a strong role in the development of disease. Alteration of force generated cell signalling results in the knock-on alteration of many cellular

functions such as cell adhesion, migration or proliferation (Lehoux *et al.*, 2006). Two main haemodynamic forces exist: (i) cyclic strain and (ii) shear stress (Figure 1.3).
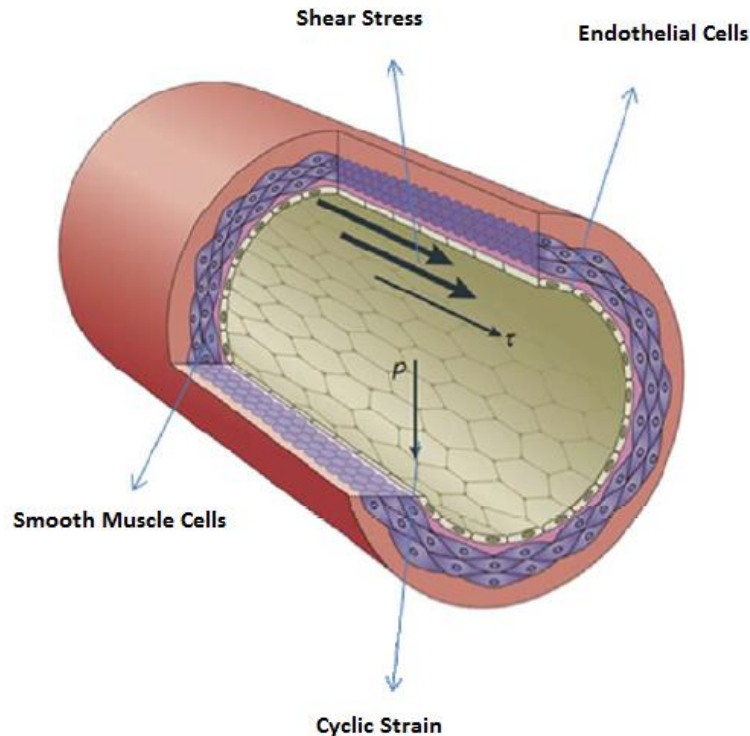
Figure 1.3: Forces affecting Endothelial Cells in the Vasculature. This illustrates the haemodynamic forces - P represents the pressure of the cyclic strain, and r represents the shear stress – both of which are influential on the endothelial cell layer. Pressure is normal to the vessel wall, resulting in circumferential stretching, while shear stress is parallel to the vessel wall and exerted longitudinally in the direction of blood flow (Hahn and Schwartz, 2009).

1.2.1 Cyclic Strain

Contraction of the heart causes pulsatile (a pulsing flow with periodic variations) changes in blood pressure on the arterial side of the circulatory network. The aorta expands at the peak of this blood pressure cycle (systolic) and then steadily contracts as the pressure decreases (diastolic) from the blood flowing downstream. Cyclic strain is generated by the pulsation of the blood vessels as blood is pumped through by the heart (Collins *et al.*, 2005). It results in the vessel wall stretching in the circumferential and longitudinal direction, however the vessel wall becomes thicker or thinner so that force per unit of wall is consistent (Lehoux *et al.*, 2006). This equilibrium is described by Laplace's Law (Laplace, 1899):

$$T = \frac{\text{Pr}}{h}$$

Where **T** = Wall tension (or force per unit length of the vessel), **P** = Blood pressure, **r** = radius and **h** = thickness of the vessel wall. Arteries also remodel in response to change of fluid flow so that the vessel diameters are matched to the blood volume (Schaper, 2009).

Cyclic strain can affect smooth muscle cells (Qi *et al.*, 2010) but is predominantly influential on endothelial cells, playing an important role in cell migration (Von Offenberg Sweeney *et al.*, 2005) and permeability (Collins *et al.*, 2005). At pathophysiological levels though, cyclic strain results in haemodynamic dysregulation leading to atherosclerosis (Ando and Yamamoto, 2011). It has a visual effect on endothelial cell morphology, where it increases cell proliferation, results in the formation of actin stress fibres, and the cell realignment perpendicular to the force vector. The actin cytoskeleton and its regulatory proteins are believed to play an important role in the pathogenic effects of cyclic strain. Further investigation is still on-going, as there are proteins which have a regulatory effect on the dynamic activity of the actin cytoskeleton that are still to be fully characterised (Hahn and Schwartz, 2009). For example, the LIM proteins, Zyxin and Paxillin, have been recently observed to exhibit mechanosensory properties, affecting the actin cytoskeleton in response to strain (Watanabe-Nakayama *et al.*, 2013). As discussed later in this chapter, these proteins are observed to bind with LASP-1, which itself binds to Palladin. This strengthens the hypothesis that Palladin and LASP-1 play a role in force induced cytoskeletal remodelling, meriting the investigation into these proteins.

Endothelial cells subjected to cyclic strain show moderate production of Reactive Oxygen Species (ROS), which becomes increased under pathological conditions (Bundey, 2007). Furthermore, cyclic strain has been observed to also upregulate Nitric Oxide Synthase (NOS) in endothelial cells (Fleming, 2010), where pathological levels of strain appear to increase upregulation more than physiological levels. When converted, the endothelial-derived Nitric Oxide (NO) can react with the ROS, which further reduces the availability of NO in the cell (Rojas *et al.*, 2006). It is thought that the accumulation of ROS can also initiate an inflammatory response which plays a part in development of atherosclerosis (Kou *et al.*, 2009).

1.2.2 Shear Stress

While cyclic strain is a haemodynamic force that can affect endothelial and smooth muscle cells in the vessel, shear stress is a force that only affects endothelial cells. This shear stress is the frictional force per unit area that blood exerts as it flows over the endothelial cell layer. Shear stress is expressed as units of force / unit area (Newton per meter squared [N/m^2] or Pascal [Pa], or dynes/cm^2; 1 N/m^2 = 1Pa = 10 dynes/cm^2). Under normal physiological conditions the endothelium is exposed to roughly 10 dynes/cm^2. In the case of this atheroprotective laminar shear, shear stress can be expressed using the Hagen-Poiseuille formula (Katritsis *et al.*, 2007):

$$\tau = \frac{4\mu Q}{\pi r^3}$$

Where τ = shear stress, μ = blood viscosity, Q = flow rate and r = vessel radius.

The endothelium is subjected to shear stress of approximately 10-70 dynes /cm2 (Thorin and Thorin-Trescases, 2009). Endothelial cells *in vivo* exhibit an elongated shape that is orientated in parallel to the direction of the blood flow in relatively straight regions of the vasculature. The frictional force induces two general levels of molecular response exclusive to endothelial cells – the acute rapid response over short time periods, or delayed long term changes that are dependent on protein synthesis. In disturbed shear – the type seen at branching points and curvatures of the arterial tree (Figure 1.4) - the acute response is sustained (Hahn and Schwartz, 2009).

The immediate response of the laminar shear-induced remodelling is cell elongation, wherein actin stress fibre and microfilament formation, and intracellular junction disruption are observed within the first three hours of shear (Li, Haga and Chien, 2005; Johnson *et al.*, 2011). As a result of this shear, oxidative stress, permeability and cell turnover are low (Figure 1.4). Between 6-8 hours following laminar shear stress, changes in endothelial morphology occurs and the actin cytoskeleton is restructured. Such changes include the partial disassembly and subsequent reassembly of actin filaments at adherens junctions and focal adhesions (Osborn *et al.*, 2006). Adherens junctions are a dynamic complex present at cell-cell borders between adjacent endothelial and epithelial cells. Focal adhesions are structures through which both mechanical force and regulatory signals are transmitted. They can mediate the

anchorage of cells to ECMs also (Wehrle-Haller, 2012). The actin disassembly is augmented with many actin-binding scaffolding proteins localising to adherens junctions and focal adhesions also. Delayed or chronic shear mediated responses require the synthesis of certain proteins, which in turn may result in changes in the appropriate gene expression. The shear induced modulation of gene expression results from the binding of specific transcription factors to their target cis-element in the promoter region of the gene (Chien *et al.*, 1998; Obi *et al.,* 2009).

Studies have observed the *in vivo* alterations of shear stresses (Hahn and Schwartz, 2009; Cecchi *et al.,* 2010). The many different forms of shear, aside from steady laminar flow, include laminar pulsatile flow, or turbulent flow (Figure 1.4).
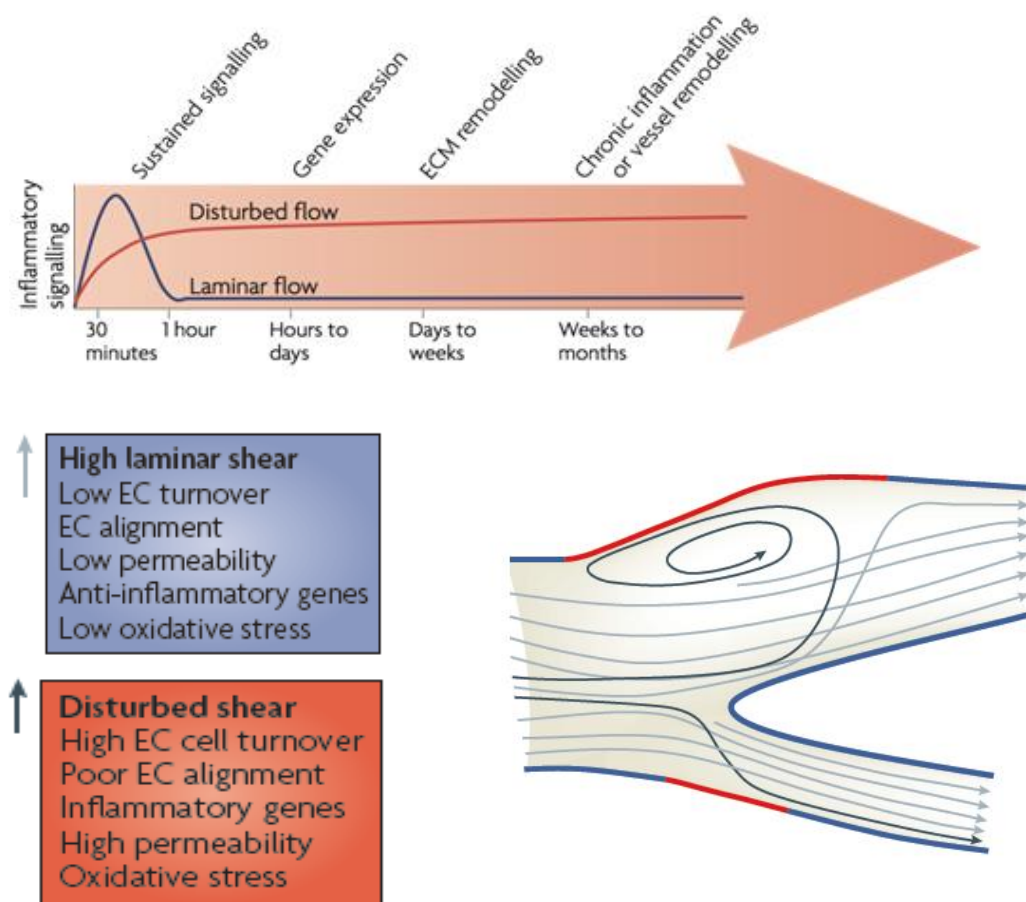
Figure 1.4: The effects of shear flow on Endothelial Cells. In regions where the arteries are straight, the blood flow is laminar (Blue coloured in this diagram). But in regions where branching of arteries occurs, complex flow patterns develop, and shear becomes disturbed (Red coloured in the diagram). Endothelial cells in regions of high laminar shear have an anti-inflammatory phenotype, and align in the direction of flow. However, in disturbed shear regions, pro-inflammatory conditions are visible where cells have poor alignment and inflammatory genes are expressed – leading to a higher occurrence of atherosclerosis. Cells under laminar flow activate various inflammatory signalling pathways, but these are downregulated after around an hour. Disturbed shear activates the same pathways, but in a long-term manner (Hahn and Schwartz, 2009).

Many shear responsive genes (e.g. Thrombomodulin, NOS, Prostacyclin and ICAM-1) are modulated by the type and rate of shear flow (Resnick *et al.,* 2003; Chien *et al.*, 1998). However the same type of shear stress doesn't apply across the whole vasculature, with different parts of the network being subjected to different forms of shear stress. As a result, some genes are regulated differently at different locations such as arterial bifurcations or curvature of the vessel. At such sites, disturbed blood flow can lead to transient vortex formations and even flow reversal. In turn this can lead to a variety of altered flow patterns. Under disturbed shear, cells have a higher proliferation rate, migration rate and deregulated cell morphology, all of which are mechanisms for initiation and the progression of atherosclerosis (Chiu and Chien, 2011). Furthermore, DNA synthesis has been observed to be significantly higher in areas of disturbed shear, as opposed to the areas exposed to laminar shear (Estrada *et al.*, 2011).

1.2.3 Mechanotransduction

Mechanotransduction refers to the process by which the endothelial cells possess the ability to take mechanical force and convert this force into biochemical signals which subsequently change the function of the cells (Orr *et al.*, 2006b; Hahn and Schwartz, 2009). The signals are altered depending on the difference in the force caused. For instance, exposure to laminar, disturbed or oscillatory shear flow can generate different endothelial responses. A group of receptors known as mechanosensors are utilised here, differentiating between physiological and pathological haemodynamic stimuli (Liu *et al.,* 2013; Katsumi *et al.*, 2004). Many possible mechanosensors have been suggested to function in sensing and being regulated by flow, such as platelet and endothelial cell-adhesion molecule-1 (PECAM-1), vascular endothelial (VE)-cadherin and various integrins (Hahn and Schwartz, 2009).

Integrins are membrane-associated glycoproteins which are generally found at the basolateral surface of endothelial cells. These proteins are composed of an α and a β subunit. There are 18 α and 8 β subunits which can be arranged into different receptors with alternative binding properties and tissue distributions (Hynes, 2002, Barczyk, Carracedo and Gullberg, 2010). Each subunit consists of a large extracellular domain (which binds directly to ECM proteins), a transmembrane spanning region, and a short cytoplasmic domain (Hynes, 1999). The cytoplasmic domains interact with signalling molecules and cytoskeletal proteins in order to regulate cellular events (Shyy and Chien, 2002). Such cytoskeletal proteins are actin-binding, and include talin, α-actinin and

ZASP (Bouaouina *et al.*, 2012). The cellular events include signal transduction, cytoskeletal organisation and cell motility. Integrins are unique in their ability to regulate "inside out" signalling, where the intracellular signals affect binding affinity to ECM ligands, affecting cell adhesion, progression and motility (Shattil, Kim and Ginsberg, 2010). Integrins can also regulate "outside-in" signalling, whereby they are capable of transmitting signals into the cell from the surrounding matrix and affecting cell growth, gene expression and programed cell death (Hynes, 2002).

Integrins are only able to bind to their binding partners when there are a minimum number of them present at focal adhesions. Their affinity is relatively weak - when integrins are loosely distributed across the cell surface, there is no strong adhesion present. To be more effective, several integrins must localise at the adhesion. The low affinity is actually necessary, as otherwise, there would be increased binding of cells, which would result in a lack of motility. By making and breaking focal adhesions, the cell can move and restructure if needed (Puklin-Faucher and Sheetz, 2011).
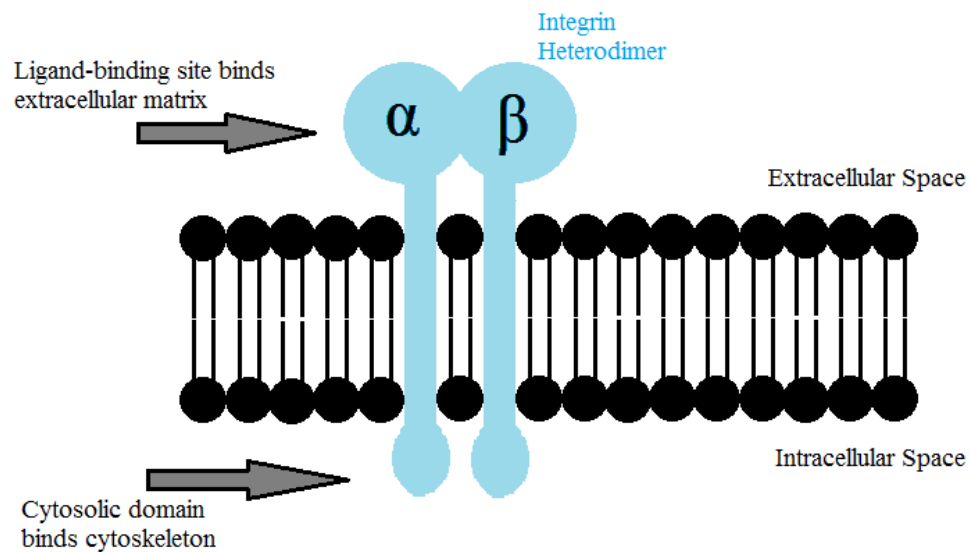
Figure 1.5: Basic structure of the integrin heterodimer. Integrins are composed of the extracellular domain which binds directly to extracellular matrix proteins, a transmembrane spanning region, and a short cytoplasmic domain which binds to actin-binding proteins in the cytoskeleton.

It has been observed that integrins are highly sensitive to haemodynamic forces. For instance integrin activation plays an essential role in flow-mediated Nitric Oxide release (Zaragoza *et al.*, 2012). Under static conditions, the mechanosensitive integrins are in an inactive conformation, and various signalling molecules are unphosphorylated or assembled as a signalling complex (Shyy and Chien, 2002). Studies have shown that the onset of laminar shear stress triggers a conversion of integrins to a high affinity state,

followed by their binding to the subendothelial ECM (Orr *et al.*, 2005). This binding is specific depending on integrin and matrix, and is important for cellular development, cell adhesion, maintenance and repair (Harburger and Calderwood, 2009). For example, shear flow is observed to trigger the activation of the Mitogen-Activated Protein (MAP) kinase p38 when endothelial cells are coated on collagen, but not on fibronectin. The same shear flow can induce activation of the nuclear factor kappa-B (NF-κB) transcription regulator on fibronectin, but not collagen (Orr *et al.*, 2005). There is less evidence for integrin activation through cyclic strain, but it has been suggested that these forces trigger integrin activation in order to increase cell adhesiveness, which leads to new binding and signalling (Schwartz and Simone, 2008).

Kinases are important regulatory proteins with respect to integrins. They respond to activation signals from growth factors, and in turn trigger specialised cellular responses. Integrin cytoplasmic domains have been observed to bind with protein tyrosine kinases (Romer *et al.*, 2006). It has been observed that shear stress is also capable of activating many kinases located in the cell membrane, focal adhesions and cytoplasm. For example, the PI3-K – Akt and protein kinase-A pathways which regulate the activation of endothelial NO synthase are activated following shear. Also of note is the Focal Adhesion Kinase (FAK), which is a ubiquitously expressed cytoplasmic protein tyrosine kinase that has been observed to regulate numerous endothelial cell functions (Grinnell and Harrington, 2012). When activated, FAK is autophosphorylated and associates with c-Src, another kinase. Following this, c-Src phosphorylates paxillin and p130cas, which act as scaffolds for recruitment of various adaptor proteins and signalling intermediates (Donato *et al.*, 2010).
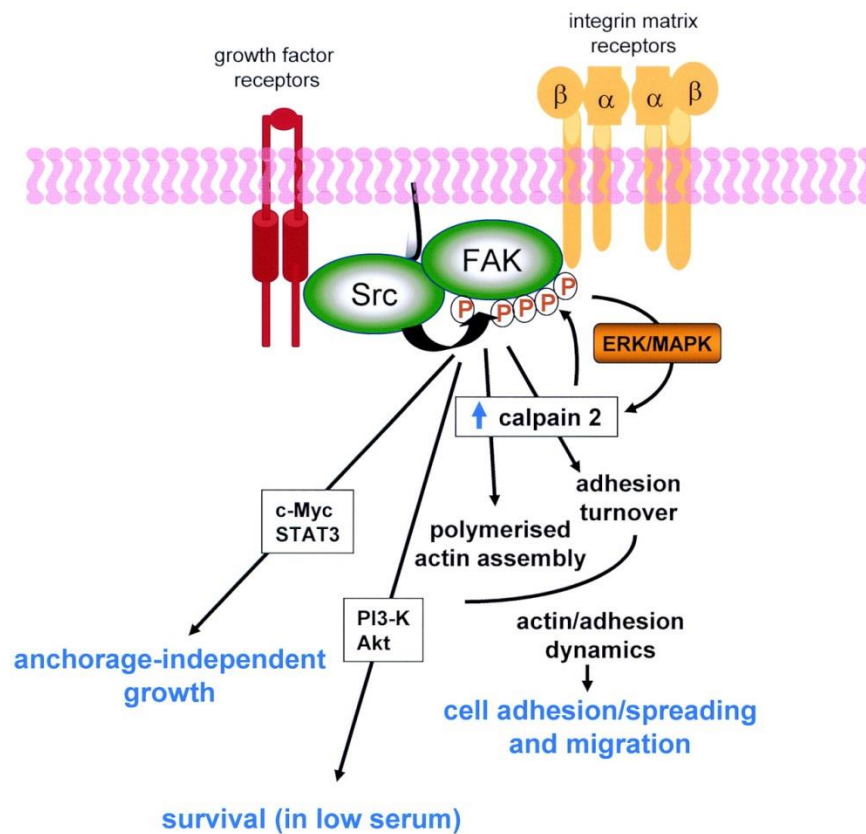
Figure 1.6: Focal Adhesion Kinase phosphorylation. The phosphorylation of FAK is Src-induced and coordinates adhesion dynamics, cell migration, survival, and anchorage-independent growth. The Src-induced phosphorylation of FAK is required for the rapid assembly of actin stress fibres and the formation of focal adhesions that promote initial cell adhesion and spreading, events that are in part mediated by calpain activity. Src-induced phosphorylation of FAK also promotes focal adhesion turnover and cell motility via calpain activation, most likely by linking calpain to upstream regulation by the extracellular signal related kinase/MAP kinase pathway (Westhoff *et al.,* 2004).

Phosphorylation of p130cas by FAK associated Src also leads to activation of MAP kinase and cell migration. MAP kinases are involved in directing cellular responses to an array of stimuli, such as osmotic stress, heat shock and proinflammatory cytokines. They regulate many cellular functions such as proliferation, gene expression, differentiation, mitosis, cell survival, and apoptosis. There is increasing evidence that FAK and Src play a critical role in the interactions between integrins and cadherins, where activated Src and/or FAK can regulate cadherin complex stability (Canel *et al.*, 2013; Koenig *et al.*, 2006).

1.3 EXTRACELLULAR MATRICES

As discussed in the last section, the integrins can bind to the extracellular matrix (ECM) in a specific manner, depending on type of integrin or matrix, which can affect the cellular development. The ECM exists to serve many functions, such as providing

18

anchorage for cells, separating different tissues, and regulating cellular communication (Orr *et al.*, 2006b; Abedin and King, 2010). ECM formation is essential for other processes such as growth or wound healing (Davis and Senger, 2005). The extracellular domains of integrins bind directly to ECM proteins such as fibrinogen, fibronectin and collagen (Orr *et al.*, 2006). As illustrated in Figure 1.7, some of these ECM proteins are capable of altering cellular function and phenotype through the activation of specific integrins which support the flow activation of inflammatory pathways such as NF-κB (Orr *et al.*, 2005). Activation can promote the migration of cells and the breakdown of cell-cell adhesions, which results in elevated endothelial permeability (Mehta and Malik, 2006). Integrin responses to mechanical force can be dependent on specific integrin-matrix interactions. Localised vascular homeostasis has a direct effect on the function of endothelial cells through these interactions of matrices with corresponding integrins, followed by specific signal transduction from the activated integrin. Endothelial cells plated on fibronectin or fibrinogen matrices activate NF-κB in response to flow, whereas cells on collagen do not.

NF-κB (nuclear factor kappa-light-chain-enhancer of activated B cells) is a protein complex that controls the transcription of DNA (Orr *et al.*, 2005). NF-κB controls many inflammatory genes, being observed to be chronically active in many inflammatory diseases, such as atherosclerosis (Liu *et al.*, 2012). While it is difficult to observe NF-κB signalling in an *in vivo* model, it has been observed that endothelial cell-specific inhibition of NF-κB results in a reduction of the development of atherosclerosis in an *in vivo* ApoE−/− mouse model (Gareus *et al.*, 2008). Activation of NF-κB is essential for the Tumour Necrosis Factor α (TNF-α) response. TNF-α is a potent pro-inflammatory cytokine, which triggers endothelial activation resulting in increased vascular permeability (Kempe *et al.*, 2005). Flow-induced NF-κB activation is downstream of conformational activation of integrins. This results in the binding of new integrins to the subendothelial ECM and subsequent signalling events (Orr *et al.*, 2005).

The inhibitory IkBα subunit is degraded and NF-κB is phosphorylated, which allows NF-κB to translocate into the nucleus following flow. Both subunits of NF-κB undergo posttranslational modification also. This modification includes the phosphorylation of p65 Ser536 in the C-terminal transactivation domain, which is important for expression of target genes (Petzold *et al.*, 2009). Changes following shear in the sub-endothelial ECM differ depending on matrix (Orr *et al.*, 2006).
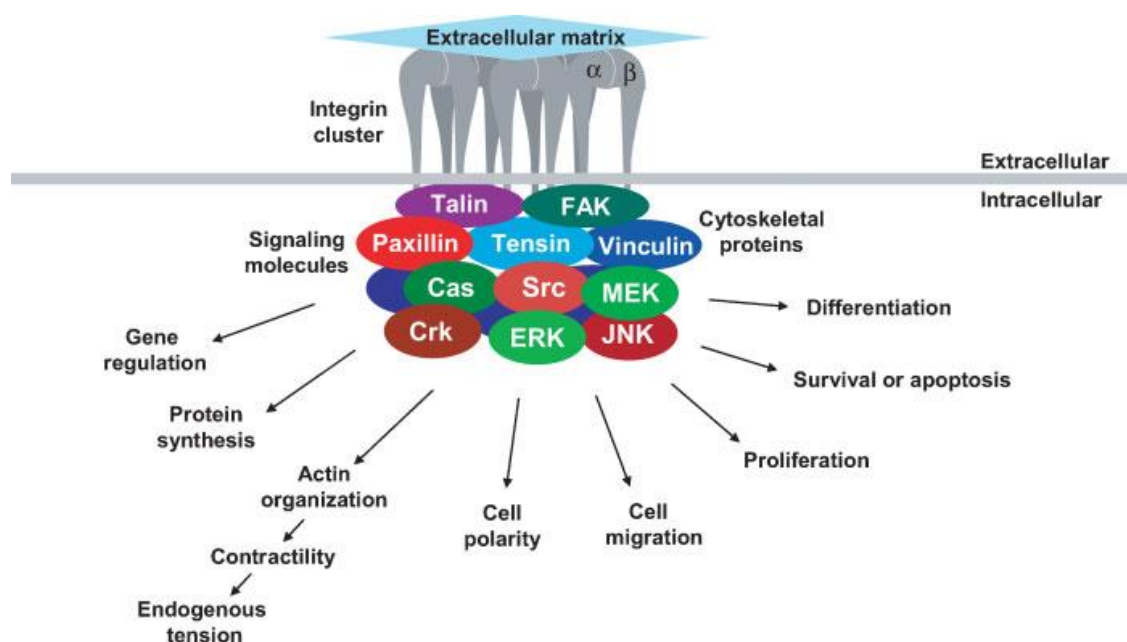
Figure 1.7: General model of Cell-Matrix Interactions and their downstream regulation. The integrin cluster interacts with the extracellular matrix outside of the endothelial cells. These integrins recruit cytoplasmic proteins which, along with other cell surface receptors, can control and regulate many cellular processes and functions (Berrier and Yamada, 2007).

1.3.1 Fibrinogen

The ECM glycoprotein (i.e. a protein bound to a carbohydrate), fibrinogen, plays a major role within the vasculature. It is a large, complex, dimeric glycoprotein composed of three pairs of polypeptides: two Aα, two Bβ, and two γ. These polypeptides are linked together by 29 disulphide bonds, some of which are depicted in Figure 1.8. The two subunits are composed of a D domain which contains a globular region and an E domain which contains disulfide bonds that links the two subunits (Mosesson, 2005).

Fibrinogen is known for a long time to induce endothelial cell attachment, spreading and migration (Suehiro *et al.*, 1997). It is converted into fibrin by thrombin; the fibrin is subsequently polymerised to form a haemostatic plug that, together with platelets forms a blood clot. Fibrinogen has been identified to be a major independent risk factor for CVD with elevation of appearing to correlate with the increasing prevalence of risk factors (Tousoulis *et al.*, 2011). There are several mechanisms for this to occur. Fibrinogen can bind to activated platelets specifically, via glycoprotein IIb/IIIa - which contributes to platelet aggregation. Furthermore, fibrinogen is observed to increase in inflammatory states. Interestingly, there is little fibrinogen or fibronectin present beneath the endothelium in most of the vasculature, but these proteins are observed at sites of disturbed flow *in vivo* (Orr *et al.*, 2005).
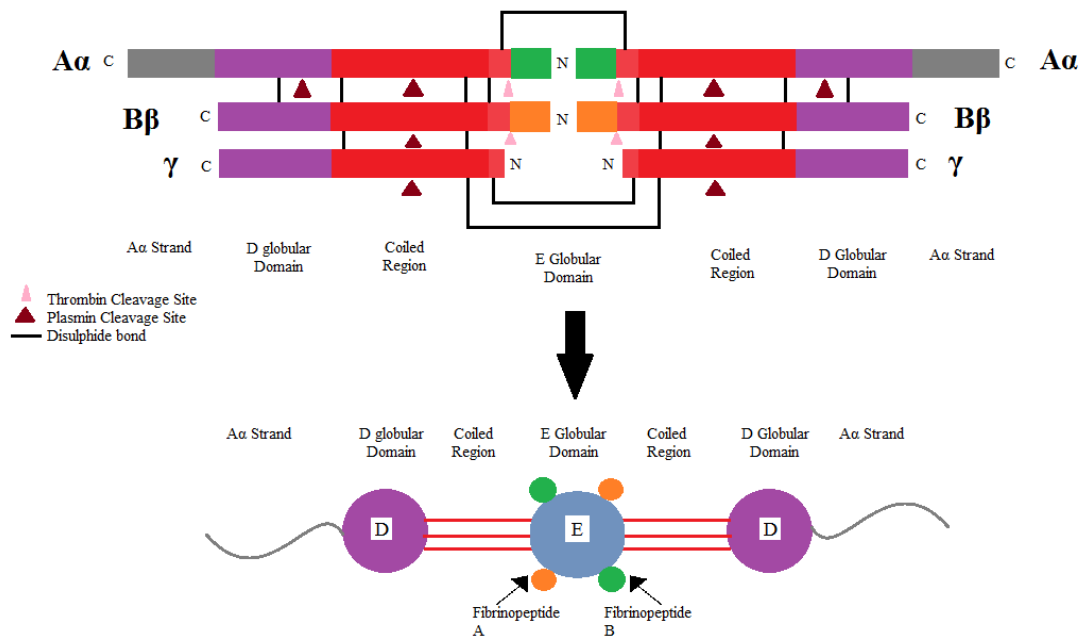
Figure 1.8: Fibrinogen. This schematic illustrates the structure of fibrinogen, consisting of two Aα, two Bβ, and two γ polypeptides. These polypeptides are orientated in such a way that all six N-terminal ends meet and form the central E domain. Two regions of coiled α helices stretch out on either side of the E domain, each consisting of one Aα, one Bβ, and one γ polypeptide. Each of the coiled regions ends in a globular D domain, consisting of the C-terminal ends of Bβ, and γ, as well as part of the Aα polypeptide. The C-terminal end of the Aα peptide then sticks out from each D domain as a long strand, where they can interact with each other or with the E domain during fibrin clot cross-linking.

1.3.2 Fibronectin

Fibronectin is a glycoprotein which connects cells with collagen fibres in the endothelial cell matrix. The protein works by binding collagen and surface integrins, which causes the cytoskeleton to reorganize; thereby allowing for cell motility. It consists of a series of modular domains in an inactive unfolded form. When stimulated, it undergoes conformational rearrangements; revealing previously concealed fibronectin-binding sites and triggers fibronectin matrix assembly (Wierzbicka-Patynowski and Schwarzbauer, 2003). Adjustments of the contractility or matrix rigidity can potentially regulate matrix assembly and structure (Berrier and Yamada, 2007). It has been shown that fibronectin secreted from endothelial cells could enhance the spreading and adhesion of cells on a fibrinogen matrix (Zou *et al.*, 2012). This suggests that this cell-matrix interaction could be indirect. Furthermore, it may be mediated by fibronectin as a bridging molecule.
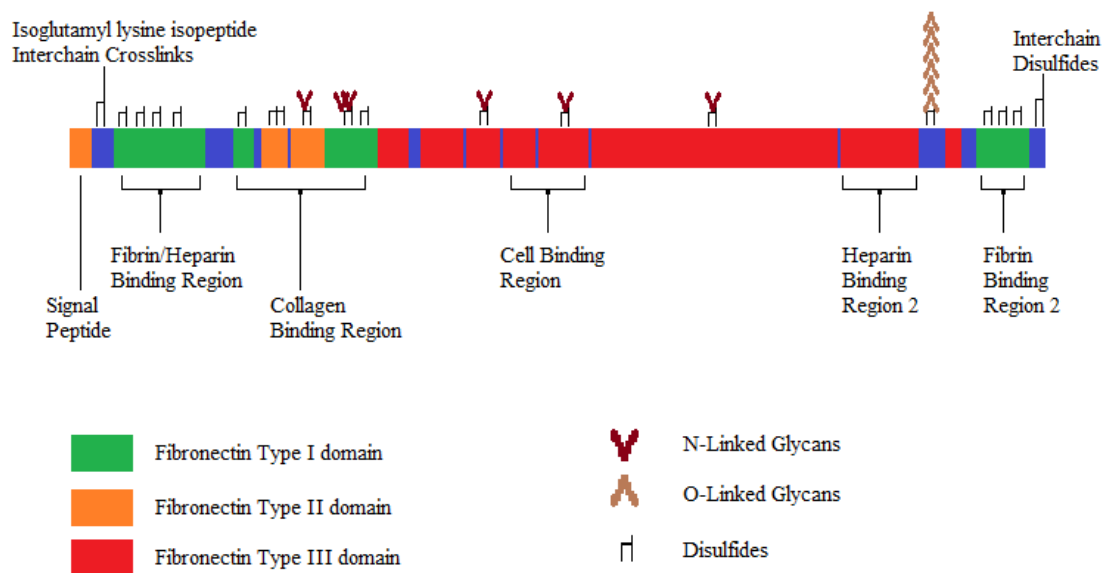
Figure 1.9: Fibronectin. This schematic illustrates the structure of fibronectin, consisting of two heterodimers; the A chain and the B chain, containing the type III connecting segment region. The multiple domains of fibronectin have binding affinities for collagen, heparin, fibrin and other specific cell membrane receptors.

Following shear stress, fibronectin becomes more uniformly distributed beneath endothelial monolayers and organizes into bands of densely packed fibrils. Studies have implicated the shear stress stimulation of the integrin αVβ3 through activation of endothelial cells seeded on a fibronectin matrix, which results in increased binding and cell adhesion (Tzima *et al.*, 2001; delPozo *et al.*, 2000). Studies indicate the integrin activation following shear flow is localised to the edge of cellular lamellipodia. The αVβ3 integrin has been observed to be highly active at cell-cell junction formations, with many of the proteins involved in junction formation also being involved with this integrin in actin recruitment, organisation and maintenance. It has also been observed that laminar shear stress enhances the migratory properties of endothelial cells via the α5β1 integrin. These fibronectin receptor subunits serve as central mechanotransducers in endothelial cells (Urbich *et al.*, 2002). The α5β1 and αvβ3 integrins associate with the Shc adaptor protein, which is able to couple integrin signalling to the MAP kinase cascade and is essential for endothelial cell adhesion and survival (Danen and Yamada, 2001). Previous studies observe that this interaction of Shc and the α5β1 and αvβ3 integrins is stimulated through shear stress (Jalali *et al.*, 2001). As α5β1 is upregulated, the downstream MAP kinase cascades and FAK are activated, stimulating cell migration.

1.3.3   Collagen

Collagen is a major fibrous protein in the ECM and in connective tissue. Multiple types of collagen exist which are distinguished by the ability of their helical and non-helical regions to associate into fibrils, to form sheets, or to cross-link different types of collagen (Lodish *et al.*, 2000). Type I collagen is observed in skin and bone, and the Type III collagen frequently associates with it. Type I collagen can be observed to act upon endothelial cells, altering their morphology to a spindle shape and aligning cells into solid cord-like assemblies (Whelan and Senger, 2003). Type IV is the type mainly seen in the basement membrane of the vasculature however (Hohenester and Yurchenco, 2013). Type IV collagen is a sheet-forming type which is observed to have a critical scaffolding function in basement membranes. This particular type of collagen promotes cellular adhesion and proliferation (DeCaterina and Libby, 2007). It forms a network structure that involves its interaction with other basement membrane components (Genové *et al.*, 2005). Collagen IV molecules consist of two α1 (IV) chains and one α2 (IV) chain. These chains can interact indirectly with cells through low affinity laminins (Hohenester and Yurchenco, 2013), or by strong interactions mediated by nidogen, a glycoprotein which binds to laminin (Mokkapati *et al.*, 2011). Both of these proteins are basement membrane components (Liliensiek *et al.*, 2009). Each of the α-chains consists of three domains: an N-terminal 7S domain, a middle triple-helical domain, and a C-terminal globular non-collagenous (NC1) domain. It is speculated that the α-chains self-assemble to form sets of triple-helical molecules which self-associate via the NC1 domains and their middle triple-helical domains to form spider web-like scaffolds which interact with the laminin network in forming a basement membrane scaffold (Tanjore and Kalluri, 2006).
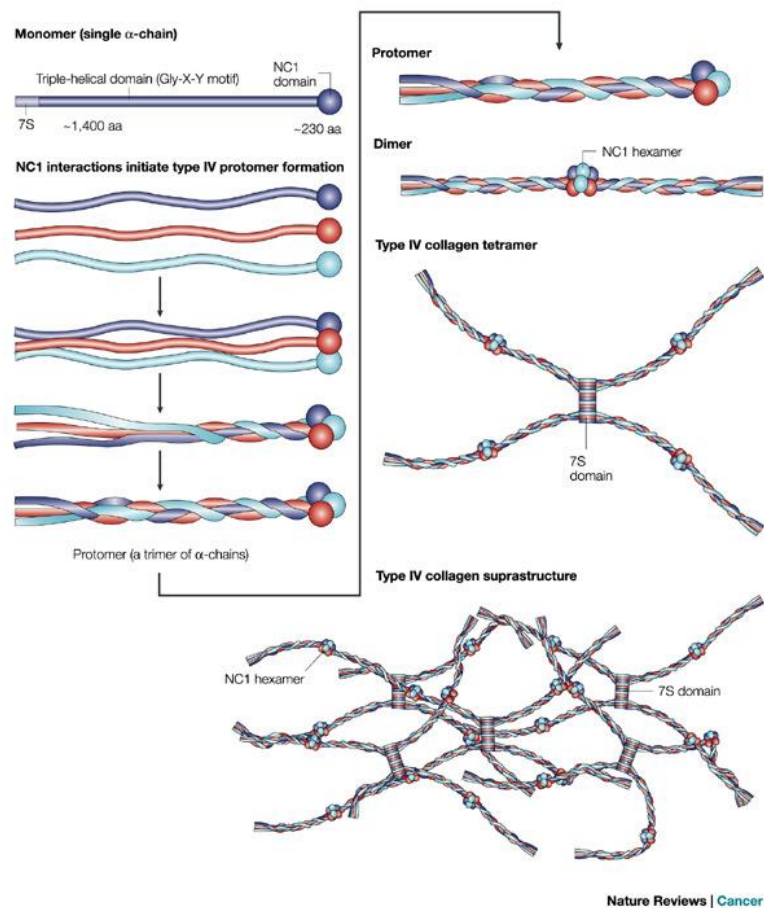
Figure 1.10: Collagen. The type IV collagen α-chains have three similar domain structures: an amino-terminal 7S domain, a middle triple-helical domain, and a carboxy-terminal globular non-collagenous (NC-1) domain. The NC1 domains are thought to associate together, leading to protomer trimerization. This trimerization proceeds like a zipper from the carboxy-terminal end, resulting in a fully assembled flexible protomer. Two type IV protomers associate via their C-terminal NC1 trimers to form an NC1 hexamer. Afterwards, four protomers interact at the glycosylated N-terminal 7S region to form tetramers. These interactions form the nucleus for a type IV collagen scaffold. The scaffold evolves into a type IV collagen super structure, with the help of end to end associations and also lateral associations between type IV collagen protomers (Kalluri, 2003).

ECM composition remains relatively stable in healthy adult tissue, but this balance is subject to change (Wight and Potter-Perigo, 2011). Degradation of Type IV collagen can occur in the basement membrane under both physiological and pathological conditions (Kalluri, 2003). Under these conditions, the triple helices of collagen can unfold, enabling other matrix proteins such as fibronectin to interact with native collagen *in vivo*. Such fibronectin-collagen interactions may mediate the adhesion of cells to collagen, form non-covalent crosslinking of fibronectin and collagen in migratory pathways, and also regulate the removal of denatured collagenous materials from blood and tissue (Pankov and Yamada, 2002).

Endothelial production of collagen also appears to be inhibited with increased cyclic strain (Wilson *et al.*, 2009). Studies on cells seeded onto a glycosylated form of collagen have observed the halting of the alignment of endothelial cells normally seen during shear stress (Kemeny *et al.*, 2011), suggesting that collagen expression in endothelial cells may be hindered with exposure to both kinds of haemodynamic force, affecting the balance of matrix composition. It has been observed that shear stress is capable of inducing NF-κB activation on fibrinogen and fibronectin matrices, but not on collagen. Despite the production of ROS during shear, there is a lack of flow-induced NF-κB activation when endothelial cells are seeded onto a collagen matrix, which is suggestive that collagen somehow regulates cellular sensitivity to ROS (Orr *et al.*, 2005). Certain integrins fail to be activated on nonpermissive matrices such as collagen. The ligation of one integrin can affect activation of other integrins in a knock on effect (Gonzalez *et al.*, 2010). It was hypothesised then that expression of Palladin or its interacting proteins may be affected by the specific ECM related signalling mechanisms following mechanical stimulation of the endothelial cell. The results of this are discussed in Chapter 3.

1.4 THE CYTOSKELETON

The structure of the endothelial cell in response to mechanics are largely determined by the alteration of the cellular cytoskeleton, which itself is mainly composed of microtubules, intermediate filaments and actin (Choi and Helmke, 2008). The microtubules are the largest, having a diameter of about 25nm, the intermediates filaments are roughly 10nm, and the actin microfilaments are the smallest component at approximately 8nm in size (Insall and Machesky, 2001). These structural filaments are each assembled from monomeric precursors that are reappropriated through the exact spatial and temporal control of multiple cellular processes (Osborn *et al.*, 2006). The cytoskeleton is capable of building a scaffold to define cell shape, but is still flexible so as to tolerate haemodynamic forces. It is not a constant structure though, as actin fibres re-align in the direction of shear (Oberleithner *et al.*, 2007). It follows that the cytoskeleton plays an important role in the modulation of haemodynamic forces, whereby it transmits them through the cell, and transduces the mechanical force into a bio-chemical signal which finally leads to an alteration of cellular function. The disruption of the actin cytoskeleton in such a way can sufficiently negate the effect of

shear stress mediated signalling and changes in gene expression (Imberti *et al.*, 2000). Cell migration and tissue remodelling require a co-ordinated cross talk between the intermediate filament, microtubule and actin cytoskeletal networks. Recent studies have indicated that the intermediate filaments and their associated proteins such as Myosin IIa are important components in mediating this crosstalk (Even-Ram *et al.*, 2007; Chang and Goldman, 2004).

1.4.1 Microtubules

Microtubules act as rigid reinforcing rods which sustain both tension and compression. Actin filaments act along with them to resist the breaking down of the cell and facilitate the transmission of forces which allows the cytoskeleton to determine cell shape and structure (Abu Shah and Keren, 2013). They also play a role in the mitotic division of cells, where they aggregate and form a mitotic spindle, which assists in chromosome partitioning and cell division (Woolner *et al.*, 2008). Microtubules possess a uniform structural orientation, by where the wall of a microtubule is composed of a helical array of tubulin heterodimers, each composed of one α-tubulin and one β-tubulin molecule, arranged in an alternating manner (Hu *et al.*, 2006). These heterodimers polymerize end to end, giving the filament polarity. The actual tubules are composed of 13 "protofilaments" composed of heterodimers, all encircling a hollow core. This results in the microtubules possessing a rigid structure, contrary to the other filament systems.

These microtubules work as tracks for motor proteins such as myosin (Lyle *et al.*, 2012). By using the microtubule motors to travel along actin filaments, many molecules of myosin generate enough force to contract muscle tissue. The proteins are also able to move vesicles and organelles through using this function (Thompson and Langford, 2002). There are also a number of proteins which regulate microtubule stability, mostly by binding along the length of the microtubules, as opposed to capping the ends (Tirnauer and Bierer, 2000).

1.4.2 Intermediate Filaments

Intermediate filaments are flexible but strong polymers that work to prevent excessive stretching of the cells by external forces, as well as providing mechanical support for the cells. When structural integrity is disrupted, repair and re-establishment is accomplished by the microtubules and actin microfilaments, being mediated by the

intermediate filaments until the cell reverts to a more structurally sound state (Chang and Goldman, 2004). There is a continuous network of intermediate filaments from the nuclear envelope to attachments known as desmosomes and hemi-desmosomes on the plasma membrane. Mechanical forces are transmitted through these desmosomes from cell to cell, and through hemi-desmosomes from cell to ECM (Delva *et al.*, 2009).

In contrast to the highly conserved actin microfilaments and tubulins, the protein subunits of intermediate filaments are varied in sequence and size (Chang and Goldman, 2004). Another difference is the lack of polarity they have, which facilitates spontaneous self-assembly under physiological conditions (Godsel *et al.*, 2008). During filament assembly, the monomers intertwine as they organize into a rope-like structure with considerable tensile strength (Kreplak and Fudge, 2007). The subunits are encoded by multiple different genes, but do share some characteristics, such as a general size of around 10nm in diameter.

1.4.3   Actin

Actin is a highly conserved, ubiquitous and vitally important protein in the cell. The human vasculature displays six actin isoforms, which can be divided further into three groups: alpha (α), beta (β) and gamma (γ). The α-actins are found to be mainly expressed in muscle cells and function in the cellular contraction whereas the other isoforms can be found in non-muscle cells as cytoskeletal components (Borisy and Svitkina, 2000). Actin contributes greatly to the function of cells through formation of cytoskeletal structures and localisation of actin-binding proteins which play other roles themselves in cell motility. Such actin-binding proteins have multiple domains for the organisation of actin, as well as protein scaffolding and signal transduction (Hu *et al.*, 2006). An imbalance in actin dynamics is indicative of a cell's pathological state. Actin carries out its main functions through rounds of polymerisation and de-polymerisation in a network of actin filaments (Cooper and Schafer, 2000). The filaments extend and form various structures, such as lamellipodia, pseudopods or filopodia. Furthermore, actin filaments bind to specific actin-binding proteins to form other structures (Figure 1.11). For example, the protein myosin and other actin-binding proteins will combine with actin to form bundles called stress fibres which apply tension between structures on the plasma membrane (Bershadsky *et al.*, 2006). These structures are then either bound together, or to the ECM, so by manipulating the filaments, the adhesive formations can be modulated. The actin cytoskeleton is organised into microfilaments,

which themselves have actin monomers as their core subunits. These monomers exist in a globular form – referred to as G-Actin - which associates together in long filamentous forms, known as F-Actin (Figure 1.11). These F-Actin strands group together in a helical shape to form microfilaments. Actin microfilaments possess a defined polarity, with the faster growing ends known as "barbed ends" and the slower growing ends known as the "pointed ends". The barbed end is favoured for growth, with actin filaments in cells strongly orientated with the barbed ends facing outward to the cell surface.
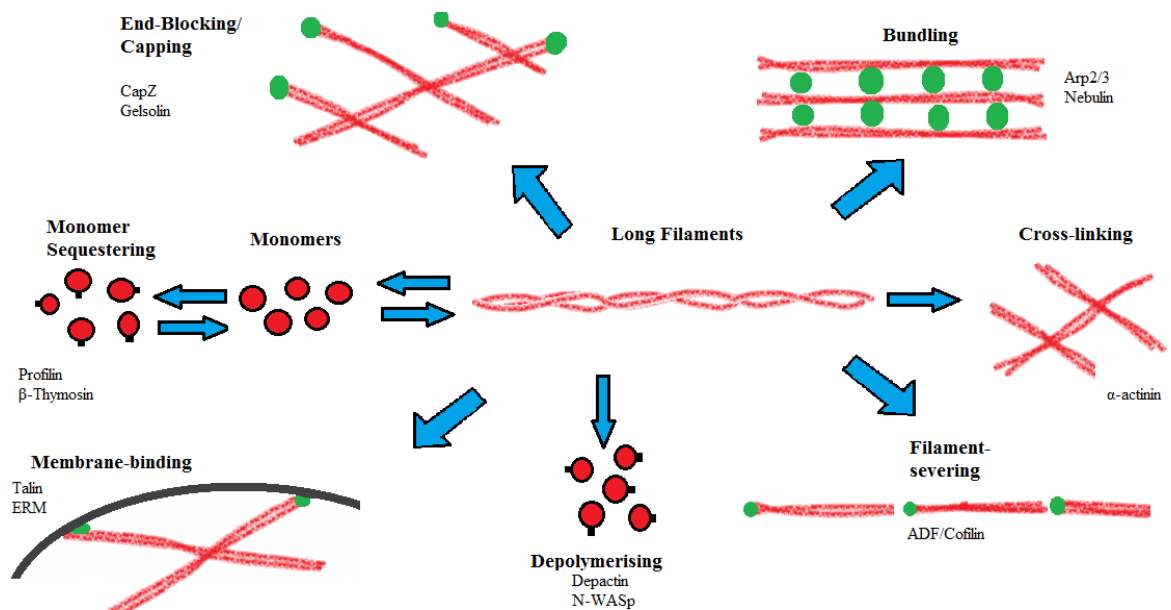
Figure 1.11: Actin and binding proteins. This figure demonstrates the various functions actin filaments may have, along with the different proteins that interact with them. Actin-binding proteins can be loosely grouped into categories that function in sequestering G-actin into F-actin filaments, anchoring actin to membrane adhesion complexes, severing or depolymerisation of actin filaments, cross-linking or bundling actin, or capping the ends of filaments. The Palladin protein plays a role in bundling and crosslinking.

Actin-binding proteins regulate the organisation of cellular actin filaments. These proteins can be organised into families that are able to bind the monomers, sever filaments, cap filament ends, cross-link filaments or stabilise filaments (Dominguez, 2004). Such proteins possess actin-binding sites to enable the cross-linking of proteins and filaments as well as providing stability for other higher order assemblies of actin filaments. For example, the actin-binding α-actinin is found in the cortical actin network, at intervals along stress fibres and on the cytoplasmic side of cell adhesion

plaques. It is vital for the attachment of actin filaments to the Z-lines in skeletal muscle cells, and to the dense bodies in smooth muscle cells (Klaavuniemi *et al.*, 2004). It also plays a role in the binding of actin to the membrane in other cell types. The Palladin protein, as discussed later, is also as an actin-binding protein, localising to stress fibres, focal adhesions and z-lines (Mykkänen *et al.*, 2001; Parast and Otey, 2000; Dixon *et al.*, 2008).

Another actin based structure is the stress fibre. Stress fibres consist of roughly 10-30 actin filaments grouped together in straight bundles, along with cross-linking proteins and Myosin II motors. These structures transverse the cell, and terminate in dense plaques at the cell base (Pellegrin and Mellor, 2007). Within stress fibres, the individual actin filaments are bundled together through the cross-linking proteins. The myosin motors move, sliding the actin filaments past one another, allowing the fibre to contract. The proteins also facilitate the transmission of the contractile generated forces they produce to the ECM via focal adhesions. Contraction against the focal adhesion structures allows the force generated by myosin motors and filament growth and rearrangement to move and reshape the cell. Under normal conditions, cells are protected and reinforced by the ECM. When this support matrix in compromised, or when haemodynamic force is increased, the cells are stimulated into rapidly forming stress fibres. They then become aligned in the direction of flow within the vessels. The molecular mechanisms underlying the regulation of stress fibre thickness in response to mechanical stimuli is still under investigation (Tojkander *et al.*, 2012; Hotulainen and Lappalainen, 2006).

There are three classes of stress fibre, defined by their subcellular location: dorsal stress fibres, ventral stress fibres and transverse arcs (Hotulainen and Lappalainen, 2006). Dorsal stress fibres are formed by formin-mediated actin polymerisation at focal adhesion sites. They are attached to focal adhesions at one end, which tethers them to the cell base. The other end displays a loose matrix of actin filaments. These fibres elongate from focal adhesions to form short filaments containing α-actinin (Pellegrin and Mellor, 2007). Myosin then associates to these filaments, displacing the α-actinin. Because of the single polarity they possess, dorsal stress fibres are not contractile in nature. Instead they work by providing rigidity to the cell, and allow the cells to spread out in the blood vessel in an adaptive response to shear stress.

Ventral stress fibres are the most common subtype of stress fibre; found lying along the base of the cell and attached to focal adhesions at each end. The ventral stress fibres can form from the joining of two dorsal stress fibres to form a structure anchored at each end with the focal adhesion. Ventral stress fibres are contractile in their central region. At this localisation, the fibres from the opposing ends meet and generate a tension across the entire structure, on account of them being tethered to the focal adhesions at either ends. This allows for the resulting force to be transmitted to the substratum (Noria *et al.*, 2004).

The dorsal stress fibres may either join each other directly, or else meet at a transverse arc which then disassembles (Pellegrin and Mellor, 2007). The transverse arcs are formed through the end to end joining of actin bundles to myosin bundles beneath the dorsal surface of migrating cells directly behind the lamella. Transverse arcs are not anchored to the plasma membrane by focal adhesions so they transmit their force to the ECM indirectly via dorsal stress fibres (Ciobanasu *et al.*, 2011).
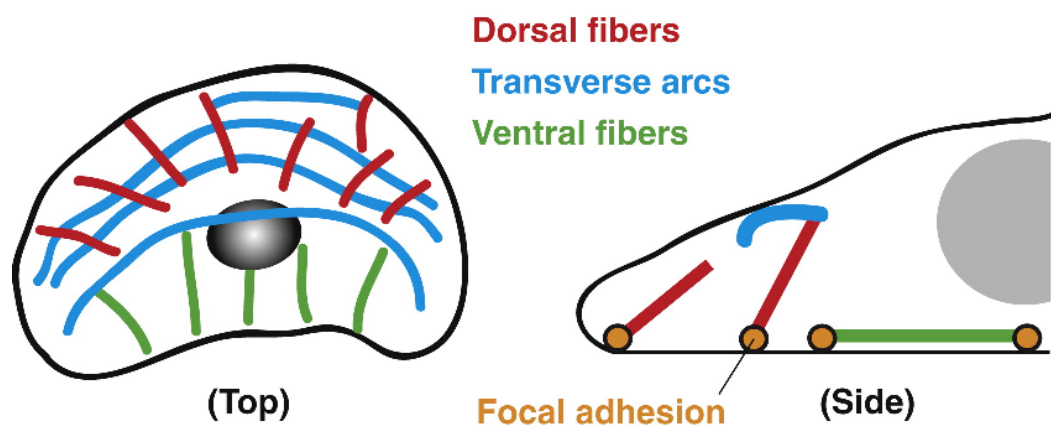
Figure 1.12: Actin Stress Fibres. This figure summarizes the distribution of the three classes of stress fibres in cells. The ventral fibres are formed when two dorsal fibres fuse together with a transverse arc. (Lord, 2011).

Stress fibres structures contain regularly spaced "thickenings" called dense bodies. These dense bodies consist of several actin-binding proteins, scaffolding proteins and signalling kinases. One such protein observed within dense bodies is Palladin, the investigation and characterisation of which forms the major aim of this thesis. As the cell is subjected to haemodynamic force, the expression of actin will change on account

of the remodelling of the cell inducing a change in the fibres. It was theorized that the expression of Palladin would follow, changing in its expression levels in response to the same haemodynamic forces.

1.5 THE PALLADIN PROTEIN

The actin-binding protein Palladin, and its hitherto unknown characterisation within the aortic endothelial cell, form the main aim and focus of this thesis. Discovered in the year 2000, this member of the Myotilin-Myopalladin-Palladin family plays a role in cytoskeletal organisation (Parast and Otey, 2000). It is also involved in cell development, scar formation, embryonic development and cell motility. Mutations in Palladin have been shown to play a role in diseased states (Pogue-Geile *et al.*, 2006). While alterations in Palladin expression are characteristic in these diseases, changes in expression are not exclusive to pathological states. The protein appears to be responsive to haemodynamic forces, with upregulation being observed in human adipose-derived stem cells subjected to cyclic strain (Wall *et al.*, 2007). As stated previously, the only characterisation of Palladin in endothelial cells was the observation of the protein within the endothelial cell nuclei in human coronary vessels with atherosclerosis (Jin *et al.*, 2010). A major aim was therefore to observe the expression of protein within endothelial cells subjected to haemodynamic force.

1.5.1 Isoforms of Palladin

The Palladin protein itself exists in multiple cell type specific isoforms, arising from alternative splicing of the *PALLD* gene (Table 1.2). The *PALLD* gene is unusually large and complex, spanning 400kb in size and containing at least 25 exons (Goicoechea *et al.*, 2010). Three of these exons – the first, third and twelfth – are 5' noncoding exons, that are specific for one of three possible transcription start sites (Rachlin and Otey, 2006). It has been proposed that the different isoforms may serve distinct cellular functions. While the 200kDa isoform is the largest (and the isoform of which all the smaller isoforms can be considered to be derived from), it is the 90kDa isoform which is generally the most commonly observed isoform in cell types (Parast and Otey, 2000; Rachlin and Otey, 2006; Henderson-Jackson *et al.*, 2011).

Table 1.2: Palladin isoforms in specific cell types. The table lists some of the specific cell and tissue types which display different specific isoforms of Palladin.

Isoform	Cell Type	References
200	Heart/ Smooth Muscle	Wang and Moser, 2008
	Bone	Rachlin and Otey, 2006
140	Developing Epithelial derived cell lines, Adult tissues rich in muscle / cardiac muscle	Rachlin and Otey, 2006
90	Smooth Muscle	Jin *et al.*, 2007
	Fibroblasts	Goicoechea *et al.*, 2010
	Lung and Bladder	Wang and Moser, 2008
	(Ubiquitously expressed in most tissues)	Parast and Otey, 2000
65	Pancreas	Goicoechea *et al.*, 2010
	Uterus	Wang and Moser, 2008

The multiple isoforms possess different combinations of proline-rich domains in the N-terminal end of the molecule, which are sites for protein-protein interactions (Figure 1.13). These regions are flanked by numerous serine residues (predominant phosphorylation sites in Palladin) and are homologous to the ones contained in zyxin, vinculin and VASP family members (Parast and Otey, 2000). In the C-terminal, Palladin has Ig-like domains which mediate filamentous actin (F-actin) cross-linking (Goicoechea *et al.*, 2008). The Ig domain is involved in protein-protein interactions, appearing in both extracellular and intracellular proteins (Barclay, 2003). These domains generally contain about 100 amino acids, and consist of seven to nine beta strands folded in a sandwiched beta sheet fold form (Otey *et al.*, 2009). The Ig domains have been observed previously to associate with the actin cytoskeleton in a number of protein families, including myosin light chain kinase and Myotilin (Heikkinen *et al.*, 2009). The Ig domains of Palladin show a homology to those found in these protein families. Sequence comparison indicates that Palladin is most homologous to Myotilin, displaying similar domains in both the C-terminal and N-terminal regions (Mykkänen *et al.*, 2001). However, despite these very close similarities, the two proteins are differentially expressed in tissue, with Myotilin expression being much more restricted, being found within the Z-disc of skeletal muscle and cardiac muscle (Otey *et al.*, 2005).
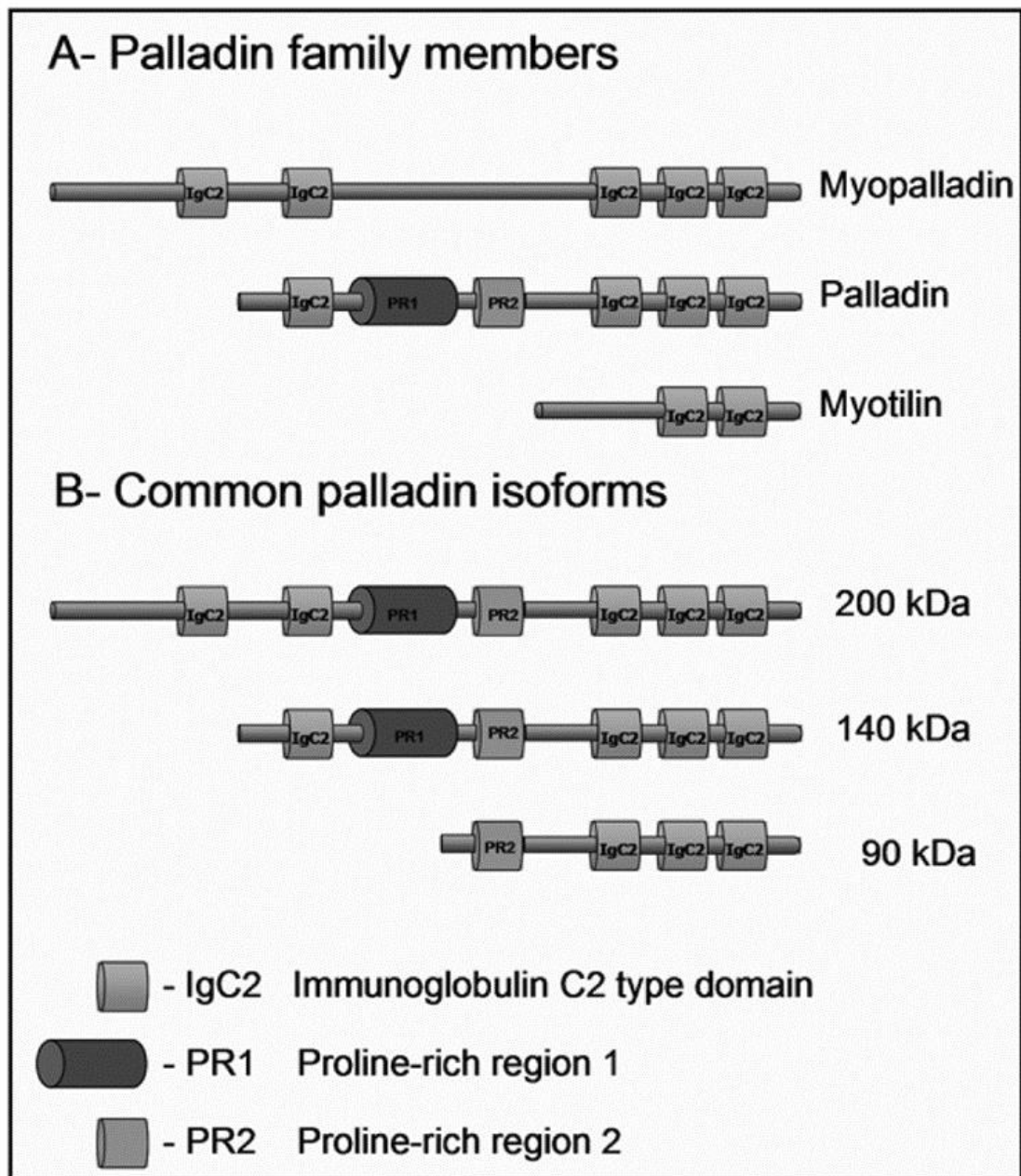
Figure 1.13: Isoforms of Palladin. This schematic is representative of the major palladin isoforms, palladin family members and their domain organization. Myotilin contains two C-terminal Ig domains, while Myopalladin has two N-terminal and three C-terminal Ig domains, similar to the Ig domain structures of Palladin. Palladin isoforms are composed of a combination of between three to five Ig-like domains, and at most two proline-rich domains. While the diagram lists the main 90,140 and 200 kDa sized isoforms, to date there are 7 fully categorized isoforms in total, with preliminary data on an 8th and 9th being investigated. These main three isoforms contain proline-rich domains that the other sizes do not (Goicoechea *et al.*, 2008).

Palladin has been observed in structures containing contractile actin filament bundles, such as stress fibres or sarcomeres (Parast and Otey, 2000; Mykkänen *et al.*, 2001). The Ig3 domain, but not Ig4 or Ig5 domain, is observed to bind to F-actin in a salt-dependent

manner, suggestive of an electrostatic interaction (Goicoechea *et al.*, 2008). Notably, while the Ig4 domain does not bind to F-actin, fragments that contain both Ig3 and Ig4 appear to exhibit a greater affinity for actin when compared to the Ig3 domain alone (Dixon *et al.*, 2008). It appears that this is so because of actin-binding residues in the Ig3-Ig4 linker region enhancing the electrostatic interaction between the Ig3 domain and F-actin. However this linker region alone is unable to bind to actin. The Ig1 and Ig2 domains are still under investigation, as they only appear in certain isoforms - the 140kda sized form has the Ig2 domain near the N-terminus, while the canonically "full" 200kDa form has the Ig1 and Ig2 domain, as well as Ig3, Ig4 and Ig5. The alterations in these Ig domains in different isoforms can result in the isoform specific binding of Palladin to other proteins (Rachlin and Otey, 2006).

1.5.2   Protein Interactions of Palladin

Palladin can associate with many other proteins. It co-localises with α-actinin (Beck *et al.*, 2011; Grooman *et al.*, 2012), another prominent actin-binding protein which itself assists in organization of the cytoskeleton, and acts as an adaptor in multi-protein complexes associated with actin filaments (Figure 1.14). α-actinin also plays an important role in cell-matrix and cell-cell adhesion (Otey and Carpen, 2004). The Palladin protein co-localizes with α-actinin in focal adhesions, dense regions and cell-cell junctions as well as recruiting α-actinin to stress fibres via its poly-proline segments (Rachlin and Otey, 2006). Studies show that a short sequence of Palladin, in amino acids 222-280, specifically mediates the interaction with α-actinin with the binding site in α-actinin located within the C-terminal domain (Rönty *et al.*, 2004).
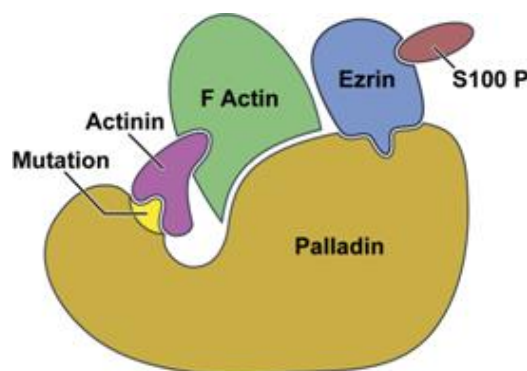
Figure 1.14: Interaction of Palladin with other proteins. This diagram illustrates how Palladin could interact with F-actin, and other actin-binding proteins such as Ezrin or α-actinin (Pogue-Geile *et al.*, 2006).

Palladin is also observed to bind to CLP36, a member of the PDZ-LIM family of proteins, which associates to α-actinin and localizes to the actin cytoskeleton (Maeda *et al.*, 2009). Palladin also binds to other actin associated proteins such as VASP (Boukhelifa *et al.*, 2004), profilin (Boukhelifa *et al.*, 2006), ezrin (Mykkänen *et al.*, 2001), and Eps8 (Goicoechea *et al.*, 2006). VASP and its related proteins (Mena, Ena and EVL) regulate actin filament growth and cell motility, and also function as actin cross-linking proteins (Price and Brindle, 2000; Schirenbeck *et al.*, 2006). VASP forms complexes with profilin, suggesting that VASP and Palladin may work together in recruiting profilin to actin polymerisation sites (Krause *et al.*, 2003; Witke, 2004; Boukhelifa *et al.*, 2005). Profilin can also enhance actin growth through the binding with monomeric actin, thereby occupying an actin-actin contact site. This can result in profilin catalysing the changing of actin-bound ADP into ATP, thereby converting the poorly-polymerizing ADP-actin monomers into readily-polymerizing ATP-actin monomers. Ezrin, which is a member of the ERM (Ezrin/Radixin/Moesin) family of actin-associated scaffolds, is typically a part of the cytoskeleton but in smooth muscle cells it is localized along microfilaments (Mykkänen *et al.*, 2001). Fragments of Ezrin were observed binding to the Ig2 and Ig3 domains of Palladin in SMCs, however full length Ezrin did not interact (Mykkänen *et al.*, 2001). This suggests that Ezrin must be activated to bind to Palladin. Activation via phosphorylation and/or phosphatidylinositol bisphosphate binding can disrupt the intramolecular association, revealing binding sites for actin and several other molecules. Ezrin may also bind to cell surface adhesion molecules, cell signalling molecules or cytoskeletal proteins including actin (Neisch and Fehon, 2011). Eps8 is a substrate for the EGF receptor and directly binds to actin, regulating the length of the filaments. Palladin and Eps8 co-localise in the dorsal membrane ruffles that form after cells are treated with certain growth factors, and also in the podosomes of vascular smooth muscle cells (Goicoechea *et al.*, 2006). The large number and diversity of proteins which bind to Palladin are suggestive that it also has an indirect effect on actin organization as a scaffolding molecule, being responsible for organising a group of other proteins to ensure that actin assembly, bundling and depolymerisation occur in the correct order for cell motility to occur (Dixon *et al.*, 2008).

Table 1.3: Binding partners of Palladin. The table below summarizes the major published binding partners of Palladin protein, and their binding sites.

Interacting Protein	Interaction Site in Palladin	References
α-actinin	Between amino acids 222-280, 90kDa isoform	Parast and Otey, 2000; Rönty *et al.*, 2004
Eps8	N-terminal poly-proline sequences of 90kDa isoform	Goicoechea *et al.*, 2006
Ezrin	2 C-terminal IgC2 domains of human Palladin	Mykkänen *et al.*, 2001
Integrin αvβ5	Between amino acids 298-772 of 90kDa isoform	Lai *et al.*, 2006
LASP-1	N-terminal poly-proline sequences of 90kDa isoform	Rachlin and Otey, 2006
Profilin	N-terminal poly-proline sequences of 90kDa isoform	Boukhelifa *et al.*, 2006
Spin90 and Src	N-terminal poly-proline sequences of 90kDa isoform	Rönty *et al.*, 2007
VASP	FPXPP motifs in 90kDa and 140kDa isoforms	Boukhelifa *et al.*, 2004

1.5.3 Effects of Palladin Expression

The expression of Palladin is required for many essential cellular functions, with regular embryogenesis a prime example. In Palladin knockout mice models, embryos were observed to die within 15 days and exhibit developmental abnormalities such as failure for the neural tube to close (Luo *et al.*, 2005). It has been demonstrated that Palladin-null fibroblasts were also lacking in the β1 integrin subunit, with research indicating that Palladin is involved in the proteolysis process of the β1 integrin. The integrin itself is also known for playing a role in cell adhesion; downregulation of it may be an underlying effect resulting from adhesion and migration defects in the cell (Liu *et al.*, 2007). The expression of Palladin therefore may be necessary for the adhesion of cells to the ECM, likely through the stabilization of the β1 integrin by Palladin (Luo *et al.*, 2005). Palladin also interacts with integrin αvβ5 at the focal adhesions and likely links it to the cytoskeleton, but this interaction has not been well characterized (Lai *et al.*, 2006). Focal adhesions in knockdown cells have been observed to dramatically reduce, with only a few peripheral adhesions remaining, correlating with a reduction in number and strength of stress fibres (Parast and Otey, 2000). Furthermore, knockdown of Palladin has been observed to cause a decreased F-actin to G-actin ratio, disordered stress fibres, and a significant delay of wound healing due to decreased cell migration (Jin *et al.*, 2009, 2010).

Over-expression of Palladin also results in huge changes to the actin cytoskeleton, with increase of actin bundles being observed (Rachlin and Otey, 2006). Notably the overexpression phenotype appears to differ depending on isoform; overexpression of the 140kDa isoform displays compact star-like actin arrays, compared to the robust actin-cables of the 90kDa overexpression. Palladin has been observed to be rapidly upregulated in response to exposure to the Transforming Growth Factor β1 (TGF-β1) cytokine (Rönty et al., 2006). Reviews have pointed out that TGF-β1 stimulation acts along with increased matrix rigidity to influence wound healing (Hinz, 2007), as well as the induction of podosomes (Varon et al., 2006). Podosomes are dynamic, actin-rich structures which are involved in the adhesion of cells to solid substrates, as well as playing a role in tissue invasion and matrix remodelling (Buccione et al., 2004; Linder, 2007). In many adult organs, Palladin is observed to be upregulated after injury near a wound site, where cell migration and tissue remodelling occur (Rönty et al., 2006; Goicoechea et al., 2009). Palladin is also is upregulated downstream of angiotensin II treatment in vascular smooth muscle cells. Angiotensin II influences the hypertrophy of the vessel wall which occurs during chronic hypertension, and also increases the synthesis of contractile proteins in aortic smooth muscle. The experimental overexpression of Palladin in SMCs was shown to increase their migration rate in vitro (Jin et al., 2007). When looking at the roles of Palladin in cell migration, a unifying theme emerges, as illustrated in Figure 1.15.

The Rho family of small GTPase signal transduction enzymes has been seen to regulate Palladin expression. Investigation of expression following treatment of cells with rho-inhibitors showed a loss of Palladin along with the loss of stress fibres and focal adhesions. This indicates Palladin expression is regulated by RhoA signalling and by actin dynamics, but it is unclear as to whether the RhoA-ROCK pathway acts directly on palladin or indirectly through its modulation of actin dynamics (Jin, 2011). It has been further shown that Palladin interacts with the SH3 domains of the SPIN90 protein, and is required for Src induced cytoskeletal remodelling (Rönty et al., 2007). Src is a non-receptor kinase which regulates cell adhesion, motility, and invasion by remodelling of the actin cytoskeleton, as well as being a key player in the formation of podosomes (Brunton et al., 2004). It can also bind to Eps8 (Otey et al., 2009). Palladin was observed to phosphorylate in cell expressing active Src, and that Src kinase resulted in the translocation of Palladin and SPIN90 to membrane protrusions. The knockdown

of Palladin led to inhibition of SPIN90 relocation, suggesting that perhaps Palladin may target Src to control Src-dependent events.
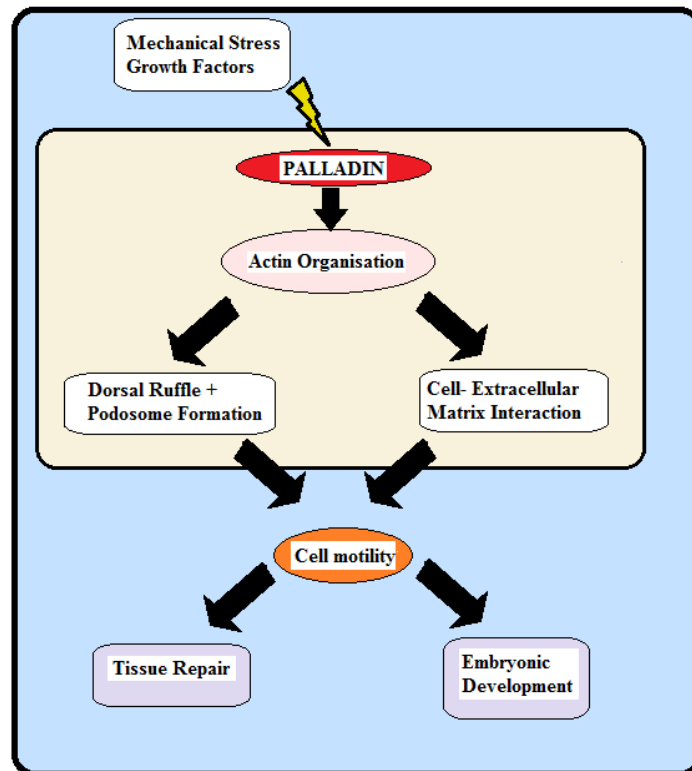
Figure 1.15: Palladin in Cell Migration. This model illustrates a working model for the role that Palladin plays within multiple processes required for cell migration across tissue boundaries. Following a stimulation of some kind, Palladin expression is altered, which organises the actin cytoskeleton. This has knock on effects on the shape and interactions of the cell, which in turn affect cell motility and subsequent functions. The protein can translocate to the nucleus upon stimulation, suggesting that it may also have a signalling function in excitation-transcription (Jin, 2011).

Knockdown of Palladin also affects the expression of LASP-1, one of its binding protein partners. As it localises to actin stress fibres, it has been proposed that Palladin also binds to the LASP-1 protein, which in turn binds the proteins zyxin and Ena/VASP to co-ordinate the actin organisation events required to re-orientate, and thicken the actin stress fibres in order to adapt to haemodynamic stresses (Yoshigi *et al.*, 2005; Hoffman *et al.*, 2006; Furman *et al.*, 2007).

1.5.4 LASP-1

The proline domains of the extended N-terminal region of the 140kDa Palladin protein isoform contains binding sites for many protein families, including a site for binding of Lim and SH3 domain protein 1, better known as LASP-1. LASP-1 is an actin and membrane associated protein, which functions as a cytoskeletal scaffold (Chew *et al.*, 2000). It also contains several conserved domains that function as protein interaction sites (Grunewald and Butt, 2008). These domains consist of an N-terminal LIM domain, followed by an actin-binding nebulin repeat domain and a C-terminal SH3 domain that facilitates its binding to Palladin, as well as other proteins such as VASP (Li *et al.*, 2004; Rachlin and Otey, 2006) (Figure 1.16). LASP-1 was originally discovered as the first member of a newly defined LIM-protein sub-family of the nebulin group characterised by the combined presence of the LIM and SH3 domains (Tomasetto *et al.*, 1995). The SH3 domain appears as 80% identical and 86% conserved to that of nebulin, which itself is a characterised binding partner for Myopalladin (Bang *et al.*, 2001). The siRNA knockdown of Palladin leads to loss of LASP-1 at actin stress fibres and redirection to focal adhesions without changing actin filaments (Rachlin and Otey, 2006). Thus it appears Palladin is necessary to recruit LASP-1 to actin stress fibres but not to focal adhesions.

The *LASP-1* gene is approximately 4.0kb long, transcribing the protein 261 amino acids long and 37kDa in molecular weight. The protein is ubiquitously expressed, playing a major role in the cytoskeleton architecture, cell migration and proliferation, as well as having a major function in embryogenesis (Grunewald and Butt, 2008). It also regulates the functions of podosomes in cells (Stölting *et al.*, 2012). LASP-1 in human cells is phosphorylated by cAMP- and cGMP dependent protein kinases (PKA and PKG) at serine 146 (Terasaki *et al.*, 2004). This renders the protein more cytosolic (Nakagawa *et al.*, 2006). It is also phosphorylated at tyrosine 171 by Abelson tyrosine kinase (Abl). Phosphorylation at tyrosine 171 is also associated with loss of LASP-1 from focal adhesions and furthermore with initiation of cell death, but without changes in the dynamics of migratory processes (Lin *et al.*, 2004).

LASP-1 is a haemodynamic responsive adaptor protein, given that it binds directly to actin and plays a role in cell-cell and cell-matrix adhesion. Together with Palladin, it localises in actin rich structures in the cell such as lamellipodia, suggesting that it plays an essential role in actin cytoskeleton organisation at leading edges of migrating cells

(Chew *et al.*, 2002; Lin *et al*., 2004). In non-motile cells, LASP-1 has been observed to localise to the peripheral edge of the cell. Subsequent exposure to migration-stimulating growth factors causes a rapid relocalisation to the focal adhesions, followed by a later localisation towards the membrane ruffles. Membrane ruffling is significantly increased in cells over-expressing LASP-1 which suggests an important role for LASP-1 in generating and/or regulating these structures.
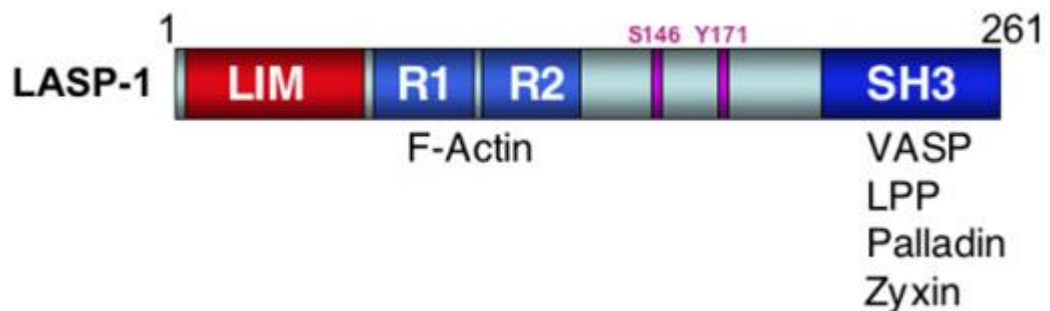
Figure 1.16: LASP-1. This schematic illustrates the domains of the LASP-1 protein. The binding sites of Palladin and other proteins are indicated at the appropriate domains. Palladin is observed binding at the SH3 domain. Domains marked R1 and R2 represent nebulin regions. It is at these sites where filamentous actin is seen to bind. Known phosphorylation sites at serine 146 (S146) and tyrosine 171(Y171) are marked with pink boxes (Grunewald and Butt, 2008).

LASP-1 has been observed to be upregulated in many cell cancers (Tang *et al.*, 2012), with over-expression correlating with tumour size and lymph node metastasis (Frietsch *et al.*, 2010; Grunewald *et al.*, 2007A). The knocking down of LASP-1 therefore resulted in a strong inhibition of proliferation and migration of cancer cell lines, also showing a reduction in the binding of zyxin – a LASP-1 binding partner – to focal contacts (Grunewald *et al.*, 2006; Grunewald *et al.*, 2007B). LASP-1-null mice have been generated, which displayed slightly lower body weights but developed normally and had no overt phenotypic abnormalities (Chew *et al.*, 2008).

To date, several research studies have been carried out to investigate its regulatory mechanisms. Results have been conflicting however. It was suggested that *LASP-1* gene transcription was controlled by the *p53* tumour suppressing gene, with *p53* inactivation inducing the overexpression of LASP-1 (Wang *et al.*, 2009). However, overexpression of LASP-1 was not observed to be associated with *p53* mutations in a breast cancer cell line (Frietsch *et al.*, 2010). The same paper also showed that an inverse correlation between LASP-1 and the tumour suppressor PDEF (Prostate-derived Ets transcription

factor) could not be demonstrated. But then in invasive breast cancer cells, PDEF did show an ability to repress LASP-1 expression (Turner *et al.*, 2008).

The depletion of LASP-1 by RNAi, or overexpression by transient transfection both appeared to disrupt the ability of cultured cells to migrate normally (Lin *et al.*, 2004). It would appear that the temporary and more permanent alterations (both overexpression and knockdown) of LASP-1 alternatively affect the protein expression levels, and that levels must be maintained to precise limits. The regulatory mechanisms appear to be still a matter of debate.

1.5.5 Drebrin

Another F-actin-binding protein of interest is the developmentally regulated brain protein, more commonly referred to as Drebrin (Grintsevich *et al.*, 2010). It has been suggested that it is a likely binding partner to Palladin, but has not been investigated in much detail (Li *et al.*, 2011), prompting the investigation of this protein here. Whilst mainly found in brain tissue, it has been documented to be found in a diverse range of other cell types e.g. renal glomeruli, keratinocytes and basal cell carcinomas (Peitsch *et al.*, 2003; Peitsch *et al.*, 1999). The protein appears in different isoforms – Drebrin A and Drebrin E1 and Drebrin E2, referring to adult and embryonic forms – which arise from alternative splicing of the *DBN1* Gene (Jin *et al.*, 2002). The *DBN1* gene is approximately 2.6kb long, transcribing a protein 649 amino acids long (Toda *et al.*, 1993). The molecular weight of the protein appears to be 70-72kDa, however due to its unusually slow SDS-PAGE mobility it appears at around 120kDa when protein is examined on a gel (Peitsch *et al.*, 2001).

All of the Drebrin isoforms similarly display a single actin depolymerisation factor domain at the N-terminal, followed by a non-conserved central region and a SH3 domain in the C-terminal (Keon *et al.*, 2013) (Figure 1.17). Changes in the non-conserved region result during development result in the different isoforms. The E1 isoform is thought to function in migration, and is replaced by the E2 form during embryogenesis, where is also functions in migration as well as development of axons and dendrites (Keon *et al.*, 2000). This E2 isoform is the only one observed in other cell types of a non-neuronal origin (Peitsch *et al.*, 2005).
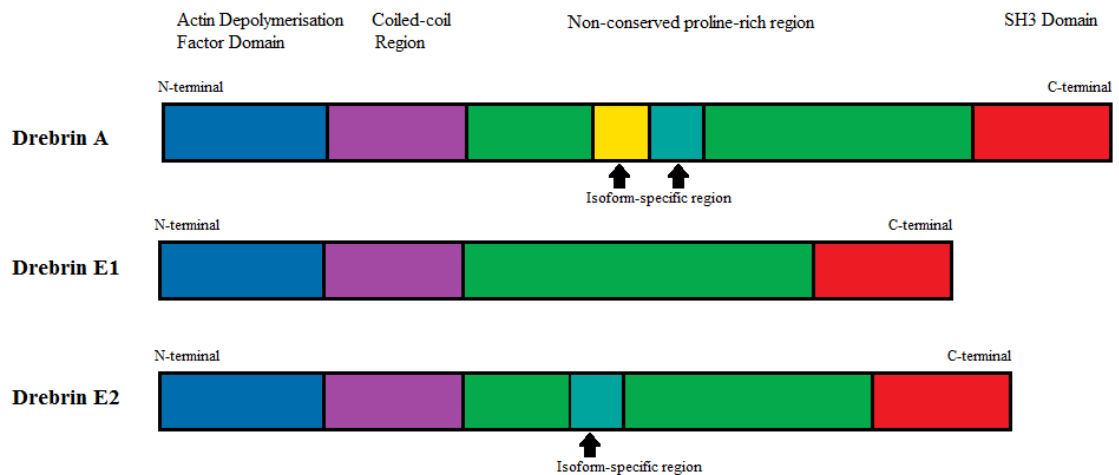
Figure 1.17: Drebrin isoforms. This schematic illustrates the structure of the Drebrin protein and its isoforms. Each isoform – the adult form and the two embryonic forms – all contain the same actin depolymerisation factor (ADF) domain at the N-terminal, and a SH3 domain at the C-terminal. The non-conserved proline-rich regions differ, with the adult isoform containing specific regions not observed in the embryonic forms. The E1 isoform differs from the E2 isoform in that it is truncated within the non-conserved region.

It has been found that Drebrin plays a role in cell-cell interactions and remodelling of the actin cytoskeleton (Butkevich *et al.*, 2004). As the protein binds to actin, it has been observed to induce helical changes in the actin structure (Sharma *et al.*, 2012). Drebrin is mostly observed bound with actin microfilament bundles associated with plaques of cell-cell contact sites representing adhering junctions (Majoul *et al.*, 2007), although this may be through its association with other actin bundling proteins. Drebrin itself has not been found to possess F-actin severing, bundling, capping or nucleating activities itself (Li *et al.*, 2011), suggesting that the protein may regulate actin stability by interacting with other actin associated proteins instead (Mikati *et al.*, 2013; Peitsch *et al.*, 2005). The Drebrin protein has been suggested to also play a role in regulation of cell adhesion due to the ability to recruit or modulate the activity of other actin regulating proteins, for example the F-actin bundling Eps8 protein (Li *et al.*, 2011). Drebrin has been shown to bind via proline domains with profilin, a protein which itself prominently binds to Palladin (Witke, 2004; Mammoto *et al.*, 1998) indicating a link between the proteins. The Drebrin protein is believed to be involved in induction of Podosomes – actin rich adhesion structures which contribute to matrix remodelling (Linder and Aepfelbacher, 2003). Palladin also localizes to podosomes (Goicoechea *et al.*, 2006), as does LASP-1 (Stölting *et al.*, 2012) reinforcing the idea of a link between the proteins, as well as indicating a potential site of interaction.

Notably, Drebrin can inhibit the actin-binding proteins tropomyosin and α-actinin, two proteins that co-localize together, but generally appear in cells more frequently than Drebrin (Mikata *et al*., 2013; Ishikawa *et al*., 1994). However, in experiments concerning the overexpression of Drebrin, it appeared to perform this function in different ways depending on the protein. Drebrin competes with tropomyosin to bind to actin, with overexpression observed to cause the dissociation of tropomyosin from actin filaments. With α-actinin, Drebrin appears to inhibit its actin-binding and actin cross-linking activities. The resulting inhibition leads to the actin filaments developing a thick and curved phenotype. Overexpression of Drebrin A or E2 isoforms has been observed to result in the co-localization of Drebrin with the actin filaments and the formation of dendritic-like cell processes (Shirao *et al.*, 1994; Terakawa *et al.*, 2013; Ishikawa *et al.*, 2007). The overexpression can lead to the change in cell phenotype, with neuronal-like protrusions with ruffled membranes developing (Majoul *et al.*, 2007). Investigations of Drebrin knockdown using human glioma cells showed the resulting effects to be much more modest (Terakawa *et al.*, 2013). This could likely be due to the depletion of Drebrin being compensated by other proteins, namely tropomyosin or α-actinin. However, some effects can still be observed.

Drebrin has been noted to be a major component associated with the actin filaments located at adherens junctions in regular endothelial cells (Peitsch *et al.*, 1999; Keon *et al.*, 2000). Recent studies on the knockdown of shRNA-based knockdown of Drebrin E2 in HUVEC cells which were subsequently subjected to shear stress showed potential impairments of cell-cell adhesion that did not appear in static cells (Rehm *et al.*, 2013). This critical weakening of cell-cell junctions is characterised by the reduced transendothelial electrical resistance, rupturing of cell-cell contacts, and the loss of nectin (cellular adhesion proteins) from the adherens junctions.

In a number of cells, a limited amount of Drebrin is observed to be present at the plasma membrane, but upon establishment of cell-cell contacts, the endogenous Drebrin is redistributed to the plasma membrane in an already pre-assembled form of Drebrin particles called "drebrosomes" that are transported along cytoskeletal elements (Peitsch *et al.*, 1999). These particles may in fact be analogous to endothelial microparticles.

1.6 MICROPARTICLES

The aforementioned perturbations of haemodynamic conditions (e.g. laminar shear stress) affect multiple endothelial functions, including cell apoptosis, permeability and remodelling. Brodsky *et al.,* (2004) detail a link between high shear stress and release of submicron particles, known as microparticles (MPs), derived from endothelial cells. In contrast, Boulanger *et al.,* (2007) demonstrate an inverse correlation between endothelial microparticle circulation and baseline shear stress values, suggestive of an increased release following apoptosis of endothelial cells triggered by low laminar stress. Microparticles are of particular interest as they are complex structures which possess a wide array of cell surface receptors, mRNA and proteins (Reich and Pisetsky, 2009), and are formed and released by various stimuli under numerous (patho-) physiological conditions.

The term "Microparticles" (MPs) is used to describe small vesicles of a varied size, from 100-1000nm. First documented in the late 1960s and thought to be "cell dust" (Wolf, 1967), microparticles are composed of small fragments of membrane released from the cell. Burnier *et al.,* (2009) discussed how published research has subsequently shown how they actually play an important role within the vasculature, due to possessing various membrane proteins and other intracellular components from their parent cell. For example, they are understood to play a role in cell-cell communication through the transfer of various components such as microRNA, mRNA and proteins (Mause *et al.,* 2010). Microparticles also promote coagulation via thrombin generation and exposure of negatively charged phospholipids on their membrane surface, and can directly affect endothelial cell function by stimulating cells to produce cell-specific cytokines, tissue factors, and cell-adhesion molecules such as PECAM-1, E-selectin or vitronectin (Keuren *et al.,* 2006; Diamant *et al.,* 2004). Microparticle function appears to be dependent on vesicle components, which itself is dependent on the cell type from which they originate (Muralidharan-Chari *et al.,* 2010).

Table 1.4: Diseases related to elevated microparticles of different origins. The table below summarizes the different cardiovascular diseases related to increase in microparticles.

	Endothelial MPS	*Platelet MPS*	*Erythrocyte MPS*
CVD related to increase of MPS	Hypertension, Atherosclerosis, Acute Coronary Syndrome, Acute Ischemic Stroke, Impaired angiogenesis,	Hypertension, Atherosclerosis Acute Coronary Syndrome, Stroke, Myocardial Infarction	Blood Clotting, Pulmonary Embolisms, Deep Vein Thrombosis
References	Burnier *et al.*, 2009; Mallat *et al.*, 2000; Williams *et al.*, 2007; VanWijk *et al.*, 2003	Burnier *et al.*, 2009; Preston *et al.*, 2003; VanWijk *et al.*, 2003	Gelderman and Simak, 2008

Many types of cells including platelets, endothelial cells, erythrocytes and leukocytes all produce microparticles, under normal physiological conditions (Reich and Pisetsky, 2009). Upon cellular activation, or indeed apoptosis, there is a change in the composition and number of microparticle sub-populations. While microparticle release in a physiological state is relatively low, elevated levels have been observed in the circulation of CVD patients (Mikirova *et al.*, 2011). These microparticles have been implicated in playing a role in inflammation and coagulation leading to impaired vascular function in diseases such as atherosclerosis, hypertension and diabetes (Tushuizen *et al.*, 2011).

1.6.1   Microparticle Formation

Microparticle formation and release has been observed in both the physiological state and the pathological state (Azevedo, 2012), but with aberrant levels observed in the unhealthy pathological state. This observation highlights the potential of MPs to serve as a molecular and cellular *'vexillum'* for certain diseases such as CVD, metabolic syndrome, kidney disease and diabetes. Two mechanisms elicit microparticle formation, namely apoptosis and cell activation. Both use different pathways in microparticle biogenesis. During apoptosis, the cell will contract and DNA fragment, followed by the subsequent observation of membrane blebbing (VanWijk *et al.*, 2003). However, these blebs are somewhat different than microparticles formed *via* cell activation, in both size and protein composition. It is thought that the actin-myosin cytoskeleton works in creating a contractile force which drives the formation of these membrane blebs (Croft *et al.*, 2005). As the contraction occurs, membrane-actin linkages are seen to weaken

focally, resulting in bleb formation as the membrane is forced through areas of weakness. A myosin counterforce retracts the blebs, and this process repeats in a cycle. Actin and myosin become concentrated at the base of the blebs, and they become lined with a thin border of membrane-associated actin. The cycle of contractile force and bleb formation continues until the cell enters a condensation stage, where it shrinks into small apoptotic bodies as dissolution of polymerised actin occurs (Croft *et al.*, 2005).

Shedding of microparticles is a process that can also occur independently of apoptosis (Sapet *et al.*, 2006). The term "cell activation" encompasses both physiological and pathological stimuli leading to microparticle release. For example, in platelets and endothelial cells, shear stress represents one such stimulus. Stimulation with cytokines or thrombin can also elicit release (Bucciarelli *et al.*, 2012) as can an increase in plasma homocysteine levels (Sekula *et al.*, 2011). Endothelial cells, monocytes and vascular smooth muscle cells have all been shown to release microparticles after activation by cytokines, bacterial lipopolysaccharide or reactive oxygen species (Azevedo, 2012).

Upon cell activation, the release of microparticles is both time- and calcium-dependent (VanWijk *et al.*, 2003), with shedding occurring within minutes of agonist stimulation. Cell activation, by various stimuli, results in the release of calcium from the endoplasmic reticulum stores in the cytosol, which in turn results in downstream activation of μ-calpain. μ-calpain is a calcium-dependent cytosolic protease which cleaves talin and α-actin, leading to decreased binding of integrins to the cytoskeleton and a reduction in cell adhesion and integrity. The inhibition of calpain has been shown to prevent the release of microparticles (Azevedo, 2012). Cytosolic calcium increase activates certain kinases and inhibits phosphatases. This, coupled with calpain activation, ensures the cleavage of the cytoskeleton, leading to disruption of the cell, facilitating microparticle release. Loss of adhesion between the membrane lipid bilayer culminates in further blebbing of the membrane, which can in turn leading to shedding of microparticles. In addition to calpain, other molecules are also thought to be involved in calcium-dependent microparticle release (Azevedo, 2012). In support of this, there are several mechanisms responsible for the disruption of the membrane. Phosphorylation of myosin light chains by myosin light-chain kinase (MLCK) stimulates the contractile activity of myosin, with myosin ATPase activation creating movement between actin and myosin filaments. It is thought that this movement may create tension in the plasma membrane which leads to bleb formation and microparticle release (Azevedo, 2012). The precise interaction between cell membrane and

cytoskeleton leading to microparticle formation however is still not fully characterised. In this regard, recent data implicates a role for the ROCK-II isoform in thrombin-induced microparticle release from endothelial cells (Sapet *et al.*, 2006).

1.6.2 Apoptotic Bodies and Exosomes

The formation of microparticles shares some similarity to that of apoptotic bodies and exosomes. Following apoptosis of the cells, small apoptotic bodies (also known as apo-bodies) can be formed as the cell shrinks and subsequently fragments. These bodies may contain various subcellular organelles and fragments of DNA. Some microparticles can also be released at this point as membrane blebbing occurs. The apoptotic bodies are much larger in size than microparticles (Table 1.5), are less regular in shape (VanDommelen *et al.*, 2012) and are released in the final stages of apoptosis, unlike microparticles which are released earlier by cells (Azevedo, 2012).

Table 1.5: Comparison of types of vesicle released from cells. The table below summarizes the different types of vesicles released from cells, and their individual characteristics.

Property	*Microparticles*	*Exosomes*	*Apoptotic Bodies*
Origin	Plasma Membrane	Intracellular Endocytotic-lysosomal system	Not determined
Size	100-1000nm	50-100nm	1000-4000nm
Appearance (via SEM)	Irregular	Cup-shaped	Irregular
Mechanism of Release	Shedding from plasma membrane	Exocytosis of MVB	Apoptosis
Markers	Tissue Factor, PS, Cell Surface Markers	LAMP1 CD63	Genomic DNA,PS, Histones
References	Ling *et al.*, 2011; Azevedo, 2012; Holtom *et al.*, 2012	Dignat-George and Boulanger 2011; Keller *et al.*, 2006; Holtom *et al.*, 2012	Ling *et al.*, 2011; VanDommelen *et al.*, 2012; Théry *et al.*, 2001

It has been postulated that the exosomes may play an important role in the regulation of cardiovascular function (Azevedo, 2012). Exosomes are smaller than microparticles (usually less than 100 nm) but they are much more homogenous in size than microparticles. Analyses have shown how all mammalian cell exosomes share common characteristics including size, density, structure, and protein composition (Keller *et al.*, 2006). These proteins include many cytoplasmic proteins such as actin, tubulin and annexins (Théry *et al.*, 2001). Exosomes also possess the ability to potentiate signalling

events that they originally promoted, by similar mechanisms to microparticles. Exosomes are believed to have a role in cell-cell communication, via directly stimulating cells by receptor-mediated interactions or by transferring varied molecules from cell to cell (Camussi *et al.,* 2010).

Exosome formation is quite distinct from that of microparticles – with their release from cells mainly orchestrated by the endocytotic-lysosomal system. Their biogenesis occurs when intracellular multi-vesicular bodies are exocytosed and fuse with the plasma membrane (Camussi *et al.*, 2010). The exosome displays major histocompatibility complex (MHC) Class I or II molecules on its surface, implicating a role in antigen presentation (Théry *et al.*, 2002; Clayton *et al.*, 2001). It is believed that through using exosome therapies, it is possible to prime the immune system to recognize certain tumour-specific antigens, and subsequently launch an appropriate immune response toward cancer cells without damaging neighbouring healthy cells (Tan *et al.*, 2010). Exosomes released from tumour cells have been shown to stimulate cells of the immune system in such a way, reducing tumour growth (Skog *et al.*, 2008), with evidence suggesting the exosomes show a function in transporting RNA, which could also be utilised as a biomarker and diagnostic tool (Cho *et al.*, 2009).

1.6.3 Endothelial Microparticles

Recent advances have been made with specific regard to endothelial microparticles. These submicron vesicles are released as a result of endothelial cell blebbing, with a higher release rate observed in dysfunctional endothelial cells. EMPs vary in size, phospholipid and protein composition (Horstman *et al.*, 2004). While they vary in these aspects, they exclusively display certain endothelial proteins e.g. vascular endothelial cadherin (VE-Cadherin) and E-selectin, which are unique antigenic signatures that differentiated them from other microparticles (Dignat-George and Boulanger, 2011). They represent a small but important subset of all microparticles (Martínez *et al.*, 2005; Mezentsev *et al.*, 2005) but are still found to be quite influential, playing a role in inflammation and various other endothelial functions.

1.6.3.1 Microparticles and Endothelial Physiology

Under physiological conditions, endothelial microparticles can have benefits, displaying cytoprotective effects on endothelial cells by reducing apoptosis, presumably acting as

an adaptavive response to various stimuli. Moreover, low concentrations of microparticles from human umbilical vein endothelial cells (HUVECs) have been shown to actually promote the formation of capillary-like structures (Mezentsev *et al.*, 2005; Burnier *et al.*, 2009).

Endothelial microparticles are implicated in angiogenesis whereas ones from certain cell lines are thought to facilitate the invasion of ECMs, and evasion of the immune response. The effect of microparticles on angiogenesis is widely debated, as it seems that some microparticles (e.g. platelet-derived) are pro-angiogenic, whereas others, such as endothelial-derived, have been reported as both pro- and anti-angiogenic (Burnier *et al.*, 2009; Martínez and Andriantsitohaina, 2011; Camussi *et al.,* 2010). One could hypothesise that these contrasting physiological effects may be due to various permutations and combinations of MP-cellular aggregates, such as platelet-MP.

The pro-angiogenic abilities of endothelial microparticles have been observed through the matrix metalloproteinase activity they contain. Endothelial cells produce these matrix metalloproteinases, and store them in secretory vesicles (Nguyen *et al.*, 1998). The endothelial cells release these vesicles which are then enhanced by angiogenic factors (Taraboletti *et al.*, 2002).

1.6.3.2 Microparticles and Endothelial Dysfunction

HUVECs decorated with high levels of microparticles *in vitro* showed an inhibitory effect on angiogenesis (Taraboletti *et al.*, 2002). Isolated microparticles in pathological concentrations have been observed to affect angiogenesis by uniform shortening of total capillary length and branching points (Mezentsev *et al.*, 2005) while also enhancing apoptosis (Distler *et al.*, 2011). It has been postulated that one of the mechanisms for this occurrence may be microparticle-mediated induction of oxidative stress in the treated cells.

Endothelial microparticles appear to play an important role in immune response, as well as having roles in intracellular signalling and cell adhesion events (Philippova *et al.*, 2011). They have potent pro-inflammatory effects, with deleterious consequences (Chironi *et al.*, 2009). These processes are all linked to pathogenesis of CVD, and because circulating microparticle numbers are altered in many forms of CVD, a role for microparticles in CVD initiation, progression and pathogenesis is therefore likely. Elevated levels of endothelial microparticles have been observed to correlate with the

loss of flow-mediated dilation and arterial stiffness (Viera *et al.*, 2012). They are also known to be elevated in acute coronary syndromes (Bernal-Mizrachi *et al.*, 2003; Mallat *et al.*, 2000) and in severe hypertension with end organ damage (Preston *et al.*, 2003) – conditions associated with endothelial injury and a pro-thrombotic state. It is suggested that they display an ability to also directly affect the endothelial cells of patients with myocardial infarction by hindering their nitric oxide pathway (Boulanger *et al.,* 2001).

The endothelium possesses the ability to release vasodilators such as prostacyclin, endothelium-derived hyperpolarizing factors and nitric oxide (NO) (Mostefai *et al.*, 2008). Changes in the ability to release these factors are fundamentally linked to development and progression of CVD. NO is fundamental for proper endothelial function, being required for the inhibition of adverse stimuli (e.g. ROS) (Dimmeler and Zeiher, 1999). When the vasculature is subjected to hypoxic conditions, cells are metabolically compromised which results in cellular dysfunction. Neutrophils adhere to the endothelial cell layer (mediated by adhesion glycoprotein surface complexes) and are then able to accelerate cell dysfunction through a wide range of cytotoxic mechanisms (Vince *et al.*, 2009). The neutrophils in turn mediate a variety of responses harmful to the other cells, one of them being ROS production.

Enhanced ROS production has also been seen very early in the atherogenic process, suggesting the link between ROS and apoptosis (Dimmeler and Zeiher, 2000). Microparticles stimulate ROS production in endothelial cells in an EGFR-dependent manner (Burger *et al.*, 2011) and endothelial-derived NO reacts with these elevated level of superoxides (O_2-), thereby reducing NO bio-availability (Rojas *et al.*, 2006). It has been reported that microparticles are also able to decrease the expression of NO, thus altering the balance between the production and release of the NO and ROS (Martin *et al.*, 2004) and contributing to increased endothelial dysfunction and potential synthesis of microparticles and apo-bodies.

A study by Holtom *et al.,* (2012) investigated the co-culture of plasma-derived microparticles with TNF-α treated HUVECs (which caused them to model endothelium inflammation) and observed that the inflammation leads to enhanced levels of ROS in cells, causing dysfunction. They further suggest that the inflammation of the endothelium caused the release of pro-inflammatory microparticles, which contribute to prolonged endothelial cell activation. The increasing ROS production levels lead to

elevated cellular oxidative stress, which impairs endothelial function and elicits development of vascular remodelling of disease.

Published data on microparticles point to a repetitive "feed-forward" sequence where the release and subsequent elevation of microparticle levels are a result of endothelial dysfunction, but also something which exacerbate and potentiate dysfunction (Brodsky *et al.*, 2004). It appears that when the number of circulating microparticles reaches a certain clinical threshold, that they become an important factor in the pathophysiology of disease, impacting the endothelium and other cells. These other cells can include monocytes, which endothelial microparticles bind to and activate. Doing so can enable the microparticles to migrate further through the endothelium (Horstman *et al.*, 2004).

1.6.3.3 Microparticles and Endothelial Normalisation/Repair

It is possible though that, under certain conditions, endothelial microparticles could contribute to the sorting of factors that prevent cell detachment and apoptosis (Dignat-George and Boulanger, 2011). There is growing evidence that perhaps endothelial microparticles may be released as part of a negative feedback mechanism to counter the cellular dysfunction associated with CVD, i.e. underpin a cellular adaptive response (Tushuizen *et al.*, 2011). The role of microparticles as a way of normalizing and repairing cells following insult is a matter of debate. These pro-survival properties of endothelial microparticles have also been documented in the literature. It has been suggested that endothelial microparticles might elicit normalisation of endothelial dysfunction via two mechanisms: either direct interaction with cells to promote normalization, or activation of endothelial progenitor cells to mediate endothelial cell repair (Hoyer *et al.*, 2010). It has been demonstrated that microparticle release could protect against apoptosis by diminishing cellular levels of caspase-3 via caspase "trapping" in the microparticles (Abid-Hussein *et al.,* 2007).

1.6.3.4 microRNA in Endothelial Microparticles

Diehl *et al.,* (2012) investigated miRNA content in endothelial microparticles and have shown that certain miRNAs are present (e.g. miRNA-451 and miRNA-486). miRNA-451 is known to inhibit the expression of macrophage migration factor, which is a pro-inflammatory cardiac depressant that can lead to impaired ventricular function (Bandres *et al.*, 2009). miRNA-486 meanwhile targets mRNAs that encode the phosphatase and

tensin homolog (*PTEN*) and Forkhead box protein O1A (*FOXO1A*) genes, which serve as negative components of the phosphoinositide-3-kinase (PI3-K) /Akt signalling pathway (Small *et al.*, 2010). PI3-K is an important regulator of integrin signalling, and prior to cell migration, increases integrin avidity (Trusolino *et al.*, 2000), whilst Akt is essential for the eNOS activation (Fleming *et al.*, 2005). By targeting *PTEN* and *FOXO1A*, miRNA-486 helps enhance the PI-3-K/Akt signalling pathway, leading to sustained cell survival.

1.6.4   Microparticles: Clinical Perspectives

Microparticle research is still in its early stages, but shows great promise and clinical relevance. There is much evidence that the levels, composition, and function of microparticles can be modified depending on the environment in which they are released, pointing to their potential usage in diagnostic, prognostic and therapeutic settings (Andriantsitohaina *et al.*, 2012).

1.6.4.1 Diagnostic / Prognostic Potential

Elevated levels of microparticles from platelets, monocytes, or endothelial cells are found to correlate with most cardiovascular risk factors (e.g. hypertension or obesity) putatively indicative of a poor clinical outcome (Dignat-George, 2008). As such, circulating microparticles isolated from blood show the potential to be utilised as biomarkers of overall vascular competence (Table 1.6). Quantifying and qualifying microparticle content of blood could also be utilised to detect early signs of CVD, even pre-clinical horizon, and as a method of monitoring response to treatments (Viera *et al.*, 2012). There are various methods to analyse microparticles, but as discussed in Chapter 1.6.4.3, they are not without issue.

Table 1.6: Microparticle source and antigenic signature used in their detection by Flow Cytometry. In this table, a list of specific characterisation markers for microparticles of various cellular origins is documented.

Microparticle origin	*Markers*	*References*
Endothelial	CD31 CD34 CD54 CD51 CD105 CD106 CD144	Burnier *et al.*, 2009; Bernal-Mizrachi *et al.*, 2003; Mallat *et al.*, 2000; Williams *et al.*, 2007; Taraboletti *et al.*, 2002; Gelderman and Simak, 2008
Platelet	CD41 CD41a CD42a CD42b CD61 CD62P	Burnier *et al.*, 2009; Preston *et al.*, 2003; VanWijk *et al.*, 2003
Erythrocyte	CD235a CD36	Burnier *et al.*, 2009; Gelderman and Simak, 2008; VanSchravendijk *et al.*, 1992

1.6.4.2 Therapeutic Potential

Using microparticles themselves as a treatment is a potential future application. A putative role for platelet microparticles in endothelial repair has been noted (Siljander, 2011). They have advantages over regular drug delivery methods in that they display a natural stability in blood and can deliver functional RNA to cells. Furthermore, patient-derived microparticles have been suggested as a method to potentially overcome the obstacle of immune rejection in the host (VanDommelen *et al.*, 2012).

In employing microparticles as therapeutic tools, it may be possible to engineer custom designed microparticles with modified properties (Martínez and Andriantsitohaina, 2011). They can be employed to induce over-expression of key proteins or molecular entities, e.g. miRNA, in cells. Moreover, transfection of microparticle-producing cells with certain proteins and delivering them to target cells (e.g., to replace/repair an already existing mutated protein) may represent a way of transferring information and altering cell function. They potentially could also be used to deliver miRNA/mRNA directly to cells to elicit therapeutic effects at the genomic level, i.e. to serve as a micro-cellular therapeutic.

Zernecke *et al.*, (2009) were able to observe miR-126 within apoptotic bodies. In theory, it could also be observed in regular microparticles or exosomes. This miRNA supports the proliferation, migration, tubule formation and sprouting of endothelial cells. When these apo-bodies were incubated with HUVECs, they observed transfer of the microRNA into recipient cells followed by production of the anti-inflammatory chemokine CXCL12 by the cells. miR-126 mediated CXCL12 abundance enhanced the CXCR4-mediated recruitment of progenitor cells, contributing to repairing of the vascular wall following injury.

1.6.4.3 Detection Methods and Issues

As mentioned previously, there are methods to detect microparticles in samples, albeit not without some issues. Simak and Gelderman (2006) list and discuss the various methodologies commonly employed in the laboratory setting to analyse and characterise microparticles in blood samples, ranging from antigen detection by flow cytometry to microplate affinity assays employing Annexin V to detect Phosphatidylserine. Nomura *et al.*, (2008) noted that an assay method using standard enzyme-linked immunosorbent assay (ELISA) protocols may also be a cost effective method in MP analysis.

Technical issues and sensitivity limitations still exist with diagnostic tests however in detecting smaller size microparticles and exosomes, such as distinguishing the different types of microparticles (Dignat-George and Boulanger, 2011; Mayr *et al.*, 2009). While ELISA-type immunoassays could measure the total amount of a microparticle-associated antigen, they lack an ability to provide single vesicle information. Annexin V assays also show a disadvantage in that they will only be able to detect the subset of microparticles with accessible Phosphatidylserine on their surface. There are a large amount of endothelial microparticles that do not bind annexin V, rendering such an assay uninformative. Furthermore, as annexin V is a natural plasma protein, endogenous levels are present on physiological levels of circulating microparticles, masking and attenuating aberrant PS detection (Philippova *et al.*, 2011; Gelderman and Simak, 2008).

Flow Cytometry is a more robust analysis method, being able to analyse large numbers of microparticles in a single sample, based on size, granularity and antigens displayed by the MPs. However the small particle size and dim signals still challenge the sensitivity threshold of many commercially available flow cytometers. Research is on-

going regarding the optimal way to separate the individual populations (Robert *et al.*, 2012), with Flow Cytometry analysis, pre-centrifugation (to separate based on size) or a combination of both being the current optimal methods. Nolte-'t Hoen *et al.*, (2011) have developed a fluorescence-based, high-resolution Flow Cytometric method for quantitative and qualitative analysis of nano-sized membrane vesicles such as microparticles and exosomes, highlighting the fact that technology is getting closer to a more definitive method of characterisation.

Following the subjection of the cell to haemodynamic forces (in particular, laminar shear stress), the level of Palladin protein in the cell was noted to increase, but then decrease over time (Chapter 3). It was thought that the protein may be released from the cells via the endothelial microparticles. It was hypothesised that upon investigating the amount of protein in microparticles, there would be increases in the amounts of protein observed at the different time points.
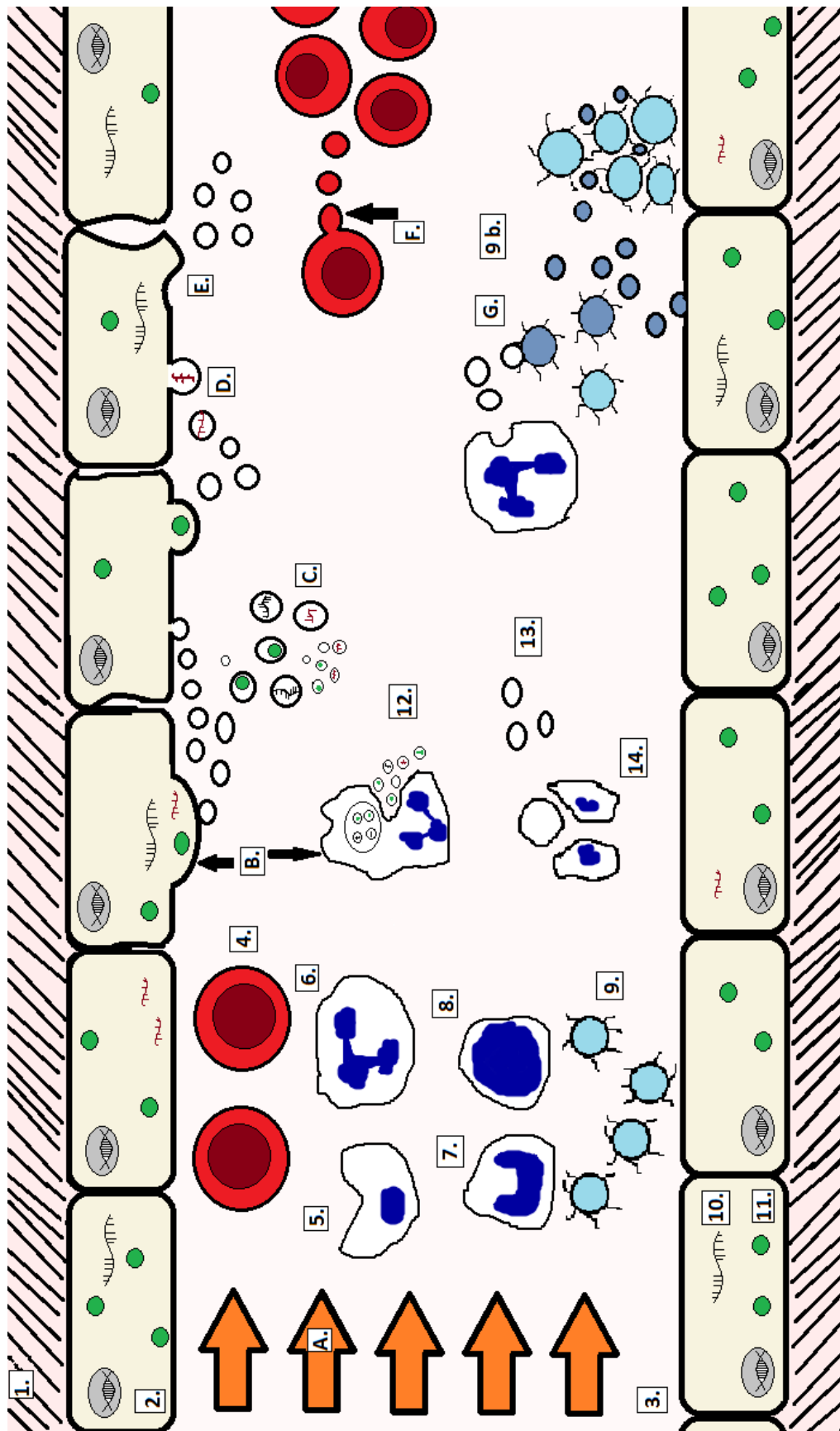
Figure 1.18: Microparticles in the Vasculature. This figure displays the presence of microparticles, exosomes and apoptotic bodies, and demonstrates their formation, and how they influence other cell types. Key:

1) Tunica Media - Layer of Smooth Muscle Cells in the vessel.
2) Tunica Intima - Monolayer of Endothelial Cells.
3) Lumen – Contains the blood, which is composed of plasma and various blood cells
4) Red Blood Cells.
5) Macrophage.
6) Neutrophil.
7) Monocyte.
8) Lymphocyte.
9) Platelets.
    9b) Activated Platelets.
10) RNA inside the cell.
11) Protein inside the cell.
12) Exosome release from cells (Via exocytosis of Multi-vesicular bodies in the cell).
13) Microparticles released from cells.
14) Apoptotic Bodies.

Different processes occur in the release of Microparticles:

A) Shear stress – Flow of blood across the cells. Increased flow stimulates microparticle release.
B) Membrane Blebbing.
C) Microparticles and Exosomes contain Protein, RNA, miRNA.
D) Microparticles are able to affect cells downstream, transporting molecules from one cell to another. These activate the cell, resulting in release of calcium from the endoplasmic reticulum, which results in downstream activation of calpain μ. Calpain cleaves talin and α-actin, leading to decreased binding of integrins to the cytoskeleton and a reduction in cell adhesion.
E) The cytoskeleton starts de-stabilising, causing increased release of microparticles.
F) Red blood cell microparticles facilitate formation of enzyme complexes which cause other red blood cells to coagulate together.
G) Microparticles released from Neutrophils can activate platelets, which stimulates the release of platelet microparticles. This in turn causes the coagulation of platelets.

1.7 AIMS AND OBJECTIVES

The work presented here in this thesis investigates the expression of the Palladin protein, and the PALLD gene which encodes it, within Human Aortic Endothelial Cells. The protein has been observed in endothelial cells, however it has not been characterised fully within this cell type. Experiments were performed to characterise the genetic and proteomic expression in response to the haemodynamic forces expressed within the vasculature, namely laminar shear stress and cyclic strain. Since the Palladin protein is known to be an actin-binding protein, it was hypothesised that Palladin expression alters as the cell shape changes in response to haemodynamic stimuli.

As stated, Palladin may also interact with the ECM within the vasculature, having been seen to play a role in stabilising integrins and linking them to the cytoskeleton (Luo *et al.*, 2005; Lai *et al.*, 2006). Integrins are highly influenced by haemodynamic stimuli such as laminar shear stress, which converts the integrins to a high affinity state, allowing them to bind to the subendothelial extracellular matrix (Orr *et al.*, 2005). This binding is specific depending on integrin and matrix, and is important for cellular development, maintenance and repair (Harburger and Calderwood, 2009). Certain ECMs have been shown to interfere with integrin signalling under shear stress (Orr *et al.*, 2006). Based on this understanding, the effects of ECMs on the shear induced expression of Palladin within the endothelial cell were investigated.

Upon extracting the Palladin protein from HAECs and analysing it through mass spectrometric methods to further characterise its protein complex, the link between Palladin and two other actin-binding proteins – LASP-1 and Drebrin – was highlighted. The response of these proteins to haemodynamic forces (namely laminar shear stress) was then investigated, as was the expression of these proteins when the cells are cultured on ECMs. By doing so, a comparative profile of each protein could be observed and compared against the others. Through comparing the patterns of expression of each protein under these conditions, it was hoped that an understanding could be formed with regards to how Palladin, LASP-1 and Drebrin interact in the same network with one another in the vasculature.

The expression of these proteins was also investigated within the release of endothelial microparticles. Following the haemodynamic stimuli of the cells (especially with laminar shear stress), an increase in presence of EMPs is observed. It was hypothesised that the changes in protein expression at later time points (i.e. where the protein expression level decreases a few hours after an initial increase) could be explained by the release of excess protein via the microparticles. The particles released from cells cultured on the ECMs were also similarly probed. Since the protein levels can be affected by culturing of the cells on matrices, investigative experiments were performed to observe if the matrices affected the release of proteins of interest from the cells also.

Following these experiments where the particles were probed for the proteins of interest, it was investigated if these particles may also have an effect on expression levels of protein in other cells. Since microparticles can be used to signal other cells downstream, initial experiments were performed incubating regular HAECs with

conditioned cell media containing increased volumes of EMPs. Initial experiments also to observe the release of Palladin via EMPs taken from human blood samples post-exercise were performed, in order to characterise the protein release in an *in vivo* setting as opposed to the *in vitro* nature of the other experiments.

Finally, experiments to observe the cell migratory patterns of cells where Palladin had been knocked down were carried out. They were performed to determine the functions of Palladin in cell migration and adhesion. In doing so, a more definitive and complete characterisation of the Palladin protein within the vasculature could be presented with the work described here.

CHAPTER TWO

MATERIALS AND METHODS

2.1 MATERIALS

2.1.1 Reagents and Chemicals

Table 2.1 below lists the reagents and chemicals used, alongside the company where each item was sourced:

Table 2.1: Reagents and Chemicals used in experiments.

Applied Biosystems, CA,USA	High Capacity cDNA Reverse Transcription Kit, Scrambled control siRNA.
ATCC-LGC Standards, Middlesex,UK	HEK-293 Human Embryonic Kidney cells.
Bio-Rad, Hercules,CA,USA	10X Tris/Glycine/SDS Running buffer, Laemmli sample buffer, TEMED.
Cell Applications, CA,USA	Rat Aortic Smooth Muscle Cells (RAOSMCs).
Dako, CA,USA	Fluorescent mounting media, Polyclonal Rabbit Anti-human VonWillebrand Factor (vWF) antibody.
Eppendorf, Cambridge,UK	50X TAE Buffer.
Eurofins MWG Operon, Ebersberg,Germany	Gene Specific Primers – *PALLD*, *18S*, *LASP-1*, Drebrin – *DBN1*.
Fermentas, York,UK	Green dream Taq 10x Buffer, Taq polymerase, Precision Plus® Protein Ladder.
GE-Healthcare, Buckinghamshire,UK	Goat monoclonal to Mouse IgG (HRP-conjugated) secondary antibody.
Invitrogen, CA,USA	AlexaFluor-488 goat anti-Mouse secondary antibody, AlexaFluor-488 goat anti-Rabbit secondary antibody, DH5α E-coli competent cells, GIBCO™ Distilled Water, Phosphate buffered saline (PBS), Rhodamine Phalloidin, RNase free distilled water, SYBR® Safe Solution, Trizol® Reagent.
Lennox Laboratory Supplies LTD, Dublin,Ireland	100% Ethanol, 100% Industrial Methylated Spirits (IMS).
Merck Bioscience, CA,USA	ProteoExtract® S-PEK Antibody Control Kit, ProteoExtract ® S-PEK subcellular proteome kit.
Millipore,	FlowCellect™ MitoLive Kit,

MA,USA	Goat derived, Anti-Rabbit IgG (HRP-conjugated) secondary antibody, Mouse monoclonal anti-LASP-1 primary antibody, Rabbit polyclonal Anti-Drebrin A/E isoforms primary antibody, Rabbit Polyclonal Anti-GAPDH primary antibody.
Pierce Biotechnology, *IL,USA*	BCA assay kit, Co-immunoprecipitation kit, Restore stripping buffer, Supersignal West Pico chemiluminescent substrate.
Promocell, *Heidelberg, Germany*	Cryo-SFM serum free medium for cryopreservation, Endothelial Cell Growth Medium MV, Endothelial Cell Growth Medium MV Supplement Mix: (Fetal Calf Serum (FCS) 5.0% (v/v), Endothelial Cell Growth Supplement (ECGS) 0.4% (v/v), Endothelial Growth Factor (EGF) 10ng/ml, Hydrocortisone 1μg/ml, Heparin 90 μg/ml) Human Aortic Endothelial Cells (HAECs), Human Aortic Smooth Muscle Cells, Human Aortic Smooth Muscle Cell Growth Medium.
Proteintech Group, Inc., *Chicago,IL*	Rabbit Anti-Human PALLD (Palladin) Polyclonal antibody.
Qiagen, *West Sussex,UK*	HiSpeed Plasmid Midi-prep kit.
Roche Diagnostics, *Basal,Switzerland*	FastStart Universal SYBR Green Master (Rox), Protease inhibitor cocktail.
Sigma Chemical Company Ltd, *Dorset,UK*	Acetic Acid, Acetone, Agarose, Ammonium Persulfate, Ampicillin, Bovine serum albumin, Collagen, Chloroform, DAPI Nuclear Stain, DMSO, Dulbecco's Modified Eagle Medium, Fetal bovine serum, Fibrinogen, Fibronectin,

	Goat Serum,
	Hydrochloric acid,
	Isopropanol,
	Kanamycin sulphate,
	Palladin specific siRNA (SASI_Hs01_00197888)
	Paraformaldehyde (1X solution),
	Penicillin/Streptomycin (100X),
	0.1% (w/v) Ponceau S solution,
	RPMI-1640 media,
	Sodium Acetate,
	Sodium Chloride,
	Sodium Deoxycholate,
	Sodium Orthovanadate,
	Tris-HCl pH 7.4,
	Triton X-100,
	Trypsin-EDTA (10X),
	Tween®-20.
Thermo Fisher Scientific, Leicestershire,UK	Methanol, 10X PBS solution, pH 4.0 Buffer solution (Phthalate), pH 7.0 Buffer solution (Phosphate), pH 10.0 Buffer solution (Borate).

2.1.2 Instrumentation

Table 2.2 lists the instrumentation used, and the company where each item was sourced:

Table 2.2: List of instrumentation used in experiments.

Applied Biosystems, CA,USA	Applied Biosystems 7900HT Fast Real-Time PCR machine with sequence detection software (SDS).
Bennett Scientific Ltd., Devon,UK	Clifton Duo ® Water Bath.
Bio-Rad, Hercules,CA,USA	MJ-Mini gradient thermocycler, Mini-PROTEAN Tetra Cell System (4-gel system includes electrode assembly, Electrophoresis PowerPak®, companion running module, tank, lid with power cables, mini cell buffer dam, Transfer module)
BioTEK, VT,USA	Microplate Reader.
Eppendorf, Cambridge,UK	Centrifuge 5430R, Centrifuge 5810R.

Flexcell International Corp, *NC,USA*	Flexercell® tension plus™ FX-4000T System.
Labtech, *East Sussex,UK*	Nikon® Eclipse TS100 phase-contrast microscope.
Mason Tech, *Dublin,Ireland*	Nanodrop 1000™ System.
Medical Supply Company, *Dublin,Ireland*	Horizontal Agarose Gel Electrophoresis rig.
Millipore, *MA,USA*	Guava EasyCyte FACS System.
Stuart Scientific Ltd, *Staffordshire,UK*	Block Heater, Orbital Shakers, Rotator, See-Saw Rocker, Vortex.
Syngene, *Cambridge,UK*	G-Box fluorescence and chemi-luminescence gel documentation and analysis system.
Taylor-Wharton, *USA*	Liquid nitrogen cryo-freezer unit.
Thermo Fisher Scientific, *Leicestershire,UK*	Holten LaminAir laminar flow cabinet.
VWR International Ltd. *West Sussex,UK*	Haemocytometer, Nalgene ® Freezing Container for cryotubes.

2.1.3   Consumables/Plasticware

The companies listed in Table 2.3 provided the consumables and plasticware used for experiments:

Table 2.3: List of consumables and plasticware used in experiments.

Applied Biosystems, *CA,USA*	96-well Optical Plates for qRT-PCR, Adhesive covers for 96-well Optical Plates, Adhesive cover application tool.
Becton Dickinson, *NJ,USA*	BD Vacutainer™ Blood Tubes (Buffered sodium citrate (0.105 M)
Bio-Rad, *Hercules, CA,USA*	Thick mini trans-blot filter paper, 10X Tris/Glycine/SDS Running buffer.
Bioo Scientific, *Austin, TX,USA*	Exomir™ Kit, Duo-Syringe Filter Assembly.
Dunn Labortechnik GmBH, *Asbach,Germany*	(Pronectin coated) 6-well Bioflex plates.
GE-Healthcare, *Buckinghamshire,UK*	Whatman® Filter Paper.

Invitrogen, *CA,USA*	MP-100 Microporator, Neon® Transfection System (Microporator tubes, Solution E buffer, solution R buffer, 10μl and 100μl gold tips).
Medical Supply Company *Dublin,Ireland*	0.2 ml PCR tubes, 0.5 ml polypropylene tubes.
Pall Life Science, *NY,USA*	Acrodisc 32 mm syringe filter with 0.2 μm super membrane, Nitrocellulose transfer membrane.
Sarstedt AG & Co. *Numbrecht,Germany*	6-well Cell+ Tissue Culture dishes, 100mm Cell+ Tissue Culture Dishes, Cell Scrapers, Cryotubes, Individually Wrapped and plugged Sterile Serological Pipettes – 2ml, 10ml and 25ml size, Individually wrapped sterile aspiration pipettes – 2ml size, Polypropylene Reagent & Centrifuge Tubes (15ml), Polypropylene Reagent & Centrifuge Tubes (50ml),
VWR International Ltd. *West Sussex,UK*	Cover slips, Glass slides.

2.1.4   Preparation of Stock Solutions and Buffers

2.1.4.1 Immunoblotting

Transfer Buffer (1X)

Tris-HCl	25mM
Glycine	192mM
Methanol	20%

RIPA Cell Lysis Buffer Stock (1.28X)

HEPES, pH7.5	64mM
NaCl	192mM
Triton X-100	1.28% (v/v)
Sodium Deoxycholate	0.64% (v/v)
SDS	0.128% (w/v)
dH$_2$O to final volume	500ml

RIPA Cell Lysis Buffer (1X)

1.28X RIPA Stock	1X
Sodium Fluoride	10mM
EDTA, pH8.0	5mM
Sodium Phosphate	10mM
Sodium Orthovanadate	1mM
Protease Inhibitors	1X

Sample Solubilisation Buffer (4X)

Tris-HCl, pH6.8	250mM
SDS	8% (w/v)
Glycerol	40% (v/v)
β-Mercaptoethanol	4% (v/v)
Bromophenol Blue	0.008% (w/v)

TBS wash Buffer

Tris-HCl, pH7.4	50mM
NaCl	150mM

Coomassie Stain

Coomassie Brilliant Blue R250	0.2%
Methanol	45%
Glacial Acetic acid	10%
dH$_2$O	44.8%

Coomassie stain filtered using a 0.25μm filter.

Coomassie Destain Solution

Methanol	20%
Glacial Acetic acid	10%
dH$_2$O	70%

2.1.4.2 Molecular Biology Buffers and Medium

SOC Media

Tryptone	2% (w/v)
Yeast Extract	0.5% (w/v)
NaCl	10mM
KCl	2.5mM
$MgCl_2$	10mM
$MgSO_4$	10mM
Glucose	20mM

Lysogeny Broth (LB) Media

Tryptone	1% (w/v)
Yeast Extract	0.5% (w/v)
NaCl	171mM

Lysogeny Broth (LB) Agar (1L)

Agar	15g

Made up to 1L with LB media

Antibiotics

Ampicillin	100 μg/μl
Kanamycin	50 μg/μl

Antibiotics are dissolved with dH_2O and sterilised using a 0.25μm filter. Aliquots may be stored at -20°C, but kept wrapped in tinfoil to avoid degradation through exposure to natural light.

TE Buffer

Tris	10mM
EDTA (pH8.0)	1mM

DNA Loading Buffer

Sucrose	40% (w/v)
Bromophenol Blue	0.25% (w/v)

2.2 METHODS

2.2.1 Cell Culture Techniques

In the culturing of cell types, each technique was undertaken in a sterile environment using a Holten LaminAir laminar flow cabinet. All cell types were grown in a 37°C humidified atmosphere containing 5% CO^2. Any containers entering incubators or laminar cabinet was sprayed with 70% Industrial Methylated Spirits (IMS) to prevent contaminants. Items such as pipette tips or micro-centrifuge tubes were first autoclaved and cooled to 17-20°C prior to use.

2.2.1.1 Human Aortic Endothelial Cell (HAEC) Culture

Human Aortic Endothelial Cells are a strongly adherent cell line that forms a confluent contact inhibited monolayer with distinct cobblestone morphology. HAECs (Promocell) were derived from the thoracic aorta of a fifty-nine-year-old human male post-mortem. The isolated endothelial cells were maintained in Endothelial Cell Growth Medium MV supplemented with a separate SupplementMix® of various growth factors. When added to the medium, the final concentrations are 5% (v/v) FCS, 0.004% (v/v) ECGS, 10ng/ml of EGF, 90μg/ml of Heparin, and 1μg/ml of Hydrocortisone. These hormones and chemicals help in regulating angiogenesis and cell growth. The Penicillin/Streptomycin mixed antibiotic was also added to give a final concentration of 100 U/ml penicillin and 100μg/ml streptomycin. These HAECs were cultured in 100mm x 20mm culture dishes along with 35mm 6-well plates. Cells involved in cyclic strain experiments were grown in Bioflex® series 6-well culture plates (Dunn Labortechnik GmBH) with a flexible, pronectin bonded growth surface. For immunofluorescence analysis involving sheared HAECs, cells were seeded onto sterilised glass cover slips in 6-well plates. HAECs between passages 5-10 were used for experimental purposes.

2.2.1.2 Trypsinisation of Adherent Cell Lines

For sub-culturing of cells, trypsinisation of adherent cells was required. Adherent cells were passaged in a cell culture dish at 70-90% confluence. For trypsinisation, the PBS, 1X trypsin and cell culture medium was pre-warmed to 37°C in the water bath. Using a sterile aspiration pipette, growth media was removed from the confluent monolayer and cells were washed with 4mls PBS. The cell culture dish was gently swirled for 30 seconds in order to neutralize trypsin inhibitors present in serum. This PBS was

aspirated afterwards in the same way, following which 1ml of 1X trypsin/EDTA solution in PBS was added to the cells. The cells were left for no more than 5 minutes, with regular observation of the cells state of detachment on the microscope. At the point at which roughly 50% of the cells are loosened, the culture dish was gently tapped on the side in order to detach the cells from the growth surface. When cells were observed to be detached completely, 8mls of full media was added to the cells to neutralise the trypsinisation. The cell suspension was carefully mixed by carefully pipetting up and down. This 9mls of suspended cells was split among 3 new sterile culture dishes. Each dish had a fresh 5mls of full media also added to them. At 70-90% confluence, a full dish contains $1.5\text{-}2.0\text{x}10^6$ cells, meaning that the plates with new passages will start off with roughly $5 - 6\text{x}10^5$ cells. Media is changed early the day after splitting and cells are then fed every second day with 6mls of pre-warmed fresh media.

2.2.1.3 Cryogenic Preservation and Recovery of Cells

For long term storage, cells were maintained in a liquid nitrogen cryo-freezer unit (Taylor-Wharton, USA). Following trypsinisation, cells were centrifuged at 700 rpm for 5 minutes at 17-20°C. The supernatant was aspirated, and the pellet was re-suspended in 5mls Cryo-SFM. 1.6ml aliquots of this were transferred to sterile cryotubes and frozen in a -80°C freezer, at the rate of -1°C/ minute using a Nalgene Mr Frosty® cryo-freezing container. Following overnight freezing at -80°C, the cryotubes were transferred to the cryo-freezer unit. For cell recovery, Cryotubes were rapidly thawed in a 37°C water bath. Following this, they were resuspended in pre-warmed PBS and centrifuged at 700rpm for 5 minutes to separate the cells from the DMSO. Once this was done, the cell pellet was resuspended in 3mls of media and added to a culture dish with 5mls of fresh media. Early the next day, the medium was removed, washed with pre-warmed PBS to remove DMSO, and 6mls of fresh growth medium was added.

2.2.1.4 Cell Counting

For healthy cell growth during certain experimental procedures cells needed to be seeded at precise numbers and densities. In order to do this, cell counts were performed using a Neubauer chamber haemocytometer.

2.2.1.4.1 Cell Counting using a Haemocytometer

For this method, cells were trypsinised and re-suspended in cell media as per protocol. The Haemocytometer is cleaned with IMS and left air-dry inside the laminar hood. A sterile cover slip is placed over the top of the chamber. The cell suspension is gently mixed to achieve a homogenous concentration. 20μl of this suspension is pipetted into the groove in the haemocytometer, where surface tension spreads this over the haemocytometer's marked grid for counting (Figure 2.1). Using the 10X objective lens, the numbers of cells in the four outer squares were counted. The average count per square, when multiplied by $1x10^4$, determines the cells per ml. This number is multiplied to adjust for dilution factor, and also by the total volume of the cell suspension i.e. x9 if the total volume is 9mls.
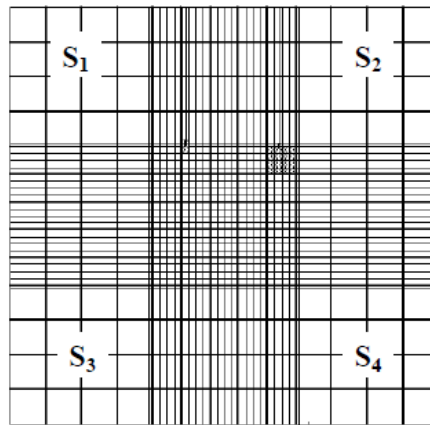
Figure 2.1: Haemocytometer. The Haemocytometer grid has four corner squares (S1-S4), each containing 16 smaller squares arranged in a 4X4 pattern. Using a 10X objective lens, the cells in each corner square were counted. For cells touching the border lines, only the ones on the right and upper lines were counted, and ones on the left on the bottom lines were disregarded.

2.2.2 Physiological Assays
2.2.2.1 Cyclic Strain

For cyclic strain assays, HAECs were seeded onto six-well pronectin-coated BioFlex Plates at a density of $5x10^5$ cells per well. The silicon membrane of the plates allows for a controlled physiological strain of the cells using a microprocessor controlled vacuum (Banes *et al.*, 1985). 24 hours post seeding, cells were subjected to cyclic strain using a Flexercell® Tension Plus™ FX-400T™ System (10% strain; 60 cycles/min) for a series of time points (0-48 hours). Following time points of strain, cells were harvested for either Western Blotting, or for mRNA extraction and qRT-PCR analysis. Media was also retained and stored at -20°C for endothelial microparticle analysis.

(A) **(B)**
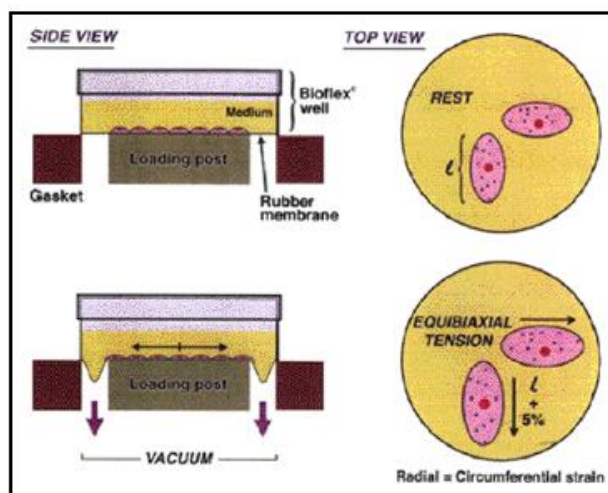
Figure 2.2: The Flexercell® Tension Plus™ FX-4000T System. Figure 2.2 (A) shows the setup of the Flexercell system, designed for cyclic strain of cells. Figure 2.2 (B) demonstrates how the vacuum of the docking setup applies strain on the cells, in an equibiaxial manner, stretching the pronectin coated membrane over the loading posts.

2.2.2.2 Non-Pulsatile Laminar Shear Stress

For laminar shear stress studies, HAECs were seeded into a 6-well cell culture plate at a density of 2×10^5 and allowed to reach full confluency. Prior to shearing, the medium was replaced with 4mls of fresh medium. The cells were sheared at 10 dynes/cm^2 for a series of time points (0-48 hours) on an orbital shaker (Stuart Scientific mini orbital shaker OS) set to a speed of 230rpm. The speed was determined using the following equation (Hendrickson *et al.*, 1999):

$$Shear\ Stress = \alpha\sqrt{\rho n(2\pi f)^3}$$

Where
α = radius of rotation in cm
p = density of liquid in g/l
n = liquid viscosity 7.5×10^{-3} dynes/cm^2 @ 37°C
f = rotation per second

As a control, plates containing static endothelial cells were maintained. They were cultured in the same incubator, but on a different shelf to avoid vibrational interference from the orbital rotator. Following shearing experiments, the cells were harvested for either (i) protein (ii) mRNA (iii) Immunoprecipitation of protein for Mass Spectrometric

analysis; or (iv) fixing *in situ* for immunofluorescence staining. Media was also retained and stored at -20°C for future endothelial microparticle analysis experiments.

2.2.2.2.1 Laminar Shear Stress of Cells Seeded on an Extracellular Matrix

For experiments where the effects of ECMs on protein and gene expression were investigated, 6-well plates were pre-prepared. Under sterile conditions, each well of a 6-well plate was fully covered with 1ml of PBS containing either: 10μg/ml fibrinogen (at a pH of 8.0), 10μg/ml fibronectin or 20μg/ml collagen, depending on which matrix was being investigated. The plate was then incubated overnight at 4°C. The next day, PBS was aspirated and cells were seeded, later being subjected to laminar shear stress as described previously.

2.2.2.3 Endothelial Microparticle (EMP) Analysis of Media Samples

In this study, EMPs were isolated and their content was analysed to investigate the presence of Palladin or other proteins. Confluent endothelial cells were subjected to laminar shear stress or cyclic strain, and equal amounts of culture medium were collected into 15ml conical centrifuge tubes. This tube was centrifuged at 2250rpm for 15 minutes at 4°C in order to remove cells and cell debris. Supernatant was collected and aliquoted into micro-centrifuge tubes (1ml per tube). Following the extraction methods of Vion *et al.,* these micro-centrifuge tubes were spun at 14000rpm for 30 minutes at 4°C (Vion *et al.,* 2013). The media was aspirated, leaving the EMP pellet. The microparticle pellets were pooled together in a total of 1ml of 1X PBS. The single micro-centrifuge tube was centrifuged at 14000rpm for 30 minutes at 4°C. The PBS was aspirated, and the pellet re-suspended in 20μl fresh 1X PBS. The samples were stored at -80C. Else they were prepared for Western Blotting (Chapter 2.2.5.1) or FACS analysis (Chapter 2.2.3).

2.2.2.4 Endothelial Microparticle (EMP) Analysis of Blood Samples

For samples taken from an *in vivo* model (i.e. blood samples), the blood was drawn from participants using a 19C needle into 5ml BD Vacutainer ® tubes containing 1x PBS/ Sodium Citrate (to help stabilise the blood and prevent clotting). Ethics approval was granted for this study from the DCU research ethics committee (DCUREC/2008/64 and DCUREC/2009/172). Blood was drawn from patients at 2 time

points: Post-Exercise, and 1 hour Post-Exercise – designated a relaxed state. This exercise was quantified using the Borg Scale of Perceived Exertion. The scale assays how the patient perceives the difficulty of activities. The scale starts at 6, characterised by "no feeling of exertion" i.e. when the patient is at a resting rate. Moderate activities such as a brisk walk ("fairly light" to "somewhat hard") register 11 to 14 on the scale. Vigorous activities, i.e. running on the treadmill up to the highest level of sustainable activity, rate from 15 to 20 on the scale ("hard" to "extremely hard"). Multiplying the score by 10 gives an approximate heart rate (Borg, 1982). The patients exercise consisted of roughly 30 minutes of running on a treadmill, achieving a score from 15-20 within the last 10 minutes of running. This raises heart rate in the patient, which elevates the increase of blood flow; leading to an increase in microparticle release.

Once blood was withdrawn, each Vacutainer tube was centrifuged at 2250rpm for 15 minutes. The plasma layer – 2.5mls - was removed and filtered through an Exomir Kit dual-filter of 0.22μm and 0.02μm (Bioo Scientific) to trap the microparticles and exosomes in separate filters. The filters were separated, with each filter being flushed through with 1ml RIPA buffer. The buffer obtained was flushed through the respective filter again another 2 times, before being collected into separate micro-centrifuge tubes (Figure 2.3). Both tubes were centrifuged at 14000rpm for 30 minutes at 4°C. The supernatant was then gently aspirated, with care made not to aspirate the EMP pellet. The pellet was re-suspended in 20μl fresh 1X PBS and stored at -80°C.
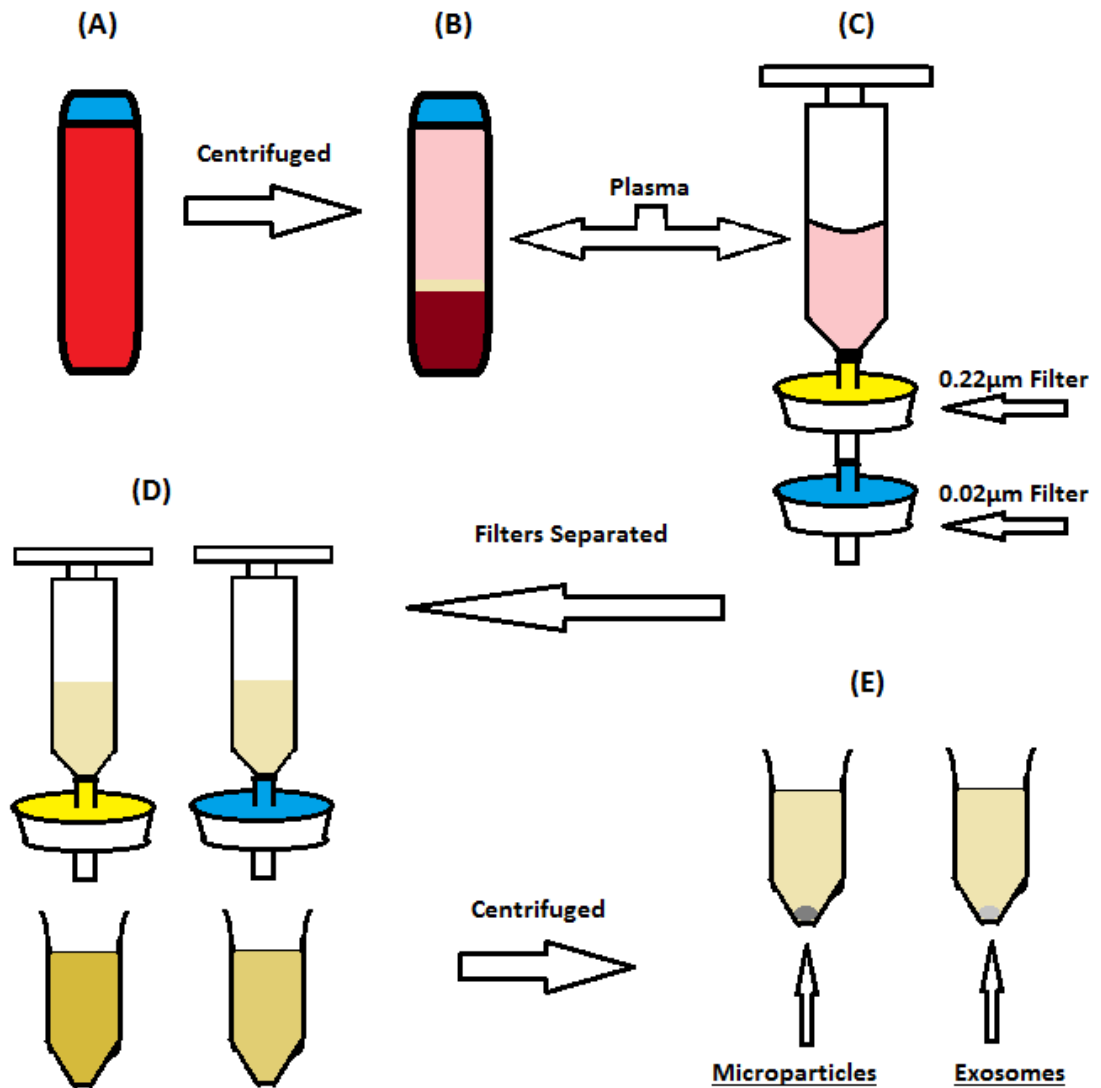
Figure 2.3: Extractions of Microparticles and Exosomes from Blood. Blood was withdrawn from patients and collected in Vacutainer tubes (A). These tubes were centrifuged in order to separate the plasma from the red blood cells and white blood cell/platelet layer (B). Plasma was removed and syringed through the Exomir dual filter assembly, with microparticles being retained in the 0.22μm upper filter, and exosomes retained in the lower 0.02μm lower filter (C). These filters were separated, with each one being flushed through using sterile syringes and 1ml RIPA buffer each (D). The RIPA was re-added and flushed through the respective filters a second and third time to ensure complete extraction of particles from the filters. The resulting samples of RIPA buffer containing either microparticles or exosomes was centrifuged to collect the particles (E). Supernatant was aspirated (after taking an aliquot for analysis) and the pellet was re-suspended in PBS before being stored at -80°C until use.

2.2.3 Molecular Biology Techniques

2.2.3.1 Reconstitution of Plasmid cDNA

A DNA based plasmid for Palladin-GFP (gifted to the laboratory by Professor Carol Otey, University of North Carolina) was presented which was afterwards reconstituted. Using flame sterilised forceps and scissors, a 1cm^2 area of filter paper containing the plasmid was cut out and placed within a sterile 1.5ml micro-centrifuge tube. 100μl of endotoxin-free, sterile TE buffer was added to the tube before being vortexed for 5 seconds and incubated at 17-20°C for 5 minutes. Following this, the mixture was again vortexed for 5 seconds and the tube was centrifuged for 15 seconds at 1000rpm. Supernatant was collected to be used in bacterial transformations.

2.2.3.2 Transformation of Competent Cells

Plasmids were transformed into DH5α electro-competent *E.coli* bacteria to facilitate rapid replication and purification of a higher volume of the plasmid DNA. Under sterile conditions, approximately 5-10μl of the reconstituted DNA supernatant was added to a vial containing 25μl of competent bacterial cells. The bacteria/DNA mixture was incubated on ice for 30 minutes, allowing the bacteria to come into contact with the DNA. The mixture was heated at 42°C for 30 seconds to disrupt the bacterial membrane, allowing the DNA to enter the cell. The heated mixture was placed back on ice for 2 minutes to help the bacteria retain the plasmids. Many bacteria will not survive the rapid change of temperature, but enough retain integrity to keep the plasmid. 500μl of room temperature SOC media is added to the mix before incubating again for 30 minutes, shaking at 150rpm at 37°C. This allows the transformed bacteria to recover and divide again. Transformed bacteria were spread on LB agar plates containing Kanamycin antibiotic: one plate with 40μl, and the other with 400μl. These spread plates were inverted and incubated overnight at 37°C. After 12-16 hours, successfully transformed colonies were visible for selection. Either plate is usable for picking colonies, but using the 40ul plate allows for colonies to be more spread out, assuming there were viable bacteria. The 400ul spread plate is retained for backup in case bacterial growth is not optimal on the other plate.

2.2.3.3 Midi-preparation of Plasmid DNA from Bacterial Colonies

Under aseptic conditions, colonies were selected from successful spread plates using a wire loop and inserted into bacterial tubes containing 5mls of LB broth supplemented with 5μl of Kanamycin antibiotic (at a stock concentration of 30ng/μl). Bacterial tubes were placed on a rotator at 37°C for 6-8 hours to create a larger volume of bacteria in the logarithmic growth phase. After reaching this phase, this starter culture was incubated at 37°C, shaking at 150rpm overnight (16-20 hours) in autoclaved baffled culture flasks - containing 145mls of LB broth with the appropriate ratio amount of antibiotic (145μl). At 16-20 hours, the culture flask was removed and cells were collected in a 50ml conical centrifuge tube. This was achieved by centrifuging 50mls of the cells in LB broth mixture at 3000rpm for 20 minutes at 4°C. Following this, supernatant is discarded and more broth is added; after which the tube is centrifuged at the same conditions. This is repeated until all the LB broth is pelleted. A Qiagen HiSpeed Plasmid Midi-prep kit is then used to extract the plasmid from this pellet. The bacterial pellet is re-suspended in 6mls of chilled P1 buffer (50 mM Tris-Cl, pH 8.0; 10 mM EDTA and 100 μg/ml RNase A) provided. For

A further 6mls of Buffer P2 (1% SDS (w/v), 200 mM NaOH), is added to lyse the cells. This mixture is shook for 30 seconds before incubating at 17-20°C for 5 minutes. 6mls of chilled Buffer P3 (3.0M potassium acetate pH 5.5) is added to neutralise the cell lysis and the tube is shaken for 30 seconds to ensure uniform mixing. The cell lysate mix is poured into a Qiagen Midi-cartridge and incubated at 17-20°C for 10 minutes while the cell debris settles. A Hi-speed Midi-prep tip is calibrated by allowing Equilibration buffer (750 mM NaCl, pH 7.0; 15% isopropanol (v/v); 0.15% Triton® X-100 (v/v); 50 mM MOPS) to flow through it. Cell lysate is filtered through this tip whereby the DNA binds to the resin column. Bacterial cell protein is removed by washing the column with 20mls of Wash buffer (1.0 M NaCl; 50 mM MOPS, pH 7.0). DNA is eluted with 5mls of QF Elution buffer (1.25 M NaCl; 50 mM Tris-Cl, pH 8.5) and 3.5mls of isopropanol is added to precipitate the DNA. The mixture was inverted a few times and allowed to precipitate at 17-20°C for 5 minutes, before getting filtered through the QIA-precipitator filter module provided. Plasmid bound to the precipitator filter was washed with 2mls of 70% (v/v) ethanol, dried by flushing air through, and then eluted with 500μl sterile dH$_2$O. The eluted DNA was flushed through the precipitator once again to remove any unbound DNA. The sample was subjected to spectrometric analysis using the NanoDrop™ system. The quality of the DNA was analysed through measurement of the

ratio of absorbance at 260nm and 280nm. Pure DNA with no bound protein impurities will have an A260/A280 ratio of 1.8-1.9.

2.2.3.4 Agarose Gel Electrophoresis

Agarose Gel Electrophoresis was employed to visualise the presence of plasmid DNA and reverse transcribed cDNA, and as a means to quality control both standard PCR and qRT-PCR samples post amplification. The agarose gel apparatus consists of a horizontal gel rig with electrodes, a buffer chamber, a gel plate and a plastic comb. The 1% (w/v) agarose solution is prepared as 1g agarose added to 99mls 1X TAE buffer in a conical flask. The solution was heated in a microwave to dissolve the agarose until the solution went clear. The solution was cooled to a warm temperature but not too cool - otherwise the agarose would start setting. After cooling, 10μl of 1X SYBR ® Safe solution – a fluorescent DNA stain - was added to the liquid agarose. The gel plate was sealed at the sides with autoclave tape to prevent leaking, and the comb was placed in the allotted groove in the plate walls. The agarose mix was poured into the gel plate and covered with tinfoil while setting, due to the SYBR ® Safe solution's light sensitivity. At ~30 minutes later when the gel was set, the tape was removed, and the gel was placed into the rig. The chamber was filled up with 1X TAE buffer until it sufficiently covered the top of the gel. The comb was removed, allowing the buffer to enter the wells, and samples and a ladder marker were loaded.

For plasmids, ~1-2μg was loaded with 6μl loading buffer. For qRT-PCR samples, 10μl of each sample was added to 6μl loading buffer. Standard PCR products didn't need loading buffer, as the Fermentas® PCR buffer allows for straight loading of samples. The gel rig is covered in tinfoil and the gel electrophoresed for ~1 hour at 100V - until the loading buffer is seen to run at least three-quarters of the way down the gel. Samples are visualised using the G-Box fluorescence gel documentation and analysis system.

2.2.3.5 Ethanol Precipitation

Ethanol precipitation was used in cases where DNA samples needed to be purified and concentrated. For every 100μl of DNA Sample, 10μl of Sodium Acetate and 200μl of 100% ethanol were added. The mixture was gently inverted to mix and incubated for 10 minutes at -80°C, before being centrifuged at 13000rpm for 20 minutes at 4°C. The supernatant is carefully aspirated and the pellet is washed in 70% ethanol, and again centrifuged at 13000rpm for 10 minutes at 4°C. The supernatant is removed and the

pellet is air-dried at 17-20°C. It is then re-suspended in 30µl of sterile RNase free distilled water.

2.2.4 Transfections with Plasmids and siRNA
2.2.4.1 Microporation

The transfection of siRNAs and plasmids has always been a complicated technique to perform, with endothelial cells being a difficult cell to transfect (Yockell-Lelièvre *et al.*, 2009). The electroporation method uses electrical energy to create pores in the cell membrane, and then drives the siRNA/plasmid into the cell to be expressed. However this resulted in large percentages of cell death. Kim *et al* described a method using a capillary tip and pipette system which acted as a substitute for a cuvette and electroporation reaction chamber which was more effective and resulted in 70-80% cell survival. They also indicated that the cell viability depended on the change in pH caused by electrolysis during electroporation (Kim *et al.*, 2008). The Invitrogen Neon® Transfection System was developed based on these findings. The MP-100 model available utilises a gold plated pipette tip as an electroporation chamber to transfect cells. The small surface area allows for a uniform electric field to be generated with minimal heat generation, pH variation or oxide formation that can be problematic in other electroporation protocols.

(A)   **(B)**   **(C)**
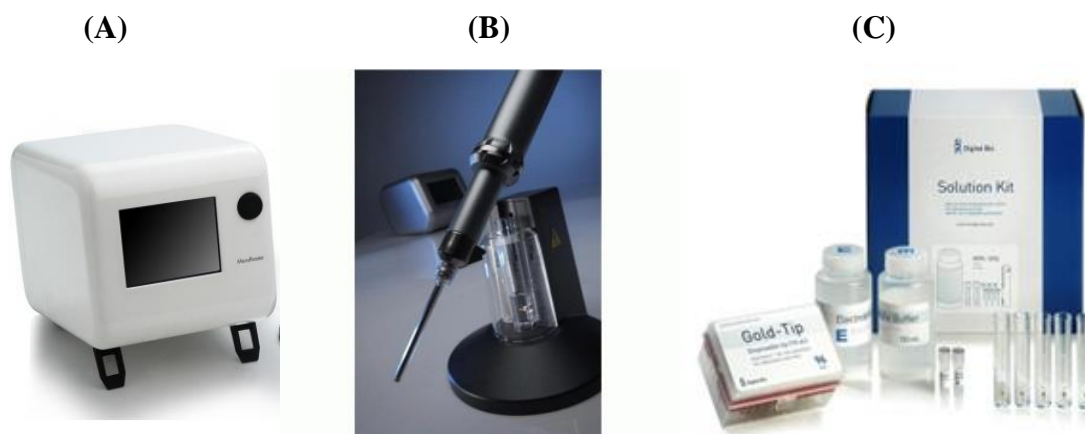
Figure 2.4: The Invitrogen Neon® Transfection System. This electroporation technique consists of (A) The microporation unit that facilitates the voltage settings needed for transfection, (B) the microporation docking station containing the electroporation buffer and specialised fixed volume pipette to electroporate the cells suspended in the gold tips; and (C) the microporation kit containing the necessary microporation solutions, tips and microporation tubes.

Prior to transfection, each well of a 6-well plate to be used was pre-incubated with 2mls of antibiotic-free growth media in the tissue culture incubator. This equilibrates the media in the plate so that the sensitive transfected cells adapt quickly to the media and remain viable. Plates of cells at 50-70% confluency were trypsinised, collected in cell media and counted as documented previously. This level of confluency works better with transfections as the cells are in a dividing phase, making the membrane easier to open, without damaging the cell. They were then aliquoted, with each aliquot containing 550,000 cells (5×10^5 cells + 10% extra to allow for centrifugation losses) for each planned transfection and centrifuged at 700rpm for 5 minutes at 17-20°C. Supernatant was removed and each aliquoted cell pellet was re-suspended in 110μl of Buffer R, a proprietary resuspension solution. The cell/buffer mix was transferred to a sterile 1.5ml micro-centrifuge tube and 1.5μg plasmid DNA/50nM siRNA was added. The microporation tube was set up in the docking station with 3.5mls E2 buffer, a proprietary electroporation solution. The cell mixture was pipetted using a special microporation pipette into a 100μl gold tip, with care taken not to have any bubbles appear in the mixture (bubbles break the connection in the electroporation and result in an uneven charge that destroys all the cells contained in the tip). For HAECs, the desired pulse conditions are 1000V voltage, 30ms Pulse Width, and a 3 pulse number. The pipette was docked into the microporation station and the program was run. Following the microporation the 100μl cell sample was transferred instantly to a well of the six-well plate containing 2ml pre-incubated media. Cells were incubated overnight, with the media being replaced the next day.
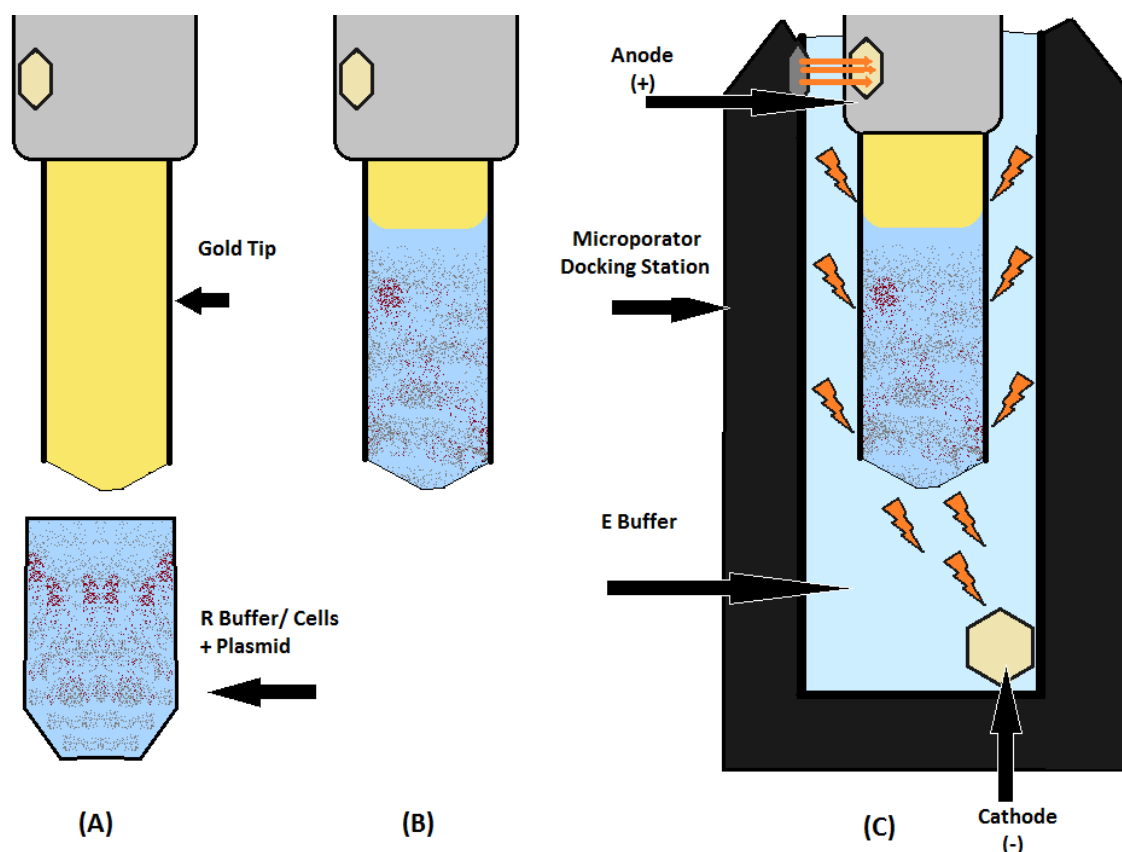
Figure 2.5: Electroporation of Cells using Microporator. Figure 2.5 (A) shows the pipette with a retractable gold tip, about to collect the R Buffer / Cells and Plasmid mix. As seen in (B), care is taken to avoid any bubbles appearing between the mixture and the tip. This tip is placed into the microporation tube containing E buffer, which has been set up inside the Microporator Docking Station (C). The docking station is connected to a module which facilitates the charge used to electroporate the cells. The electrical charge is passed from the station, through the Anode in the pipette. The charge (represented in orange) passes through the gold tip, and down through the cell mixture until it reaches the cathode at the bottom of the microporation tube. This process causes the cells to open pores in their membrane which allows the siRNA/plasmid to get transfected into the cell.

2.2.4.2 Cell Migration Assay of Transfected siRNA Knockdown Cells

Post-transfection, the cells were seeded as described. Controls were also set up, with non-transfected cells. At 30 hours post-transfection the cells were determined (through Western Blotting) to be at the optimal stage of siRNA knockdown. At this time point, the cells were subjected to a scratch wound healing assay. A circle on the underside of the plate was marked to mark a zone for imaging. Under sterile conditions, a 200ul pipette tip was used to scrape a line through this zone, leaving behind a wound of 1mm in diameter. Cells were imaged on a microscope at repeated time points to determine cell migration.

2.2.4.3 xCELLigence™ Assay of Transfected siRNA Knockdown Cells

The xCELLigence™ system (Roche, Basal, Switzerland) is a novel system that allows monitoring of cell migration or adhesion in real-time without any labelling, or need to image the cells at specific time points. The system works by measuring the electrical impedance across the integrated micro-electrodes at the base of specialised cell culture plates (Ke *et al.,* 2011). These plates – named the E (Electrode) and CIM (Cellular Invasion/Migration) plates, respectively measure cell adhesion and cell migration. The impedance measurement is used to provide quantitative information about the cells, including number, morphology and viability. The presence of the cells on the electrodes alters the local ionic environment at the electrode/solution interface leading to increased electrode impedance. The impedance is measured using a dimensionless parameter called the Cell Index (CI) which is derived from the relative change in electrical impedance. The CI is characteristically set at zero when cells are absent or not-adhered to the electrodes. Under the same physiological conditions, when more cells are attached, the CI values are larger. Thus, CI is a quantitative measure of cell number present in a well. Change in a cell status, such as cell morphology, cell adhesion, or cell viability will lead to a change in CI.

On the day of the experiment, the experimental parameters were set up on the RTCA software as follows.

1. Exp Notes tab: Experimental information, purpose, name etc. were entered.
2. Layout tab: In this tab, wells are highlighted to enter information on the cell number, type, treatment etc. within that well. This is what will decide whether you are doing individual or multiple well analyses. For the purposes of this experiment, triplicates were performed.
3. Schedule tab: This is what determines the length of the experiment and timing of intervals between sweeps – where the impedance is measured. Step one is for initial back ground reading to calibrate the software. This is performed first before the cells are added. A second cycling step is then added; 300 sweeps at 5min intervals were selected. This gives a monitoring of adhesion/migration of just over a 24 hour period.
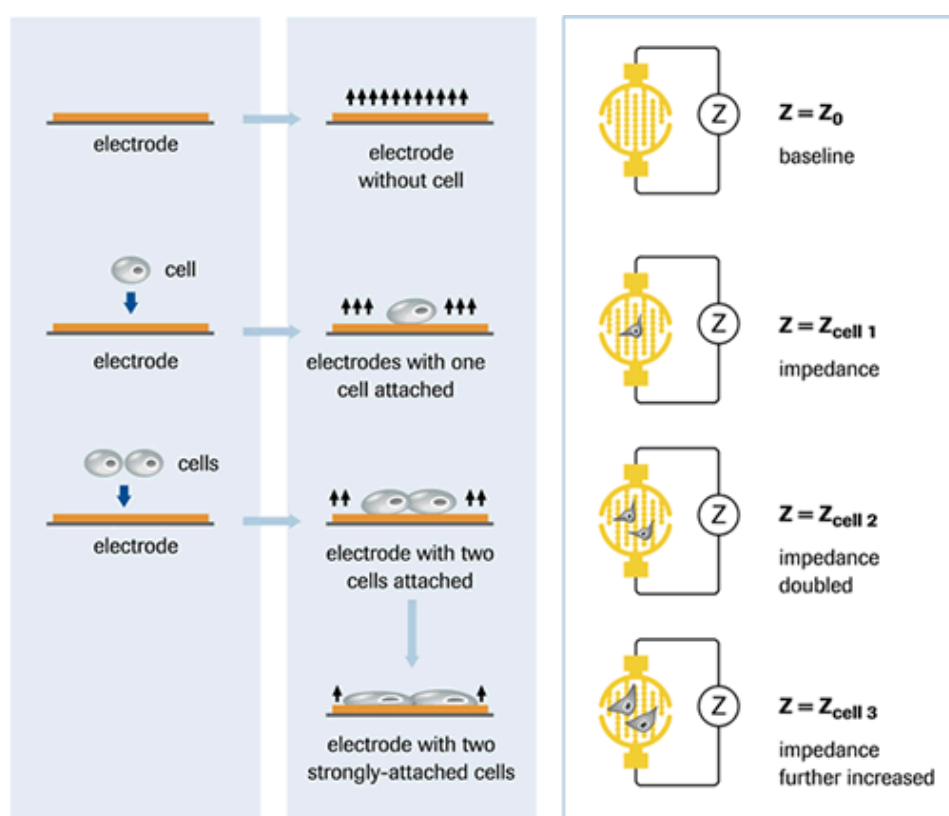
Figure 2.6: The xCELLigence™ System. This schematic illustrates how the xCELLigence™ system functions. The Cell Index value is set to zero when the electrode has no cells present. Presence of cells on the electrodes alters the environment at the electrode/solution interface leading to increased electrode impedance. Impedance increases as more cells attach or migrate across the electrode, which increases the Cell Index value. This value is recorded in five-minute increments and graphed with the specialised software.

For migration assays, firstly the HAECs were transfected with siRNA as per previously described methods, and incubated for 30 hours – the optimum time for knockdown. At approximately 45 minutes prior to the completion of this time point, the CIM-plates were disassembled according the manufacturer's instructions (Figure 2.7). CIM-Plates are single use, disposable devices used for performing cell migration assays on the instrument. The CIM-Plate 16 comprises a plate cover (lid), an upper chamber and a lower chamber. The upper chamber has 16 wells that are sealed at the bottom with a microporous polyethylene terephthalate (PET) membrane containing microfabricated gold electrode arrays on the bottom side of the membrane. The median pore size of this membrane is 8μm. The lower chamber has 16 wells, each of which serves as a reservoir for media and any chemo attractant for the cells in corresponding upper chamber wells.

160 μl of serum-free medium was added into the lower chamber with no air bubbles allowed to form, and the upper chamber then placed onto it. Another 50 μl of serum-

free medium was added into each well ensuring the surface of the well was fully covered and no air bubbles were present. The plate was allowed to incubate for 30 minutes at 37°C to allow the plate to acclimatise to the conditions. Meanwhile, cells were trypsinised and counted. Upon completion of the incubation, the CIM-plate was scanned for one minute - allowing the setting of the baseline value for the plate. 30,000 cells per condition were added per well into the upper chamber of CIM-Plate. The CIM-plate was incubated for another 30 minutes at 17-20°C while these cells settled and adjusted to the media. Initial adhesion of cells was measured at 5 minute intervals from 0-24 hours. Data was recorded and analysed using the specialised software.
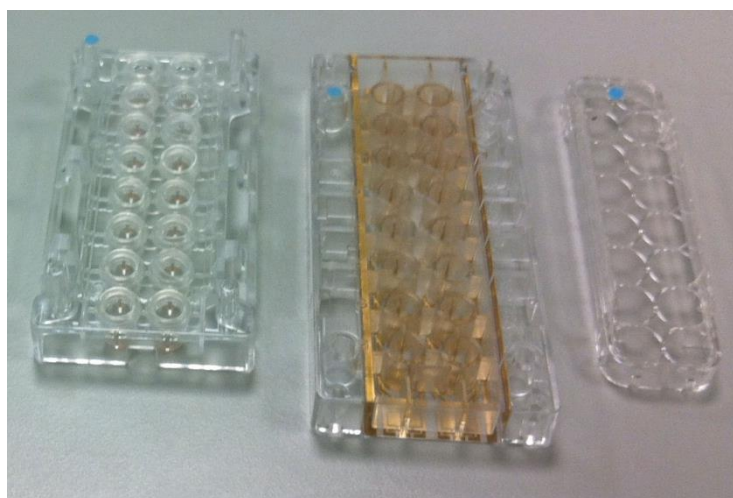
Figure 2.7: The CIM Plate. This illustrates the plate used for cell migration assays on the xCELLigence™ system. Left: Lower chamber plate containing the chemoattractant. Middle: Upper, electrode containing, chamber plate to which the cell suspension is added. Right: Plate cover.

2.2.5 Immuno-Detection Methods

2.2.5.1 Immuno-Blotting (Western Blotting)

2.2.5.1.1 Preparation of Whole Cell Lysates

For the purposes of Western Blotting, cell lysate was prepared in the following manner. Cell culture media was aspirated from culture dishes, and the plates were immediately placed on ice. They were washed three times with PBS solution – 6mls for a 100mm cell culture dish; or 1ml for each well of a 6-well plate. Following the complete aspiration of this PBS, cells were harvested with a cell scraper and 1X radioimmunoprecipitation assay (RIPA) cell lysis buffer. For immunoprecipitation experiments, a cell lysis buffer was provided in the Pierce® Co-immunoprecipitation kit. The manufacturer's manual recommended this buffer for use instead of RIPA, but

all other volumes and protocol remained the same. 250µl of buffer per 58cm^2 dish (or 40µl per well of a 6-well plate) was added to the cells and they were left incubate on ice for 5 minutes. The cells were then scraped off, with the cell suspension collected in a 1.5ml micro-centrifuge tube. This suspension was rotated at 4°C for 1 hour and centrifuged at 10000rpm for 20 minutes at 4°C to pellet the triton-insoluble material from the sample. A 50µl aliquot of supernatant was taken for immediate use in a BCA assay, with the remaining supernatant being also aliquoted and stored at-80°C for future use in Western Blotting.

2.2.5.1.2   Bicinchoninic Acid (BCA) Assay

The BCA assay is a biochemical assay used to quantify the total amount of protein in solution. It works on two reactions; firstly the ability of peptide bonds to reduce Copper (Cu2+) ions under alkaline conditions to produce Cu+. Secondly, the reduced copper ions react with bicinchoninic acid to form a complex that strongly absorbs light at 562nm. A 96-well plate is prepared with a range of BSA standards (from 0.0 to 2.0 mg/ml, increasing 0.2mg/ml increments) along with protein samples to be measured, and the RIPA buffer used. For each sample, 10µl was pipetted per well, and in triplicate. Two separate reagents are supplied in the commercially available assay kit (Pierce Chemicals); Reagent A (an alkaline bicarbonate solution) and Reagent B (a copper sulphate solution). A mixture of one part Reagent B to 50 parts Reagent A is mixed; 200µl of this is added to every well containing either 10µl of protein lysate, RIPA buffer, or BSA standard. The plate is covered and incubated at 37°C for 30 minutes. Following this incubation, absorbance is read at 562nm using an ELx800 microplate reader (Biotek). Results of known standards and unknown samples are graphed on an Excel spreadsheet in order to obtain protein concentrations using the known readings on a standard curve.

2.2.5.1.3   Sodium Dodecyl Sulfate-Polyacrylamide Gel Electrophoresis (SDS-PAGE)

SDS-PAGE resolves cellular proteins based solely on their electrophoretic mobility. During SDS-PAGE, proteins are moved by an applied current through a cross-linked polyacrylamide gel in the presence of the negatively charged detergent Sodium Dodecyl Sulfate. SDS binds to protein molecules and denatures them to their primary structure. Electrostatic repulsion between the bound SDS molecules causes the proteins to unfold

to a similar shape, removing secondary and tertiary structure as a factor in the separation. The amount of SDS bound is proportional to molecular weight of the polypeptide. As such, SDS-polypeptide complexes are able to be separated through the polyacrylamide gel in accordance with the size of the polypeptide (Laemmli, 1970).

10x100mm sized glass plates (one flat front plate, and one back plate with 1.0mm spacer) were cleaned, rinsed with 70% ethanol and dried completely. The components of the BioRad electrophoresis system were assembled according to manufacturer's instructions. The short plate was placed over the long plate, leaving a 1.0mm gap between the two, and the assembly was sealed tight using the provided locking frame and stand. The stand comes with a rubber base to keep the gel sealed from leaking. A 10% resolving gel was prepared as listed in Table 2.4:

Table 2.4: 10% SDS-PAGE Resolving Gel composition. The table documents the components of the SDS-PAGE resolving gel and the volumes needed to make the gel. The given volume for 1 gel when prepared leaves extra solution behind in a 50ml tube (which can be used to indicate when the gel has set). For creating two gels, 1.5X the volumes listed for a single gel was prepared. This allows for extra solution to indicate when the gel had set.

Reagent	Volume for 1 gel	Volume for 2 gels
dH$_2$O	4.0ml	6.0ml
1.5M Tris-HCL pH 8.8	2.5ml	3.75ml
30% Acrylamide-Bis	3.33ml	5ml
10% SDS	100μl	150ul
10% Ammonium Persulfate	50μl	75ul
TEMED	5μl	7.5ul

The 10% APS is made in dH$_2$O; excess APS can be aliquoted and stored at -20°C to be thawed out for single use. Both 10% APS and TEMED are added just before pouring the gels, as they start polymerisation of the gel. Having added these, approximately 5-6mls of resolving gel mix is poured gently between the two plates, avoiding bubble formation. Once the gel is filling up ~80% of the way, a layer of isopropanol is then poured on top to remove any air bubbles, and to provide an even surface on the gel. The gel is then allowed to polymerise for 40 minutes at 17-20°C.

Once polymerisation has finished, the isopropanol is poured off the top of the resolving gel, rinsed with dH$_2$O, and dried using filter paper. The 4% stacking gel is prepared as documented in Table 2.5 and poured on top of the resolving gel. Any bubbles present

are removed with a pipette tip, and the comb is inserted. The gel is then left to set for 20-30 minutes.

Table 2.5: SDS-PAGE 4% Stacking Gel composition. The table documents the components of the 4% SDS-PAGE stacking gel and the volumes needed to make it. As with the resolving gel, 10% APS and TEMED are added and mixed just prior to pouring.

Reagent	Volume
dH$_2$O	3.05ml
0.5M Tris-HCL pH 6.8	1.25ml
30% Acrylamide-Bis	675μl
10% SDS	50μl
10% Ammonium Persulfate	50μl
TEMED	5μl

Upon polymerisation of the stacking gel, the gel is inserted into the electrophoresis chamber containing the required electrodes, as designated in Figure 2.8. If only a single gel is being run, a buffer dam is placed on the opposite side; otherwise the second gel plate is inserted. The plate holder is locked into the buffer tank, and ~800mls of 1X Tris/Glycine/SDS Running Buffer is added, in such a way that the inner chamber is filled to the very top. The gel will fail to run properly if not full, generating an uneven electrophoresis indicated with a curve in the sample buffer line in the gel. Once the buffer has been added, the combs are removed. Unpolymerised acrylamide in the wells is flushed out with a pipette tip and Running Buffer.
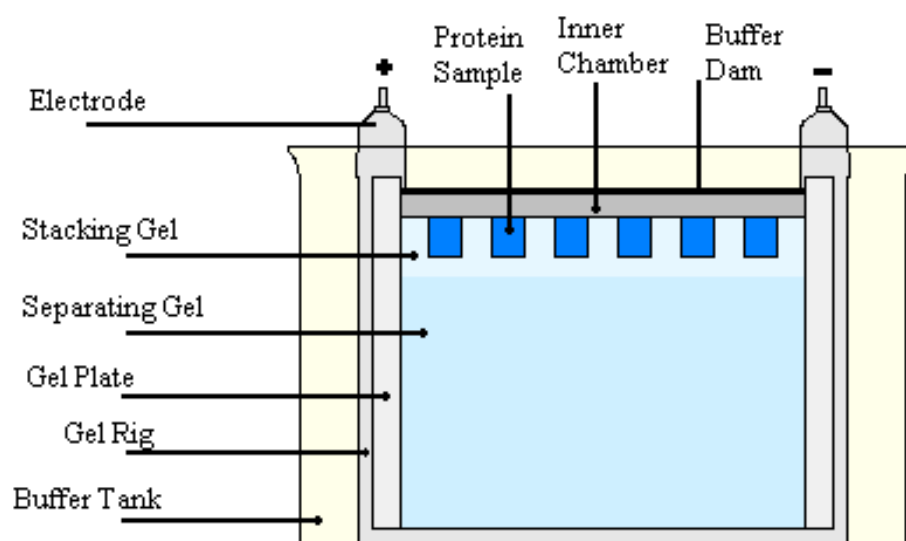
Figure 2.8: Schematic design of SDS-PAGE Gel orientation inside buffer tank. This figure illustrates the orientation of the SDS-PAGE gel when loaded and placed inside the tank full of running buffer. The lid of the tank connects the electrodes to the PowerPak™ which regulates the electrical charge needed to separate the proteins on the gel.

Protein samples are prepared in 4X sample solubilisation buffer (SSB) to give the optimal concentration of protein depending on protein investigated (Table 2.6) and 1X SSB in a total volume of 30ul. Samples are boiled at 95°C for 5 minutes and held shut with micro-centrifuge clips (to prevent pressure opening the sample and the heat evaporating it). Samples are immediately placed on ice once boiled, then loaded into individual lanes in the SDS-PAGE gel. In a separate lane, 5μl of Precision Plus ® protein molecular weight marker is also inserted. The inner chamber is topped up with more Running Buffer and the lid is shut and connected to a PowerPak™. Samples are electrophoretically separated for 20 minutes at 80V, before being subjected to 100V for 120 minutes, or until the sample buffer reaches the bottom of the gel.

Table 2.6: Protein loading volumes. This table documents a list of proteins investigated by Western Blotting analysis, and the quantity of each protein loaded into the SDS-PAGE gels to carry out the investigation.

Protein Name	Protein Loaded per lane (μg)
Palladin	30μg
LASP-1	30μg
Drebrin	40μg

2.2.5.1.4 Transferring to a Nitrocellulose Membrane

Following separation on a gel, the proteins then transferred to a membrane whilst still maintaining their relative position and resolution. The wet transfer method (Towbin *et al.*, 1979) was the method for transfer in all Western Blot experiments. Prior to completion of the SDS-PAGE method, a piece of nitrocellulose membrane was cut to the same size as the gel. It, along with filter papers and fibre pads are soaked for 15 minutes in ice-cold Transfer Buffer. This equilibrates the membrane to the transfer buffer and also allows for easier dilution of any SDS complexes bound to the gel that may impede a successful protein transfer. Once the gels are run, they were removed from the gel plates, and the stacking gel was removed. The gel, membrane, filter papers, and fibre pads were assembled in specialised cassettes supplied in the Mini-PROTEAN Electrophoresis System (BioRad) according to the schematic in Figure 2.9. The cassette was checked to be free from air bubbles (which prevent proper transfer of protein) and inserted into the cassette holder containing the electrodes required for transferring.
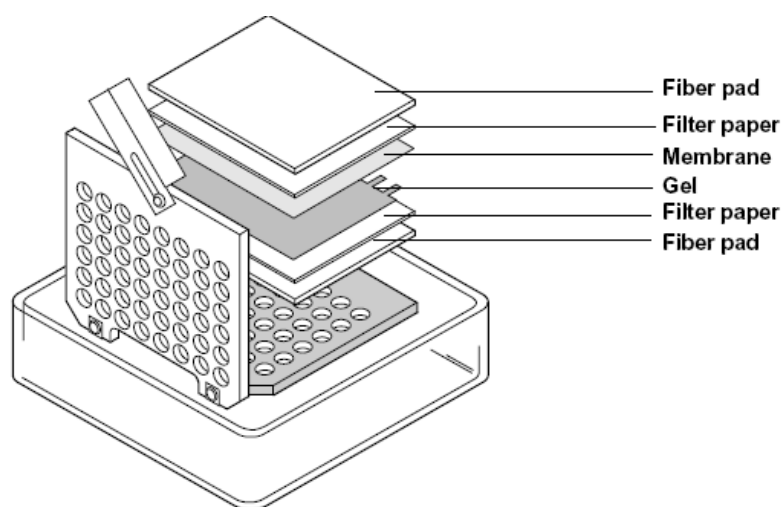
Figure 2.9: Transfer Cassette Schematic. This figure shows the schematic of the transfer cassette used to transfer the electrophoresed proteins from an SDS-PAGE gel to nitrocellulose membrane. The black coloured side is assembled face down, and overlaid with a fibre pad, filter paper, resolved gel, nitrocellulose membrane, filter paper and fibre pad in that order before being sealed with the cassette clamp.

The cassette holder was placed in the buffer tank with a cooling ice-block and filled with ice-cold transfer buffer, as shown in Figure 2.10. The cassette is orientated to allow the charge to pass through, transferring the protein from the gel to the membrane. Transferring was performed for 2 hours at 100V with the tank surrounded in ice.

Alternatively, a stirring bar was placed inside the tank, and the transfer was performed overnight at 50V in a cold room at 4°C, with the stirring bar rotating.
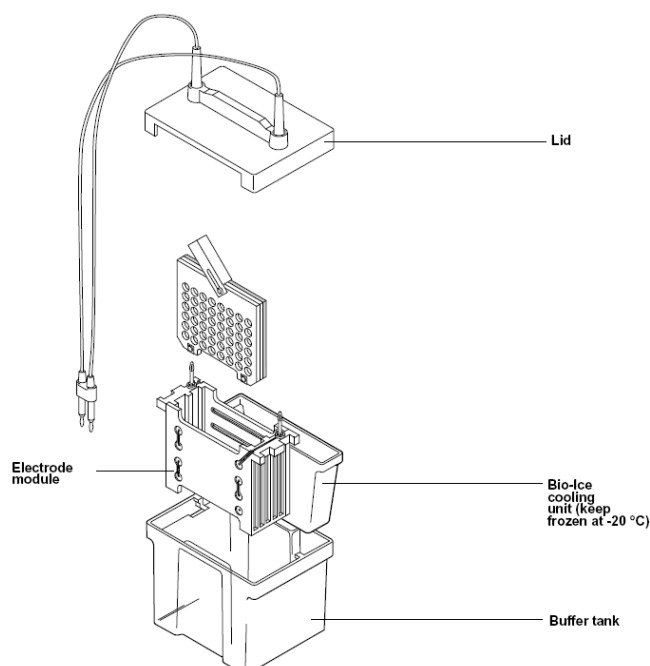
Figure 2.10: Setup of Transfer of protein from Gel to Membrane. This figure illustrates preparation of the gel within a transfer cassette prior to transferring of protein to a nitrocellulose membrane.

The tank transfer system was assembled in the illustrated manner. The transfer cassette was placed in the correct orientation of the electrode module. The module was placed into the buffer tank with a -20°C cooling block to keep the buffer as cold as possible. The lid was shut in the correct orientation and the transfer was started.

2.2.5.1.5   Ponceau S Staining

Ponceau S Stain was a method used to validate that protein had transferred to the membrane successfully. Ponceau S is a negative stain, which binds to positively charged amino acid groups of proteins. Following transfer, the membrane is placed in a disposable plastic container and is overlaid with roughly 10mls of Ponceau S stain. It is swirled around for 30 seconds before the stain is poured off. Transferred protein is visible as a red band on the white membrane. Following visualisation, the membrane is overlaid with dH$_2$O and placed on a See-Saw Rocker for 5 minutes with gentle rocking and regular changing of water, until the stain has been removed.

2.2.5.1.6   Coomassie Gel Staining

A secondary method to determine transfer of protein is through staining of the SDS-PAGE gel to visualise protein bands or absence thereof. This technique ensures the transfer method worked, as well as determining that immunoprecipitation assay techniques work as expected (a minimal number of bands should be observed). The SDS-PAGE gel is overlaid with $0.25\mu m$ filtered Coomassie Blue solution while incubating on the See-Saw rocker at $17-20^{o}C$ for 2-4 hours. Following this, the Coomassie Blue solution was removed, and the gel was de-stained, whilst rocking, in destain solution until the protein bands appeared clear and visible with no background staining, changing the solution regularly.

2.2.5.1.7   Immunoblotting and Chemiluminescence Band Detection

Following protein transfer, the nitrocellulose membranes are subjected to blocking in a 5% (w/v) BSA/ TBS with 0.1% Tween solution. For membranes to be probed with Drebrin antibodies, the solution used is a 2.5% (w/v) BSA/TBS with 0.1% (v/v) Tween solution. Membranes are subjected to 1 hour in transfer buffer on a See-Saw rocker at $17-20^{o}C$. Once blocked, the membranes are washed for 5 minutes in TBS with 0.1% Tween (v/v) to remove excess solution. Subsequently, the membranes are incubated with gentle rocking for 2 hours at $17-20^{o}C$ with the appropriate primary antibody (Table 2.7) in 6mls of 5% (w/v) BSA/TBS. Alternatively; the antibody was incubated overnight, rocking at $4^{o}C$.

Table 2.7: Primary Antibody solutions. This table displays the optimised primary antibody dilutions for proteins monitored by Western Blotting, along with the commercial and animal sources of these antibodies.

Type of Antibody	Commercial Source	Animal Source	Initial Antibody concentration	Antibody Dilution in BSA/TBS	Amount of antibody used per blot (6mls)
Palladin Polyclonal	ProteinTech	Rabbit	16μg/100μl	1:1000	0.96μg
GAPDH Polyclonal	Millipore	Rabbit	100μg/100μl	1:2000	3μg
LASP-1 Monoclonal	Millipore	Mouse	100μg/100μl	1:2000	3μg
Drebrin Polyclonal	Millipore	Rabbit	100μg/100μl	1:500	12μg
vWF Polyclonal	Dako	Rabbit	100μg/100μl	1:2000	3μg

Upon completion of the primary antibody incubation step, the antibody was removed and washed three times for 5 minutes in Wash Buffer (TBS with 0.1% Tween) while rocking. The membranes were incubated with an appropriate Horseradish Peroxidase (HRP)-conjugated secondary antibody in a 5% BSA/ TBS with 0.1% Tween solution, as dictated in Table 2.8. The membranes were incubated at one hour with gentle rocking at 17-20°C. Membranes were then washed three times in Wash buffer for 5 minutes each time, while rocking at 17-20°C, before being subjected to detection by chemi-luminescence. Supersignal ® West Pico (Pierce) chemi-luminescent substrate is prepared and used to detect HRP-conjugated secondary antibody binding. The HRP enzyme catalyses the conversion of the substrate into a sensitized reagent in the vicinity of the protein-antibody complex, which produces a carbonyl group that emits light as it decays to a single carbonyl. The full reaction takes less than two minutes to occur (the prepared substrate is incubated with the membrane for two minutes each time). Once this substrate is added, the signal will remain at a plateau level for 30 minutes before it slowly shows signs of degrading. Overall light emission will continue for several hours, but is no longer optimum after 30 minutes. Following the 2 minute incubation, excess substrate was removed and the chemiluminescent signal was detected using the high sensitivity camera of the G-Box fluorescence and chemi-luminescence gel documentation and analysis system. The system is able to expose the blot to light at controlled times, and obtains multiple pictures at different exposure times from the

same blot in a single session. These high definition images can also be saved on a computer in a variety of formats, providing advantages over dark room methods of developing. Western Blot bands were observed at 2 minutes of exposure time unless otherwise stated. Scanned blots were examined with ImageJ™ densitometry software (http://rsbweb.nih.gov/ij/index.html). The software determines the quantitative measurement of optical density which arises from the darkness of the bands on the blot. The software measures the density of each band (set within the same size measurement area) to determine the comparative amounts of detected protein expressed in each sample. The values of the protein of interest are divided by the respective value for the control protein (usually GAPDH) and a definitive value is obtained. Results are graphed and expressed relative to the baseline, untreated sample value.

Table 2.8: Secondary Antibody solutions. This table displays the optimised primary antibody dilutions for proteins monitored by Western Blotting, along with the commercial and animal sources of these antibodies.

Secondary Antibody Source	Reactivity	Commercial Source	Proteins detected	Initial Antibody concentration	Antibody Dilution in BSA/TBS	Amount of antibody used per blot (6mls)
Goat	Rabbit	Millipore	GAPDH Drebrin Palladin	100μg/100μl	1:2000	3μg
Sheep	Mouse	GE Healthcare	LASP-1	82μg/100μl	1:2000	2.46μg

2.2.5.1.8 Membrane Stripping

For the purposes of blotting for proteins of similar weights on the same membrane (GAPDH and LASP-1 both are in the 35-40kDa range) membranes were stripped using Restore ® Western Blot stripping buffer (Pierce). The stripping of both primary and secondary antibody from the membranes was carried out in accordance with manufacturer's instructions. The membrane was washed in TBS-T buffer to remove the chemi-luminescent substrate. It was incubated, whilst rocking, in Restore ® Western Blot stripping buffer for no more than 15 minutes. The membrane was removed from the stripping buffer and washed in TBST, before being re-blocked as described in

Chapter 2.2.5.1.7. After completion of this step, membranes were incubated in the appropriate secondary antibody and developed as described above to test for the removal of the primary and secondary antibodies from previous blotting procedures. Once a clear result on the G-Box system was observed the membrane was washed again in TBST washing buffer to again remove the chemi-luminescent substrate. It was re-blocked again for 30 minutes, and re-blotted with the alternative primary and secondary antibodies, following the methods described previously.

2.2.5.2 Immunoprecipitation of Protein

Immunoprecipitation of intact protein complexes is known as co-immunoprecipitation (Co-IP). Co-Immunoprecipitation works by selecting an antibody that targets a known protein that is believed to be part of a complex of proteins. The antibody is used to immunoprecipitate the protein of interest (also known as a bait protein) and also pulls out any other proteins (a.k.a. prey proteins) that may interact with it.

Co-immunoprecipitation was carried out to extract protein from HAECs, using a Pierce® co-immunoprecipitation kit according to manufacturer protocols. The Co-IP kit works by directly immobilizing protein-specific antibodies onto an agarose support with an amine-reactive resin. This resin prevents co-elution of antibody heavy and light chains that may co-migrate with relevant bands, masking results. The association of other proteins with Palladin, LASP-1 and Drebrin was investigated in this study.

Following lysis of cells as described in Chapter 2.2.5.1.1, the lysate was subjected to pre-clearing to reduce non-specific protein binding. This meant preparing a spin column with 80ul of Control Agarose Resin provided in the kit. This was centrifuged at 1000g for 1 minute, before 100ul of 1X Coupling Buffer (0.01M sodium phosphate, 0.15M NaCl; pH 7.2) was added. Following another centrifugation, the column was incubated with 200ul of cell lysate at 17-20°C for 1 hour, with end over end mixing. The column was centrifuged, with the pre-cleared lysate collected for use with an antibody bound column.

To prepare the antibody bound columns, the spin columns firstly had 50μl of Coupling Buffer added to them before centrifuging for 1 minute at 1000g at 17-20°C. Controls were also prepared – one with an inactivated control resin, and another with activated resin but with Quenching Buffer (1M Tris-HCl) added instead. The resins were washed twice with 200μl of 1X Coupling Buffer with the column being centrifuged at the same conditions. The columns were then plugged and 75μg of antibody in 200μl 1X Coupling

Buffer was added, along with 3μl of 5M Sodium Cyanoborohydride (NaBH₃CN) solution. The spin columns were screwed shut and rotated gently for 3 hours. Plugs were removed and the spin columns were centrifuged, removing excess antibody. The spin columns were washed twice by centrifuging 1X Coupling Buffer through them twice, before 200μl of Quenching Buffer was centrifuged through. The columns were incubated on a rotator for 15 minutes at 17-20°C with 200μl of Quenching Buffer and 3μl of Sodium Cyanoborohydride. The screw cap was removed and the column was washed by centrifugation: twice with 200μl of 1X Coupling Buffer, then six times with 150μl of Wash Solution (1M NaCl). The columns were ready to be used for immunoprecipitation.

The spin columns were washed twice by centrifuging through with 200μl of IP Lysis/Wash Buffer (0.025M Tris, 0.15M NaCl, 0.001M EDTA, 1% NP-40, 5% glycerol; pH 7.4), before the plugs were inserted and 200μl of pre-cleared cell lysate was added. Columns were rotated for 4 hours, or overnight at 4°C. Following this, the columns were centrifuged (with the flow through kept to determine binding affinity), before being washed three times by centrifuging 200μl of IP Lysis/Wash Buffer through. The Co-IP protein was eluted by incubating at 17-20°C for 5 minutes with 50μl of Elution Buffer, and then centrifuged once more at 1000g for 1 minute.

For storage, the spin columns are washed twice with 200μl of 1X Coupling Buffer, centrifuging after each wash. They then are plugged and sealed with 200μl of 1X Coupling Buffer and stored at 4°C. The Co-IP samples were validated using SDS-PAGE and Coomassie staining, or else Western Blotting. Once validated, they were sent to the National Institute for Cellular Biotechnology, Dublin (NICB) for Mass Spectrometric analysis using MALDI-TOF methods.

2.2.5.3 Proteocellular Fractionation

Proteocellular fractionation was performed to investigate the localisation of Palladin in HAECs following haemodynamic stimulation. The ProteoExtract® sub-cellular proteome extraction kit (Merck Biosciences) was used according to manufacturer's instructions to separate the different sub-cellular sections: the cytosolic fraction; the membrane/organelle, the nuclear and the cytoskeletal fractions. The extraction kit works by taking advantage of the differential solubility of the subcellular compartments in different proprietary reagents provided in order to sequentially lyse the different fractions from the cells attached to the plate. The other cellular fractions remain

attached to the plate until their specific reagent is used to extract them. Early destruction of the cell that might occur from cell scraping, or trypsinisation is thereby avoided, leaving each fraction intact.

The translocation of Palladin from the different sub-cellular components under haemodynamic forces was documented. For adherent cells, this protocol was performed directly onto cells on a six-well culture plate, and all extraction steps were carried out in the 4^oC cold room. Media was removed, and the cells were washed twice with 800μl of ice-cold wash buffer per well, being incubated for 5 minutes, while being gently rocked each time. Following removal of wash buffer, each of the wells was overlaid with 400μl of ice-cold Extraction Buffer 1 and 1X protease inhibitor cocktail. The culture plates were incubated for 10 minutes with gentle rocking. Following this incubation, the supernatant (Fraction 1 – the cytosolic fraction) was carefully transferred to a 15ml polypropylene tube, and stored on ice, or at -80^oC if being kept for future use. 400μl of Extraction Buffer II with 1X protease inhibitor cocktail was then added to each well of the plate, covering all the plate. The plates were incubated for 30 minutes with gentle agitation. Following this, the supernatant (Fraction II – the membrane/ organelle fractions) was transferred to a 15ml tube, and also stored on ice, or at -80^oC for long term storage. Extraction Buffer III with 1X protease inhibitor and 0.5μl benzonase was prepared next, with 200μl covering each well. After a 10 minute incubation with gentle agitation, the supernatant (Fraction III – the nuclear fraction) was transferred to a 15ml tube and kept on ice or stored at -80^oC until use. Finally, cells were covered with 200μl of 17-20°C Extraction Buffer IV and 1X protease inhibitor cocktail. Cells were gently agitated for 5 minutes, and the remaining cell structures (Fraction IV – the cytoskeletal fraction), were collected into a 15ml tube, and stored at the same conditions of the other fractions. The protein in the samples was precipitated (Chapter 2.2.5.3.1) to concentrate the volume, and then were analysed for Palladin expression in each of the four cellular fractions by Western Blotting according to the protocols dictated in Chapter 2.2.5.1.

Following probing for Palladin, the blots were stripped according to protocol in Chapter 2.2.5.1.8, and probed using the ProteoExtract® S-PEK Antibody Control Kit. This is a set of four monoclonal antibodies, each one specific for one of the different four extracted fractions (Table 2.9). These antibodies were used as a control as opposed to GAPDH on account of the levels of GAPDH changing dependent on fraction.

Table 2.9: List of Control Antibodies for Proteocellular Fractionation. These antibodies were used in the detection of protein expression from cells subjected to time points of shear, and subsequently fractionated. After probing for the protein of interest, the blot was stripped and re-probed for the fraction-specific antibody listed.

#	Fraction	Antibody	Type of Antibody	Size of Protein	Initial Antibody Concentration	Amount of antibody used per blot (5mls)
1	Cytoplasm	Anti-HSP90a	Mouse	90	1.26mg/ml	5μg
2	Membrane/ Organelle	Anti-Calnexin	Mouse	67/90	2.0mg/ml	5μg
3	Nuclear	Anti-PARP-1	Mouse	85/116	0.1mg/ml	5μg
4	Cytoskeleton	Anti-Vimentin	Mouse	58	0.5mg/ml	0.5μg

2.2.5.3.1 Protein Precipitation

Before Western Blot analysis of the fractionation samples could be performed, the samples needed to be concentrated and the protein precipitated using acetone. This ensured the fractionations were of a manageable volume that would fit into the wells of an SDS-PAGE gel. Each fractionation was defrosted, but kept cold on ice. A volume of acetone, equal to 5X the fractionation sample, was added, and the mixture was vortexed gently followed by centrifugation at 1000rpm and 4°C for 15 seconds. The samples were incubated at -20°C for 1 hour, with regular inversion of the samples every 10-15 minutes to prevent them from freezing. Afterwards, the mixture was centrifuged at 15000g for 5 minutes at 4°C and the supernatant was removed. The protein pellets were allowed to air dry until the acetone was removed. Samples were re-suspended in 20μl of SSB loading buffer and run on SDS-PAGE.

2.2.5.4 Immunofluorescence Imaging

Immunofluorescence imaging was carried out on glass coverslips to determine the localisation of Palladin, LASP-1 or Drebrin and their association with actin. The same antibodies as listed in Table 2.7 were used to probe the fixed cells. Coverslips were made suitable for use by dipping in ethanol and flame sterilising over a Bunsen burner flame. Once cooled, they were placed in the sterile well of a 6-well plate, and overlaid with approximately 1ml of PBS. Coverslips were incubated overnight at 4°C. The

following day, the PBS was aspirated and the coverslips were blocked for 1 hour at 17-20°C with 5mg/ml of denatured BSA. BSA was denatured by boiling at 60°C for 30 minutes and then sterile-filtering through a 0.25μm filter. HAECs were trypsinised and counted according to the previous methods, with 1.5x10^{5} cells in 1ml of culture media suspension being plated to each well, and allowed to adhere in the 37°C incubator overnight.

On the third day, cells were washed with 1ml of prewarmed PBS, then fixed by covering them with 1ml of 3.5% (v/v) Para-formaldehyde/PBS solution and incubating at 17-20°C for 10 minutes. The coverslips were washed twice with PBS before the cells were permeabilised with 0.2% Triton X-100 in PBS. The solution was left on the cells at 17-20°C for 5 minutes before they were washed twice again with PBS. Cells were blocked with 500μl per well of PBS, supplemented with 1% (w/v) BSA and 1% (v/v) Goat Serum, for 1 hour, while gently rocking. Blocking solution was removed and cells were incubated in 5μl of primary antibody, (0.8μg for Palladin, 5μg for LASP-1) diluted 1:100 in 500μl of fresh PBS with 1% BSA and 1% Goat Serum, for 2 hours at 17-20°C while gently rocking. For Drebrin, the dilution was 1:50 (10μg), as opposed to 1:100 for Palladin or LASP-1.

Following incubation, cells were washed three times in TBS buffer. Secondary goat anti-rabbit (or anti-mouse depending on primary antibody) Alexa Fluor 488 (a 2mg/ml green FITC-conjugated stain) was prepared in the blocking solution at a dilution of 1:500, with 500μl being added to each well. The cover slips were incubated in the dark at 17-20°C gently rocking for an hour, before being washed three times with PBS. Cover slips were then incubated with a secondary stain – Rhodamine Phalloidin, which stains actin red – at a dilution of 1:40 in blocking solution for 20 minutes at 17-20°C in the dark. An optional step at this point was to wash the cover slips, and then incubate with DAPI stain at a 1:3000 concentration, in order to stain the nucleus. Otherwise, the cover slips were washed three times with PBS to remove excess Phalloidin, before being carefully extracted, inverted, and mounted on ethanol-washed microscope slides using a drop of Dako mounting media. Slides were covered in tinfoil, and kept at 17-20°C for 1-2 hours to allow the media to set. The slides were examined on the fluorescent microscope, or else stored at 4°C.

2.2.6   Gene Expression Analysis
2.2.6.1 RNA Isolation

In order to investigate gene expression following haemodynamic cell stimuli, RNA needed to be extracted. The method employed in the lab involved the use of Trizol® reagent in RNAse-free conditions. Trizol ® is a ready to use reagent for isolation of total RNA from cells and tissues, maintaining the RNA integrity whilst disrupting the cells and dissolving the cell components (Chomczynski and Sacchi, 1987).

Following stimulus of HAECs, the cells were washed 3 times with PBS before being lysed with Trizol ® reagent. 500μl of reagent was added to each well of a six-well plate, with care given to make sure the cells were covered with it. The cells were stored on ice for 5 minutes to allow complete dissociation of complexes. Trizol ® samples were collected and pooled together (if subjected to the same treatment). For every 1ml of Trizol ® used, 0.2mls of chloroform was added, and samples were vigorously shaken for 15 seconds. They were incubated for 10 minutes at 17-20°C and centrifuged at 13000 rpm at 4°C for 20 minutes. The mixture separated into a lower red phenol-chloroform phase, an interphase and an upper colourless phase (where the RNA resides). To precipitate RNA, the upper phase is transferred to a new micro-centrifuge tube, where 500μl of Isopropanol for every 1ml of upper phase is added. This is inverted 5-8 times and incubated at -20°C overnight. The following day, the sample is incubated at 17-20°C for 10 minutes and centrifuged for at 13000rpm for 15 minutes at 4°C. The supernatant was discarded, and the RNA pellet was washed in 1ml of 75% ethanol in RNAse Free dH$_2$O. The micro-centrifuge was vigorously shaken, and centrifuged at 13000rpm for 10 minutes at 4°C. The ethanol was aspirated and the pellet was air-dried before being re-suspended in 50μl of nuclease-free H$_2$O. The RNA was incubated at 60°C for 10 minutes and immediately kept on ice and prepared for quantification on the NanoDrop™ system. Otherwise, RNA was stored at -80°C.

2.2.6.2 Spectrometric Analysis of Isolated RNA

RNA concentrations were determined by measuring each sample absorbance using the NanoDrop™ ND-1000 Spectrophotometer System. The spectrometer was calibrated by measuring with RNA-free dH$_2$O as a blank sample. This was dried with lens tissue, and the RNA sample was added. 1.2μl was pipetted onto the end of a fibre-optic cable (the receiving fibre). A second fibre-optic cable (the source fibre) was then placed into contact with the liquid RNA sample, causing the liquid to bridge the gap between the

fibre-optic ends. A pulsed xenon flash lamp provides the light source, and a spectrometer analyses the light passing through the sample. The data is read and archived using special software. The NanoDrop™ automatically calculates the purity of the nucleic acid samples by determining the ratio between the absorbance at 260 nm and at 280 nm (ABS260/ABS280). Pure DNA - without any protein impurities - has a ratio of 1.8 whereas pure RNA has a ratio of 2.0. Lower ratios indicate presence of proteins, whereas higher ratios imply the presence of organic reagents.

2.2.6.3 Reverse Transcription of mRNA

In this process, mRNA was transcribed into double stranded complementary DNA (cDNA) by a reverse transcriptase enzyme. A High Capacity cDNA Reverse Transcription Kit (Applied Biosystems) was used. Isolated mRNA samples are aliquoted into 0.2ml PCR tubes but diluted in Ultra-Pure GIBCO water so that the final concentration stands at 1000ng of RNA in 10μl of water. Added to this sample was 10μl of a master mix, which contained the following:

4.2μl of GIBCO™ water

2μl of RT Buffer – a standard buffer

2μl of Random Primers - These are used to produce cDNA from all over the mRNA sequence. The cDNAs produced are shorter in length, but there is an increased probability that the 5' ends of the mRNA are converted to cDNA.

1μl of Multiscribe™ - This recombinant RNA-dependent DNA polymerase uses single-stranded RNA as a template in the presence of the random primers to synthesize a complementary DNA (cDNA) strand.

0.8μl of dNTPs – These are dGTP, dCTP, dATP and dTTP – deoxynucleotide triphosphates which are used in providing bases to synthesise DNA.

The 20μl in the PCR tube was briefly spun down in a centrifuge to ensure the sample is mixed and collected at the base of the tube. Using the desktop PCR machine, the samples were run at the following conditions:

25°C for 10 minutes,

37°C for 120 minutes,

85°C for 5 minutes.

The cDNA products were quantified on the NanoDrop™ to check concentration and purity of samples. Products are then ready for use in PCR; or else stored at -20°C.

2.2.6.4 Design of PCR Primer Sets

For Polymerase Chain Reactions, DNA primers were designed using the online Primer3 website: http://frodo.wi.mit.edu/primer3 in accordance with the standard rules to primer design. When given a gene template sequence, this software considers many factors such as melting temperature, length, GC content or likelihood of primer-dimer formation, in order to evaluate acceptable primer pairs (Untergasser *et al.*, 2012). Each primer was also designed to anneal to exon-exon border regions so as to only amplify the reverse transcribed cDNA instead of genomic DNA - leading to less genomic DNA contamination prone products in qRT-PCR.

Using another website - http://www.basic.northwestern.edu/biotools/oligocalc.html - the designed primers were verified by BLAST analysis, to check the homology and the sequence, and also to further ensure there would be no primer-dimer formation. Furthermore, mFold analysis on the same website was used to check to make sure the chosen primer would not fold with itself. The sequences of primers used, along with their optimum temperatures and product lengths are documented in Table 2.10.

For each qRT-PCR experiment, an endogenous control needed to be selected which showed the same level of expression of the gene to be unaffected by the conditions of the experiment. This was done to ensure that any changes observed in the expression of test genes were not due to changes in the expression of the endogenous control. For all qRT-PCRs, the control used was *18S*, which is a commonly used control gene (Bas *et al.*, 2004).

Table 2.10: Table of PCR primers. These were used for the detection of gene expression from cells stimulated with haemodynamic forces. The table documents the sequences of the *PALLD* forward and reverse primers, along with those of the *18S* "housekeeping" gene. Also listed are their resulting PCR product sizes along with the annealing temperature of each set of primers.

Gene	Primer	Sequence 5'-3'	Product Length	Annealing Temperature (C)
PALLD (90kDa)	Forward	GCC TCC ACC CTA GAT GAT GA	215	59.4
	Reverse	GGT CTG AAG AAT CGC TCC TG		
18S	Forward	CAG CCA CCC GAG ATT GAG CA	324	60
	Reverse	TAG TAG CGA CGG GCG GTG TG		
LASP-1	Forward	CCA CGG AGA AGG TGA ACT GT	312	52
	Reverse	TGA TCT GGT CCT GGG TCT TC		
DBN1	Forward	TGA GAC GCT GTT GCA AAT TC	151	60
	Reverse	GAA AAG AGG TGG GGG ACA TT		

2.2.6.5 Polymerase Chain Reaction (PCR)

The standard polymerase chain reaction (PCR) was used as a quicker and cheaper way of checking that newly designed primers worked before using them in qRT-PCR analysis. PCR is a commonly used technique to amplify a single or a small number of a strand of DNA, generating millions of copies of a particular DNA sequence. PCR was used to amplify a specific target sequence of DNA within the *PALLD* and *18S* genes using gene specific primers (Table 2.10). cDNA was diluted in GIBCO water to a stock concentration of 100ng/μl. Samples were kept on ice, and made up to 25μl according to the volumes listed in Table 2.11.

Table 2.11: List of the reagents required per reaction for Polymerase Chain Reaction.

Reagent	Volume
Template cDNA (100 ng/µl)	1µl
Forward Primer (10uM)	1µl
Reverse Primer (10uM)	1µl
dNTPs (2.5mM)	2µl
10X DreamTaq™ Buffer	2.5µl
MgCl$_2$ (25mM)	0.5µl
GIBCO Water	16.875µl
Taq Polymerase	0.125µl
Final Volume	25µl

This mix was placed into a MJ-Mini gradient thermocycler (Bio-Rad) with hot-lid for thermal cycling. Samples were subjected to an initial denaturation step of 92C for 2 min. This was followed by 30 cycles of:

92°C for 1 minute,

Primer specific annealing temperature (See Table 2.10) for 1 minute,

72°C for 1 minute.

Followed with a final extension step of 72°C for 5 min. Samples were then stored at 4°C. PCR products were visualised using agarose gel electrophoresis (Chapter 2.2.3.4).

2.2.6.6 Quantitative Real Time PCR (qRT-PCR)

Following the optimisation of primers by standard PCR, they were used in qRT-PCR. This technique follows the same principle of PCR, with amplified DNA being quantified in real-time as it accumulates in the reaction. This quantification is facilitated using SYBR green dye. This specific dye fluoresces only when bound to the minor groove of double stranded DNA. The fluorescence is read by a laser at the end of every cycle – hence, the amount of cDNA product formed during the PCR cycles can be quantified in real-time and graphed. Relative quantification is used to analyse changes in gene expression in one sample relative to the untreated reference sample. This method compares the Cycle Threshold (Ct) value of one target gene to another (using the formula: $2\Delta\Delta CT$)—for example, an internal control or reference gene (*18S*)—in a single sample. The qRT-PCR experiments were carried out using an Applied

Biosystems 7900HT Fast Real-Time PCR machine. For each reaction, the reaction was prepared in accordance with the recipe in Table 2.12. A master mix of 90μl was prepared as triplicates of 25μl each were used for every sample. The 90μl provides extra to prevent pipetting error affecting the results. Samples were subjected to an initial denaturation step of $95^{o}C$ for 10 minutes, followed by 40 cycles of:

$95^{o}C$ for 15 seconds,

The Primer Specific annealing temperature for 1 minute,

$72^{o}C$ for 30 seconds.

After which, there was a final extension step of $72^{o}C$. Samples were prepared using *18S* gene–specific primers and run to the same specifics. Quantification of cDNA targets was normalised for differences across experiments/samples using the endogenous *18S* as an active reference gene.

Table 2.12: List of the components for qRT-PCR reaction. 25μl of this is taken for each of 3 reactions.

Component	Volume/concentration
cDNA	300 μg
Forward Primer	100pmol (roughly 2.0μl)
Reverse Primer	100pmol (roughly 2.0μl)
Universal SYBR Green PCR master mix	45μl
RNase free dH$_2$O	To a final volume of 90μl

2.2.7 Flow Cytometry

Flow Cytometry is a method used for the counting and sorting of cells and particles suspended in a fluid stream. Most flow cytometer machines can measure two types of light from cells; Light Scatter and Fluorescence.

Light scatter is the interaction of regular light with materials. The Millipore Guava® Flow Cytometer used in experiments possesses light scatter detectors opposite the laser and to one side of the laser, keeping in line with the intersection of the fluid flow/laser beam. The measurements made by these detectors are respectively called Forward Scatter and Side Scatter. Forward Scatter is used in providing information of the relative size of individual cells, and Side Scatter gives information on the granularity of cells.

Fluorescence is the property of a molecule to absorb light at one wavelength and re-emit light at a different wavelength.

This method was used to characterise the microparticles released from media as being endothelial in origin. The Guava® Flow Cytometer uses microcapillary technology in order to reduce the number of cells needed for analysis, as well as the amount of waste generated. Samples are able to be analysed from a 96 well plate as a result.

Figure 2.11: The Millipore FACS Guava EasyCyte System. Samples are loaded on the 96-well plate at the front.

2.2.7.1 Endothelial Microparticle Assay using the Millipore FACS Guava EasyCyte System

The microparticles were tagged with an APC-tagged antibody for VCAM-1 (Vascular cell adhesion molecule 1, also known as CD106). VCAM-1 is a noted endothelial cell marker, so this was used to indicate that the microparticles observed were endothelial in nature. Microparticles were prepared as listed in Chapter 2.2.2.3, following which they were resuspended with 0.2% Triton X-100 in PBS. The microparticles were incubated at 17-20°C for 5 minutes to allow them to become permeabilised before they were centrifuged again for 14000rpm for 20 minutes. The resulting pellet was resuspended in

450µl of PBS with 2% (v/v) Fetal Bovine Serum added. This suspension was divided into two Eppendorf tubes of 200µl each. One had 4µl of VCAM-1 antibody (1 µg) added to the sample, while the other was left as a blank negative control. The samples were set rocking at 4°C for 1 hour and covered in tinfoil to avoid natural light affecting the antibody, and centrifuged at 14000rpm for 20 minutes. Each pellet was then resuspended in 200µl of PBS. Each 200µl sample was added to a well of a 96-well plate before being read on the FACS Guava system.

2.2.8   Statistical Analysis

Results are expressed as a mean ± standard error of the mean, of three independent experiments (n=3), unless otherwise stated. Statistical comparisons in experiments were performed to determine if data sets were significantly different from one another using t-tests or two-way ANOVA where applicable. The t-test is used when the independent variable has two levels. ANOVA is used when the independent variable has more than two levels. A resulting p-value where $p<0.05$ indicates a significant change.

CHAPTER THREE

PALLADIN AS A HAEMODYNAMIC PROTEIN IN ENDOTHELIAL CELLS

3.1 INTRODUCTION

The results from many *in vitro* studies have shown that shear stress and/or mechanical strain can modulate the expression of genes involved in actin cellular dynamics and polymerisation functions (Kris *et al.*, 2008; Gunst and Zhang, 2008; Osborn *et al.*, 2006). As stated previously, actin is a vital protein within the cell, and plays a huge role in facilitating cell structure and motility. Furthermore, the types of mechanical stimulation can also modulate the regulation of many genes that play an important role in the patho-physiology of cardiovascular disease (CVD) through the alteration of cell fate and function (Chan *et al.*, 2010). The *PALLD* gene, which encodes for the Palladin protein, is one such gene. Palladin is a known actin-binding protein (Dixon *et al.*, 2008), having been observed in structures containing actin filament bundles (Parast and Otey, 2000). However, despite the observation of this actin associated protein in many cell types it has yet to be properly characterised within cells of an endothelial nature. The protein was briefly identified within endothelial cell nuclei in human coronary vessels with atherosclerosis (Jin *et al.*, 2010), but this appears to be the extent of an understanding of the presence/role of Palladin in endothelial cells.

The aim of the work presented in this thesis was to investigate the expression of the Palladin protein and the *PALLD* gene within Human Aortic Endothelial Cells (HAECs). The goal of this chapter however, is the cellular and molecular characterisation of the gene and protein expression response to the haemodynamic forces experienced within the vasculature, namely cyclic strain and laminar shear stress. Cyclic strain affects cell proliferation, resulting in actin stress fibre formation and cellular realignment (Von Offenberg Sweeney *et al.*, 2005). Shear stress also changes cell morphology, with immediate shear inducing stress fibre and microfilament formation, while chronic shear results in the partial disassembly and subsequent reassembly of actin filaments at adherens junctions and focal adhesions (Orr *et al.*, 2006b; Osborn *et al.*, 2006). Palladin has been shown to be an actin-binding protein, localising and functioning in different areas of the cell (Otey *et al.*, 2005; Jin *et al.*, 2010). The protein also has been shown to have a role in many actin-related cellular functions such as migration (Rachlin and Otey, 2006; Goicoechea *et al.*, 2010). Because of these characteristics of Palladin, it was hypothesised that this protein may then display differential expression levels in response to the haemodynamic forces (cyclic strain and laminar shear stress) that the endothelial

cell layer is subjected to. As actin expression changes in response to force-induced cellular remodelling, the expression in the actin-binding Palladin should also be altered.

In this chapter, following the initial characterisation of the Human Aortic Endothelial Cell (HAEC) type used in the study, Palladin is then identified in HAECs through immunofluorescence methods for visual confirmation of the presence of the protein within the cells. However, Palladin is known to exist in multiple isoforms (Rachlin and Otey, 2006). There are no commercially available antibodies specific for an individual isoform, so while the immunofluorescence images show that Palladin is present, they cannot illustrate which isoforms are being stained. The antibodies utilised in the immunofluorescence imaging experiments were also used in Western Blotting experiments; firstly to reinforce the conclusion that Palladin is present in HAECs, and secondly to distinguish the isoforms that exist in the cells. Analyses of lysates from other cell types such as HaoSMC or HEK-293 are also provided as a comparative control to show which, if any, Palladin isoforms are present in the cells. By doing this, it highlights how there are multiple isoforms visible in cell types (as demonstrated in Table 1.2), while at the same time confirming that Palladin is present in HAECs, and that it exists in multiple isoforms within the cell. The 90kDa isoform was primarily investigated; on account of it being the first Palladin isoform to be discovered, and because it is the most discussed isoform in literature (Parast and Otey, 2000; Goicoechea *et al.*, 2010; Pogue-Geile *et al.*, 2006).

The genetic and proteomic responses of this isoform in HAECs subjected to cyclic strain stimulation are first demonstrated. The cells were strained for a variety of different time points under both physiological (5%) and pathological (10%) strain models using the Flexercell system as detailed in Chapter 2.2.2.1. The rationale for using time points was that they would illustrate the pattern of expression of Palladin in the cells following both immediate and long term stimulation, showing when any changes may occur in expression over the time period. In doing so, it demonstrates whether an immediate increase of Palladin expression is subject to reduction, or if it remains elevated. Observation of the Palladin response to these strain models is achieved through qRT-PCR and Western Blotting techniques, to validate gene and protein expression, respectively. Graphs are illustrated to show the patterns of strain-induced gene expression compared with strain-induced protein expression, to determine if post-strain Palladin expression is correlated.

Results were then compared to one another to demonstrate differences in expression between the 5% physiologically and 10% pathologically strained cells in order to show the effects the different strain models have on Palladin regulation. Pathological levels of strain are responsible for haemodynamic dysregulation (Safar *et al.*, 2012; Ando & Yamamato, 2011) so was hypothesised that there would be more Palladin expressed in the pathological strain, owing to the elevated instances of cell remodelling that occur with this condition; necessitating the need for increase of actin-binding proteins to assist in restructuring the cell (Collins *et al.*, 2005).

After showing that Palladin can be expressed in different isoforms across the cell types, a brief experiment was performed to show how the patterns of expression following haemodynamic stimulation may also be different. Western Blotting is used to characterise the response of Palladin to pathological cyclic strain in Human Aortic Smooth Muscle Cells, highlighting the difference in expression trends across the different layers of the macrovasculature. Cyclic strain affects smooth muscle cells (Birukov, 2009; Qi *et al.*, 2010; Salameh and Dhein, 2013) but has been seen to be more influential on endothelial cells, where the mechanical force of strain plays an important role in cell migration (Von Offenberg Sweeney *et al.*, 2005). The role of Palladin in smooth muscle has also already been shown in greater detail (Goicoechea *et al.*, 2006; Jin *et al.*, 2011). Hence, experiments stayed investigating endothelial cells rather than further investigating Palladin in smooth muscle. Many experiments also dealt with investigating responses to laminar shear stress, which smooth muscle cells are largely not subjected to, as it causes apoptosis (Fitzgerald *et al.*, 2008).

Correspondingly to the strain experiments, the expression of the Palladin (both genomic and proteomic) response to laminar shear stress (LSS) of HAECs is also investigated in this chapter. The presence of Palladin in sheared cells is firstly illustrated with immunofluorescence imaging. As stated earlier, under normal physiological conditions the endothelium is exposed to roughly 10 dynes/cm^2 of LSS (Thorin and Thorin-Trescases, 2009). By subjecting static cells to this force, the changes in expression of Palladin can be observed in tandem with the morphological changes of the HAECs. When mechanical force is applied to the cell in the form of flow, both the orientation and the thickness of the resulting stress fibres has been shown to become altered (Gavard *et al.*, 2004; Vasioukhin *et al.*, 2000). As the actin fibres restructure at different shear time points – from both immediate and chronic shear stress, it is postulated that Palladin expression may be then altered too.

The resulting changes in expression observed initially confirm that Palladin responds to haemodynamic force, which in turn provided a foundation for further research. The characterisation of interacting proteins, and the functional role coupled with shear-induced microparticle release and are discussed in Chapters 4 and 5 respectively, while the rest of this chapter further characterises Palladin expression under shear conditions.

Following LSS, qRT-PCR and Western Blotting methods illustrated the change in expression over time points while immunofluorescence of endothelial cells displayed the localisation of Palladin within the cell. However for a more detailed and quantifiable approach to characterising the changes in Palladin expression, sheared HAECs were subjected to Proteocellular Fractionation, a technique involving the chemical separation of the different subsets of the cell - Cytosol, Membrane/Organelles, Nucleus and Cytoskeleton. It was hoped that probing each subset separately post-shear would contribute to understanding the more precise localisation of Palladin in response to haemodynamic force. Palladin has been observed to co-localise in different areas of the cell, such as the nucleus, cytoskeleton or the cell membrane (Goicoechea *et al.,* 2006; Rachlin and Otey, 2006). Through the fractionation of the cells sheared at the different time points, a pattern of adaptive localisation of Palladin can be created; whereby the shear-induced regulation of Palladin at different areas of the cell in response to laminar shear stress can be characterised.

The mechanical forces of laminar shear stress and cyclic strain are converted by the cells into biochemical signals through the process of mechanotransduction. A receptor group known as mechanosensors differentiate between physiological and pathological haemodynamic stimuli. As discussed in more detail in Chapter 1, a related group of mechanosensitive signalling molecules – integrins - are capable of affecting binding affinity to ECM ligands, affecting cell adhesion, progression and motility (Hynes, 2002; Shattil, Kim and Ginsberg 2010). Interactions of the cells with the extracellular matrix (ECM) are essential for many cell functions including proliferation and migration (Hirata *et al.*, 2008). It has long been shown that the cell function is controlled directly or indirectly by the substrate on which the cells are resting on (Gospodarowicz *et al.*, 1980; Lu *et al.*, 2011). Inside the cell, the actin cytoskeleton anchors to a cluster of integrins which themselves attach to ECMs. The types of integrins in adhesions can also switch as they mature, which may be related to distinct functions (Geiger and Yamada 2011). For example, the α5β1 integrin is initially present in focal adhesions formed on a fibronectin substrate, along with αvβ3, but is lost from these adhesions unless the

fibronectin is immobilized, in which case it forms exaggerated α5β1-containing focal adhesions (Katz *et al.*, 2000; Huveneers *et al.*, 2008).

Integrins are highly influenced by haemodynamic stimuli. Laminar shear stress converts them to a high affinity state, where they then bind to the subendothelial extracellular matrix (Orr *et al.*, 2005). This binding is integrin and matrix specific, and is important for cellular development, adhesion, maintenance and repair (Harburger and Calderwood, 2009). It has been shown that under shear stress, certain nonpermissive extracellular matrices can interfere with integrin signalling (Orr *et al.*, 2006). The failure of these integrins to be activated on the nonpermissive matrices is due to active suppression by the ligation of integrins, which can suppress the activation of other integrins through transdominant inhibition (Calderwood *et al.*, 2004). Permissive matrices include fibrinogen and fibronectin, whereas the nonpermissive ECMs include collagen and laminin (Decleva *et al.*, 2002). Fibrinogen is observed to increase with elevated CVD risk factors (Stec *et al.,* 2000) while fibronectin is also observed to increase following elevated shear stress (Steward *et al.,* 2011). The formation of actin stress fibres and upregulation of integrins such as the α5 group can enhance the permissive effects of fibronectin (Nakamura *et al.,* 2003). It appears that in CVD events, certain matrices become more permissive than they would be under normal physiological conditions. Conversely, collagen has been observed to reduce and halt endothelial cell alignment following shear stress (Kemeny *et al.,* 2011).

These ECM proteins are therefore capable of altering cell function and phenotype through the activation of specific integrins which support the flow activation of inflammatory pathways, such as NF-κB (Orr et al., 2005). As a method of investigating potential signalling pathways of Palladin, the expression of Palladin following shear stress of HAECs is assayed again, but in this case the cells have first been allowed to adhere to a variety of different ECMs – fibrinogen, fibronectin or collagen. In theory, Palladin expression will be affected by the specific extracellular matrix related signalling mechanisms following mechanical stimulation of the endothelial cell. As the actin cytoskeleton will change expression and anchor to an integrin cluster as it attaches to the ECMs, so too should the Palladin protein. In particular, different expressive patterns of Palladin should be observed between the cells sheared on the permissive versus the nonpermissive matrices.

Through the observation of these expression patterns of the sheared matrix seeded cells, coupled with the comparison to cells the patterns on uncoated culture dishes, a possible integrin-mediated signalling pathway involved in Palladin expression may be discovered or at least suggested. While further work may be needed to pinpoint the exact integrins involved in Palladin expression, the results shown here in this chapter should provide the foundation for future, more precise investigations.

3.1.1 Study Aims

The experiments performed in this chapter seek to determine if the Palladin protein is regulated by haemodynamic forces at the gene transcription and/or protein level and to determine the proteomic response following cell-matrix interactions. Therefore the overall aims of this chapter are:

- To characterise the presence of the actin-binding Palladin protein and its isoforms within Human Aortic Endothelial Cells (HAECs)

- Determining the specific patterns of Palladin expression when the vascular HAECs are subjected to time points of mechanical haemodynamic stimulation, namely cyclic strain and laminar shear stress.

- Observation of the localisation of the Palladin protein in HAECs and examination of its translocation following laminar shear stress stimulation.

- Investigation of the potential integrin signalling pathways involved in Palladin expression through interactions of the cells with permissive and nonpermissive extracellular matrices – fibrinogen, fibronectin and Type IV collagen - following laminar shear stress.

3.2 RESULTS

The first experiment presented here was a simple Western Blot using the lysates from a variety of cell types. These cell types were Human Embryonic Kidney-293, Rat Aortic Smooth Muscle cells, Human Aortic Smooth Muscle cells and Human Aortic Endothelial Cells. Lysates were probed using an antibody specific for vonWillebrand Factor. This glycoprotein is produced in the Weibel-Palade bodies in the endothelium; therefore it can be utilized as an endothelial specific marker to validate the commercially bought cell type. A band is shown to be present at 300kDa in size within the endothelial cell lysate but is absent in the other samples. This confirms the endothelial nature of the HAECs for use in the other experiments.
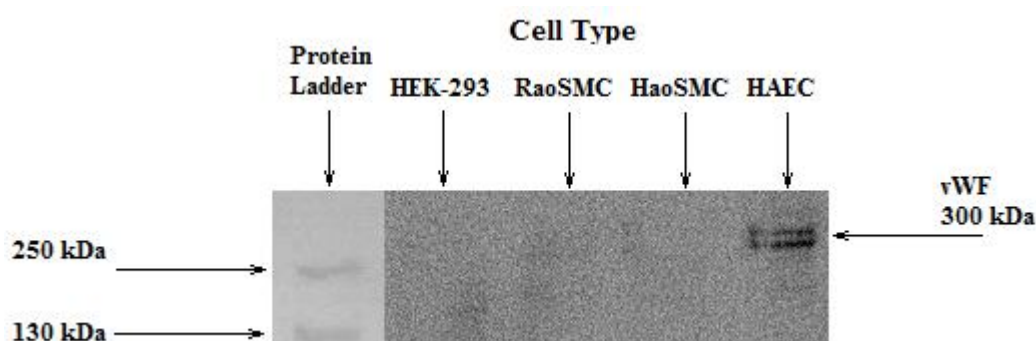
Figure 3.1: Characterisation of HAECs with vonWillebrand Factor. Western Blotting of lysates from four different cell lines (HEK-293, RaoSMC, HaoSMC and HAEC) was performed to specifically detect vonWillebrand Factor, an endothelial protein marker. The other non-endothelial cell types were used as a negative control. The endothelial cell stock analysed here was subsequently used for later experiments.

The HAECs were then probed to show the presence of Palladin – the protein of interest investigated within this thesis. Results of immunofluorescence imaging indicate that the protein is indeed present. Palladin (stained in green) can be observed in the below images localising in both the nucleus (designated as N), and to stress fibres (designated as SF). Images at closer (400X) magnification show the precise localisation of Palladin within the cell nuclei and stress fibres.

(i)   **(ii)**

(iii)   **(iv)**
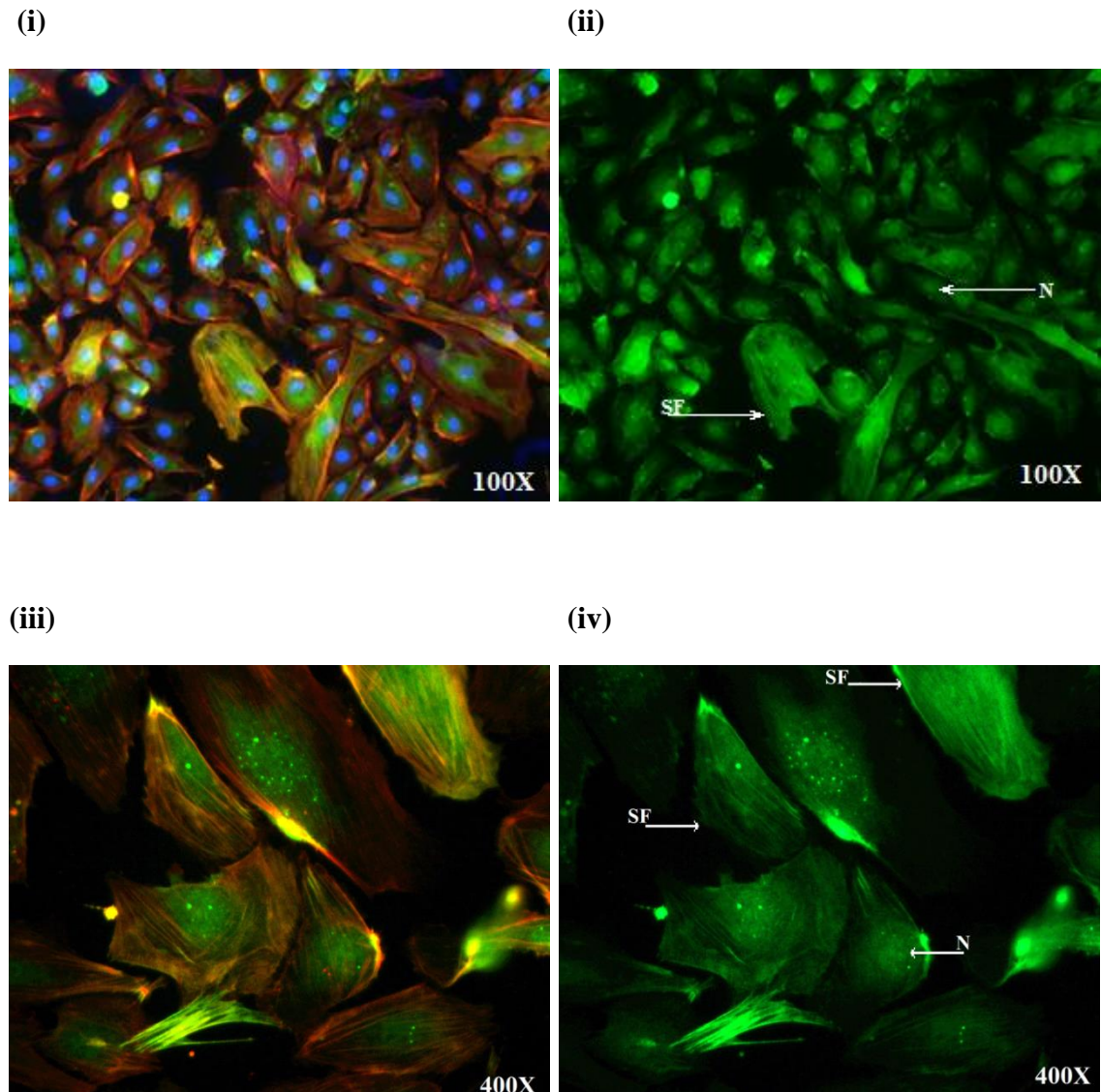
Figure 3.2: Immunofluorescence imaging of Palladin in static HAECs. In Figure 3.2 (i), the cells are stained with DAPI (a blue, nuclear-specific stain), Phalloidin (which stains actin red) and an AlexaFluor-488 conjugate that binds with the Palladin antibody (Green in colour). These cells are viewed at 100x magnification. The cells in Figure 3.2 (ii) are prepared according to the same conditions - but without DAPI or Phalloidin stain, to allow better viewing of Palladin. Palladin can be observed localising in the nucleus (N), and to stress fibres (SF). Figure 3.2 (iii) shows HAECs at 400x magnification and stained in the same manner, but without the DAPI stain. Figure 3.2 (iv) displays just the Palladin conjugated stain on the same cells as in (iii). Again, localisation of Palladin in the nucleus (N), and to stress fibres (SF) is highlighted.

After confirming that the cell stock being used was indeed endothelial in nature and that Palladin is present within them, the lysates were then probed via Western Blot to detect the separate isoform types. As before, alternative cell type lysates are probed at the same time as the HAEC lysate. Figure 3.3 below shows how Palladin is present in different combinations of isoforms depending on cell type. Presence or absence of isoforms in the cell types is summarised in Table 3.1. The 90kDa Palladin isoform - the isoform mostly discussed in literature – is notably the only type present across all the cell types examined. In HAECs, three of the other isoforms – 122, 128 and 140kDa - are also observed. These isoforms are also seen in HaoSMCs, highlighting that these are the main isoforms in the vasculature. Subsequent studies focused on the 90kDa isoform. Fainter bands are also seen in HAECs at 43kDa and 60-65kDa indicating further Palladin isoforms, albeit in lesser quantities. Protein marker is illustrated along the side to indicate the molecular weights of each of the bands. While the diagram accounts for the known isoforms listed, there appears to be light bands visible at roughly 50-55kDa. There are still undiscovered isoforms of Palladin which have yet to be fully characterised, which could account for the visibility of these bands.
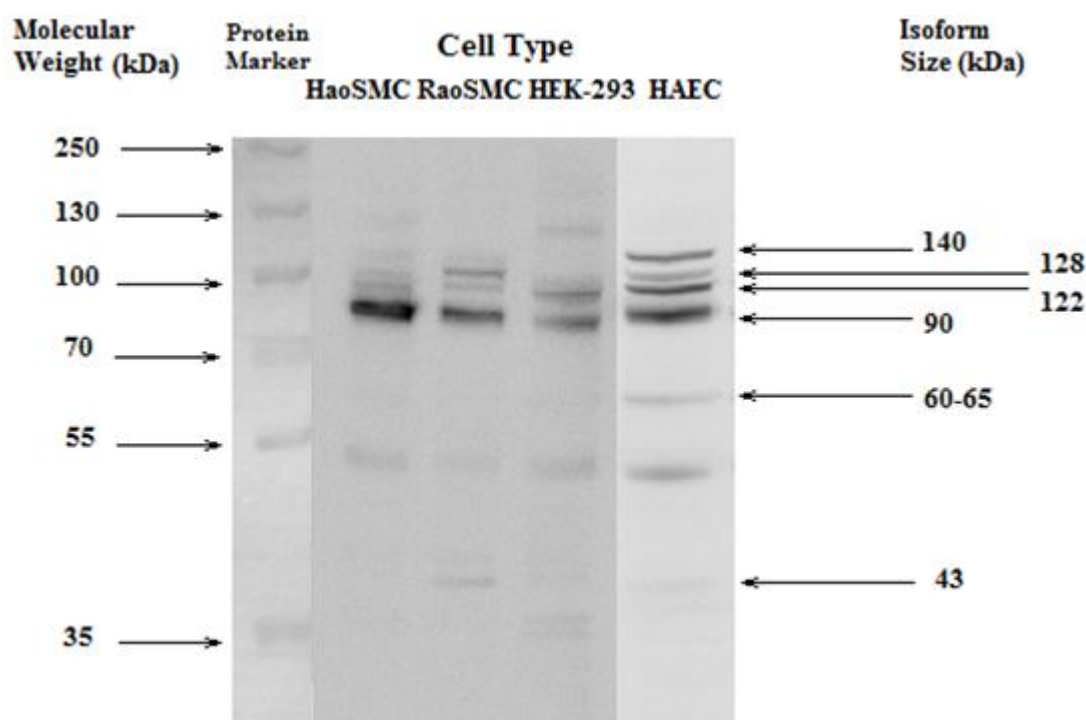
Figure 3.3: Observation of Palladin isoforms in cell types – HaoSMC, RaoSMC, HEK-293 and HAECs. Western Blotting of lysates from the four different cell types was performed to distinguish the different Palladin isoforms in cell types. The fourth cell type - HAECs - are primarily utilized within the remainder of the results, with the 90kDa isoform (the strongest band) being the primary isoform studied.

Table 3.1: List of isoforms of Palladin present in cell types. The table below summarises the data from Figure 3.3. It illustrates whether any of the known Palladin isoforms are determined to be present in the analysed cell type (Y) or absent (N).

Cell type			Isoform				
	43	60-65	90	122	128	140	200
HaoSMC	N	N	Y	Y	Y	Y	N
RaoSMC	Y	N	Y	N	Y	Y	N
HEK-293	N	N	Y	Y	N	N	N
HAEC	Y	Y	Y	Y	Y	Y	N

The HAECs were subjected to haemodynamic forces, similar to those experienced within the vasculature, to investigate their effects on Palladin expression. Since Palladin is an actin-binding protein, it was hypothesised to change in expression following force-induced cell remodelling. HAECs were subjected to cyclic strain at physiological (5%) and pathological levels (10%) of strain. Following this, expression of the PALLD gene was analysed using qRT-PCR methods. Results are expressed by the relative quantification values deduced from the analysis software.

Figure 3.4 illustrates the gene expression after cells were subjected to physiological strain for a series of time points. Within 1 hour of strain, there is over a 50% increase in PALLD gene expression. However, at 2-3 hours, the expression levels decline to below-static baseline levels. At 6 hours, expression has become upregulated again, where it reaches a similar peak to that seen at 1 hour. There is a slight decline at 24 hours, suggesting that gene expression may be declining again.

The effects of pathological strain on gene expression are shown in Figure 3.4.1. In this figure, gene expression is shown to only slightly increase within the first 2 hours of strain, staying at a plateau. It is only at 3 hours when it rises to a larger level, with a spike in the relative quantification value. Gene expression declines at 6 hours, but is still greater than baseline levels. Following this, at 24 hours expression spikes again, reaching its peak value at roughly at 2.5x the value of the static control cells.

The data for both physiological and pathological gene expression is compared in Figure 3.4.2. Here, the relative-to-baseline values are expressed alongside one another. At 1 hour, gene expression is higher at 5% strain than 10%. However, following this, the levels of 10% strain gene expression overtake that of 5% - slightly at 2 hours, but massively at 3 hours. At 6 hours, that the sample values balance to a similar, above-baseline, level. But at 24 hours, the pathologically induced gene expression outweighs the physiologically induced, with there again being a huge difference in relative gene expression between the two samples.
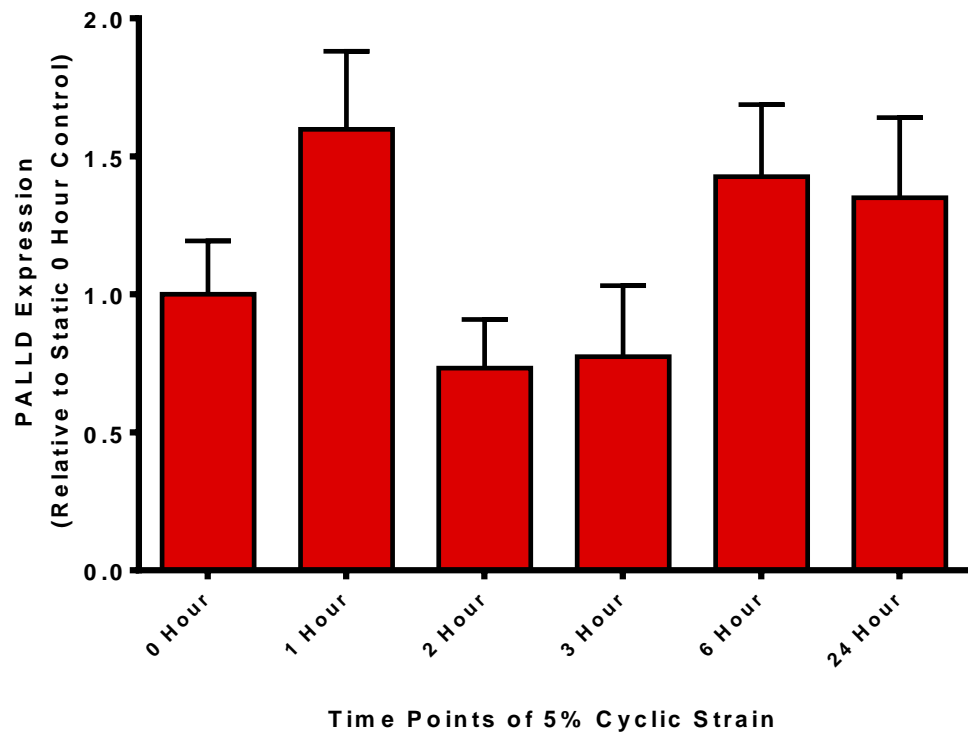
Figure 3.4: Expression of the *PALLD* gene in HAECs at 5% Cyclic Strain. mRNA was extracted from cells subjected to 5% physiological cyclic strain at varied time points, and synthesised into cDNA. qRT-PCR was performed on this cDNA to observe expression of the *PALLD* gene – the 90kDa isoform - and results were normalised against the *18S* gene. Histograms represent fold change in gene expression relative to the unstrained zero hour cyclic strain control and are averaged from three independent experiments ± SEM. Statistical analysis failed to show P<0.05.
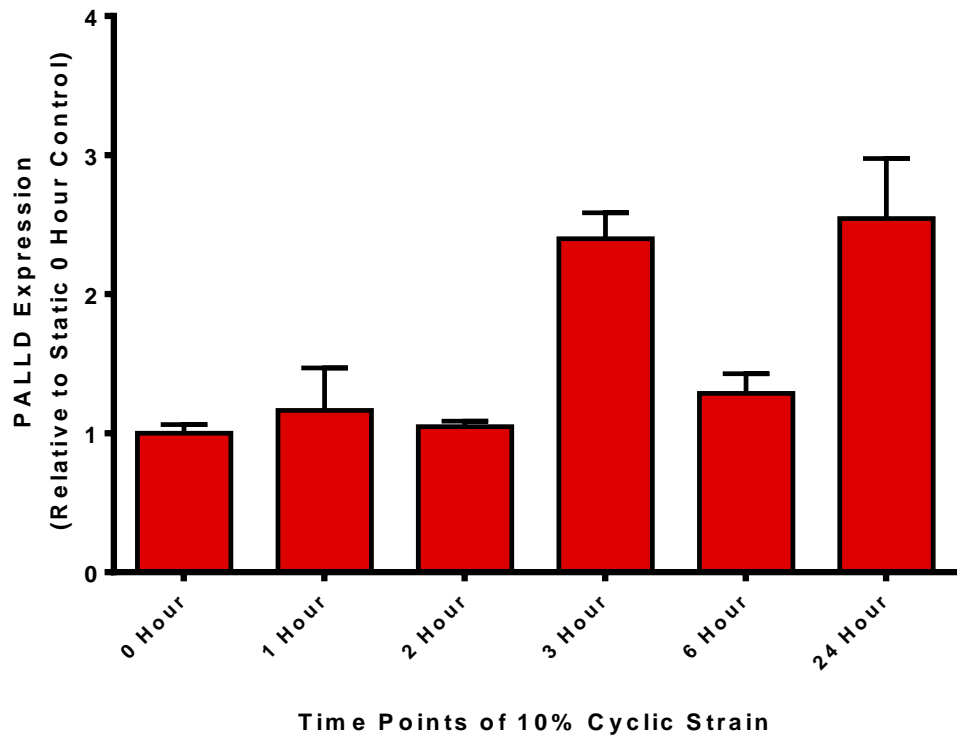
Figure 3.4.1: Expression of the *PALLD* gene in HAECs at 10% Cyclic Strain. mRNA was extracted from cells subjected to 10% pathological cyclic strain at varied time points, and synthesised into cDNA. qRT-PCR was performed on the cDNA to observe expression of the *PALLD* gene, and results were normalised against the *18S* gene. The fold changes in expression are shown on the graph relative to zero hour cyclic strain. Data is representative of three independent experiments ±SEM. Statistical analysis showed that P=0.06, showing that results were not significant.
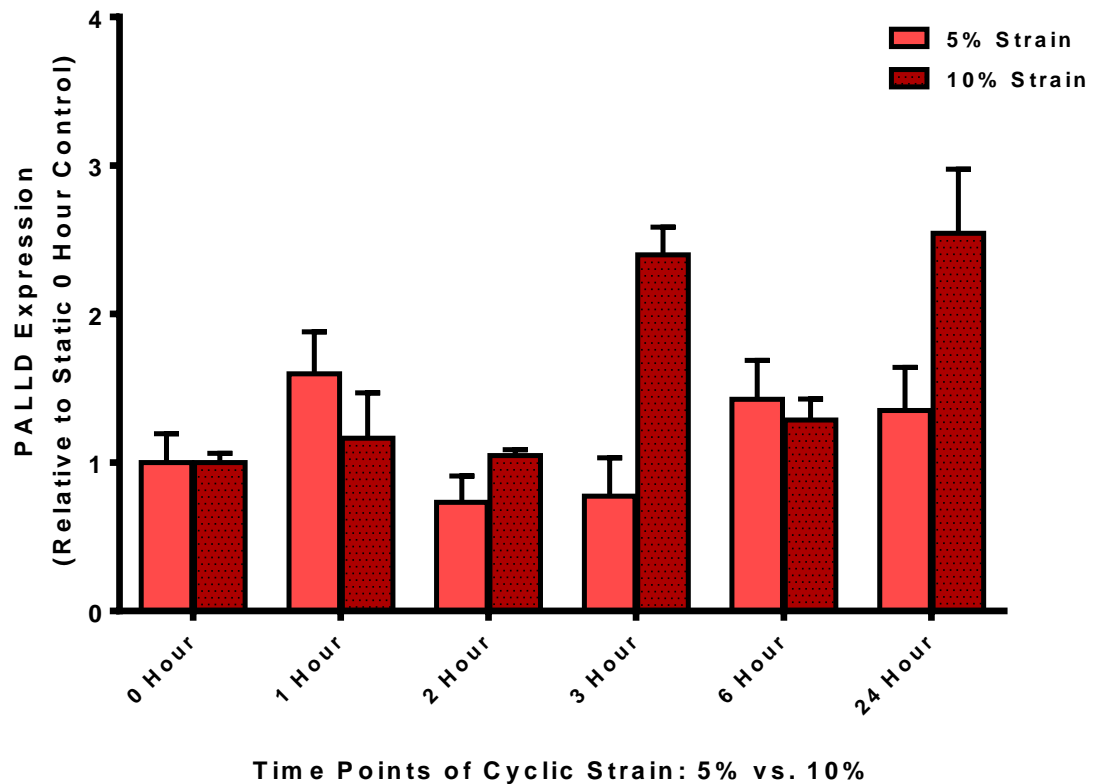
Figure 3.4.2: Comparative trends of *PALLD* gene expression in 5% vs. 10% Cyclic Strain. In this figure, Figures 3.4 and 3.4.1 are compared against each other to show the differential effects in a physiological (5% - Light Red) vs. pathological (10% - Dark Red) strain of HAECs**.**

Protein was next extracted from similarly strained HAECs, quantified and run on a Western Blot gel. The resulting membrane was probed with antibodies for Palladin and GAPDH (as an endogenous control to normalise protein expression). Figure 3.5 below shows expression within cells subjected to 5% physiological strain, where there appears to be protein bands present across all time points. The densitometric analysis of the 90kDa isoform bands show that, when normalised against GAPDH and compared to the unstrained control sample, Palladin appears to increase in expression immediately following 1 hour of physiological strain. However, expression declines steadily after increasing time points of strain, resulting in the Palladin protein becoming downregulated by 24 hours. At this point, protein expression is lower than in static cells (0 hours).

Figure 3.5.1 compares the PALLD gene expression and Palladin protein expression of HAECs both subjected to 5% cyclic strain. The expression patterns for both experiments appear similar, immediately increasing following stimulation of the cell within the first hour. However, they reduce by 3 hours of strain. There appears to be a difference in the gene and protein expression then at 6-24 hours. Even though it appears to be on a declining trend, PALLD gene expression still stays above static levels at this time. Meanwhile, at the same time points, the comparative protein expression reduces below the static baseline level. It should be noted that statistical analysis of the protein expression did not prove it to be significant (standard error between repeat analyses was too large, resulting in p-values greater than 0.05). However, a decline is shown in both gene and protein expression following the initial 1 hour peak. Taking the results together suggests that there may still be a decreasing trend of Palladin expression existing after physiological cyclic strain.
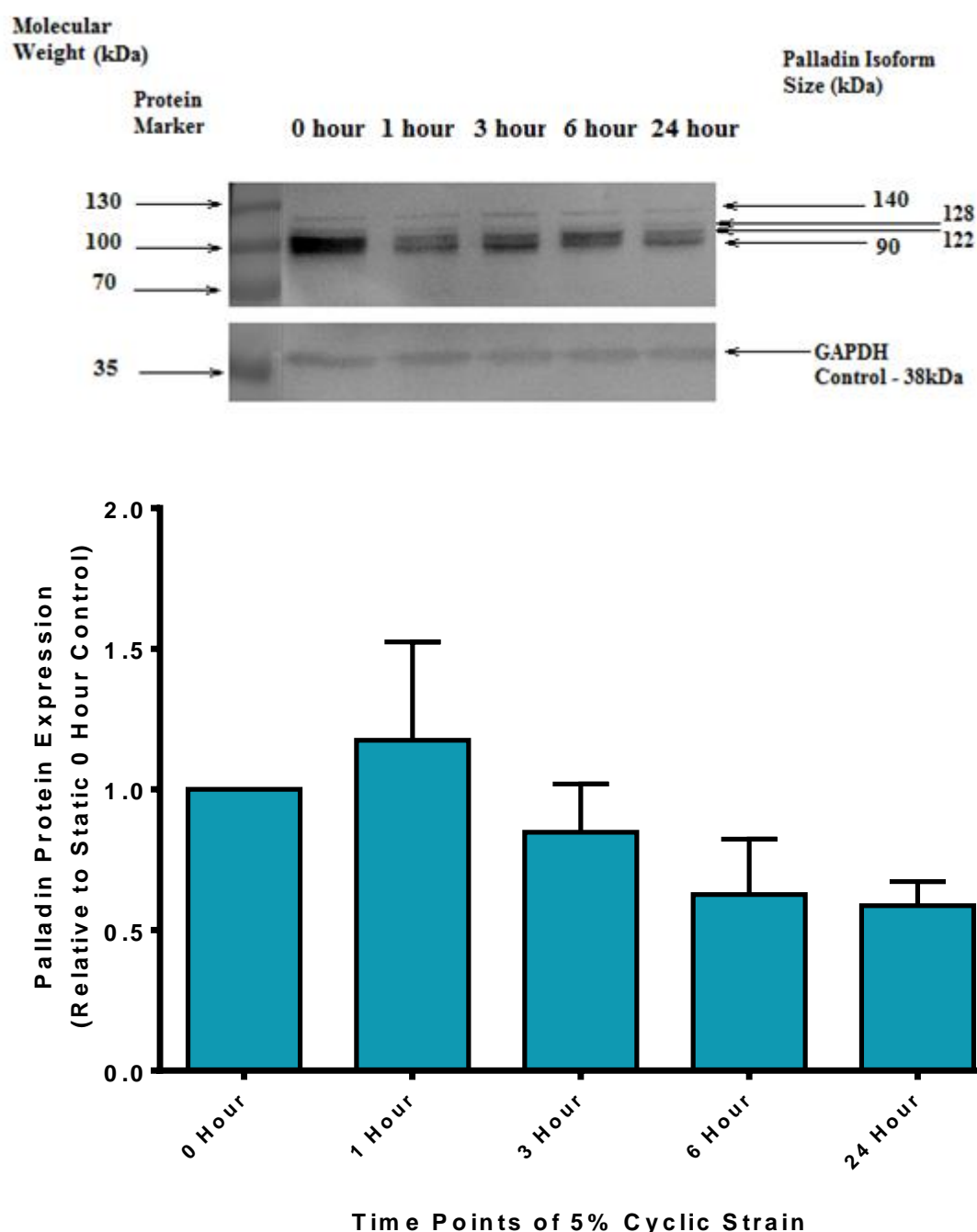
Figure 3.5: Expression of the Palladin protein in HAECs at 5% Cyclic Strain. Cells were subjected to time points of 5% physiological strain on the Flexercell system. Following each allotted time point, cells were lysed and Western Blot analysis of the protein was performed, probing for Palladin and GAPDH (as a normalizing control). Protein marker is illustrated along the side to indicate the molecular weights of each of the bands. Following Western Blotting, the blot was analysed using ImageJ densitometric quantification software. The values given for intensity of each 90kDa-sized Palladin band is given here, following normalisation against the GAPDH control bands and expressed in relative quantities compared to the zero hour unstrained cells. Data is representative of three independent experiments ±SEM. Statistical analysis however showed $p > 0.05$, indicating that the resulting changes in expression are not statistically significant.
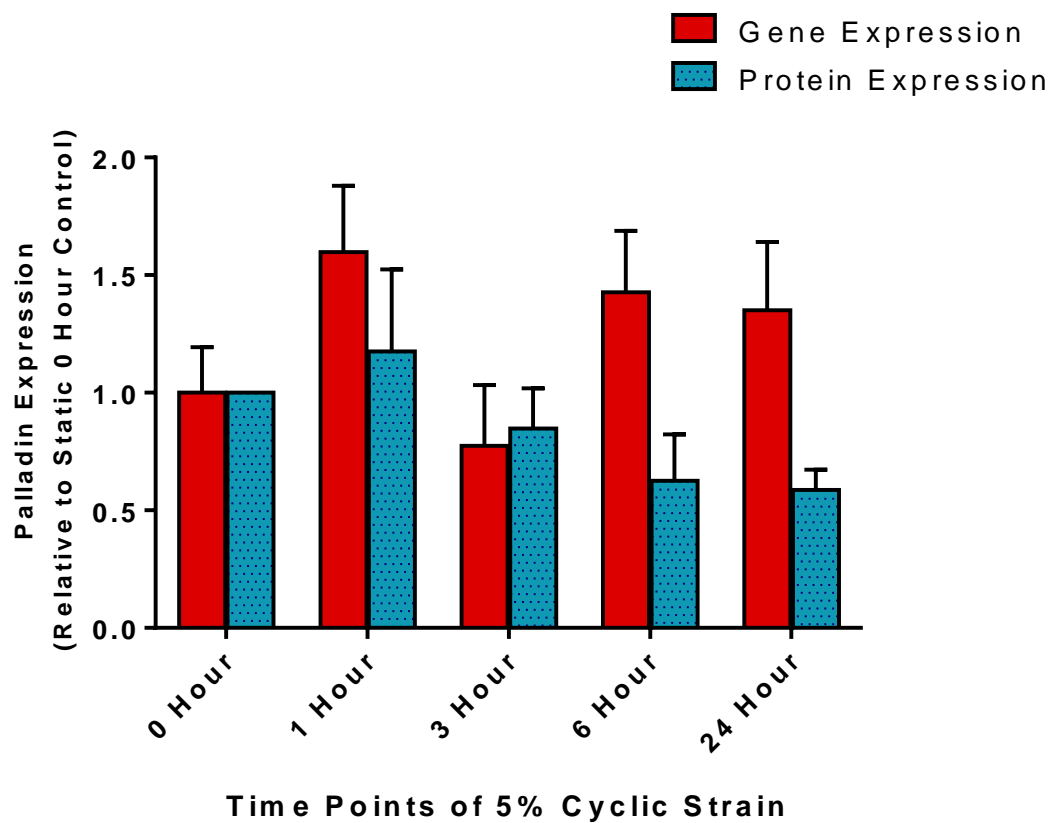
Figure 3.5.1: Comparative trends of Palladin protein expression and *PALLD* gene expression in HAECs subjected to 5% Cyclic Strain. This figure is added to compare the expression of Palladin expression following prolonged time points of 5% physiological cyclic strain. The relative-to-static cell gene expression (Red) is plotted against relative-to-static protein expression (Blue).

HAECs were next subjected to time points of pathological (10%) strain using the Flexercell system and protein was analysed as before. Figure 3.6 demonstrates how there is Palladin expressed across the different time points of pathological strain. The densitometric and statistical analysis of the 90kDa sized bands of Palladin shows that following normalisation, there is a significant two-fold increase in Palladin expression following the immediate 10% strain. The protein appears to remain around this level up to 6 hours, before the rate appears to decline. This decline still remains above the baseline (zero hours) level by 24 hours. However, it should be noted that the values for 3 hours or more of strain did not prove to be significant (p is <0.1, but greater than 0.05). This lack of significance was caused due to a larger standard error between triplicate samples affecting the analysis.

Figure 3.6.1 compares the PALLD gene expression and Palladin protein expression of HAECs subjected to the pathological 10% cyclic strain. The expression patterns for both experiments show a mildly similar pattern. Both expression levels immediately increase following stimulation of the cell within the first hour. However, the relative-to-baseline protein expression is greater than the relative-to-baseline gene expression. At 3 hours, and again at 24 hours, gene expression becomes greater than the relative protein expression.

Figure 3.6.2 illustrates the comparison of relative protein expression between the physiologically and pathologically strained HAECs. Both treatments show increase of expression within the first hour of strain, followed by a downward trend as the expression rates decrease. However, the decline is shown to be faster within the 5% strained cells, as the pathologically strained cells still express more Palladin at all the time points than the baseline static cells.
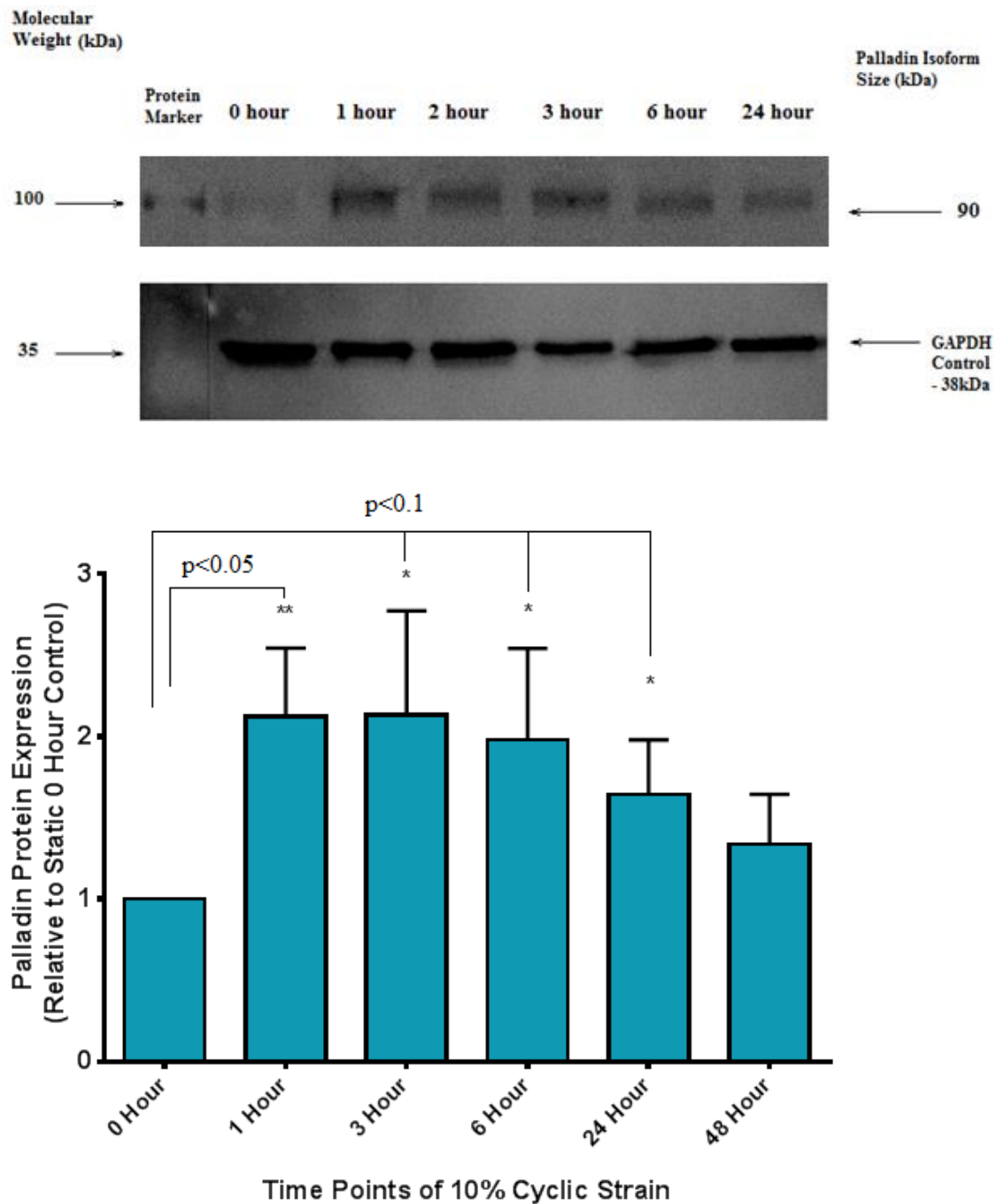
Figure 3.6: Expression of the Palladin protein in HAECs at 10% Cyclic Strain. Cells were subjected to time points of 10% pathological strain. The lysates obtained were probed using Western Blotting methods for Palladin and GAPDH (as a control). Following this, the blot was analysed using ImageJ densitometric quantification software. The values given for intensity of each 90kD-sized Palladin band is given here, following normalisation against the GAPDH control bands and expressed in relative quantities compared to the zero hour static cells. Data is representative of three independent experiments ±SEM. *p<0.1 – the results are not significant. **p<0.05.
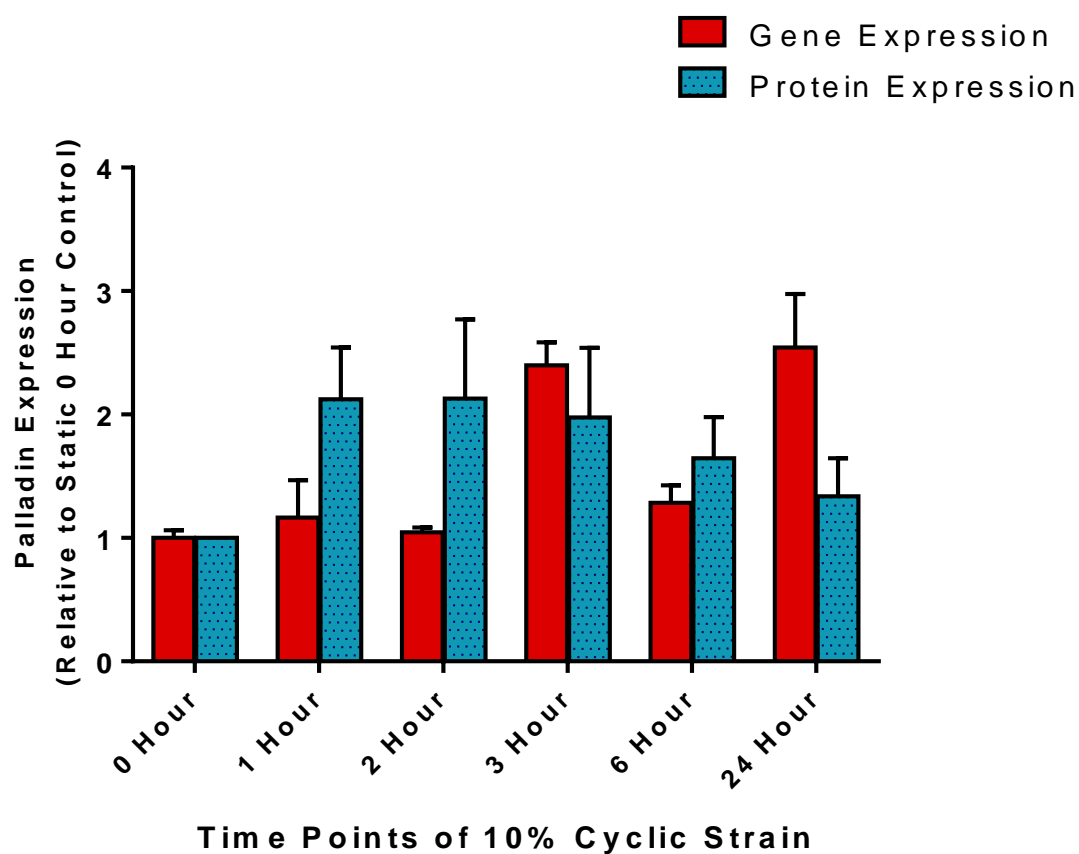
Figure 3.6.1: Comparative trends of Palladin protein expression and *PALLD* gene expression in HAECs subjected to 10% Cyclic Strain. This figure serves to compare the expression of Palladin expression following prolonged time points of 10% pathological cyclic strain. Relative gene expression is plotted (Red) against relative protein expression (Blue).
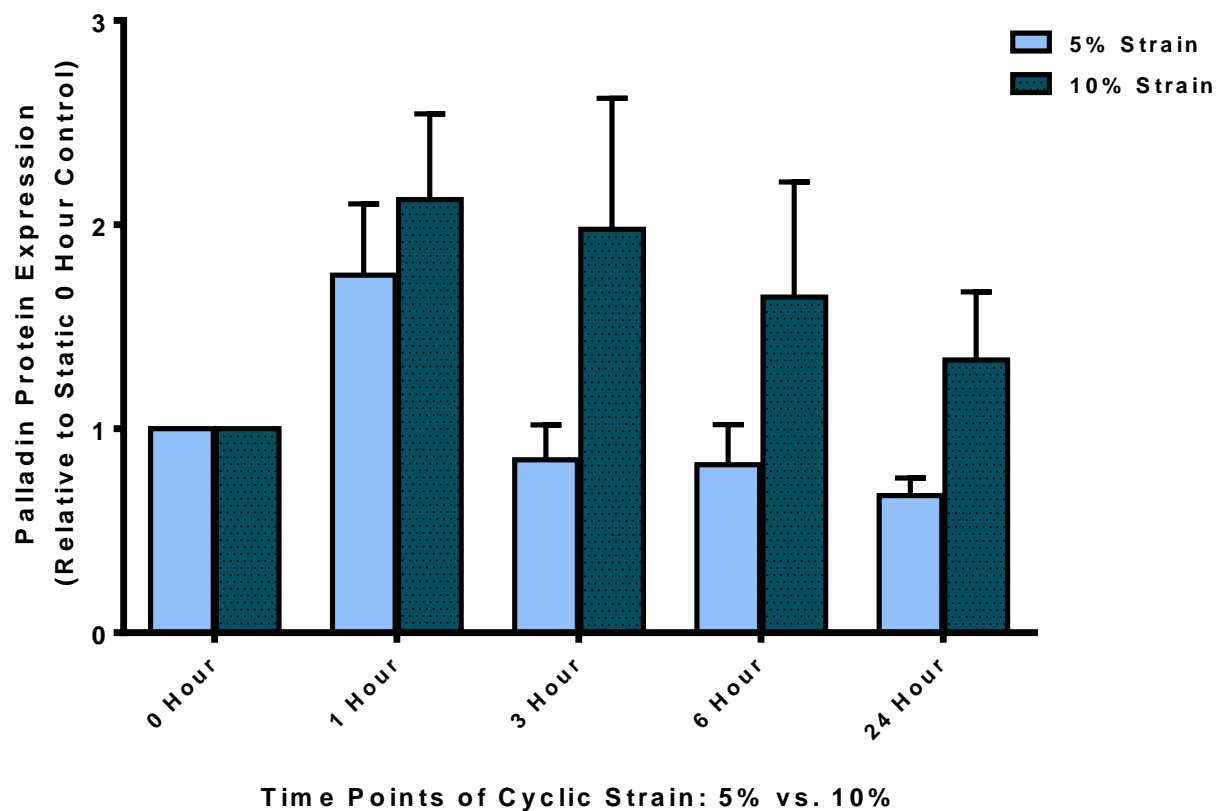
Figure 3.6.2: Comparative trends of Palladin protein expression in HAECs subjected to 5% vs. 10% Cyclic Strain. In this figure, Figures 3.5 and 3.6 are compared against each other to show the differential effects of physiological (5% - light blue) vs. pathological (10% - dark blue) strain of HAECs.

Palladin has been shown here to be upregulated in response to cyclic strain within endothelial cells. A brief experiment was devised, highlighting how Palladin is haemodynamically regulated in other cells while also showing that protein expression following haemodynamic stimulation may show different patterns across the vasculature. HaoSMCs were subjected to cyclic strain (at a 10% pathological level) for different time points. Palladin has been already been shown in the literature to be highly expressed in smooth muscle, playing an important role in cytoskeletal organisation (Jin, 2011; Wang and Moser, 2008), while previous experiments (Figure 3.3) confirmed its presence here.

Protein was obtained from the HaoSMCs and probed via the same Western Blotting methods as used before. Figure 3.7 shows strong Palladin bands for all the time points, with multiple isoforms displayed. Densitometric analysis of the 90kDa sized bands shows Palladin increasing in HaoSMCs following pathological strain. The increase following 6 hours of cyclic strain is almost two-fold. This stays increasing over 12-24 hours, where the relative expression is even greater. At 48 hours, the expression begins declining when compared to the previous 24 hour sample, but it still remains higher than the baseline sample.
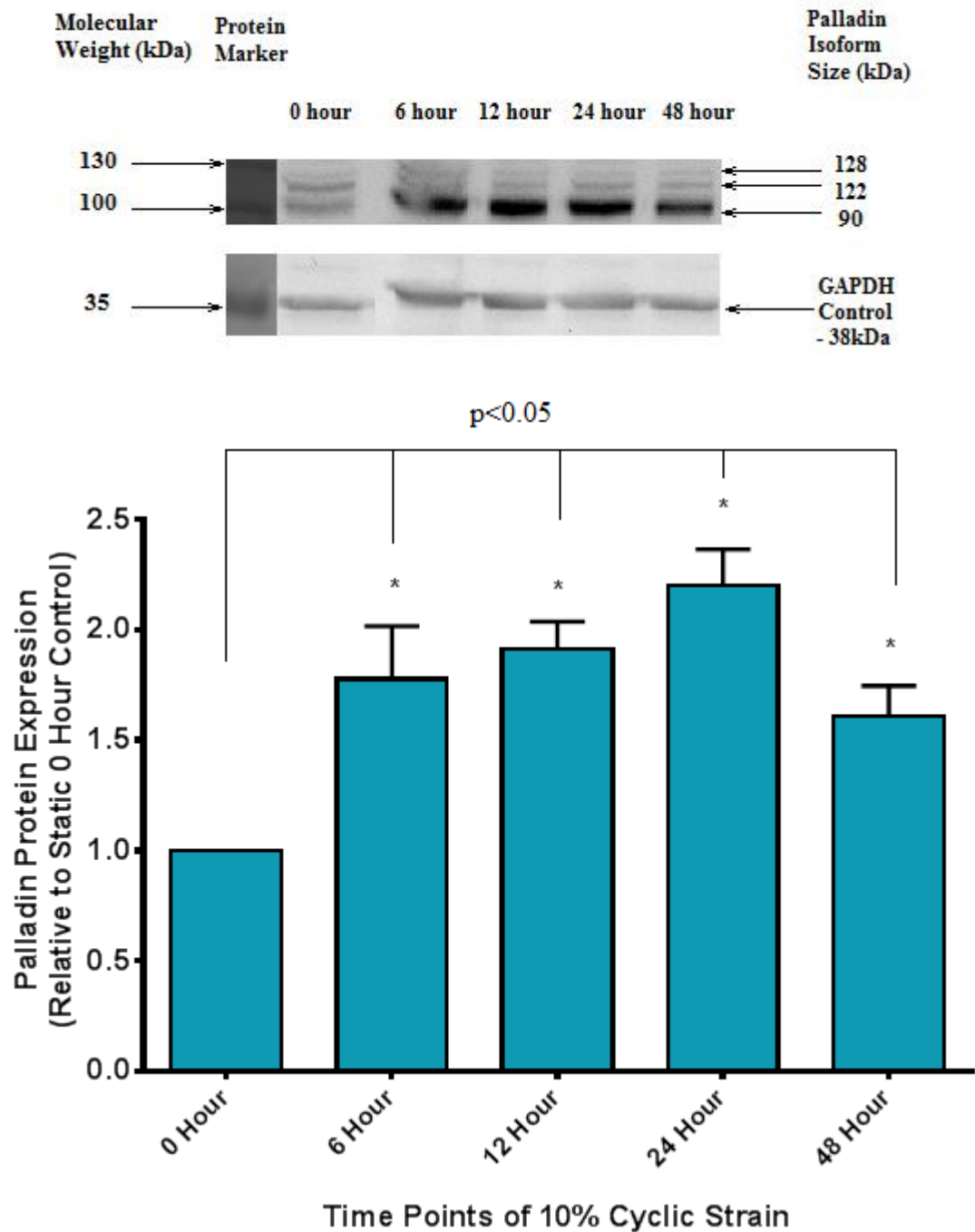
Figure 3.7: Expression of the Palladin protein in HaoSMCs at 10% Cyclic Strain. Following the Western Blotting of strained HaoSMC lysates as per previously described methods, the blot was analysed using ImageJ densitometric quantification software. The comparable values given for intensity of each of the 90kDa-sized Palladin bands are given here, following normalisation against the GAPDH control bands. The values given are expressed compared to a baseline zero hour strain. $*p < 0.05$.

Experiments stayed investigating endothelial cells rather than further investigating Palladin in smooth muscle on account of the role of Palladin in smooth muscle having been already documented in much detail by other research groups. Furthermore, smooth muscle cells are generally not subjected to the laminar shear stress that endothelial cells are. It was theorised that if Palladin is shown to change in expression following the haemodynamic cyclic strain stimulation, then it should also change when subjected to laminar shear stress. Subsequent experiments therefore continued investigating the expression of Palladin in sheared HAECs. Figure 3.8 shows the results of sheared cells that were investigated for Palladin using immunofluorescence. Palladin is visible in the cells where there is green fluorescence in the cell. Actin protein has been stained red with a Phalloidin stain. Images are provided with or without this actin stain. Following LSS, the morphology of the cells has changed, and a pattern of flow across the cells can be observed. This is illustrated by the white arrows signifying the direction of flow. As expected, Palladin is still expressed by the cell following shear. The expression of Palladin in the nucleus and stress fibres is highlighted by the letters N and SF, respectively in the figures.
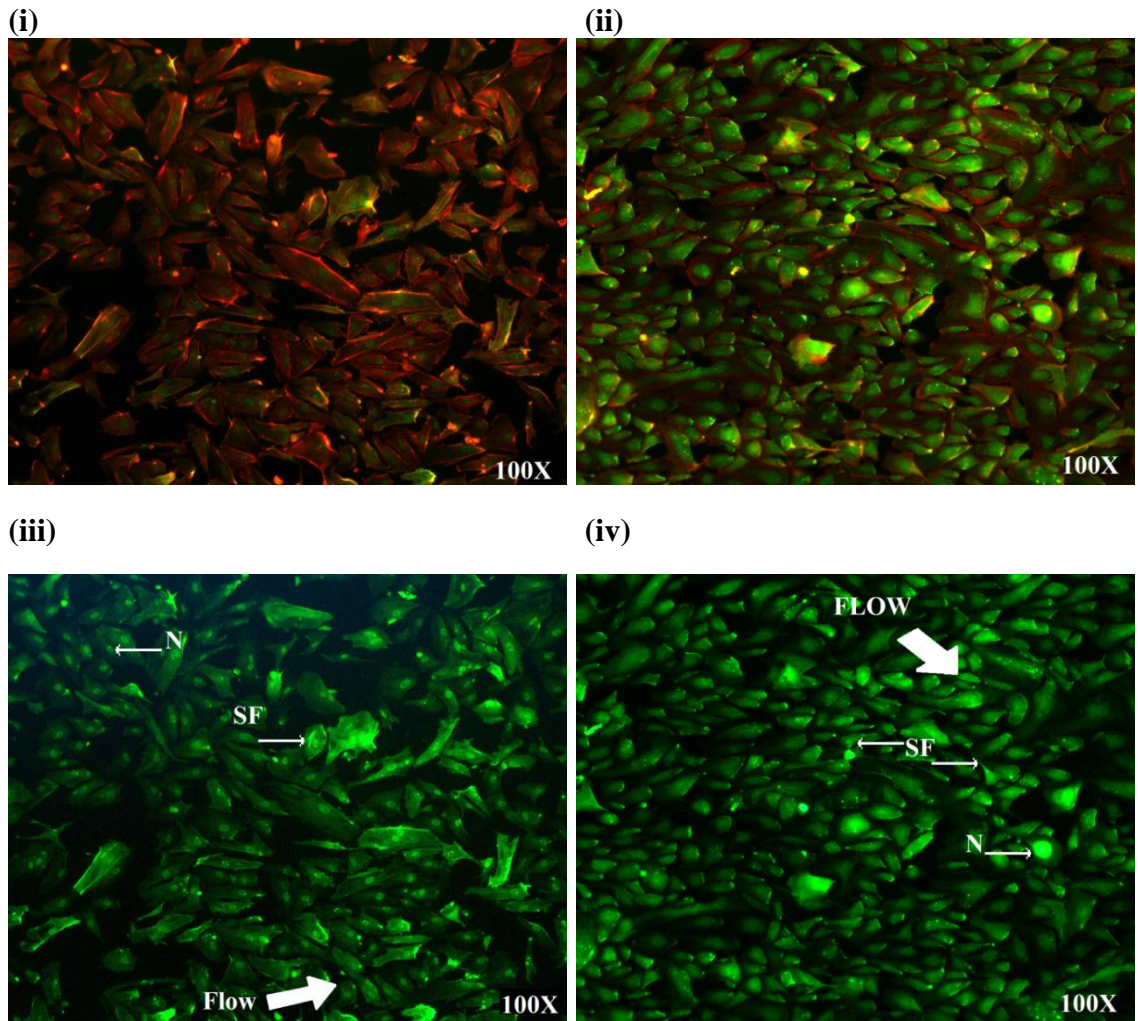
Figure 3.8: Immunofluorescence imaging of Palladin in HAECs subjected to Laminar Shear Stress at 10 dynes/cm^2. HAECs here have been subjected to either (i) 3 hours of shear or (ii) 24 hours before staining. Cells are viewed at 100x magnification. Figure 3.8 (i) and (ii) shows cells stained with AlexaFluor-488 conjugate bound to the Palladin antibody (Green), as well as staining for actin with Phalloidin (Red). The cells in Figure 3.8 (iii) and (iv) are prepared according to the same conditions as (i) and (ii) respectively - but with only the AlexaFluor-488 stain, to allow better observation of Palladin.

The response of Palladin to laminar shear stress was investigated further. Figure 3.9 demonstrates how expression of PALLD gene appears to increase immediately following shear stress, with the relative gene expression increasing after 1 hour of shear, and peaking at 3 hours, where PALLD gene expression has increased two-fold in comparison with the static baseline sample. Following this time point, expression appears to slightly decline over 6-12 hours. At 24 hours, expression increases again, but doesn't reach the early peak expression observed at 3 hours. By 48 hours, expression has returned to just below baseline levels.
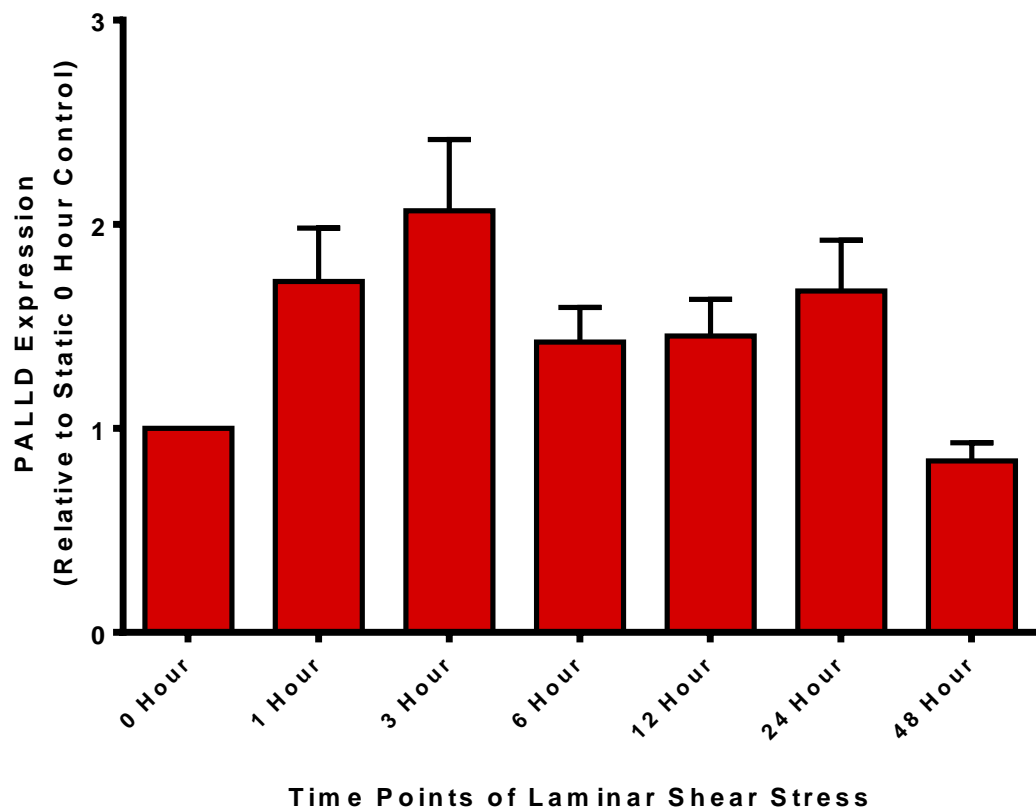
Figure 3.9: Expression of the *PALLD* gene in HAECs Sheared at 10 dynes/cm^2. This graph displays the expression of the *PALLD* gene. Following time points of shear stress at 10 dynes/cm^2, the mRNA is extracted and synthesised into cDNA which is then analysed using qRT-PCR with *PALLD* specific primers. Results are expressed relative to a zero-hour shear, i.e. static cells. Data is representative of five independent experiments ±SEM. Statistical analysis showed $p < 0.05$ for all samples.

The proteomic response of Palladin to laminar shear stress was next investigated, so as to observe if the protein expression correlated with gene expression. Western Blotting illustrated in Figure 3.10 indicated that there was an upregulation of Palladin expression following shear, as the bands showed an increase in intensity over time points, especially at 3-24 hours. Subsequent repeat experiments and normalisation against the GAPDH controls provided a more concise understanding of expression following shear. Densitometric analysis of the 90kDa isoform indicates that Palladin is indeed upregulated immediately following shear, with expression increasing over two-fold within the first hour. At 3 hours, a drop in expression is observed, while it remains above static levels. However, by 6 hours, it has once again peaked – this time almost being three times the static protein expression. At 24 hours, this reverses, with the rate of expression appearing to decline once more. By 48 hours, Palladin expression has reduced back down to the same levels observed in static cells.

Figure 3.10.1 compares the post-shear expression of protein to gene expression, in a similar manner as to how expression was compared post-strain (Figures 3.5.1 and 3.6.1). Gene and protein expression appear to follow a closer pattern to one another, with protein expression in general being slightly higher than gene expression. Between 3 and 6 hours, the similarity is less apparent. At 3 hours post-shear, relative gene expression is much higher than relative protein expression. Notably both expression levels still are greater than baseline static levels. At 6 hours, the Palladin protein expression is expressed at a greater level than the corresponding gene expression level. While both are greater than static levels, the protein expression is almost three-fold, whereas gene expression is roughly 1.5 times the static level. At 24-48 hours, relative gene and protein expression levels are once again closer with one another.
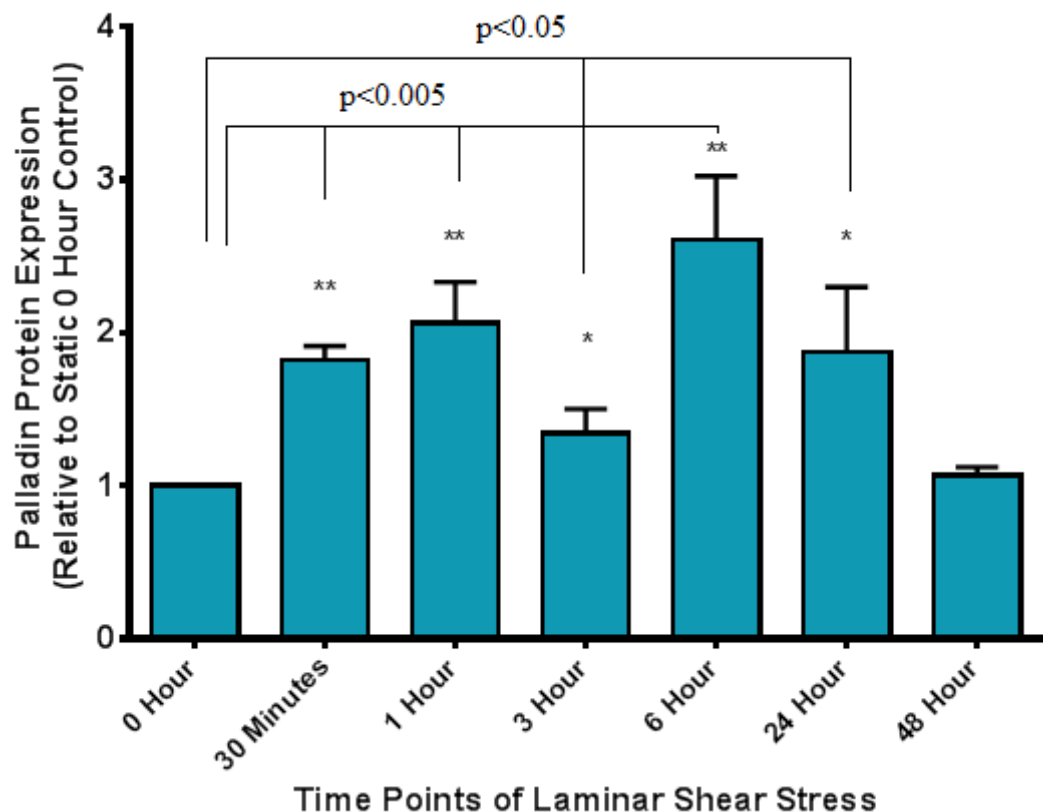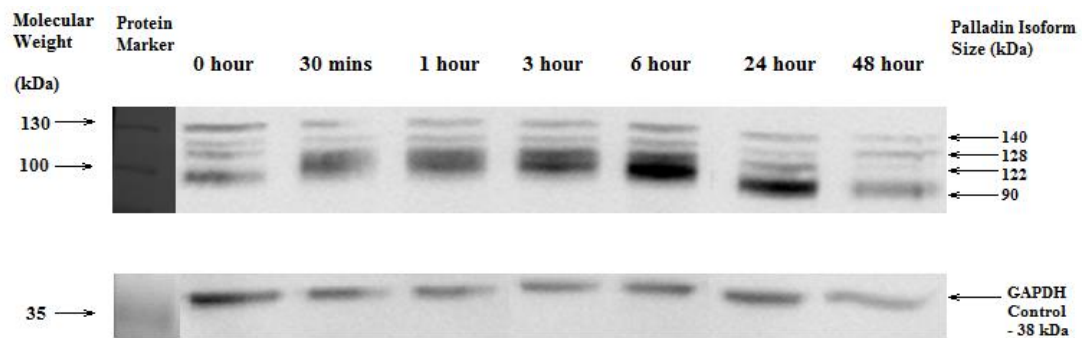
Figure 3.10: Palladin protein expression in HAECs subjected to Laminar Shear Stress at 10 dynes/cm^{2}. Following the allotted time point of LSS, the HAECs were lysed. Protein was extracted and quantified before being probed as before for Palladin and GAPDH. The multiple isoforms of Palladin are recognised by the antibody; however it is the 90kDa isoform which is subjected to analysis, its bands clearly changing more in intensity. Following Western Blotting of sheared HAEC lysates, the blot was analysed using ImageJ densitometric quantification software. The values given for intensity of each 90kDa-sized Palladin band is given here, following normalisation against the GAPDH control Western Blotting bands, and are expressed in comparison to the baseline zero hour shear. Data is representative of at least 5 independent experiments ±SEM.*$p < 0.05$. **$p < 0.005$.
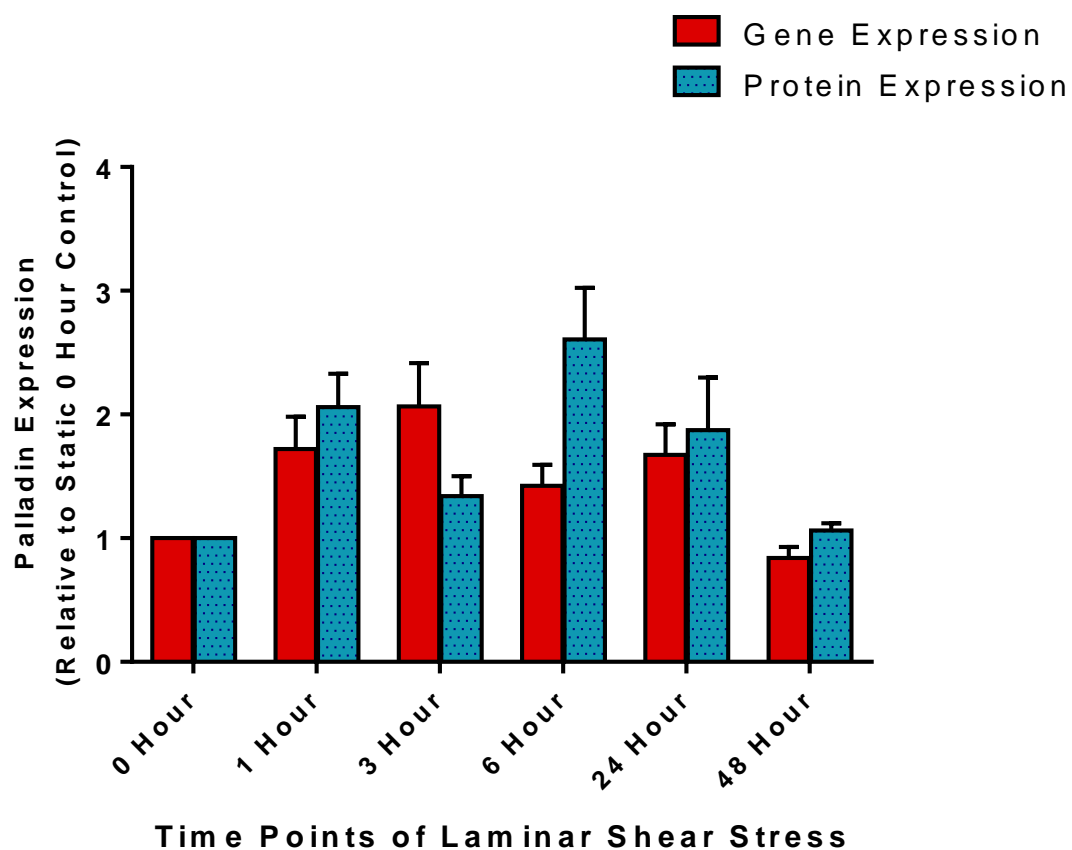
Figure 3.10.1: Comparative trends of Palladin protein expression and *PALLD* gene expression in HAECs subjected to time points of Laminar Shear Stress. This figure compares the expression of Palladin expression following time points of laminar shear stress. The relative gene expression is plotted (Red) against relative protein expression (Blue).

After investigating the proteomic response of Palladin to laminar shear stress, the localisation of protein within the cells was next investigated. Immunofluorescence imaging (Figure 3.8) had shown that Palladin localised to the different areas within HAECs following shear. For a more precise and quantifiable method to characterise changes in Palladin expression, HAECs sheared for different time points were subjected to Proteocellular Fractionation. The different subsets of the sheared cell samples - Cytosol, Membrane/Organelles, Nucleus and Cytoskeleton were separately probed via Western Blotting methods and are illustrated in the subsequent figures. Figure 3.11 illustrates the post-shear expression of Palladin in the cytosol. Notably for the first 3 hours, Palladin is barely present at all. At 3 hours there is an increase in protein, and the bands appear darker, however by 6 hours the protein has reduced in expression. It is only at 24 hours where a more definitive band is observed; showing that Palladin expression in the cytosol has peaked at this time point. Densitometric analysis confirms this pattern, with the normalised Palladin expression at 24 hours showing a seven-fold increase compared to the static sample.

Figure 3.12 demonstrates the post-shear expression of Palladin within the cell membrane and organelles. Here, the expression of bands appears fairly weakened. The 1 hour and 6 hour 90kDa bands appear to be the most definitive one present in the blot. Interestingly, the 128kDa isoform bands appear much stronger than the 90kDa bands here, suggesting an aspect of future research to investigate. The idea of different expression patterns in different isoforms is discussed later in this thesis. When the 90kDa isoform bands are analysed using densitometry and normalised, it is demonstrated that Palladin expression is in fact decreasing over the increased shear time points. There is a steady decrease in protein expression up to 3 hours of shear. After 6 hours of shear, expression slightly increases (but remains below the static expression level), before it declines at 24 hours to half the protein amount present in static cells.

Figure 3.13 continues the fractionation analysis experiment by displaying the expression of Palladin within the nuclei post shear. The 90kDa isoform of Palladin appears to steadily increase across the time points of shear. It looks similar to the pattern of expression in Figure 3.11, but without the drop in protein at 6 hours seen in the cytosol. The blot was analysed with densitometric software, and normalised against the PARP-1 nuclear protein control. Analysis showed that Palladin expression did increase at a steady rate across the shear time points, with an almost five-fold increase within the first 30 minutes of shear. At 6-24 hours the expression is ten to fifteen-fold compared to the

static level, however as a result of the differences in standard error and deviation, the results at these time points are not proven to be a statistically significant increase. However, given the steady increase pattern that has been observed up until then and that protein bands on the blot still remain quite intense, it is likely that protein level is close to the one presented.

Figure 3.14 illustrates the cytoskeletal fraction. Given that Palladin is involved in cytoskeletal structure and organisation, it was hypothesised that there would be large amounts of Palladin present post-shear. While protein bands appear weak at 0 hours and 30 minutes, strong bands are then observed at 1 hour post-shear stress. These bands appear weaker at 3 and 6 hours, before they increase again to the strongest intensity at 24 hours. When the densitometric values of these bands are normalised against the corresponding Vimentin control bands, a clearer picture of expression within the vasculature can be observed. While protein expression is relatively stable at 0-30 minutes of shear, there is a massive increase at 1 hour, reaching 10 times the baseline level. This expression slightly reduces at 3 hours, before increasing again at 6 hours. Peak expression is at 24 hours post-shear, where the relative Palladin expression is almost 20 times the static level.

A final graph is presented at the end of this part of the study. Figure 3.14.1 collects and collates the data from all the 4 fractions taken, and expresses each result as a percentage of total volume of Palladin present in the cell at a given time. Precise results are expressed in Table 3.2. Therefore, at 0 hours, 75% of the total volume of Palladin in the static cell resides within the membrane, with the other fractions of the cells each comprising roughly 5-12% of total volume. These percentages begin to change as the cells are subjected to LSS. Within the first hour of shear, while the percentages of the cytosol and nucleus remain relatively unchanged, there is an increase in percentage of cytoskeletal expression of Palladin (36.5%) at the expense of membrane expression (42.4%). After this time point, the percentages change again. While it has been shown to increase over time points, by 24 hours cytoskeletal expression remains relatively unchanged (32.9%) as it is expressed as a percentage of total Palladin in the cell. Percentage of membrane expression continues decreasing up to 24 hours (13.9%). Meanwhile, there is now more Palladin found within the cytosol (comprising 21% of total Palladin at 24 hours post-shear) and within the nucleus (32.1% of total cellular Palladin at 24 hours post-shear). Palladin is therefore proven to be a protein which is relocated during cellular restructuring in response to shear stress.
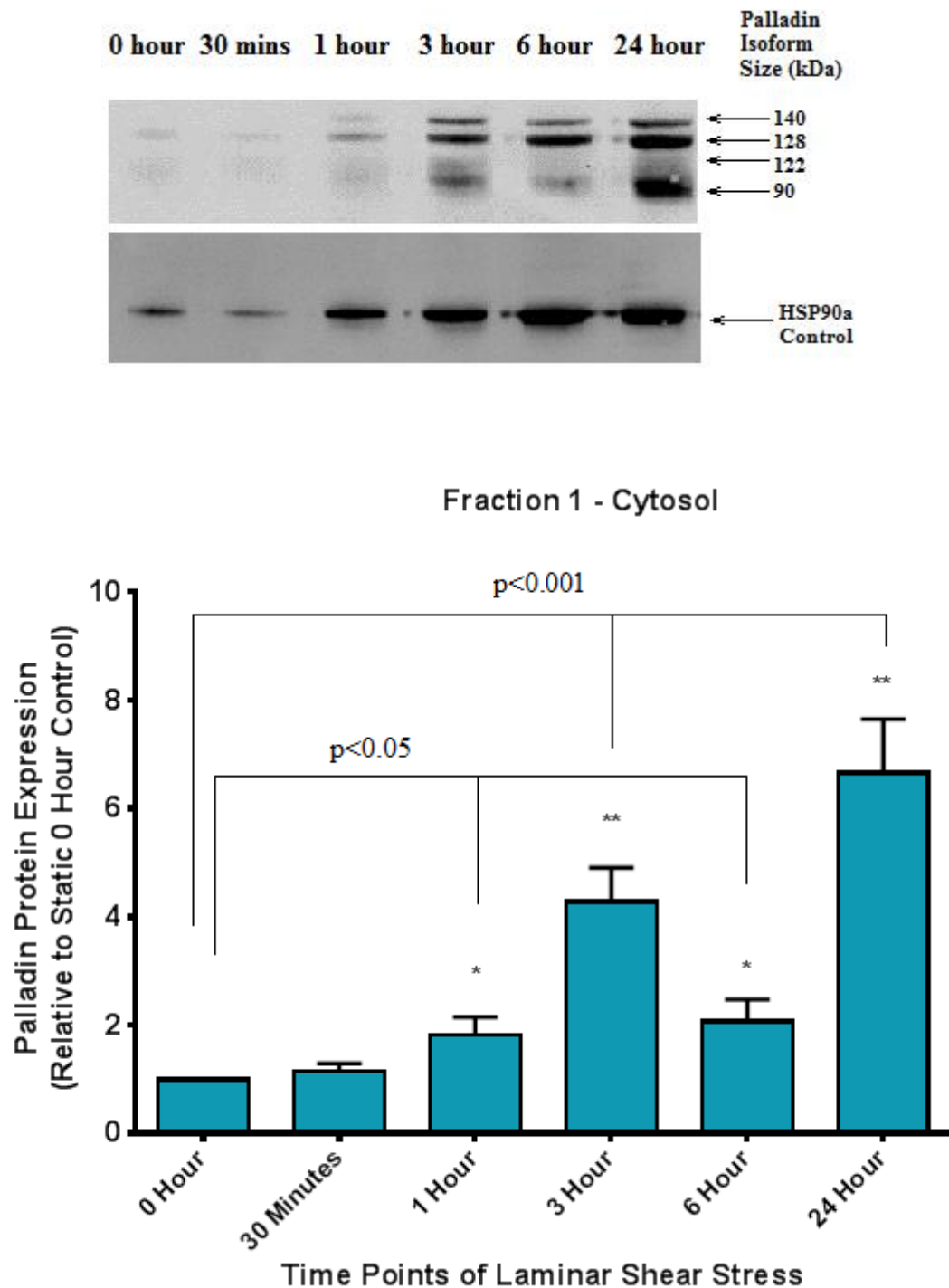
Figure 3.11: Proteocellular Fractionation of HAECs: Fraction 1 – Cytosol. Proteocellular Fractionation was applied to sheared cells in order to observe the distribution of Palladin. Protein was acetone precipitated from fractions and subjected to a Western Blot as before, with the cytosol-specific HSP90a protein employed here as a control. The blot had to be stripped according to methods described in Chapter 2.2.5.1.8 and reprobed with this antibody to achieve control bands; hence the ladder marker is not shown (the HSP90a protein is 90kDa in size itself). The Western Blot was analysed using ImageJ densitometric quantification software and normalised against the Hsp90a controls. The resulting figures are expressed in comparison to the baseline zero hour shear. *$p<0.05$. **$p<0.001$.
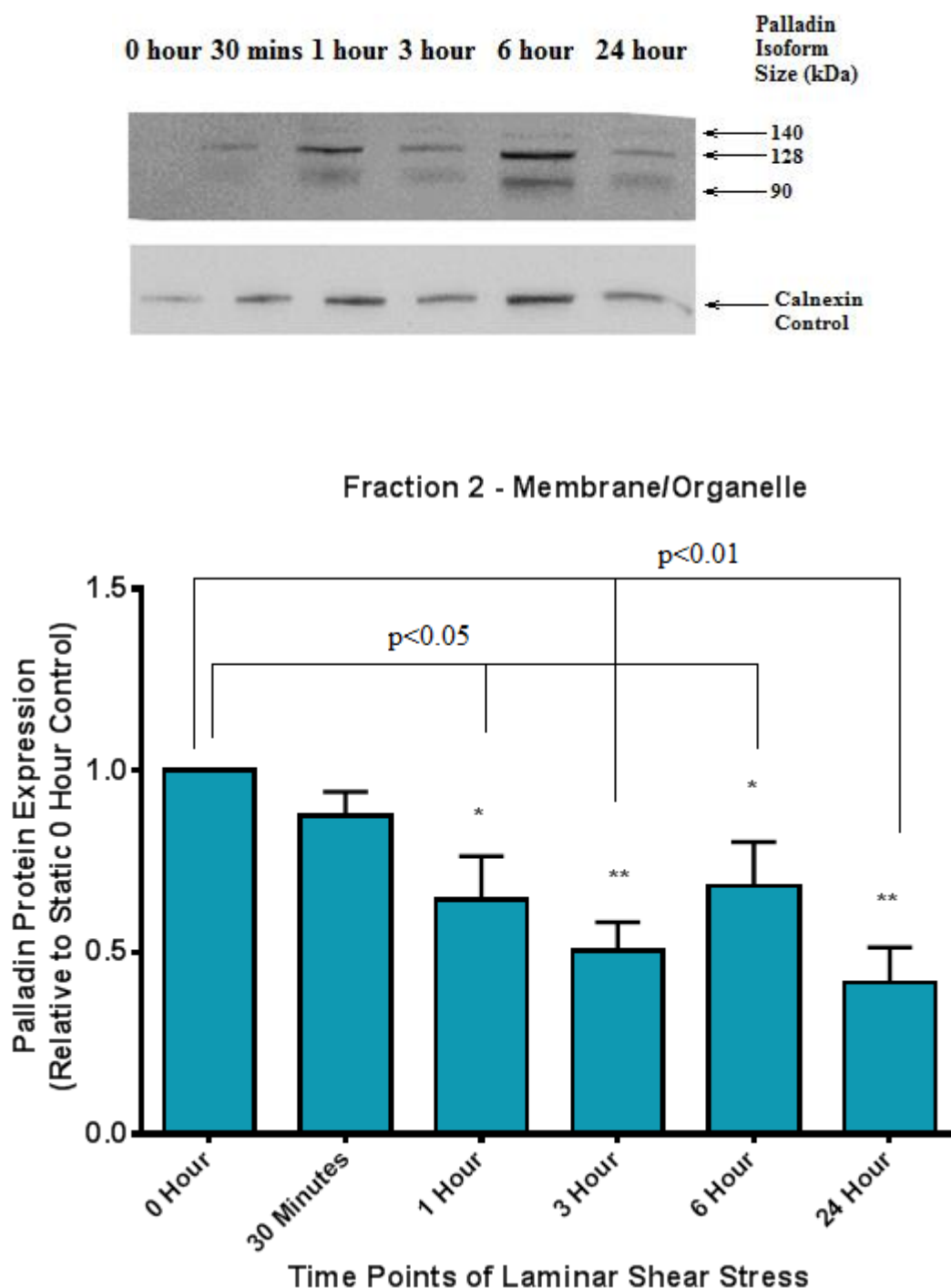
Figure 3.12: Proteocellular Fractionation of HAECs: Fraction 2 – Membrane/ Organelle.
Proteocellular Fractionation was applied to sheared cells in order to observe the distribution of
Palladin. Protein was acetone precipitated from fractions and subjected to a Western Blot as
before, with the membrane/organelle specific Calnexin protein employed here as a control. The
blot had to be stripped according to methods described in Chapter 2.2.5.1.8 and reprobed with
this antibody to achieve control bands; hence the ladder marker is not shown (the Calnexin
protein is close to 90kDa). The Western Blot was analysed using ImageJ densitometric
quantification software and normalised against the Calnexin controls. The resulting figures are
expressed in comparison to the baseline zero hour shear. *$p<0.05$. **$p<0.01$.
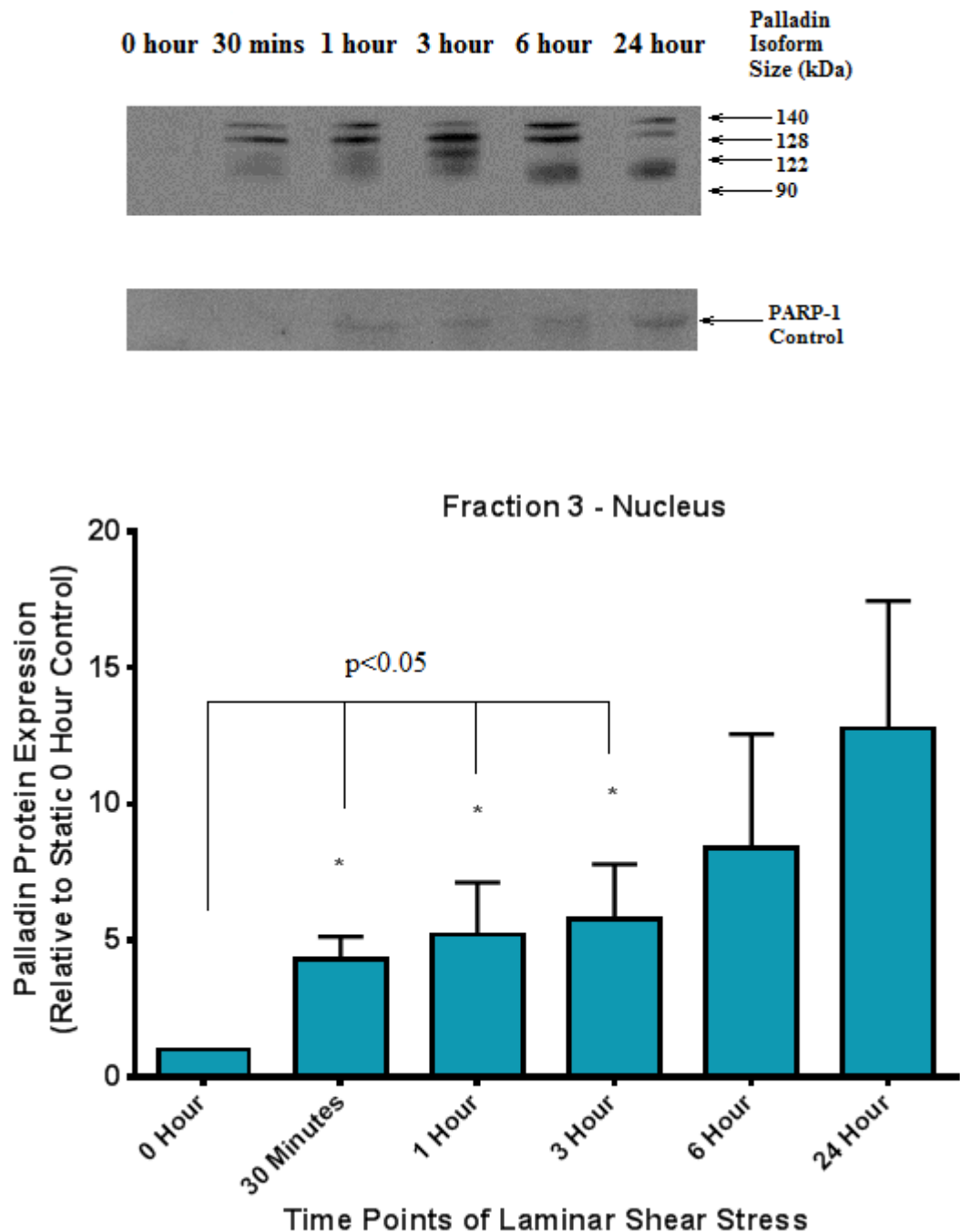
Figure 3.13: Proteocellular Fractionation of HAECs: Fraction 3 – Nuclear. Proteocellular Fractionation was applied to sheared cells in order to observe the distribution of Palladin. Protein was acetone precipitated from fractions and subjected to a Western Blot as before, with the nucleus-specific PARP-1 protein employed here as a control. PARP-1 ranges from 87-115kDa in size, so the blot had to be stripped according to methods described in Chapter 2.2.5.1.8 and reprobed with this antibody to achieve control bands; hence the ladder marker is not shown. The Western Blot was analysed using ImageJ densitometric quantification software and normalised against the PARP-1 controls. The resulting figures are expressed in comparison to the baseline zero hour shear. *$p < 0.05$.
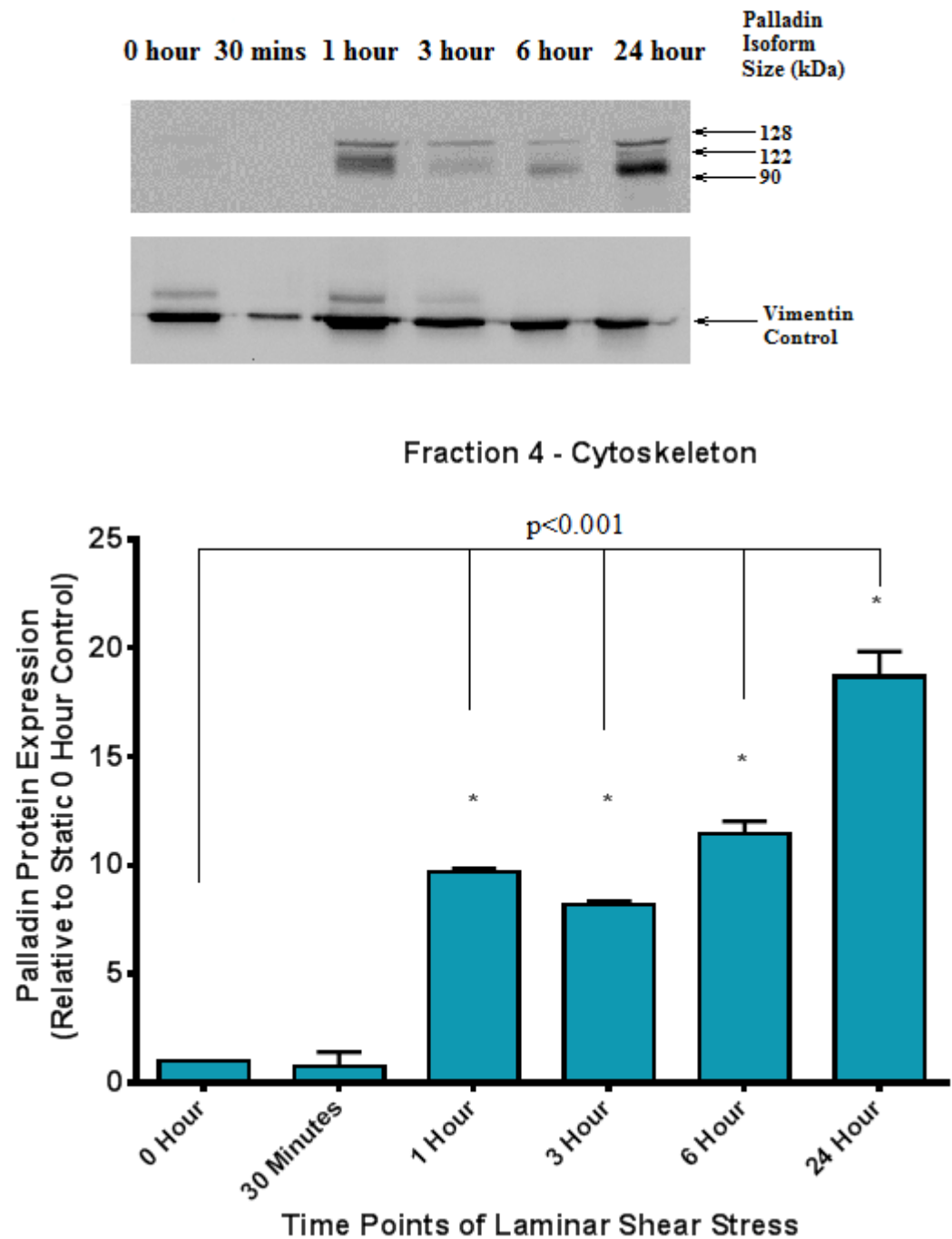
Figure 3.14: Proteocellular Fractionation of HAECs: Fraction 4 – Cytoskeleton. Cells were subjected to laminar shear stress of 10 dynes/cm^2 over a series of time points, followed by Proteocellular Fractionation. Protein was acetone precipitated from fractions, and subjected to a Western Blot to determine the presence of Palladin. Vimentin, a cytoskeletal protein was employed here as a control. Vimentin is 58kDa in size, but as the other 3 blots were stripped, this blot was stripped also in order to keep the experiment consistent. The Western Blot was analysed using ImageJ densitometric quantification software and normalised against the Vimentin controls. The resulting figures are expressed in comparison to the baseline zero hour shear. *p<0.001.

Table 3.2: Palladin Expression following time points of Laminar Shear Stress - comparative percentage total of combined fractions. The resulting data of Figures 3.11 – 3.14 was collated and expressed comparing each fraction to each other, per time point of laminar shear stress. Results are listed as percentage total of combined fractions.

			Time			
Fraction	0 hour	30 minutes	1 hour	3 hours	6 hours	24 hours
F1 - Cytosol	8.218548	7.837941	8.13956	18.56991	8.103904	21.02168
F2 - Membrane	75.20914	72.15771	42.43948	24.78771	27.87159	13.89426
F3 - Nucleus	11.19289	17.8008	12.88823	26.77485	25.96692	32.15588
F4 - Cytoskeleton	5.379425	2.20355	36.53273	29.86753	38.05759	32.92818
Total %	100	100	100	100	100	100
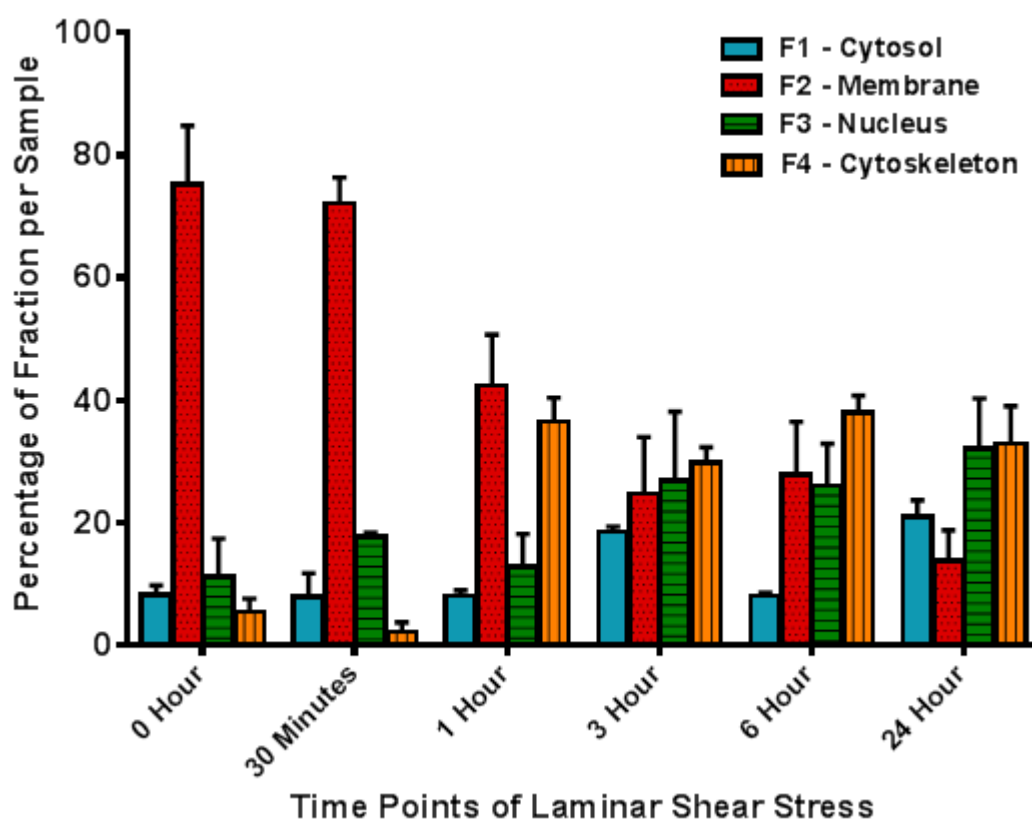
Figure 3.14.1: Expression of Palladin following time points of Laminar Shear Stress - comparative percentage total of combined fractions. This graph illustrates the percentage totals of Palladin protein in each fraction present in the cell.

Following these experiments, the expression of Palladin following shear stress of HAECs is assayed again, but in this case the cells have first been allowed to adhere to a variety of different extracellular matrices – fibrinogen, fibronectin or collagen - before being subjected to LSS. As discussed earlier, certain matrices can be permissive or nonpermissive, with the ECM types having different effects on the integrin signalling pathways - even more so following LSS. Through investigating the effects of these matrices on Palladin, it was theorised that this could help identify integrin pathways involved in gene and protein expression.

Figure 3.15 (i) shows cells seeded onto a fibrinogen (FG) matrix and stained post-shear with AlexaFluor-488 conjugate bound to the Palladin antibody (Green), as well as staining actin with Phalloidin (Red), while in Figure 3.15 (ii) only the AlexaFluor conjugated Palladin stain is presented. At the edges of the cells, there appears to be a strong intensity of staining, indicating that Palladin is expressed more. Figure 3.15 (iii) similarly shows cells – this time seeded onto fibronectin (FN) - and stained post-shear with AlexaFluor-488 conjugate bound to the Palladin antibody and co-stained with Phalloidin, while Figure 3.15 (iv) is only the AlexaFluor conjugated Palladin stain. Finally, Figure 3.15 (v) shows cells seeded onto a collagen matrix (Coll). Again, the cells are co-stained post-shear for Palladin and actin. Figure 3.15 (vi) displays only the Palladin stain. In all figures, Palladin can be observed localising in the nucleus (designated as N), Focal adhesions (designated as FA) and to stress fibres (designated as SF). Direction of flow is also illustrated. The altered morphology of the cells is visible as they have realigned in the direction of flow.

(i) FG
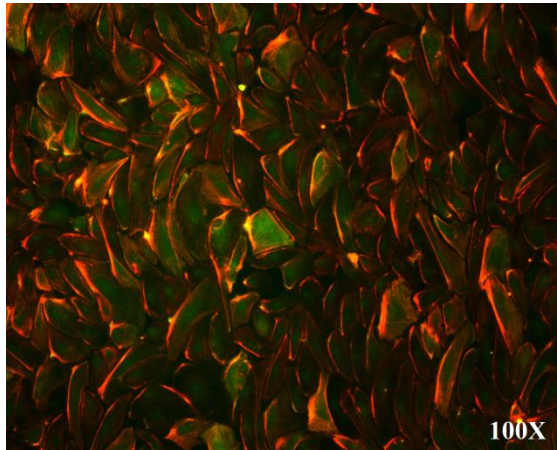
(ii) FG
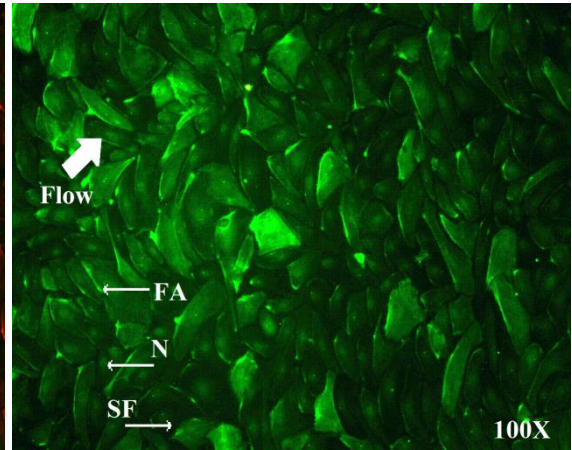
(iii) FN
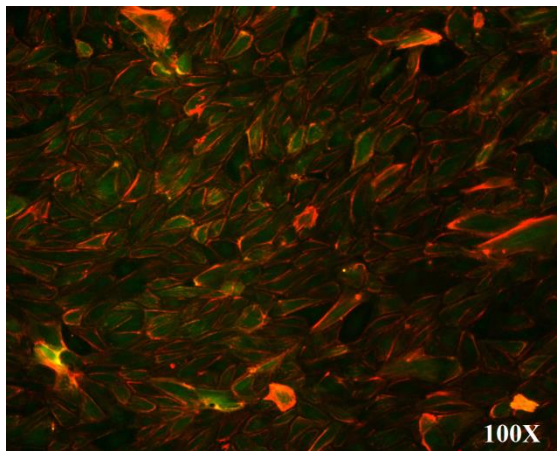
(iv) FN
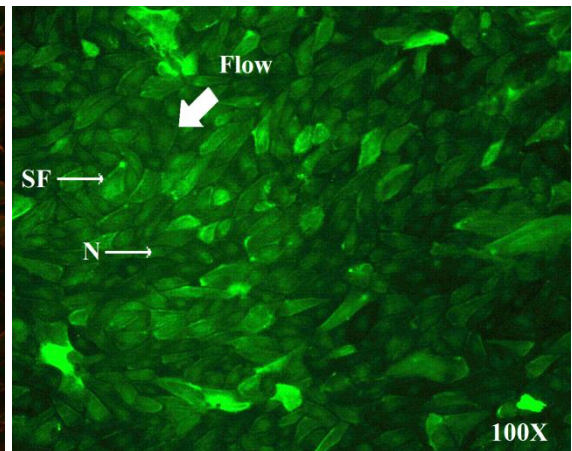
(v) Coll
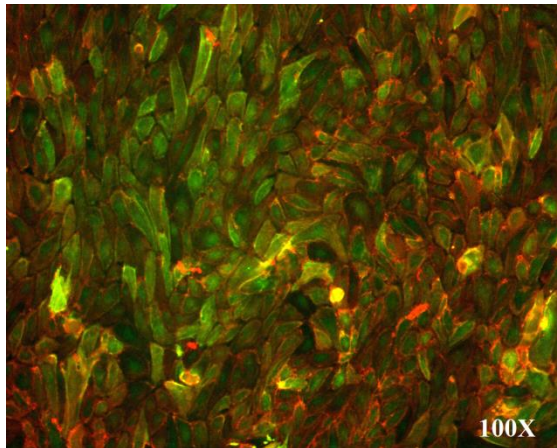
(vi) Coll
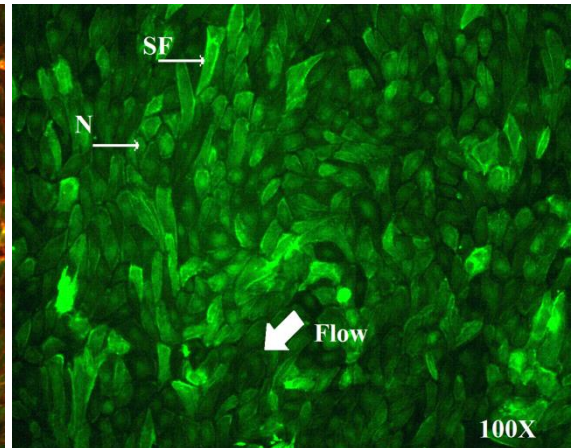
Figure 3.15: Immunofluorescence imaging of Palladin in HAECs on Extracellular Matrices subjected to Laminar Shear Stress at 10 dynes/cm^2. HAECs were grown on an assortment of ECMs and allowed to reach confluency, following which they were subjected to 24 hours of laminar shear stress. The matrices are fibrinogen (i-ii), fibronectin (iii-iv) and Type IV collagen (v-vi). Post-shear, cells were stained as outlined before. Cells are all viewed at 100x magnification. Direction of flow is also illustrated. Palladin is observed localising in the nucleus (N), Focal adhesions (FA) and to stress fibres (SF).

After showing the expression of Palladin within HAECs cultured on the different ECMs, the post-shear gene and protein expression was next investigated. First presented here are the expression patterns of cells grown on the permissive fibrinogen matrix. Figure 3.16 demonstrates the post-shear pattern is different on coated plates than that observed in Figure 3.9 (uncoated plates). Instead of increasing straight away, PALLD gene expression in fact declines within the first hour. However, this decline is reversed by 3 hours, where the expression peaks at over twice the baseline level. By the 6 hour time point, expression has declined to below-baseline levels again. The expression increases at 24-48 hours; but gene expression is still lower than the control static sample. This analysis appears to provide the first proper confirmation that post-shear Palladin expression is affected by culturing of cells on an extracellular matrix.

Palladin protein expression was then investigated, results of which are highlighted in Figure 3.17. Protein bands are visible in the Western Blot, notably they all appear more intense than the "uncoated" sample (i.e. an equal amount of protein obtained from static cells grown on culture dishes without a cell matrix). Densitometric analysis of the bands was performed, and results are expressed relative to the static cells on uncoated i.e. standard cell culture dishes. Palladin expression increases over two-fold when comparing the static uncoated cells against the static cells on the fibrinogen matrix. After the cells are sheared, the expression remains close to a two-fold increase when compared to the uncoated sample. However, when comparing to the static cells cultured on fibrinogen, the expression of Palladin begins to slowly decline for the first hour. At 3 hours expression has risen back to the level it was at 0 hours, and remains steady at this level at 6 hours also. Expression peaks at 24 hours, elevating to a higher level than the 0 hour sample (and roughly 2.5 times the expression of the static uncoated cells). Notably, expression appears to decline rapidly following this peak. At 48 hours of shear the levels of Palladin on the coated plates has fallen sharply to roughly the same level on the static uncoated cells.

Figure 3.17.1 provides a comparison of these gene and protein expression levels. By hour 1, relative protein expression is slightly higher than relative gene expression. At 3 hours, the massive peak of gene expression is greater than respective protein expression. At 6 hours the levels look similar again, but protein expression is now much greater than gene expression. After this, the gene expression stays steady as protein expression begins declining; by 48 hours, the relative-to-baseline PALLD gene expression is greater than the relative-to-baseline protein expression.
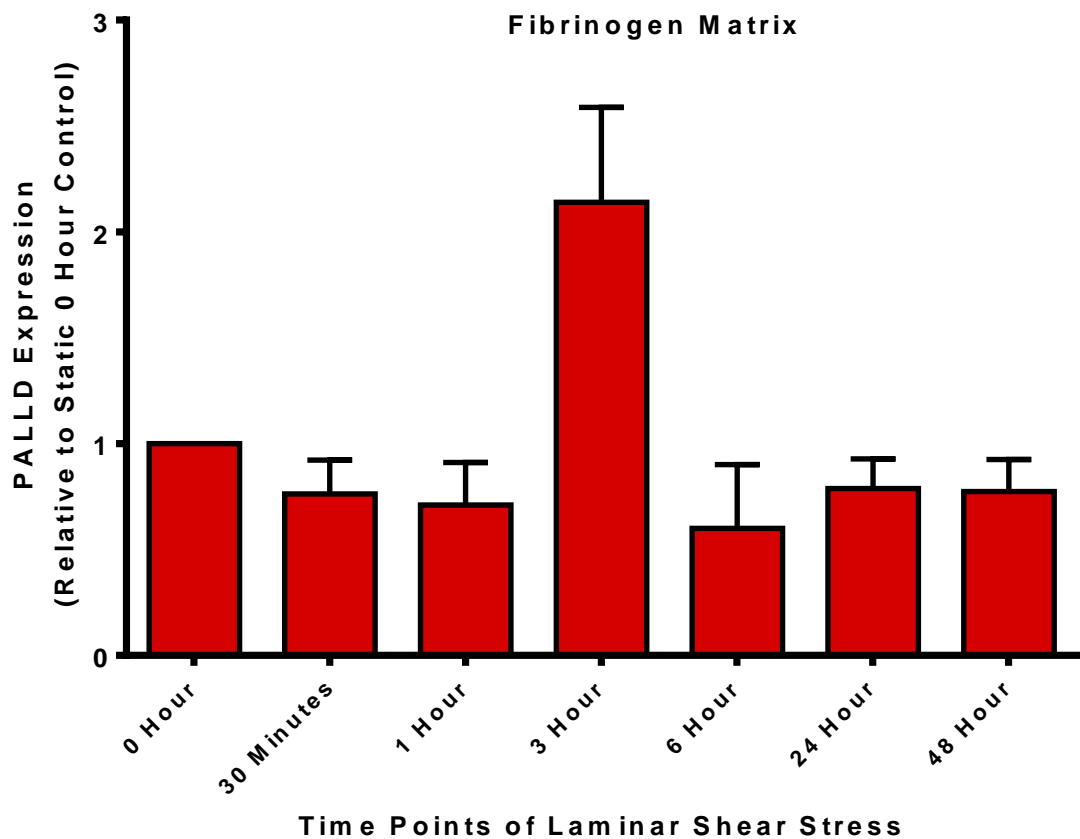
Figure 3.16: Expression of the *PALLD* gene in HAECs seeded onto Fibrinogen Matrix and Sheared at 10 dynes/cm². HAECs were seeded onto a matrix consisting of 10μg/ml fibrinogen and allowed to reach confluency. Following this, they were sheared for different time points between 0 – 48 hours. The mRNA was then extracted and synthesised into cDNA which was analysed using qRT-PCR with *PALLD* gene specific primers. Statistical analysis failed to show P<0.05.
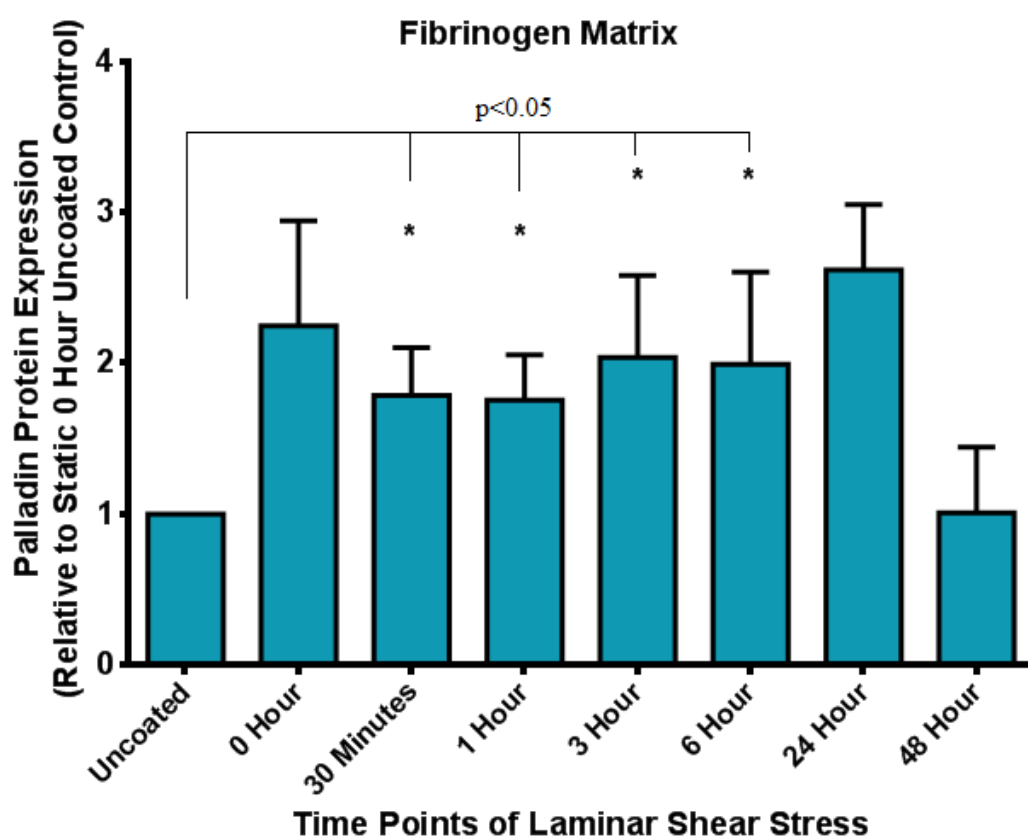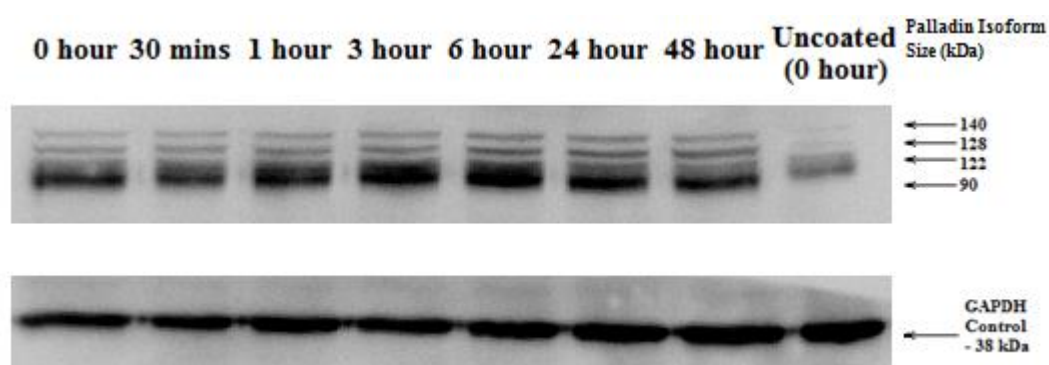
Figure 3.17: Palladin protein expression in HAECs seeded onto Fibrinogen Matrix and Sheared at 10 dynes/cm². HAECs were seeded onto a matrix consisting of 10μg/ml fibrinogen and allowed to reach confluency (18 hours post-seeding). Control HAECs were seeded at the same time onto an uncoated plate and also allowed to reach confluency. Following this, the cells on coated plates were sheared at the listed time points and then blotted for Palladin. The lysate from cells on a regular culture dish surface was also assayed as a control to illustrate the effect of the fibrinogen matrix itself on the expression of Palladin in cells. The blot was analysed using ImageJ densitometric quantification software. Results are listed relative to the static zero hours uncoated control, where cells were seeded onto regular culture plates and not subjected to laminar shear stress. *p<0.05.
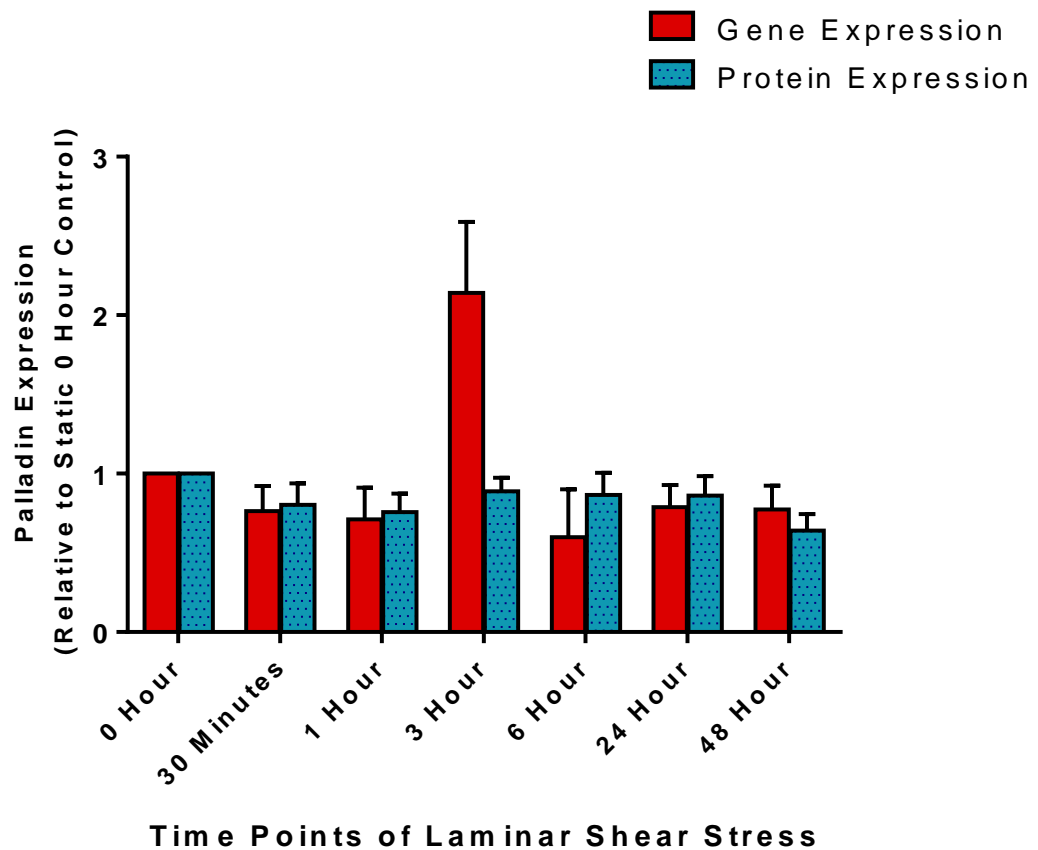
Figure 3.17.1: Comparative trends of Palladin protein expression and the *PALLD* gene expression in HAECs seeded onto a Fibrinogen matrix and subjected to time points of Laminar Shear Stress. This figure serves to compare the expression of Palladin expression on HAECs seeded on a fibrinogen matrix following prolonged time points of laminar shear stress. The relative gene expression is plotted (Red) against relative protein expression (Blue). Results are listed relative to a static zero hour control, where cells were seeded onto the matrix but not subjected to laminar shear stress.

The second ECM protein investigated was fibronectin. Like fibrinogen, this matrix is permissive, so it was thought that the expression patterns should be similar. Once again, HAECs were seeded onto this matrix, sheared at different time points and the gene and protein expression was investigated. Figure 3.18 shows PALLD gene expression increases immediately following shear, with a nearly four-fold increase of within 30 minutes of shear. This decreases at 1 hour, but expression still remains above the baseline levels, being still twice that of the control. At 3 hours, gene expression peaks (Again an over four-fold increase) before steadily declining over the next time points. By 48 hours, gene expression has regressed to almost-baseline level, with expression only slightly above that of the static cells.

Following this, the protein expression is illustrated. Figure 3.19 shows the presence of bands in all the samples. The densitometric analysis of this blot showed that Palladin expression appears to be repressed to a degree, with all sheared cells cultured on a fibronectin matrix displaying less protein than the cells on an uncoated cell culture dish. Notably though, when observing the expression of Palladin following shear, the pattern appears to follow that of regularly sheared cells (Figure 3.10), albeit suppressed. Even though Palladin expression is relatively smaller than static uncoated cells, protein still elevates within the first hour of shear, before dropping back down at 3 hours. At 6 hours expression rises again, but this falls at 24-48 hours.

Figure 3.19.1 collates the data from the gene and protein expression experiments in order to provide a comparative analysis of Palladin on sheared cells seeded on a fibronectin matrix. As shown, the relative-to-baseline gene expression level remains much more elevated than that of the relative-to-baseline protein expression. While gene expression post-shear immediately elevates to 4 times that of the static control, protein expression is only slightly above its respective control. This increased gene expression stays far more elevated than protein expression, until about 24-48 hours. At this point, gene expression is still greater, but it is reduced and much closer to protein expression.
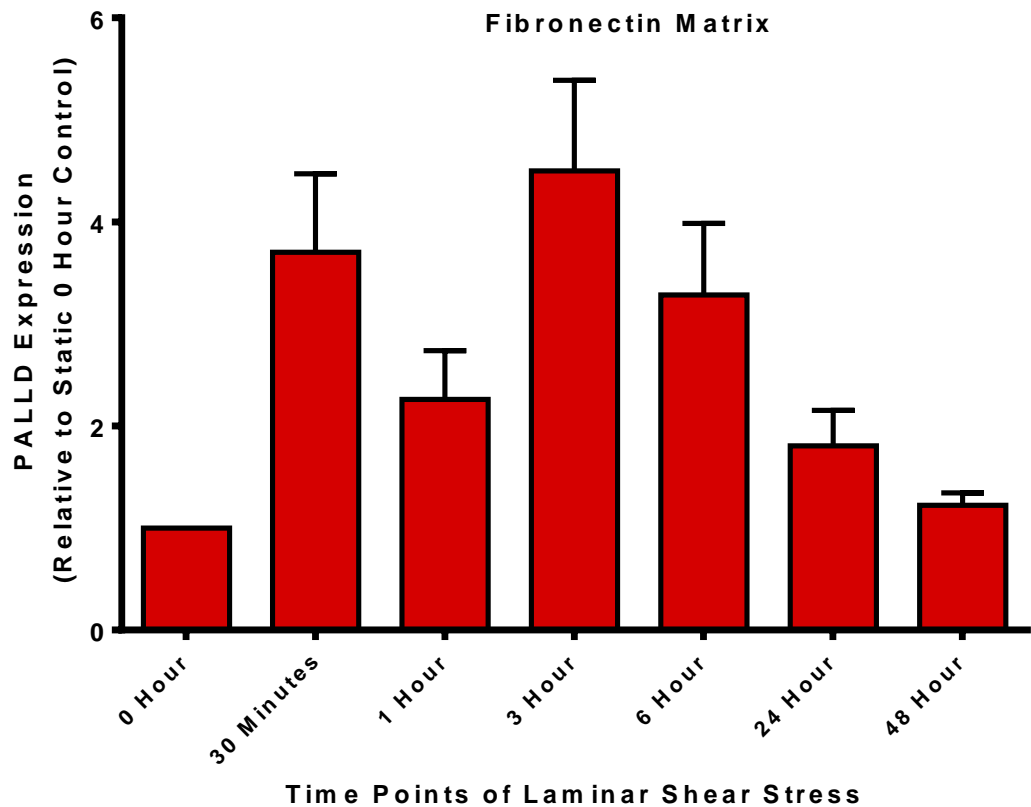
Figure 3.18: Expression of the *PALLD* gene in HAECs seeded onto Fibronectin Matrix and Sheared at 10 dynes/cm^2. HAECs were seeded onto a matrix consisting of 10μg/ml fibronectin and allowed to reach confluency. Following this, they were sheared for different time points between 0 – 48 hours. The mRNA was extracted and synthesised into cDNA which was analysed using qRT-PCR with *PALLD* gene specific primers. Statistical analysis showed $p<0.05$ for all samples.
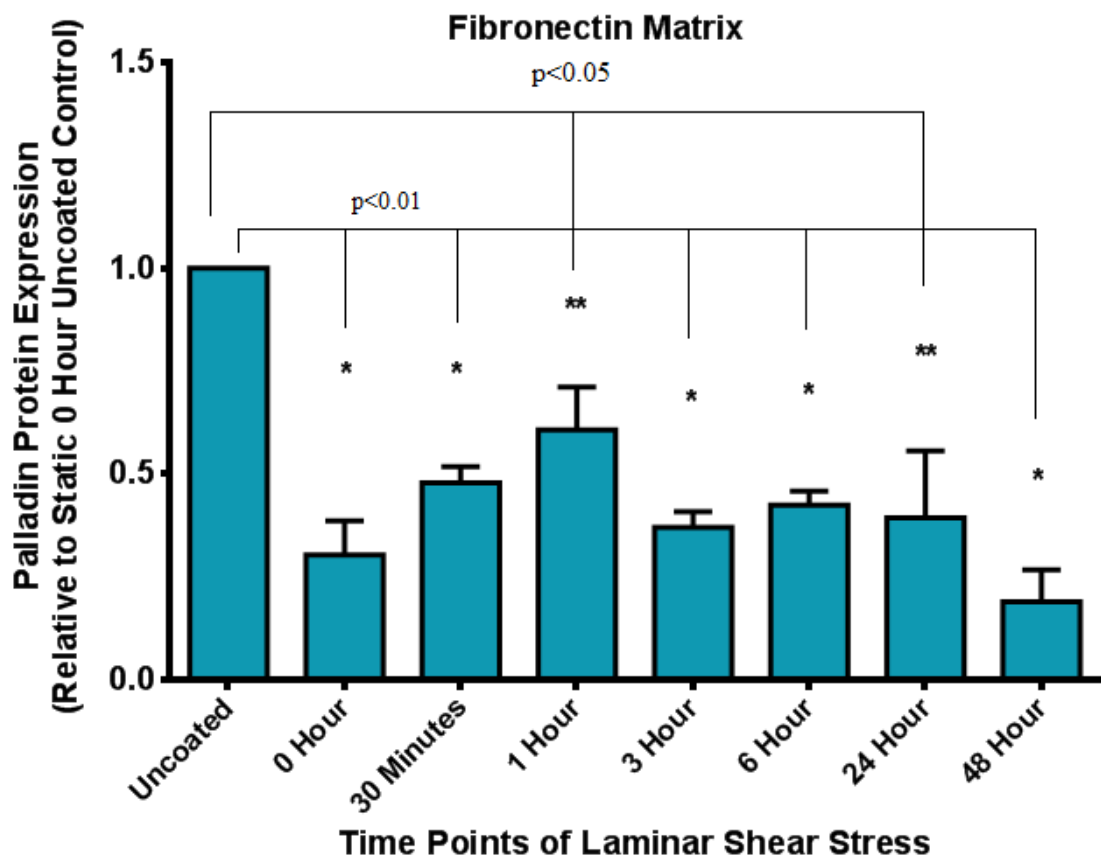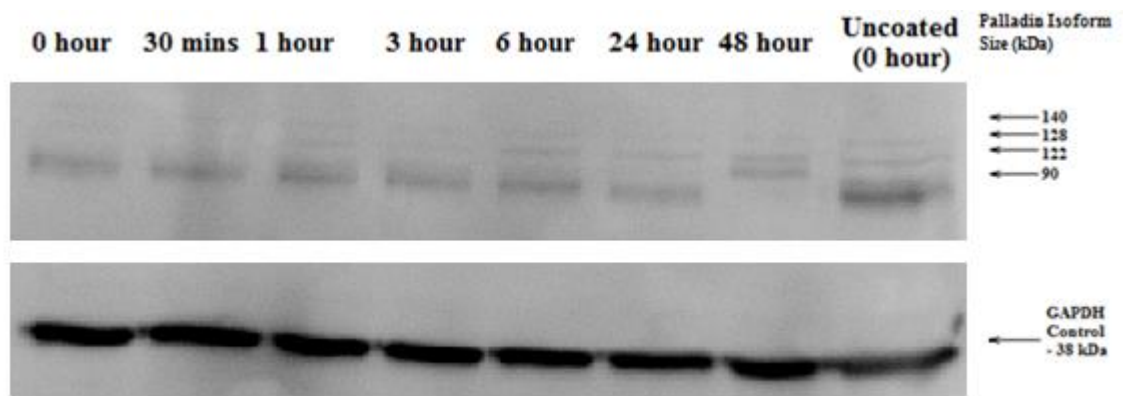
Figure 3.19: Palladin protein expression in HAECs seeded onto Fibronectin matrix and Sheared at 10 dynes/cm^2. HAECs were seeded onto a matrix consisting of 10μg/ml fibronectin and allowed to reach confluency (18 hours post-seeding). Following this, the cells grown on the matrix were sheared at the listed time points and then blotted for Palladin. Lysate from cells that were seeded onto a regular culture dish surface was also assayed as a control to illustrate the effect of the fibronectin matrix itself on the expression of Palladin in cells. The blot then was analysed using ImageJ densitometric quantification software. Results are listed relative to a static zero hour control, where cells were cultured on an uncoated culture plate and not subjected to laminar shear stress. *p<0.01. **p<0.05.
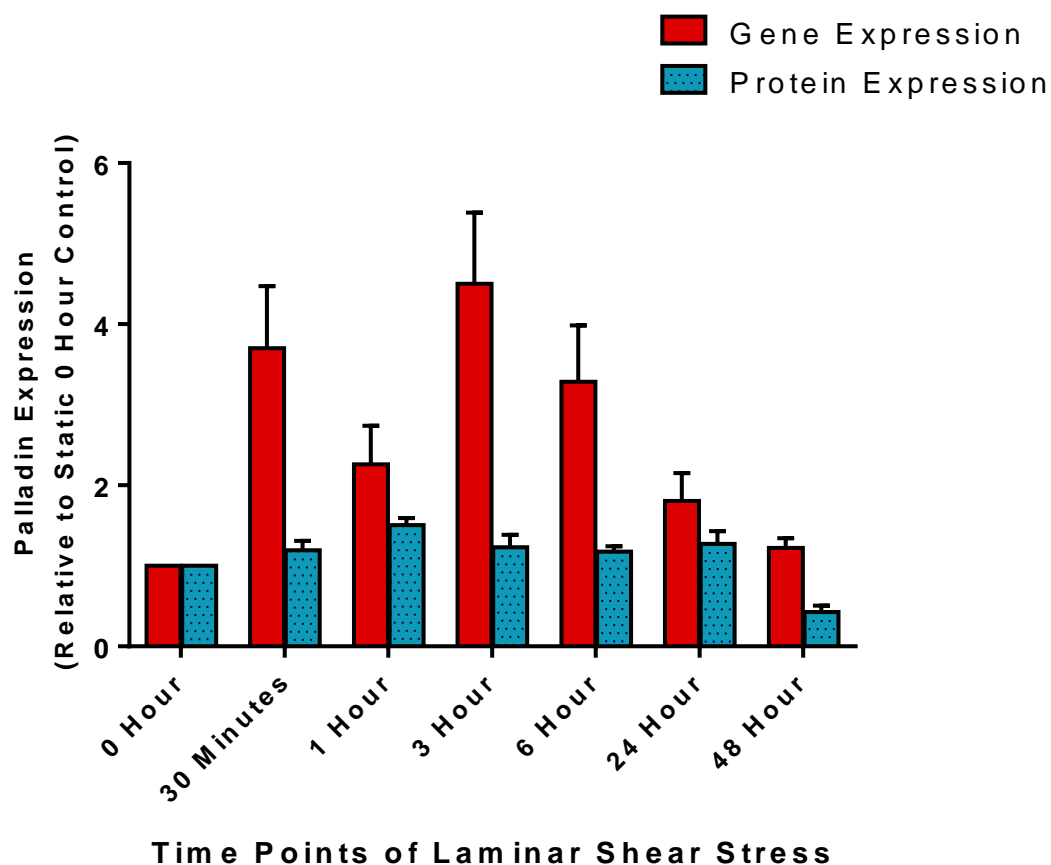
Figure 3.19.1: Comparative trends of Palladin protein expression and the *PALLD* gene expression of HAECs seeded onto a Fibronectin matrix and subjected to time points of Laminar Shear Stress. This figure serves to compare the expression of Palladin expression on HAECs seeded on a fibronectin matrix following prolonged time points of laminar shear stress. The relative gene expression is plotted (Red) against relative protein expression (Blue). Results are listed relative to a static zero hour control, where cells were seeded onto the matrix but not subjected to laminar shear stress.

Finally, Type IV collagen - a non-permissive, or passive, ECM - was investigated for its effects on Palladin expression. It was theorised to have a different influence on protein expression than that of the permissive fibrinogen or fibronectin matrices. As before, HAECs were seeded onto this matrix, sheared at different time points with the gene and protein expression then investigated. Figure 3.20 shows PALLD gene expression following shearing of cells seeded on collagen. Unusually, the expression does not appear to decline much within the first hour; staying relatively unchanged from baseline levels. At 3 hours there is an increase in gene expression, but this decreases back down again to baseline levels at 6 hours. At 24 hours, expression spikes again before dropping below the baseline level at 48 hours.

The post-shear protein expression was subsequently analysed. Figure 3.21 shows how Palladin expression appears to increase when the cells are seeded onto the collagen matrix. Comparing the static uncoated to the static cells on the matrix shows how there is a significant increase in Palladin expression, with a two-fold increase in protein. There is a slight increase of Palladin expression then following the cells being subjected to shear stress. Interestingly, with the exception of a slight decline at 6 hours, the expression levels do not change in response to shear. It should be noted that this change in expression (or lack thereof) from 30 minutes to 6 hours does not have a p-value less than 0.05 when compared to either uncoated or 0 hour static cells, meaning it is not statistically significant of a change. (However, the p-values when comparing to the uncoated static cells all had values only slightly greater than 0.05. A higher number of repeat experiments may produce less of a standard error; and proof of a significant result).

The collagen-influenced gene and protein expression were compared in Figure 3.21.1. They appear to retain a similar pattern. As shown, the relative-to-baseline protein expression is slightly higher than the respective gene expression for the first hour post-shear. At 3 hours, gene expression peaks. Here, the gene expression overtakes the protein expression slightly. This continues until 48 hours, where protein expression once again is greater than gene expression.
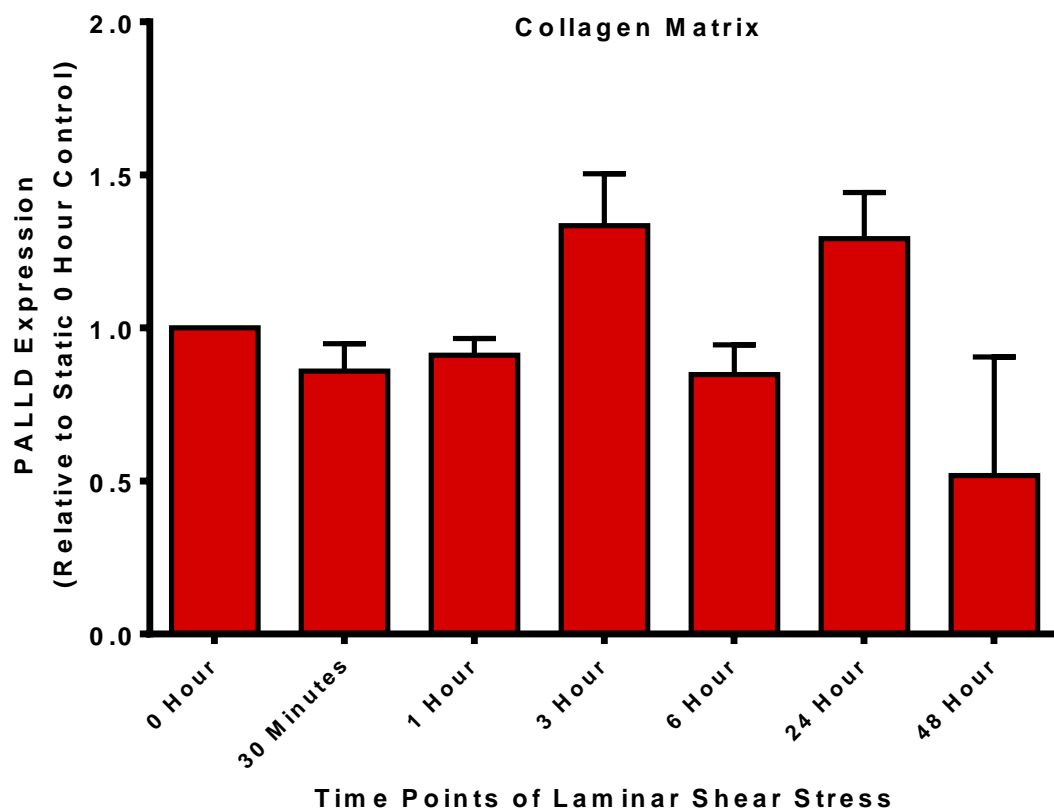
Figure 3.20: Expression of the *PALLD* gene in HAECs seeded onto Collagen matrix and Sheared at 10 dynes/cm². HAECs were seeded onto a matrix consisting of 20μg/ml collagen and allowed to reach confluency. Following this, they were sheared for different time points between 0 – 48 hours. The mRNA is extracted and synthesised into cDNA which was analysed using qRT-PCR with *PALLD* gene specific primers. Statistical analysis showed p<0.05 for all samples.
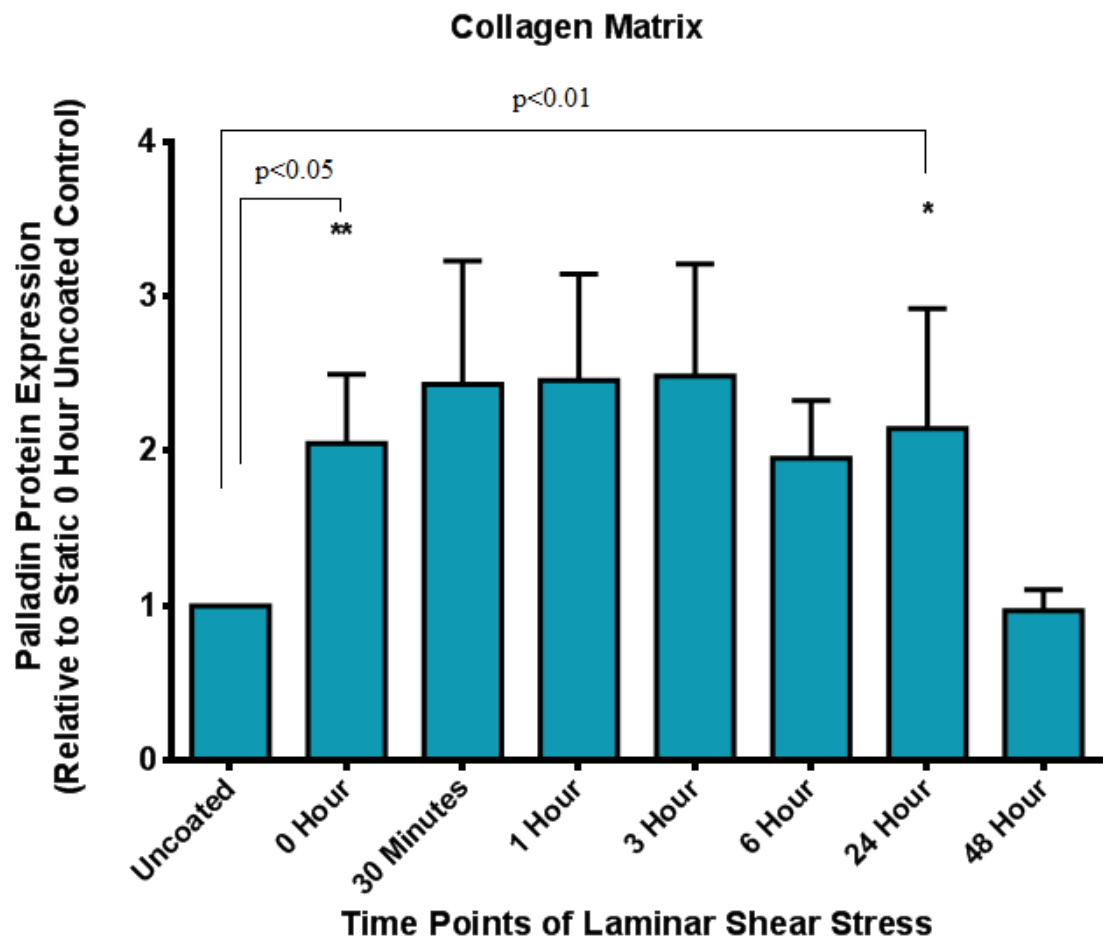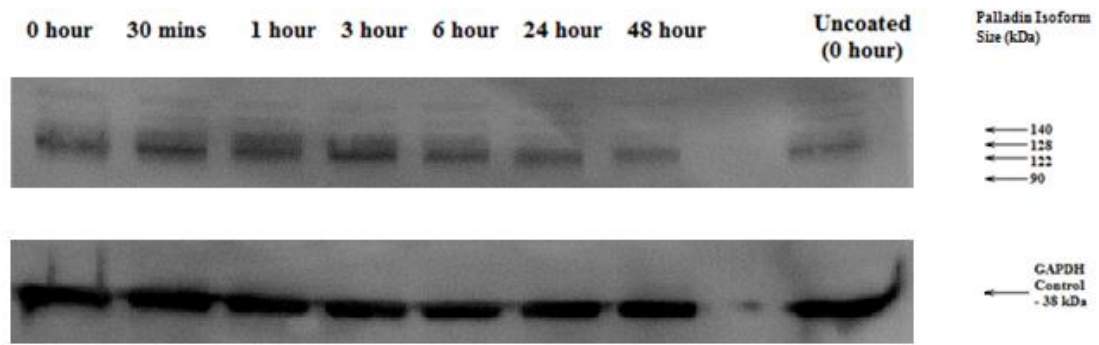
Figure 3.21: Palladin protein expression in HAECs seeded onto Collagen Matrix and Sheared at 10 dynes/cm². HAECs were seeded onto a matrix consisting of 20µg/ml collagen and allowed to reach confluency (18 hours post-seeding). Following this, the cells were sheared at the listed time points and then blotted for Palladin. The lysate from uncoated matrix cells was also assayed as a control to illustrate the effect of collagen on the expression of Palladin in cells. Blots were probed for 30 seconds – probing at lower times showed no bands, and higher times over saturated the result. The blot was analysed using ImageJ densitometric quantification software. Results are listed relative to a static zero hour control, where cells were seeded onto the uncoated culture plates, and not subjected to laminar shear stress. *p<0.01. **p<0.05.
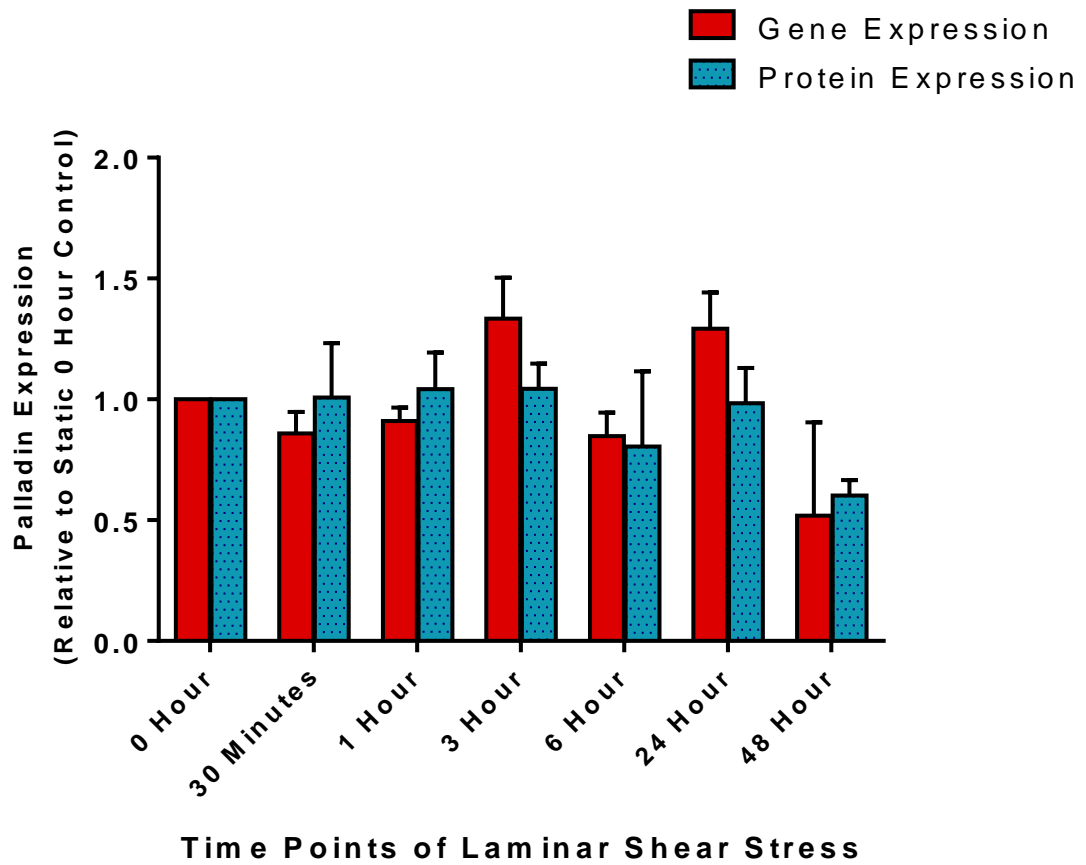
Figure 3.21.1: Comparative trends of Palladin protein expression and the *PALLD* gene expression in HAECs seeded onto a Collagen matrix and subjected to time points of Laminar Shear Stress. This figure serves to compare the expression of Palladin expression on HAECs seeded on a collagen matrix following prolonged time points of laminar shear stress. The relative gene expression is plotted (Red) against relative protein expression (Blue). Results are listed relative to a static zero hour control, where cells were seeded onto the matrix but not subjected to laminar shear stress.

3.3 DISCUSSION

The blood vessels of the human body are subjected to haemodynamic forces due to the pressure and flow created by blood. Smooth muscle cells may be influenced by cyclic strain, with strain stimulating SMC proliferation and increasing expression of extracellular matrix proteins, leading to increased organisation of the cell type (Qi *et al.,* 2010; Von Offenberg Sweeney *et al.*, 2004). The endothelial cell monolayer is also very susceptible to change in morphology as a result of its proximity to the constant flow of blood. Alterations to endothelial cell morphology are considered to be early steps in the development and progression of cardiovascular disease (Deanfield *et al.*, 2007; Hadi *et al.*, 2005). While factors such as age or diet can exacerbate the onset of morphological changes, it is the haemodynamic forces themselves such as cyclic strain and laminar shear stress which can facilitate these alterations. Increased blood flow, such as the type resulting from active sport and exercise may also elevate the haemodynamic forces applied to the blood vessels.

As a result of haemodynamic forces, the cell can alter its actin cytoskeleton in order to reinforce itself and realign in response to the change in force. The thickening and re-arrangement of actin filaments and stress fibres allows for the endothelial cell to absorb and transmit mechanical force throughout the cell – thus converting the physical pressures of haemodynamic force into biochemical signals that alter gene and protein expression. The purpose of this study was to investigate the presence and expression of the actin-binding Palladin protein, with this chapter focusing on the gene and protein response to these haemodynamic forces. Reasoning for this was the idea that if Palladin showed an elevated expression in cells subjected to increased haemodynamic forces, that it may provide a basis for understanding the change in cellular homeostasis in disease states. The protein itself could potentially show use as a disease marker, or it could indicate the expression patterns of actin-binding proteins in the cell – highlighting what proteins are upregulated or downregulated in response to disease.

The Palladin protein is expressed in many multiple isoforms derived from a singular *PALLD* gene. It is believed to be phosphorylated predominantly on serines, which can modulate cytoskeletal organisation and motility of cells (Rönty *et al.*, 2007). The different isoforms of the Palladin protein family possess multiple immunoglobulin-like domains. Most isoforms are transcribed from a series of nested promoters within the *PALLD* gene, resulting in at least three C-terminal Ig-like domains (Ig3, Ig4, and Ig5)

being present (Rachlin and Otey, 2006). Some of the other isoforms have additional Ig domains; the 140kda sized form has the Ig2 domain near the N-terminus, while the full 200kDa form has the Ig1 and Ig2 domain (Figure 3.22). The difference in binding site can mean that the different isoforms of Palladin may bind with alternative proteins, depending on difference in presence or absence of Ig domains. The actin cytoskeletal component protein, Ezrin, for instance has been observed to interact with the Ig2 and Ig3 domain, but not Ig1 (Mykkänen *et al.*, 2001). Proteins that can bind with Palladin are discussed in the next chapter. Filamentous actin itself however has been observed to bind to Palladin, via the Ig3 domain (Dixon *et al.*, 2008). Ig domains appear to be capable of generating force through an "entropic spring" mechanism (Anderson *et al.*, 2013; Grützner *et al.*, 2009). As a result of protein folding, the Ig domain can facilitate minute levels of tension on cell fibres. Several atomic force microscopy studies on other proteins with Ig-like folds indicate that Ig domains can have force-induced conformations (Kesner *et al.*, 2010). Given the presence of similar domains within Palladin, it is suggestive that the protein may have a major function with regards to the cellular response to haemodynamic force.
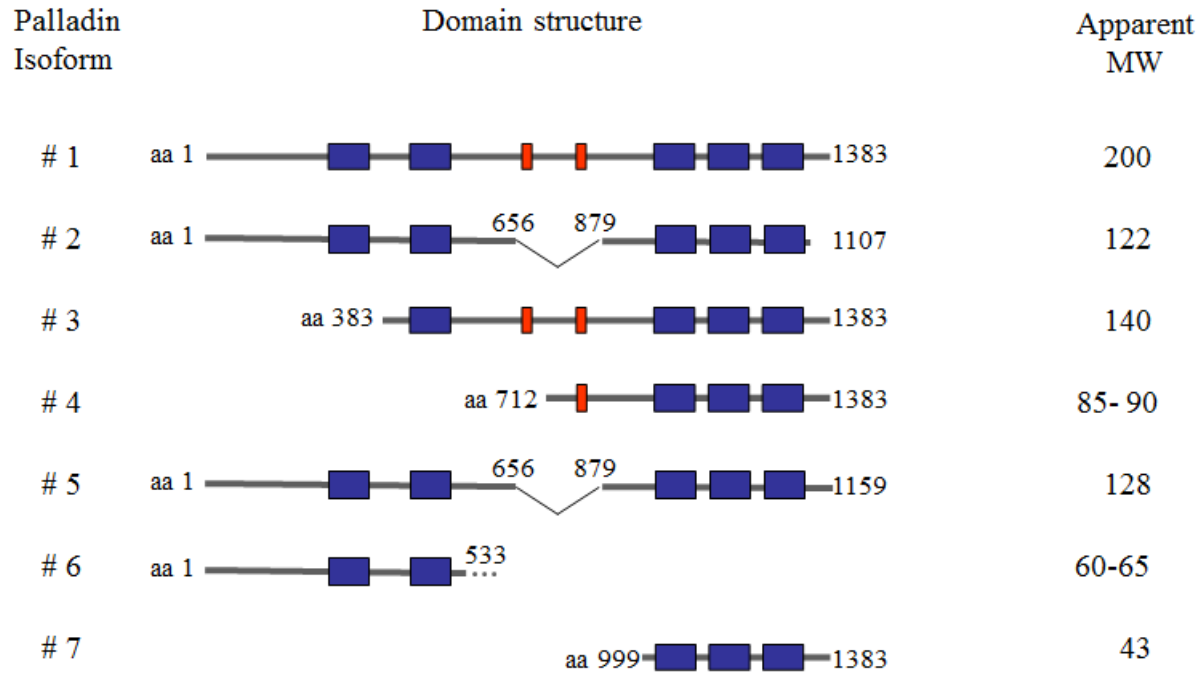
Figure 3.22: Palladin isoform structure. The Ig-like domains in this diagram are represented with a blue box. Proline-rich domains are represented with red boxes. The areas where each protein isoform is cleaved are also illustrated along with the molecular weight of each isoform.

Using an antibody that can bind to the Ig3-Ig5 domains, the expression of Palladin in HAECs was shown in Figure 3.2 via immunofluorescence imaging. Figure 3.2 (i) shows a co-stain of Palladin (stained green) along with Actin (red) and the nuclei of the cells (blue). This image shows how actin is quite plentiful in the cells, but mostly seen at the fibres at the edges of the cell. Being responsible for cytoskeleton structure, this follows expected results, as actin is needed to structure the cells. Palladin can be seen in the cytosol of the cell, but in Figure 3.2 (ii) – the same cells, without actin or nuclear stain – the protein is seen throughout the cell. Under higher magnification in Figure 3.2 (iii), the binding of actin fibres to Palladin can be observed in much closer detail. Palladin strongly binds to actin and other actin-binding structural proteins such as LASP-1 in the cell. These binding partners of Palladin are discussed in greater detail in Chapter 4.

However, while this method of investigating Palladin in the cell shows the protein, it cannot distinguish the isoforms from one another. Western Blotting methods were thusly employed using the same antibody so the different isoforms in HAECs and other various cell types could be determined. Figure 3.3 shows how Palladin is strongly expressed in vascular cells, as demonstrated by the presence of the multiple isoforms in HAECs, HaoSMCs and RaoSMCs, and the absence of some of these isoforms in HEK-293 cells. Isoforms appear differently expressed when comparing the human cell types to the rat cell type, indicating that Palladin may play different functions in the human vasculature. Figures 3.2 and 3.3 conclusively prove the presence of Palladin within Human Aortic Endothelial Cells. The HAECs appear to possess most of the major isoforms. Curiously, the 200kDa "complete" isoform is absent. This may suggest that the PALLD gene encoding for the protein is completely spliced to produce these other isoforms in HAECs. While the figure displays the known isoforms, there appears to be a light band visible at roughly 50-55kDa. This isoform has previously been identified (Luo *et al.*, 2005) but the precise configuration of its structure has yet to be properly determined. Because of the *PALLD* gene possessing the ability to be alternatively spliced, there are potentially more isoforms of the protein yet to be discovered.

In all cell types, the 90kDa isoform was the most strongly expressed band. In literature, this appears to be the most common isoform observed, so all ensuing results concern the characterisation of this isoform. Since it contains the Ig3-Ig5 domains, it shares many characteristics with some of the other isoforms (e.g. 122 or 128kDa sized) which are observed less and not completely characterised in literature. It is a likelihood that the

90kDa isoform might incorporate some of the functions of these lesser observed isoforms on account of their shared domains.

This 90kDa isoform was investigated with regard to its gene and protein response to haemodynamic forces. Figures 3.4 and 3.4.1 display the result of an investigation of PALLD gene expression following physiological and pathological cyclic strain, respectively. When cells are subjected to 5% strain - mimicking physiological strain in the vasculature – Palladin is immediately responsive, becoming quickly upregulated but then appearing to reduce in expression after an hour. In Figure 3.4.1, following time points of 10% strain of the cells - a pathological strain model - the gene expression at first seems to follow the same pattern as that of the 5% strain. However, once it reaches 3-24 hours of pathological strain, the *PALLD* expression levels elevate at a much sharper rate, reaching a two-fold increase of expression when comparing the 24 hour strained cells against the static cells. When the gene expression of the two strain models themselves are compared to one another in Figure 3.4.2, the increasing expression observed in pathological strain appears much more defined.

The immediate expression in both models is suggestive that the cell undergoes remodelling as it goes from a static state to a state more indicative of that seen in the vasculature. Cyclic strain is able to influence HAECs early following strain, forming actin stress fibres and displaying a morphological alignment of cells perpendicular to the force vector (Estrada *et al.*, 2011; Chien, 2007). As actin and actin-associated assemblies restructure in response to this immediate mechanical force, the actin-binding Palladin is immediately upregulated also. HAECs which have been subjected to cyclic strain produce Reactive Oxygen Species (ROS), which becomes increased under pathological conditions (Bundey, 2007). The accumulation of ROS can also initiate an inflammatory response which plays a part in development of atherosclerosis (Kou et al., 2009). It may be that as the pathological strain increases, the inflammatory response initiated involves the Palladin protein. As will be discussed later this chapter, in laminar shear stress, the increase of expression of Palladin in cells is indicative of an inflammatory response.

Once protein has been upregulated within the first hour of strain, post-transcriptional gene signalling mechanisms may be temporarily blocking the synthesis of protein as the cells do not require it anymore, hence the reduction in expression at 2 hours. Recent studies have investigated the role of microRNAs as post-transcriptional regulators

which control mRNA stability and act as key modulators of signal propagation (Avraham and Yarden, 2012). It may be that miRNAs regulate the cellular outcomes in response to the haemodynamic forces. Instead of regulating gene expression at the transcriptional and translational levels, miRNAs can associate with the target mRNAs to form a miRNA-induced silencing complex which causes the degradation of the target mRNAs and/or suppression of mRNA translation (Lewis *et al.*, 2003). This may be occurring here under physiological strain, as the gene expression trends towards baseline levels again by 24 hours. The same signalling mechanisms appear to have less influence when cells are subjected to pathological strain, with elevated expression observed compared to the physiologically strained cells at the same time points.

The almost instant elevation of expression following haemodynamic force is a recurring feature that is seen also in strain-induced protein expression, as well as the cellular response to laminar shear stress, which will be discussed later. As the cells adapt to chronic time points of force (at 3-24 hours), the cell undergoes a more adaptive change, necessitating an upregulation of Palladin once again. Comparing the difference in the 5% and 10% strained cells in Figure 3.4.2 shows how the gene is expressed further when in a hypertensive state (e.g. higher pressure caused by exercise/ blocked arteries). This is suggestive that the *PALLD* gene is utilised for further function (such as continued cell remodelling) in a pathological state. Such a function may be switching off the potential post-transcriptional signalling methods that influence the physiologically strained cells. It should be noted that due to large error bars in the results, the changes in gene expression failed to prove completely significant. While the changes in expression are likely, a conclusion cannot be drawn that cyclic strain changes the gene expression. Possible repeat experiments may improve the results, providing a more conclusive change in gene expression post-strain.

Consequently, the protein response to cyclic strain was investigated with the aim of strengthening the qRT-PCR data. Figure 3.5 shows the expression of Palladin at 5% strain appears to increase within the first hour, but then steadily drops to below baseline levels. Again, this is an observation of there being an immediate upregulation of protein following strain. Since the effects of strain can cause changes in cells within the first 15 minutes (Cummins *et al.*, 2007), it explains how the protein can also be appear upregulated at such an early time point. However, protein expression starts decreasing here after the 1 hour time point, suggesting possible downregulation or inhibition of protein. It should also be noted that these results did not show statistical significance

either (p>0.05). It may be that physiological strain has insignificant effects on Palladin protein expression. With that said, the trend appears to follow along the gene expression when comparing to protein expression (Figure 3.5.1) so the combined results may be representative of expression post-strain. Figure 3.5.1 further highlights how gene expression can stay elevated at 24 hours while protein expression is downregulated. A hypothesis for this could be that the protein is catabolised, being broken down into simple derivative compounds, while gene expression is still promoted as the cells realign to the cyclic strain. The lack of Palladin in strain-induced microparticles (observed in Chapter 5) suggests that the protein does not leave the cell through this manner. It could also be that the functional role of Palladin may be superseded by some other actin-binding protein in the physiological strain state. Experiments involving knocked-down cells (also in Chapter 5) appear to hint at this theory.

Under the pathological 10% strain, the protein expression is elevated much more that the 5% strain; with a significant immediate two-fold increase in protein expression within the first two hours (Figures 3.6 and 3.6.1). This expression peaks in the second hour, before levels start declining in the 3-48 hour time points. This may be a sign of post-transcriptional gene signalling occurring again. The early expression may be a result of the static cells adapting to changes in state, but this fails to account for the elevated protein expression at 48 hours compared to the static baseline. A possible reason for the protein expression remaining elevated in the chronic hypertensive state is that the cells are producing more protein in an attempt to remodel further following the more pathological haemodynamic strain. The increased strain causes the cells to change in morphology to a greater degree, which necessitates a continual synthesis of the Palladin protein.

Palladin expression in HaoSMCs under the same pathological strain models (Figure 3.7) was also investigated, with the results following a similar pattern of increase. However, the peak Palladin expression appears to take a longer time to occur, with expression levels finally peaking after 24 hours before reducing slowly. This further proves the presence of force responsive Palladin in the vasculature, with endothelial and smooth muscle cells upregulating the protein in different manners following cyclic strain. Palladin has previously been shown to be highly expressed in smooth muscle, playing an important role in cytoskeletal organisation, and may be used as a phenotypic marker for contractile smooth muscle (Jin *et al.*, 2010).The fact that Palladin expression peaks earlier in strained endothelial cells compared to strained HaoSMCs is indicative of the

endothelial cells being more responsive to force, which would make sense given that they are in direct contact with the pulsatile force from the blood.

The expression of Palladin following laminar shear stress (LSS) was also investigated because of the proximity of the cells to the blood showing a more direct effect of haemodynamic stimulation. Cells were stained post shear (Figure 3.8) in order to observe Palladin expression. Following shear, cellular structure has changed; with a pattern of flow across the cells being observed as the cells have started to re-align. It has been suggested that at this time, cells will not be fully re-aligned (Osborn *et al.*, 2006), demonstrating that Palladin is still highly expressed following shear stress. This is a possible indication it is still playing a role in actin re-organisation. Investigation of Palladin following time points of shear stress appeared to show a similar pattern of expression to cyclic strain. Following the cells being subjected to LSS, the gene expression of Palladin greatly increases within 6 hours (Figure 3.9), before it starts to reduce. Expression remains above zero hour levels, and there is an increase at 24 hours, before the gene appears to be slowly becoming downregulated by 48 hours. This pattern is indicative of an acute inflammatory response. As the cells are immediately sheared, they again respond by remodelling which requires the upregulation of Palladin.

A similar expression pattern is seen when looking at protein response to shear stress (Figure 3.10). Here, the protein significantly increases immediately following LSS, peaking at the first hour and then again from 6-24 hours, with declines in between. It appears that protein expression closely follows the pattern of gene expression where the peaks are early, and by 48 hours everything is returning to base-line levels (Figure 3.10.1). The reduction at 3 hours is interesting. An explanation may be that the protein is actively downregulated following this time point of shear stress. It is also possible that the protein may be exported from the cells at this stage. As the cells undergo a conformational change, adapting from acute shear to chronic shear (which occurs by 3-6 hours), it was hypothesised that the cells may be stimulated into releasing microparticles which contain Palladin. This hypothesis provided a foundation for experiments performed and then discussed in Chapter 5. It may also be that protein is degraded at this time, given that the cell is almost in a state of flux as it adapts from a response to acute shear to a settled adaptation to chronic shear stress (Resnick *et al*., 2003).

The upregulation of Palladin in response to immediate shear stress or cyclic strain, followed by a drop in expression over time is indicative of an acute inflammatory

response. It must be remembered though that the two types of biomechanical forces – shear stress and cyclic strain - act upon the cell differently. Shear stress applies a continuous force parallel to the cell, whereas strain stretches and relaxes the cell in a periodic manner. Therefore it is not a surprise that the expression of Palladin elevated at different time points between the two types of force. Palladin appears to be upregulated in order to facilitate cell structure as they re-organise shape in response to strain or shear. Actin remodels very quickly in response to shear (Choi and Helmke, 2008) and in strain (Chien, 2007; Birukov, 2009) following a similar but slower pattern, indicating that Palladin is important for facilitating actin re-organisation following haemodynamic forces.

While the immunofluorescence images of Figure 3.8 could highlight the presence of Palladin in sheared HAECs, the images were not useful for quantifying the precise localisation of protein. The altering expression of the protein following shear time points indicated that the protein re-localised to different areas post-shear. To investigate the post-shear localisation in a better context, Proteocellular Fractionation of HAECs was employed. This technique was utilised to extract different parts of cells (Cytosol, Membrane, Nucleus and Cytoskeleton) and determine the localisation of Palladin in each fraction following time points of LSS. Figure 3.11 illustrates the protein expression within the cytosol after LSS. Expression appears to be maintained at a steady increase until 6 hours, at which point there is a drop in protein expression. This almost correlates with the regular behaviour of Palladin in whole cell lysates, but with the 'first peak' that is normally observed at 1 hour being delayed and peaking at 3 hours instead. It is possible that following the 6 hours, as protein in whole cell lysates begins to reduce, that it gets released from other areas in the cell into the cytosol, resulting in this non-synchronous pattern.

Figure 3.12 indicates that the release of protein into the cytosol possibly originates from the membrane. Palladin expression in the membrane slowly decreases for the first few hours, due to the necessary re-localisation of the protein to other areas (e.g. cytoskeleton) in response to shear. While there is a slight increase at 6 hours, this drops down again by 24 hours. There appears to be an almost inverse pattern between expression of Palladin in Cytosol and Membrane/Organelle fractions, especially between 6-24 hours – the point of which the cells begin to adapt to chronic shear stress. This possibly suggests that Palladin begins to be utilised differently following the early

shear time-points, strengthening the idea of it being involved in the inflammatory response.

Figure 3.13 shows how Palladin expression in the nucleus is increased following LSS. There is a rapid increase of protein following 30 minutes (similar to the inflammatory response normally seen in whole cells) which remains sustained over the time course. Since Palladin is known to localise within the nucleus, it is perhaps unsurprising that this would be a site where significant increase in protein is observed. Multiple studies have shown how Palladin can localise to the nucleus in different cell lines where it can bind transcriptional regulators and influence gene expression patterns (Goicoechea *et al.*, 2008; Jin *et al.*, 2010). There is a possibility that the protein may affect signalling also in endothelial cells following LSS, but future investigation into the proteomic function inside the nucleus would be required to draw a conclusive observation.

Since Palladin is also known to be hugely involved in cytoskeletal dynamics, the localisation to this area (Figure 3.14) was of great interest. There doesn't appear to be an immediate increase following 30 minutes of shear stress, which could indicate that the Palladin expression in whole cells at this time point could be originating from other sources such as the nucleus or cytosol. Following an hour of shear, protein levels become significantly increased, and show an increasing trend over the whole time course. As Palladin plays such an important role in cell structure, the increasing relative levels here are perhaps unsurprising, due to the cell remodelling occurring following shear stress. This can help explain why protein expression is low at 24 hours in other fractions (Membrane/Organelle), as it is being relocated elsewhere.

When collecting and graphing the percentage of Palladin in each fraction together in Figure 3.14.1 and Table 3.2, it demonstrates how protein starts out being most abundant in the membrane, but following shear, it becomes elevated in the nucleus and cytoskeleton instead; indicating that there is an increase in the amounts of Palladin produced and increased function in cell structure post-shear. The percentage of Palladin found in the membrane declines greatly, illustrating that Palladin is released from the unstable membrane and relocalised as the cells restructure. Another potential reason for the membrane having a lower protein expression level could be due to the external release of Palladin from the cells through endothelial microparticles. The role of endothelial microparticles and the release of protein within them shall be discussed further in Chapter 5.

Most of these results so far illustrating the force-induced expression of Palladin are observing cells cultured on regular cell culture dishes. While they do provide a good observation of the regulation of Palladin in response to haemodynamic force, it must be emphasized that within the vasculature, these cells are naturally in contact with a variety of different extracellular matrices. As discussed in detail earlier, the cell-matrix interaction was proposed to have an effect on the role of Palladin in cellular function. Previous studies have proven that the extracellular matrix can affect Palladin expression in Smooth Muscle Cells (Jin *et al.*, 2010), so it was hypothesised that endothelial cells would be similarly affected. As stated earlier, certain matrices can be permissive or nonpermissive (i.e. passive); the type of matrix can have an effect on the integrin signalling pathways, even more so following laminar shear stress. By investigating the effects of these matrices on Palladin, it was theorised that this could help identify integrin pathways involved in protein expression.

The next area of study was to therefore investigate expression of Palladin following LSS when cells are grown on an extracellular matrix - fibrinogen, fibronectin or Type IV collagen. Cells were cultured on a matrix, sheared and then probed using immunofluorescence (Figure 3.15). This proved that Palladin was still expressed in the sheared cells when in contact with these matrices. The subendothelial extracellular matrix is largely composed of Type IV collagen and laminins (Orr *et al.*, 2005). Injury, inflammation or angiogenesis result in the degradation of the basement membrane leading to the deposition of extracellular matrix proteins such as fibronectin. In *in vivo* models, fibrinogen and fibronectin correlate with the expression of inflammatory markers such as ICAM-1 and VCAM-1 in endothelial cells (Hahn and Schwartz, 2008). HAECs grown on these matrices display a strong presence of Palladin when subjected to shear stress, suggesting that Palladin may act in a similar manner; having already been observed to show an inflammatory response to regular LSS without interaction with a ECM. The fibrinogen-seeded cells in Figure 3.15 (ii) appear to show a strong localisation of protein towards the stress fibres at the edge of the cells. Similar localisations are seen in the fibronectin or collagen-seeded cells, but of a lower intensity. These seeded cells were investigated for protein expression following an array of time points of LSS.

As seen in Figure 3.16, when the fibrinogen matrix-seeded cells are subjected to LSS time points, the pattern of gene expression is different. Instead of a sharp immediate increase, the *PALLD* gene appears to be initially downregulated. There is a sudden rise

in expression at 3 hours, which is similar to that seen in regularly sheared cells (Figure 3.9) but otherwise expression is completely altered. A possible explanation of this unusual peak may be the effect of the adaptation of the cells to a chronic shear form. It appears there is a signalling mechanism responsible for repressing the gene expression at the other time points. Fibrinogen has been shown to affect gene expression (Weijers *et al.*, 2010). However, as the cell morphology changes between 3-6 hours of shear, these changes in the cell may spur a sudden change in gene expression that briefly overrides the repressive signalling mechanism. This negation of the mechanism allows for the shear-induced upregulation of the gene to continue for the time point until the cell has finished restructuring at 6-24 hours. Investigation of these mechanisms specific to fibrinogen may be an area of future research to investigate.

When looking at the protein expression in Figure 3.17, the matrix-seeded cells also show inhibition post-shear, with immediate downregulation occurring in a similar manner to the gene expression. At 3 hours (when gene expression became briefly upregulated) a small rise in Palladin expression is seen, but expression is slightly less than the baseline fibrinogen-seeded static cells. Following the theory that the gene is in fact being repressed and the repressive mechanism stopping as the cell adjusts, then it would follow that there isn't enough time to synthesis a similar increase in protein before the gene repression continues again. When comparing the protein expression levels between cells on a matrix versus uncoated cells, it appeared that the matrix causes massive upregulated expression of Palladin. A comparison of the static cells grown on fibrinogen against static cells on an uncoated plate showed that the expression of Palladin is increased two-fold, due to interactions with the matrix. Fibrinogen has been proven to facilitate cell migration (Rybarczyk *et al.*, 2003) and can induce chemotactic activity on endothelial cells (Seeger *et al.*, 2002), indicating that as the cells migrate more on the matrix, the expression of Palladin increases as the static cells restructure and adapt to shear stress. An explanation for why in Figure 3.17 and 3.17.1 there is not so much protein expression could be that the fibrinogen stimulating the cells to produce Palladin results in a threshold being reached, leading to the cell to stop signalling for release of more protein. There may be some sort of specific inhibition of certain integrins by fibrinogen, preventing the signal that normally induces the synthesis of Palladin when cells are sheared. Fibrinogen (and fibronectin) inhibits the α2β3 integrin (Orr *et al.*, 2006), which suggests a possible integrin pathway. However, since the levels are still higher than that of an uncoated sample, it may be that there is some method by

which the immediate shear response is inhibited, but expression is still promoted by virtue of cells interacting with the cell matrix (possibly from the cells being stimulated to migrate more). As stated, this is an area of research that future investigative work may be based upon.

In Figure 3.18, cells seeded next on a fibronectin matrix and subjected to shear appear to have a relatively similar pattern of gene expression as the regularly sheared cells (Figure 3.9). There is a less of an increase in expression though at 24 hours in the cells on the matrix. Again, the cells may be adapting differently to growing on the matrix; in that they don't require upregulation of Palladin in order to adapt to chronic shear conditions. Protein expression however seems to follow the same expression pattern as seen in cells grown on uncoated plates in Figure 3.10. When comparing the gene and protein expression in Figure 3.19.1, it appears that gene expression of Palladin is much higher than protein expression. An explanation for this is that there may be elevated release of protein through endothelial microparticles. Alternatively, there could be protein deregulation occurring between 3-6 hours of shear.

Notably, all time points show much lower expression when compared to the static sample of cells on an uncoated plate. It may be a case where Palladin expression is inhibited to a certain threshold in cells by fibronectin. As mentioned before, some integrins such as α2β3 are inhibited by fibronectin, which suggests that the same integrins may be involved in the signalling pathway of Palladin. Figure 3.23 highlights how α5β1 and αVβ3 integrins binding to fibronectin specifically activate the transcription factor NF-κB (Orr *et al.*, 2005). Shear stress also activates the p21-activated kinase (PAK) in fibronectin-seeded cells. It is possible that either of these interactions may inhibit Palladin expression. Notably the PAK activation pathway is linked to increased endothelial monolayer permeability in response to shear of cells on this matrix (Orr *et al.*, 2007; Hahn and Schwartz, 2008), so the expulsion of protein from cells during shear is a possibility. However, the molecular mechanisms involved in flow-induced endothelial permeability are still under investigation. This is a curious overall result since fibronectin also plays a strong role in the migration of cells, so it would be expected that Palladin expression would increase also. It could be that the matrix on its own in this manner has a negative effect on Palladin expression; whereas in the vasculature the other matrices may counteract the protein downregulation.

When observing the cells seeded onto a collagen IV matrix (Figure 3.20), gene expression appears to also be restrained. Only at 3 hours of shear stress does *PALLD* gene expression becomes upregulated, compared with the immediate response observed in regularly cultured cells in Figure 3.10. Furthermore, while the pattern of expression is similar (decreasing at 6 hours, increasing at 24, decreasing again at 48 hours), in regular cells, the overall expression stays above zero hour baseline levels. In comparison, cells seeded onto a collagen matrix show an expression pattern that declines below baseline levels at 6 and 48 hours, demonstrating that gene expression appears to be restricted to a degree by the collagen matrix.
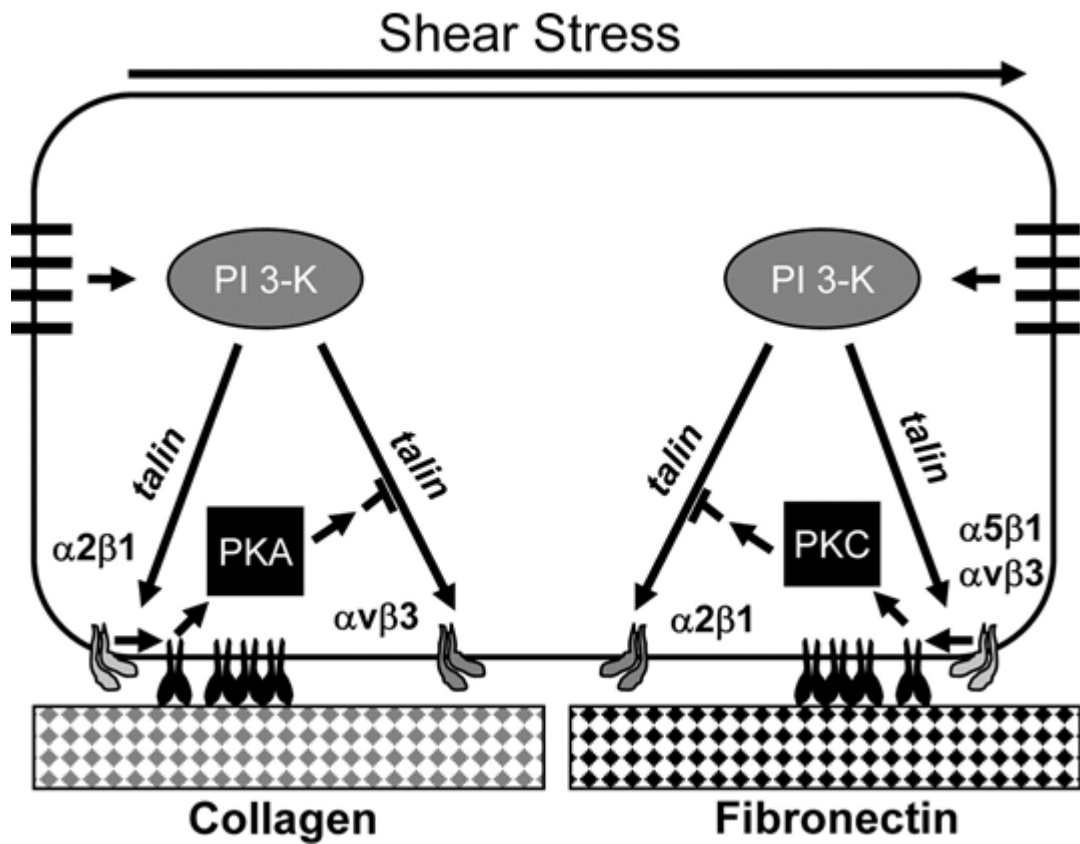
Figure 3.23: Model for flow-mediated integrin suppression. For cells seeded on a passive matrix such as collagen, the onset of flow stimulates the junctional mechanoreceptor complex to trigger activation of integrins such as α2β1 through PI 3-kinase. The binding of integrins to collagen stimulates Protein Kinase A (PKA) activation which initiates a pathway that acts upon the talin protein to suppress αVβ3. This may be an integrin which affects the expression of Palladin. For cells on the permissive fibronectin or fibrinogen matrix, the onset of flow stimulates the PI3-K dependent activation of the α5β1 and the αVβ3 integrins. The binding of these integrins stimulates the activation of Protein Kinase C (PKC), which initiates a pathway that acts upon talin to suppress the α2β1 integrin (Orr *et al.,* 2006).

Figure 3.21 demonstrates the expression of protein following LSS on a collagen matrix. The restriction of gene expression appears to result in the Palladin protein expression to be relatively sustained despite the shear stress. It would seem that there is little to no increase of protein expression for the first 24 hours of shear stress, before the levels reduce at 48 hours, most likely as the cells have fully adapted to chronic shear stress at this point. While the 30 minutes to 6 hour results fail to prove to be a significant result, the 0 and 24 hour samples are, which highlights the little to no change in the samples. Results of statistical analysis showed scores that were just outside the 0.05 threshold, so repeat experiments may provide more definitive results at these time points.

This lack of change indicates that the collagen matrix may possess some kind of method to block the signal that normally stimulates Palladin expression. The α5β1 and αVβ3 integrins are activated on fibronectin and fibrinogen, but not collagen (Orr *et al.*, 2006), which suggests that Palladin expression may be modulated through one such integrin. Flow is also observed to induce α2β1 integrin activation on collagen-plated cells, but not on fibronectin and fibrinogen. An alternative hypothesis is that an integrin such as this may act as an inhibitor of the protein expression under flow. Notably though, expression of the protein is once again higher in the cells on a coated plate as opposed to an uncoated plate. This could suggest that maybe protein levels are elevated to a threshold level following collagen stimulation, but then this doesn't account for the lack of change in protein expression following LSS time points. Again, this could suggest that the shear response is inhibited, but expression is upregulated by virtue of cells interacting with the cell matrix, migrating and necessitating the use of actin-binding proteins such as Palladin.

In conclusion, a proper specific integrin-inhibition assay would need to be performed on sheared HAECs in order to determine the precise integrin responsible for the expression of Palladin. Investigation through Western Blotting and qRT-PCR methods are limited in the sense that they can identify expression of the protein and gene, but cannot pinpoint the integrins involved in expression. However, some of the integrins suggested here would be an ideal starting point for investigation to achieve this goal. It is noteworthy that in the three different matrix-seeding experiments, expression of Palladin appears to reduce by 48 hours of shear stress. It's possible that at this point the cells have reached their maximum potential for spreading across the culture dish area. The matrices can enhance cell migration, so by 48 hours it's likely that the cells aren't remodelling anymore and as a result, Palladin is no longer required. Consequently, a

question was raised of where unwanted protein goes. Chapter 5 discusses the expulsion of Palladin from cells post-shear, through endothelial microparticle release.

This chapter however, has shown how Palladin is expressed within the vasculature, with special focus on the characterisation of gene and protein expression following both acute and chronic haemodynamic forces. It has been demonstrated how the protein is subject to upregulation and downregulation in different areas of the cell, and when in contact with extracellular matrices. The next chapter discusses the interacting proteins LASP-1 and Drebrin, and how they also function under haemodynamic force, with a focus on their shear-induced expression on extracellular matrices.

CHAPTER FOUR

PROTEIN-PROTEIN INTERACTIONS OF PALLADIN

4.1: INTRODUCTION

The connections and interactions one protein has with another can be conceptualized as being part of an interconnecting 3-dimensional signalling and regulatory network within the cell (Szklarczyk *et al.*, 2011). By observing the whole interconnecting network as opposed to observing individual proteins, one can have a "bigger picture" view; gathering better information and an understanding of how a protein functions and interacts with other proteins, as well as how it functions in different locations of the cell. Palladin has already been determined to be an important actin-binding protein (Beck *et al.*, 2013; Dixon *et al.*, 2008). It has also shown to bind to other actin-associated proteins such as VASP (Boukhelifa *et al.*, 2004), profilin (Boukhelifa *et al.*, 2006) and LASP-1(Rachlin and Otey, 2006). Based on the understanding that Palladin is part of a protein network, the next area of research concerned investigating the related protein interactions of Palladin within endothelial cells and the role these interacting proteins may play within the vasculature. To identify the protein interactions, mass spectrometry identification was utilised. This entailed performing immunoprecipation of Palladin from static HAECs using a Co-Immunoprecipitation kit. Co-IP works by covalently coupling antibodies onto an amine-reactive resin and then immunoprecipitating the antigen (also known as bait protein), pulling this protein from the cell lysate and simultaneously co-immunoprecipitating any related proteins which interact with it (also known as prey proteins). Then, using the mass spectrometric analysis, proteins found within the complex containing Palladin could be identified. Protein is digested into smaller peptides. Mass spectrometers measure the molecular weights of these peptides. Specialised software then can compare the weights to a database of known peptides, providing a probability score that the identified peptide is present in the sample. All mass spectrometry was performed courtesy of the National Institute for Cellular Biotechnology, DCU.

Following LSS, the cell undergoes functional and morphological changes (Noria *et al.*, 2004). It has been determined that Palladin plays a role in the reorganisation of the cell in response to shear. The upregulation of Palladin in order to remodel the cell requires communication with other actin-binding proteins. With these observations made, it was hypothesised that differential proteins interact with Palladin at different time points of LSS. Again, Palladin was immunoprecipitated from HAECs, but this time, HAECs were

initially sheared for different time points. It was theorised that certain proteins interact with Palladin, but at specific time points of shear stress only.

Protein interactions were further characterised and illustrated using the Search Tool for the Retrieval of Interacting Genes (STRING®) database. This is a database which quantitatively integrates interaction data from a number of sources and calculates a confidence score for known and predicted protein interactions. The score is derived by separately benchmarking the associations against the classification scheme of another database − the Kyoto Encyclopaedia of Genes and Genomes (KEGG) database. The score represents an estimate of the likelihood that a given association describes a functional link between two proteins, which is at least as specific as that between an average pair of proteins annotated on the same pathway in the KEGG database.

In this case particular regard was given to visualising the interactions of LASP-1 and Drebrin, two actin-binding proteins which were indicated following mass spectrometric analysis of Palladin. This chapter aims to further investigate the presence of LASP-1 and Drebrin within whole endothelial cells and the potential protein interactions with Palladin. With both of them being actin-binding proteins as well, we proposed that these proteins would show a response to haemodynamic force.

LASP-1 is ubiquitously expressed and is involved in cytoskeletal architecture. It has been reported to localise within multiple sites of dynamic actin assembly such as focal contacts, focal adhesions, lamellipodia, membrane ruffles, and pseudopodia, suggesting that it plays an essential role in actin cytoskeleton organisation, especially at the leading edges of migrating cells (Lin *et al.*, 2004). As mentioned, LASP-1 and Palladin interact with one another. The siRNA knockdown of Palladin leads to loss of LASP-1 at actin stress fibres and redirection to focal contacts without changing actin filaments, highlighting how Palladin and LASP-1 interact with one another. Palladin appears to bind and recruit α-actinin to stress fibres where it then binds with LASP-1 via its poly-proline segments (Rachlin and Otey, 2006). In order to further understand the interactions of these two proteins, immunoprecipitation of LASP-1 from HAECs was performed. Mass spectrometric analysis was subsequently performed to indicate the binding partners of LASP-1. By doing so, a comparison between LASP-1 and Palladin Co-IP data could be made, indicating the shared binding partners of the two proteins.

To further characterise the LASP-1 protein, its cellular response to laminar shear stress (LSS) was investigated. Subjecting HAECs to LSS has already shown that Palladin can

be upregulated immediately, indicating an inflammatory response in the cells. After later time points of shear (6 hours), the expression increases further, on account of the actin fibres further restructuring – this time to the chronic LSS. Since the Palladin protein changes because of this haemodynamic force it was hypothesised that the Palladin-associated LASP-1 protein would express a similar pattern when it was investigated.

Following this hypothesis, the expression of LASP-1 in response to shear stress was investigated further, with regards to the potential signalling pathways involved. Chapter 3 has already detailed how Palladin expression changes when cells are grown on various permissive and non-permissive extracellular matrices. HAECs were again cultured on fibrinogen, fibronectin or Type IV collagen, before being subjected to time points of LSS. Through observation of the patterns of LASP-1 expression within the matrix seeded cells, and the comparison to cells on uncoated culture dishes, the potential integrin-mediated signalling pathways involved in LASP-1 expression can be explored further.

Similar experiments were performed on the actin-binding protein Drebrin. Co-IP of Drebrin was performed to observe similar binding proteins to the ones that bind with Palladin or LASP-1. The E2 isoform of this protein is observed within cells of a non-neuronal origin and is believed to play a role within cell migration (Keon *et al.*, 2000). The protein binds to filamentous actin and competes with F-actin stabilising proteins such as α-actinin and tropomyosin (Chew *et al.*, 2005; Ishikawa *et al.*, 1994). In addition to its ability to interact with F-actin, Drebrin has been observed to form a complex with proteins such as myosin (Ishikawa *et al.*, 2007). It also has been observed interacting directly with profilin (Gordón-Alonso *et al.*, 2013; Mammoto *et al.*, 1998); a protein which itself is observed to bind to Palladin (Boukhelifa *et al.*, 2006). Furthermore, Drebrin appears to play a role in induction of podosomes in the cells (Linder and Aepfelbacher, 2003), structures which Palladin has been observed to localise to (Goicoechea *et al.*, 2006). This suggests that the two proteins, if not linked together, may at least be closely associated within the same network.

As a result of this association, the response of Drebrin to haemodynamic forces (laminar shear stress) was also investigated. It was hypothesised that this protein would respond in a similar pattern as Palladin or LASP-1, with immediate upregulation in response to shear. The LSS-induced expression of Drebrin on cells grown on ECMs was

investigated also. By repeating the similar experiments as performed in Chapter 3, only investigating Drebrin, it was hoped to gain an understanding of the function and expression of the protein as the cell interacts with ECMs. The experiments also were performed in an effort to understand the potential integrin-mediated signalling involved in Drebrin expression. As discussed previously, when the sheared cells are in contact with the matrices certain integrins can be differentially expressed. Determining the patterns of expression for Drebrin in this manner could provide an idea of the signalling pathways involved in the regulation of the protein.

4.1.1   Study Aims

The work carried out in this chapter sets out to determine the proteins which interact with Palladin. Two of these proteins – LASP-1 and Drebrin - are investigated in further detail. Their regulation by haemodynamic forces at the protein level is investigated, as is their proteomic response following interactions between cells and extracellular matrices. Therefore the overall aims of this chapter include:

- To immunoprecipitate the Palladin protein from Human Aortic Endothelial Cells and analyse the immunoprecipitated protein using Mass Spectrometry methods to determine other interacting proteins.

- To investigate specific interactions with Palladin that may occur when HAECs are subjected to Haemodynamic Force, i.e. laminar shear stress.

- Observation of the haemodynamic LASP-1 protein and its characterisation in HAECs following laminar shear stress stimulation.

- Investigation of the expression of LASP-1 and potential signalling pathways of this protein through interactions of the cells with permissive and nonpermissive extracellular matrices - fibrinogen, fibronectin and Type IV collagen - following laminar shear stress.

- Observation of the Drebrin protein and its characterisation in HAECs following laminar shear stress stimulation.

- Investigation of the expression of Drebrin and its potential signalling pathways through interactions of the cells with permissive and nonpermissive extracellular matrices - fibrinogen, fibronectin and Type IV collagen – again following laminar shear stress.

4.2: RESULTS

Co-immunoprecipitation experiments were performed on HAECs using the methods listed in Chapter 2.2.5.2. Eluted protein was assayed on a Western Blot in order to confirm presence of target protein. When a column is prepared with antibodies coupled to an activated amine-reactive resin, two control columns are prepared also – one where the activated resin has been deactivated using a provided quenching buffer, and a second where the resin was not activated in the first place. These negative controls are created to confirm that the antibody is bound to the resin, and that immunoprecipitation of protein does occur. The blot in Figure 4.1 shows that only the first eluted sample – the sample with activated resin and antibody – is Palladin protein, as the other results do not show any bands.

Furthermore, the lysate that flowed through each of the columns was also analysed by Western Blot (to confirm that Palladin was in the cells to begin with, and had been pulled out by the IP column). These flow-through samples were also run on the same Western Blot and these bands are also shown in Figure 4.1. The figure also shows a residual amount remaining un-precipitated. However the band visible is much fainter than the ones produced from the lysate flow-through from the control columns, showing that the IP was efficient. The remaining volume of the eluted sample from (i) was then analysed using Mass Spectrometry methods.

These methods entail the digestion of protein into smaller peptides, which are measured and compared to the MASCOT™ database of known peptides. Results are returned in a tabled and ranked format, listing the proteins observed within the sample (Table 4.1). Results are presented with peptide counts and probability scores, showing the likelihood that the result given is for a protein listed. All proteins are identified with probability <0.05. This is one of the parameters for the software used to analyse potential peptides in the database.

Palladin is one of the results returned, as expected. For convenience and visibility, the entry for it is presented first in the table. Other proteins listed include actin, and various other actin-associated proteins such as Myosin, Tubulin isoforms or LASP-1. The role and function of these binding proteins are detailed in Chapter 4.3.
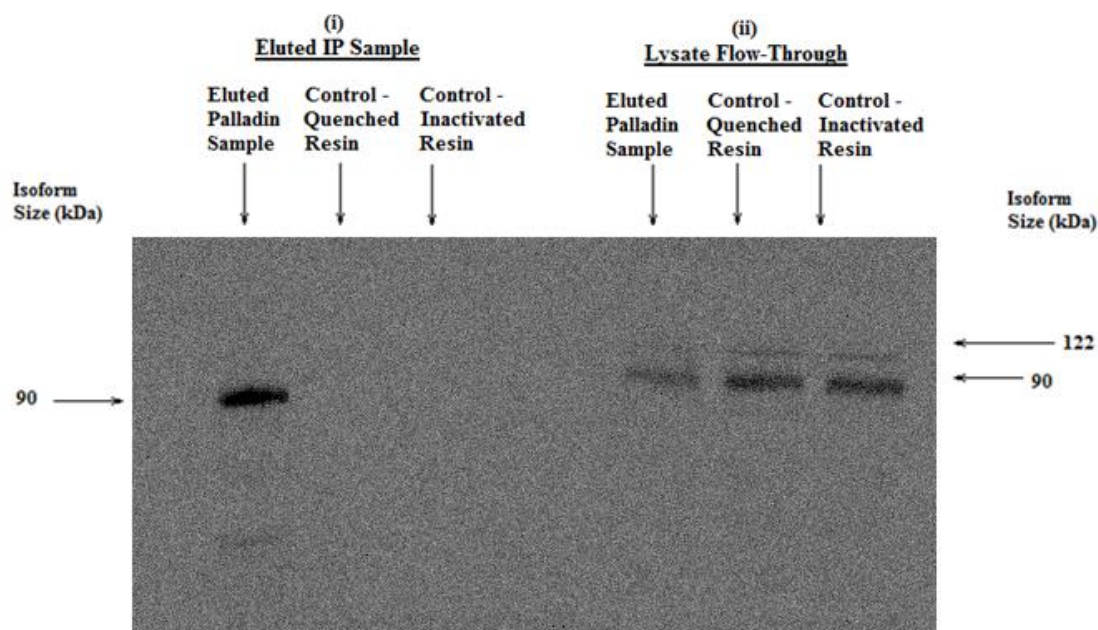
Figure 4.1: Validation of Immunoprecipitated Palladin with Western Blotting techniques. This figure demonstrates the validity of immunoprecipitation. The Palladin protein complex was precipitated from HAEC lysate and a portion of the sample was probed using Western Blotting methods. Also probed were the eluted samples from control IP columns. As observed, the control samples did not show any Palladin binding to those columns, and only appeared in the immunoprecipitated sample where antibody was bound to the activated resin.

Table 4.1: List of Proteins observed following Mass Spectrometry of Palladin Co-Immunoprecipitated from HAECs. The table below displays the results seen from a MASCOT™ search, following analysis of the eluted Palladin sample on a Mass Spectrometer.

Key to table headings:

UI = **Unique Identifier,** referring to the primary accession number of the UniProtKB database.

EN = **Entry Name,** refers to the entry name of the UniProtKB entry.

PN = **Protein Name**.

Pro = **Probability for peptides.** A lower number means a higher probability of a match.

SF = **Score Final.** This is the value of observed vs. theoretical peptide fragment mass spectrum.

P = **Peptides,** i.e. the total number of peptide matches.

UI	EN	PN	Pro	SF	P
Q8WX93	*PALLD_HUMAN*	*Palladin*	*2.56E-05*	*2.63*	*3*
P35579	MYH9_HUMAN	Myosin-9	2.68E-09	25.10	27
P08670	VIME_HUMAN	Vimentin	5.81E-10	13.64	15
P21980	TGM2_HUMAN	Protein-glutamine gamma-glutamyltransferase 2	1.03E-08	11.11	13
P62736	ACTA_HUMAN	Actin, aortic smooth muscle	1.84E-09	6.42	7
P19105	ML12A_HUMAN	Myosin regulatory light chain 12A	2.48E-09	5.72	6
P35580	MYH10_HUMAN	Myosin-10	2.72E-12	4.61	5
P60660	MYL6_HUMAN	Myosin light polypeptide 6	1.94E-09	4.66	5
Q13885	TBB2A_HUMAN	Tubulin beta-2A chain	1.05E-06	3.83	4
P35749	MYH11_HUMAN	Myosin-11	1.19E-08	2.84	3
P17661	DESM_HUMAN	Desmin	3.13E-08	2.85	3
P68371	TBB2C_HUMAN	Tubulin beta-2C chain	1.43E-05	2.57	3
Q9H4B7	TBB1_HUMAN	Tubulin beta-1 chain	4.61E-08	2.60	3
Q16643	DREB_HUMAN	Drebrin	2.26E-11	1.95	2
P07065	CKAP4_HUMAN	Cytoskeleton-associated protein 4	4.78E-05	1.83	2
P14649	MYL6B_HUMAN	Myosin light chain 6B	1.17E-07	1.89	2
Q9BYX7	ACTBM_HUMAN	Beta-actin-like protein 3	4.53E-06	1.71	2
Q71U36	TBA1A_HUMAN	Tubulin alpha-1A chain	5.16E-06	1.60	2
Q14847	LASP1_HUMAN	LIM and SH3 domain protein 1	2.45E-06	0.95	1

Palladin was identified through mass spectrometric analysis of static HAECs. Chapter 3 demonstrates how Palladin responds to haemodynamic force, with particular regards to laminar shear stress. Since the protein is upregulated immediately following shear, but changes over time points, it was believed that Palladin behaves differently depending on acute or chronic shear. With that in mind, it was hypothesised that the binding partners of Palladin may change also in response to time points of LSS. Specifically, it was believed that there may be proteins that only bind with Palladin at certain time points. The Palladin protein complex was then immunoprecipitated from HAECs which were subjected to shear time points. Again, samples were analysed using mass spectrometry and the MASCOT™ database.

The lists of proteins extracted after each time point were compared against each other to observe if there were any new and specific proteins expressed after time points of shear. Results are presented in Table 4.2, showing the unique proteins observed at specific time points. Most unique proteins appear to bind to Palladin at 30 minutes to 3 hours, or else at 24 hours – times of acute shear stress and chronic shear stress, respectively. At early time points, results appear to be groups of various histones and actin-binding proteins. At 24 hours, there are still histones and actin-binding proteins, but also a number of kinases and RNA-binding proteins. The roles of these proteins are discussed in Chapter 4.3.

Table 4.2: Unique proteins observed in Mass Spectrometric analysis of Palladin Immunoprecipitated from HAECs sheared at various time points. Palladin was co-immunoprecipitated from different time points of sheared HAECs. The immunoprecipitated complexes were again analysed using Mass spectrometry and a MASCOT™ search. The table below lists the unique proteins observed at specific time points, the roles of which are discussed in Chapter 4.3. On account of the analysis software used in the National Institute for Cellular Biotechnology being upgraded between the performance of other analyses and this analysis, the presentation of results is slightly different. As such, final score is now replaced by a general Score, and the probability for peptides is no longer presented. Results in Table 4.4 and 4.5 are presented in the older format.

Key to table headings:
UI = **Unique Identifier,** referring to the primary accession number of the UniProtKB database.
Entry Name refers to the entry name of the UniProtKB entry.
S = **Score**, a cross-correlation value of observed vs. theoretical peptide fragment mass spectrum.
P = **Peptides,** i.e. the total number of peptide matches.

30 Minutes				
UI	**Entry Name**	**Protein Name**	**S**	**P**
P06454	PTMA_HUMAN	Prothymosin alpha	8.83	5
P07355	ANXA2_HUMAN	Annexin A2	5.20	3
Q14764	MVP_HUMAN	Major Vault Protein	4.83	2
Q13470	TNK1_HUMAN	Non-receptor tyrosine-protein kinase	2.27	1
3 Hours				
UI	**Entry Name**	**Protein Name**	**S**	**P**
O75531	BAF_HUMAN	Barrier-to-autointegration factor	4.61	1
P68032	ACTC_HUMAN	Actin, alpha cardiac muscle 1	31.10	13
P68366	TBA4A_HUMAN	Tubulin alpha-4-A chain	13.25	4
P09382	LEG1_HUMAN	Galectin-1	2.23	1
P62805	H4_HUMAN	Histone H4	2.59	1
P67809	YBOX1_HUMAN	Nuclease-sensitive element-binding protein 1	3.07	1
Q01449	MLRA_HUMAN	Myosin regulatory light chain 2	2.49	1
P16401	H15_HUMAN	Histone H1.5	4.82	2
P22492	H1T_HUMAN	Histone H1t	5.93	3
P05141	ADT2_HUMAN	ADP/ATP translocase 2	2.65	1
O43791	SPOP_HUMAN	Speckle-type POZ protein	2.89	1
P35637	FUS_HUMAN	RNA-binding protein FUS	2.61	1
Q00839	HNRPU_HUMAN	Heterogeneous nuclear ribonucleoprotein U	5.05	1
Q9NZN4	EHD2_HUMAN	EH domain-containing protein 2	7.02	3
Q9P1Z9	CI174_HUMAN	Uncharacterized protein C9orf174	3.80	1

6 Hours				
UI	**Entry Name**	**Protein Name**	**S**	**P**
P60953	CDC42_HUMAN	Cell division control protein 42 homolog	2.09	1
P27658	CO8A1_HUMAN	Collagen alpha-1(VIII) chain	2.09	1

24 Hours				
UI	**Entry Name**	**Protein Name**	**S**	**P**
P52943	CRIP2_HUMAN	Cysteine-rich protein 2	5.01	2
Q96KK5	H2A1H_HUMAN	Histone H2A type 1-H	8.40	3
Q562R1	ACTBL_HUMAN	Beta-actin-like protein 2	12.01	5
P23528	COF1_HUMAN	Cofilin-1	4.16	2
O60814	H2B1K_HUMAN	Histone H2B type 1-K	2.29	1
P98179	RBM3_HUMAN	Putative RNA-binding protein 3	2.04	1
P25705	ATPA_HUMAN	ATP synthase subunit alpha, mitochondrial	6.86	3
Q8NC51	PAIRB_HUMAN	Plasminogen-activator inhibitor-1 RNA-binding protein	2.92	1
P23246	SFPQ_HUMAN	Splicing factor, proline and glutamine-rich	2.83	1
Q13724	MOGS_HUMAN	Mannosyl-oligosaccharide glucosidase	3.14	1
P49411	EFTU_HUMAN	Elongation factor Tu, mitochondrial	3.47	1
P12956	XRCC6_HUMAN	X-ray repair cross-complementing protein 6	2.65	1
Q6ZS86	GLPK5_HUMAN	Putative glycerol kinase 5	2.65	1
Q5TAX3	TUT4_HUMAN	Terminal uridylyltransferase 4	3.46	1
Q14152	EIF3A_HUMAN	Eukaryotic translation initiation factor 3 subunit A	3.06	1

Palladin had been shown to interact with a variety of proteins at this stage. The protein interactions which occur with Palladin were next illustrated using the Search Tool for the Retrieval of Interacting Genes (STRING®) database. This database collects different data from a number of sources to compare numbers of proteins together. In doing so, it can calculate a confidence score for known and predicted protein interactions. The score represents an estimate of the likelihood that a given association describes a functional link between two proteins, which is at least as specific as that between an average pair of proteins annotated on the same pathway in the KEGG database. The data from Table 4.1 was inputted into the STRING® search to highlight the network that all the immunoprecipitated proteins exist in. Results are shown in Figure 4.2, along with a visual map (also produced by the software) of the pathways and connections involved between proteins. Options exist for adding more predicted protein partners in order to observe more interacting pathways, but most have been omitted so as to show a clearer diagram. Palladin (PALLD) and LASP-1 appear to show a direct interaction, with a link between the two proteins having been documented and characterised (Rachlin and Otey, 2006). Palladin and Drebrin (DBN1) appear to have an interaction, via noted second-degree links between the Ezrin and/or α-actinin proteins.

Figure 4.2.1 illustrates the probing of immunoprecipitated Palladin which was probed separately for (i) LASP-1 and (ii) Drebrin. Bands for Palladin are shown on the same sample to confirm that this protein was initially present. The resulting bands show that LASP-1 is present in a large amount. However, bands for Drebrin are weak, suggesting that Drebrin is less associated with Palladin than LASP-1.
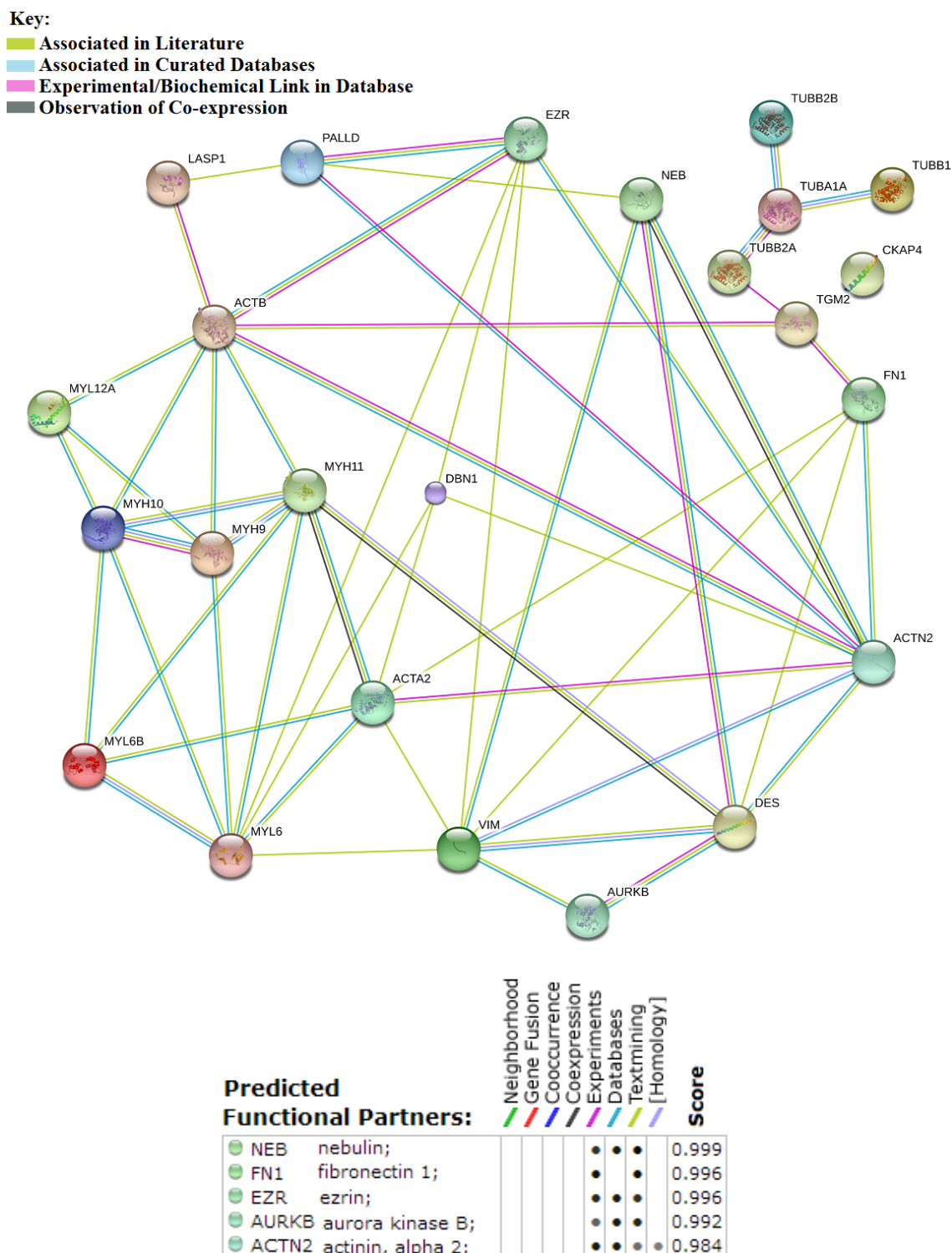
Figure 4.2: STRING® analysis of predicted protein-protein interactions. STRING® (Search Tool for the Retrieval of Interacting Genes/proteins) is a database of known and predicted protein interactions. It was used to generate a simple diagram to highlight how the Palladin, LASP-1 and Drebrin proteins most likely interact with each other and other proteins. Table 4.3 lists a key to the results. The different coloured lines represent the types of evidence for associations between proteins, as indicated. The software also provides a brief summary of the predicted functional partners of the listed main proteins, based on compilation of existing evidence, to which it assigns a score based on probability of interaction. Scores closer to 1.0 represent that interactions are more likely to occur.

Table 4.3: STRING® Diagram colour key. This key accompanies the STRING® created diagram in Figure 4.2. The coloured images represent specific proteins.

Colour	Protein	Colour	Protein
	ACTA2 Actin, Alpha 2		ACTB Actin, Beta
	MYL6 Myosin Light Chain 6		MYL6B Myosin Light Chain 6B
	MYL12A Myosin, Light Chain 12A		MYH9 Myosin, Heavy Chain 9
	MYH10 Myosin Heavy Chain 10		MYH11 Myosin, Heavy Chain 11
	TUBA1A Tubulin Alpha 1a		TUBB1 Tubulin, Beta 1
	TUBB2A Tubulin, Beta 2A		TUBB2B Tubulin, Beta 2B
	CKAP4 Cytoskeleton-associated protein 4		DBN1 Drebrin
	DES Desmin		LASP1 Lim and SH3 Protein 1
	TGM2 Transglutaminase		VIM Vimentin
	PALLD Palladin		
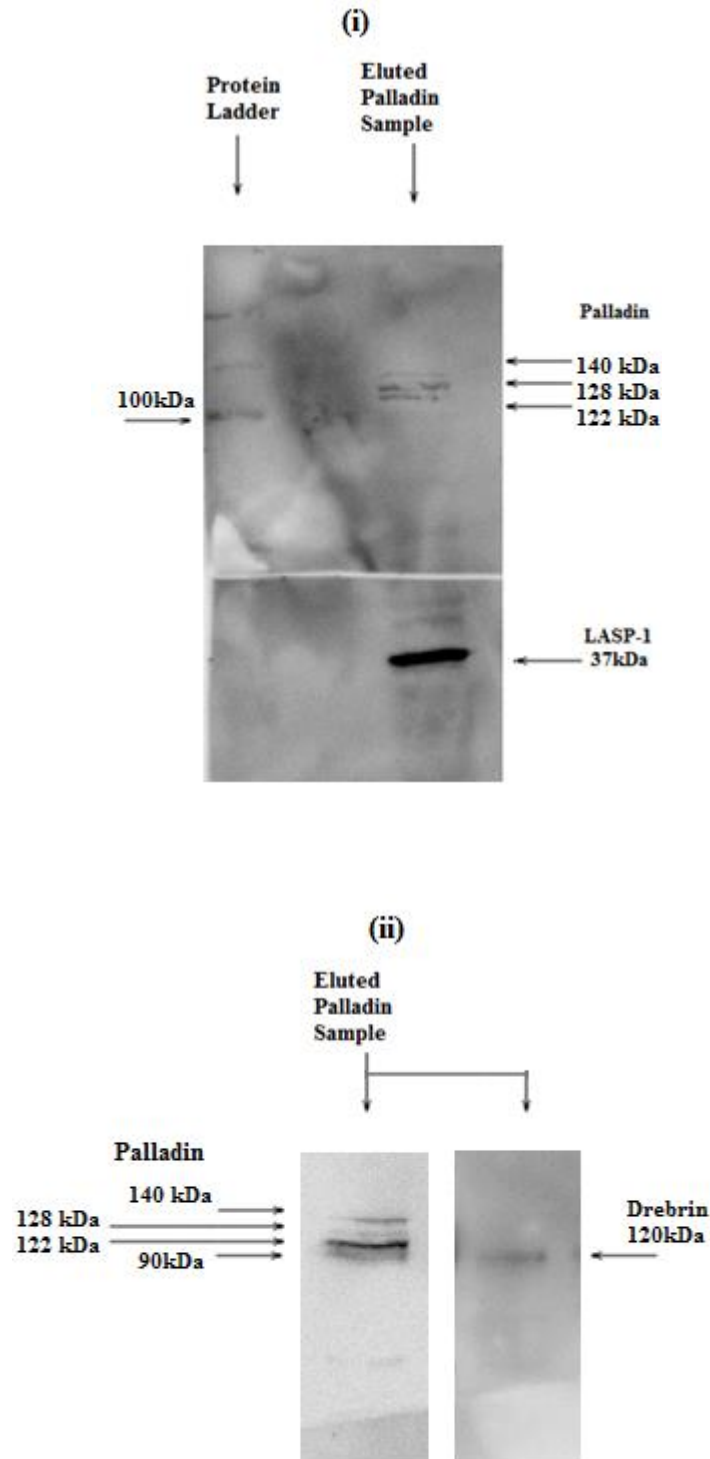
Figure 4.2.1: Western Blotting of Immunoprecipitated Palladin to probe for LASP-1 and Drebrin. In Figure 4.2.1 (i), the immunoprecipitated Palladin sample was analysed using Western Blotting methods and probed for both Palladin (at 140kDa) and LASP-1 (37kDa). The figure shows that the eluted Palladin also contained LASP-1 within the same protein complex. Figure 4.2.1 (ii) shows the probing of eluted Palladin, which was confirmed by Western Blot. The blot was stripped and then reprobed for Drebrin. Faint bands are present, confirming presence of Drebrin.

When investigating the links between proteins, particular regard was given to visualising the interactions of LASP-1 and Drebrin, two actin-binding proteins which were indicated following mass spectrometric analysis of Palladin. LASP-1 has been shown to be a known binding partner of Palladin, so its presence in HAECs was of interest. The Drebrin protein was intriguing, as it is a protein normally observed in the brain. However, like Palladin, it is actin-binding and plays a major role in cellular development. This chapter aims to further investigate the presence of LASP-1 and Drebrin within whole endothelial cells and the potential protein interactions with Palladin. With both of them being actin-binding, we proposed that these proteins would show a response to haemodynamic force.

Using LASP-1 specific antibodies, this protein was first immunoprecipitated and investigated using mass spectrometric analysis. Figure 4.3 validates the immunoprecipitation as being successful; a band is visible for the eluted LASP-1 sample, but not the control samples. When probing the lysate flow-through, a weak band is visible for the eluted LASP-1 protein, but it is much weaker than the controls – showing that most of the protein present was pulled out from the cells.

Table 4.4 highlights the actin-binding proteins that LASP-1 was found to interact with. For convenience and visibility, its entry is presented at the top of the table. Notably, Palladin does not appear in the results. However, LASP-1 did appear in table 4.1 as did proteins such as Vimentin and other actin and tubulin isoforms – showing they share a connection. Some proteins such as caveolin are highlighted as they appear to bind to LASP-1, but do not appear bound to Palladin in Table 4.1. The role and function of these LASP-1 binding proteins are detailed in Chapter 4.3.

The same specific antibodies were used to obtain immunofluorescence images of the protein within fixed HAECs (Figure 4.4). LASP-1 can be observed localising to stress fibres (designated as SF), but appears reduced in the nucleus (designated as N). This is discussed later in Chapter 4.3.
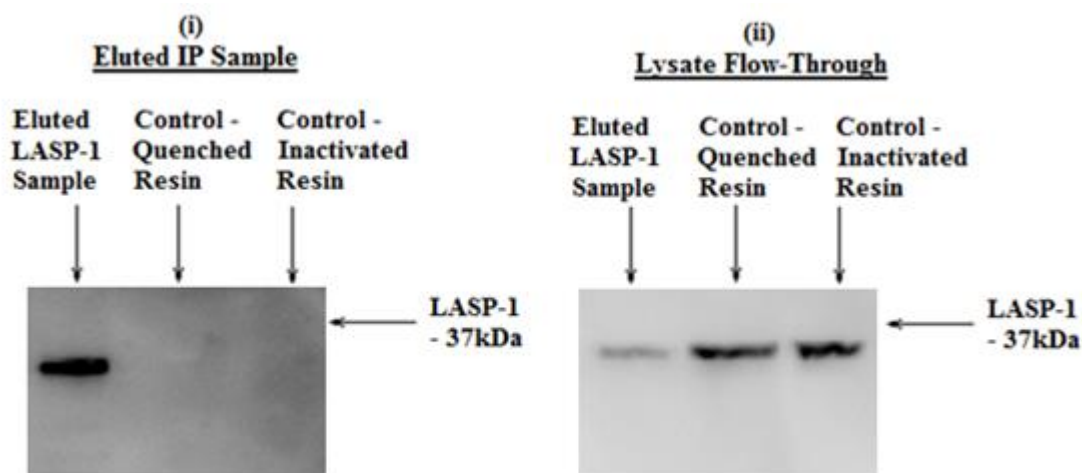
Figure 4.3: Validation of Immunoprecipitated LASP-1 with Western Blotting techniques.
After the immunoprecipitation of LASP-1 from Human Aortic Endothelial Cell lysate, some of
the protein sample eluted from the spin columns was taken and run on a Western Blot to verify
the presence of protein. Again, this sample was analysed along with the eluted samples from the
control IP columns – one column with the activated binding resin having being quenched, and
one column with an inactivated resin used instead. As shown above, the controls did not bind
any LASP-1 protein to the columns. As implemented before, lysate that flowed through the
columns was also analysed afterwards by Western Blot to verify that LASP-1 was present in the
cell lysate to begin with. Again, a small amount of LASP-1 failed to be precipitated; but most of
it was successfully collected in the eluted sample. This eluted sample was analysed using Mass
Spectrometry.

Table 4.4: List of Proteins observed following Mass Spectrometry of LASP-1 Immunoprecipitated from HAECs. This table displays the results seen from a MASCOT™ search, following analysis of an eluted LASP-1 sample on a Mass Spectrometer. As seen, multiple other hits for other proteins are observed in the table. Many of the ones listed are actin-binding and responsible for cell structure. Proteins listed in bold do not appear in Table 4.1.

Key to table headings:

UI = **Unique Identifier,** referring to the primary accession number of the UniProtKB database.

EN = **Entry Name,** refers to the entry name of the UniProtKB entry.

PN = **Protein Name**.

Pro = **Probability for peptides.** A lower number means a higher probability of a match.

SF = **Score Final.** A value of observed vs. theoretical peptide fragment mass spectrum.

P = **Peptides,** i.e. the total number of peptide matches.

UI	EN	PN	Pro	SF	P
Q14847	*LASP1_HUMAN*	*LIM and SH3 domain protein 1*	*2.37E-07*	*5.57*	*6*
P08670	VIME_HUMAN	Vimentin	6.22E-14	16.43	18
P62736	ACTA_HUMAN	Actin, aortic smooth muscle	2.45E-11	11.47	13
P60709	**ACTB_HUMAN**	**Actin, cytoplasmic 1**	**1.00E-30**	**7.67**	**8**
P17661	DESM_HUMAN	Desmin	2.18E-05	2.62	3
Q03135	**CAV1_HUMAN**	**Caveolin**	**1.44E-07**	**1.73**	**2**
Q9BYX7	ACTBM_HUMAN	Beta-actin-like protein 3	1.51E-09	1.88	2
Q71U36	TBA1A_HUMAN	Tubulin alpha-1A chain	1.48E-05	1.58	2
Q9NQC3	**RTN4_HUMAN**	**Reticulon-4**	**4.77E-11**	**1.58**	**2**
Q562R1	**ACTBL_HUMAN**	**Beta-actin like protein 2**	**1.35E-04**	**1.26**	**2**

(i)
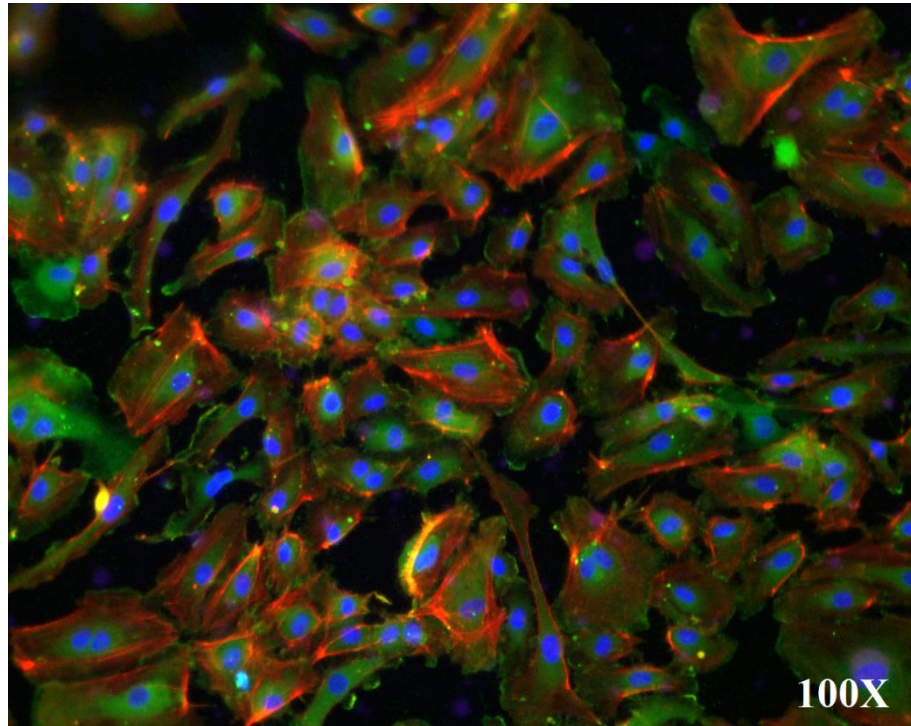
(ii)
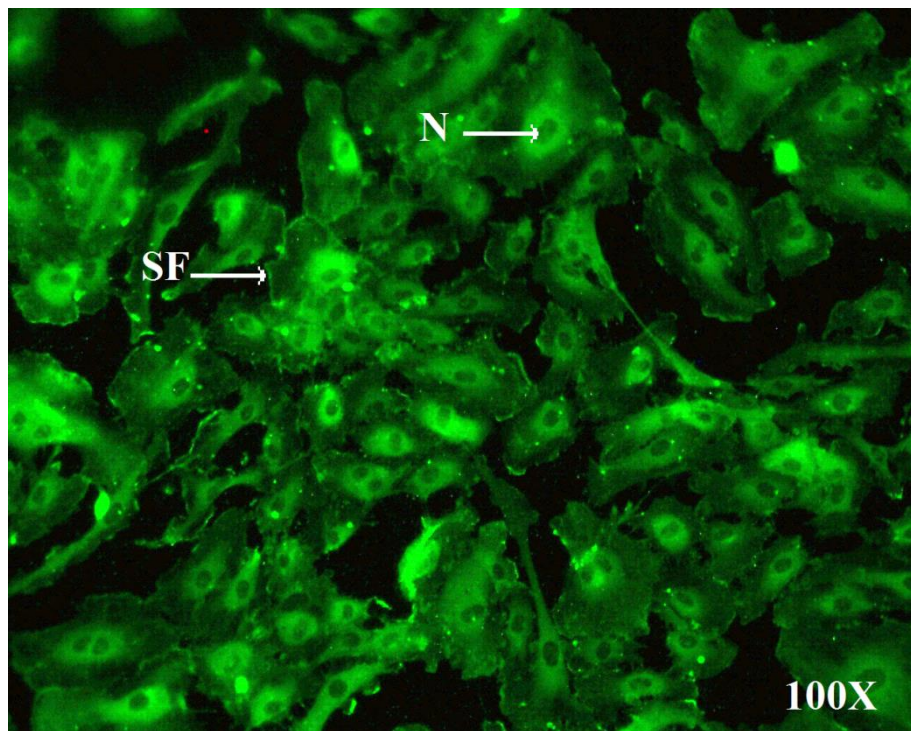
Figure 4.4: Immunofluorescence imaging of LASP-1 in static HAECs. In Figure 4.4 (i), the cells are stained with DAPI (a blue nucleus stain), Phalloidin (a red actin stain) and an AlexaFluor-488 conjugate that binds with the LASP-1 antibody (Green). These cells are viewed at 100x magnification. The cells in Figure 4.4 (ii) are prepared according to the same conditions - but without a DAPI nuclear stain or Phalloidin actin stain , so as to allow better viewing of LASP-1 in the cells.

Since LASP-1 is an actin-binding protein and it binds to Palladin, it was hypothesised that it may also be haemodynamic and therefore it follows a similar expression model. Figure 4.5 shows that, while not an exact match to Palladin, LASP-1 does have an analogous pattern. Immediately following shear, LASP-1 is significantly upregulated, increasing over 60% in expression. After this increase, it declines at 2-3 hours post-shear – not unlike how Palladin experiences a decline at the same time point. However, the decline in LASP-1 expression is not as sharp as that seen in Palladin (Figure 3.10). Protein expression stays almost steady, before increasing again at 6 hours. At 24 hours onwards, the amount of LASP-1 expressed declines again. This pattern is again similar to the expression of Palladin. However it appears that the shear-induced changes in LASP-1 protein regulation are not as drastic as that seen with Palladin.
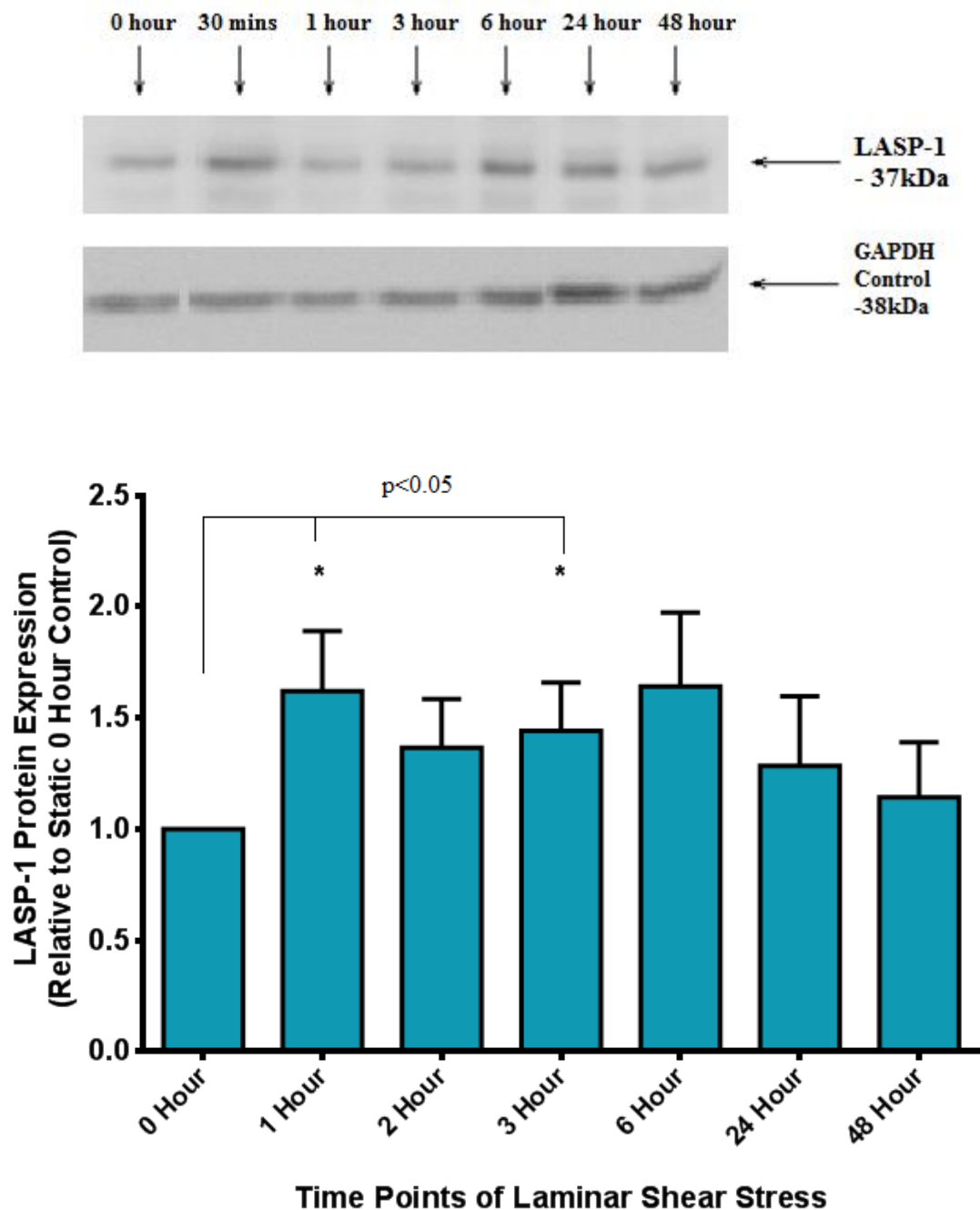
Figure 4.5: LASP-1 protein expression in HAECs subjected to Laminar Shear Stress at 10 dynes/cm^2. Following probing for LASP-1 in sheared HAECs, the Western Blot was stripped and reprobed for GAPDH to use as an endogenous control. All bands were analysed using ImageJ Densitometric quantification software. The values given for intensity of each LASP-1 band is given here, following normalisation against the GAPDH control bands, and are expressed in comparison to the baseline zero hour shear. Data is representative of at least 4 independent experiments ±SEM.*p<0.05.

The parallels between Palladin and LASP-1 expression were examined in more detail, with the probing for LASP-1 in cells cultured on extracellular matrices and then subjected to laminar shear stress. As stated previously, endothelial cells subjected to this have been shown to have specific integrins inactivated (Orr *et al.*, 2006). It was postulated that LASP-1 may be subject to the same integrin signalling mechanisms as Palladin. While we are not able to pinpoint the precise signalling mechanisms involved, through investigating the expression with these ECMs, we can at least gain an insight into what may be occurring.

Analysis involving the fibrinogen matrix (Figure 4.6) shows that the matrix alone causes LASP-1 expression to be significantly increased. Comparing static uncoated to static cells on fibrinogen shows that the matrix causes an over two-fold increase of LASP-1 expression. This increase slowly declines after longer periods of shear (albeit still remaining above baseline levels), and doesn't appear to increase any further at later time points. Investigation with the second matrix, fibronectin, showed that initially seeding the cells onto the matrix causes an upregulation in protein again. Once the cells are sheared, the expression declines back to baseline levels. It peaks at 24 hours before declining again at 48 hours. It should be noted that these results did not prove to be significant, so a definitive conclusion cannot be drawn from these results. Finally, LASP-1 expression when cells are in contact with collagen is demonstrated. LASP-1 is shown to increase when comparing the static cells cultured on this matrix to those cultured on regular dishes. The LASP-1 expression increases further post-shear, peaking at 1 hour of LSS. Afterwards, it declines at a steady rate until 24 hours, where protein expression rises again. This is not unlike the expression pattern seen following regular shear stress experiments, although the differences in expression are more disparate, and appear to be delayed with peak expression happening later than usual.
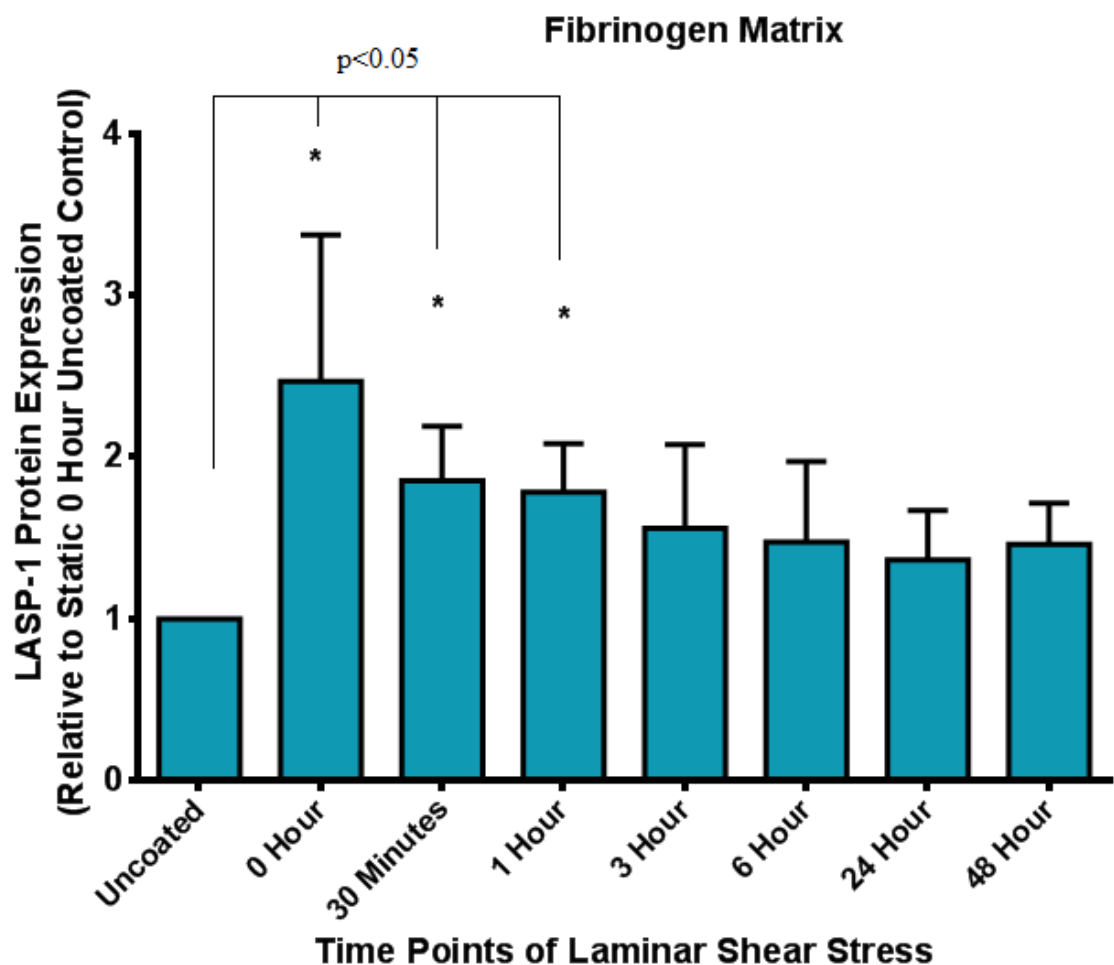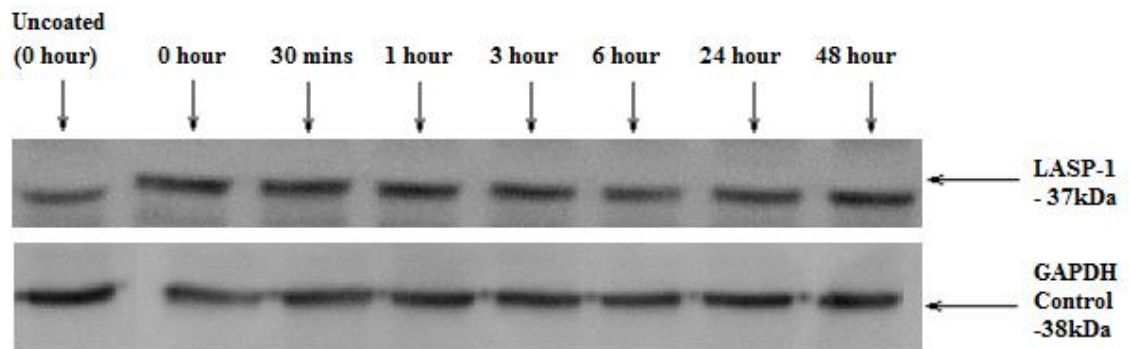
Figure 4.6: LASP-1 protein expression in HAECs seeded onto Fibrinogen Matrix and Sheared at 10 dynes/cm². HAECs were seeded onto a matrix consisting of 10μg/ml fibrinogen and allowed to reach confluency. They were then sheared at the listed time points and then blotted for LASP-1 protein. Lysate from regular HAECs was also used as a control to illustrate the effect of the fibrinogen matrix alone on the expression of LASP-1. Western Blots were analysed using ImageJ densitometry software. Results are listed relative to the static zero hour control, where cells were seeded onto regular uncoated culture dishes and not subjected to LSS. *p<0.05.
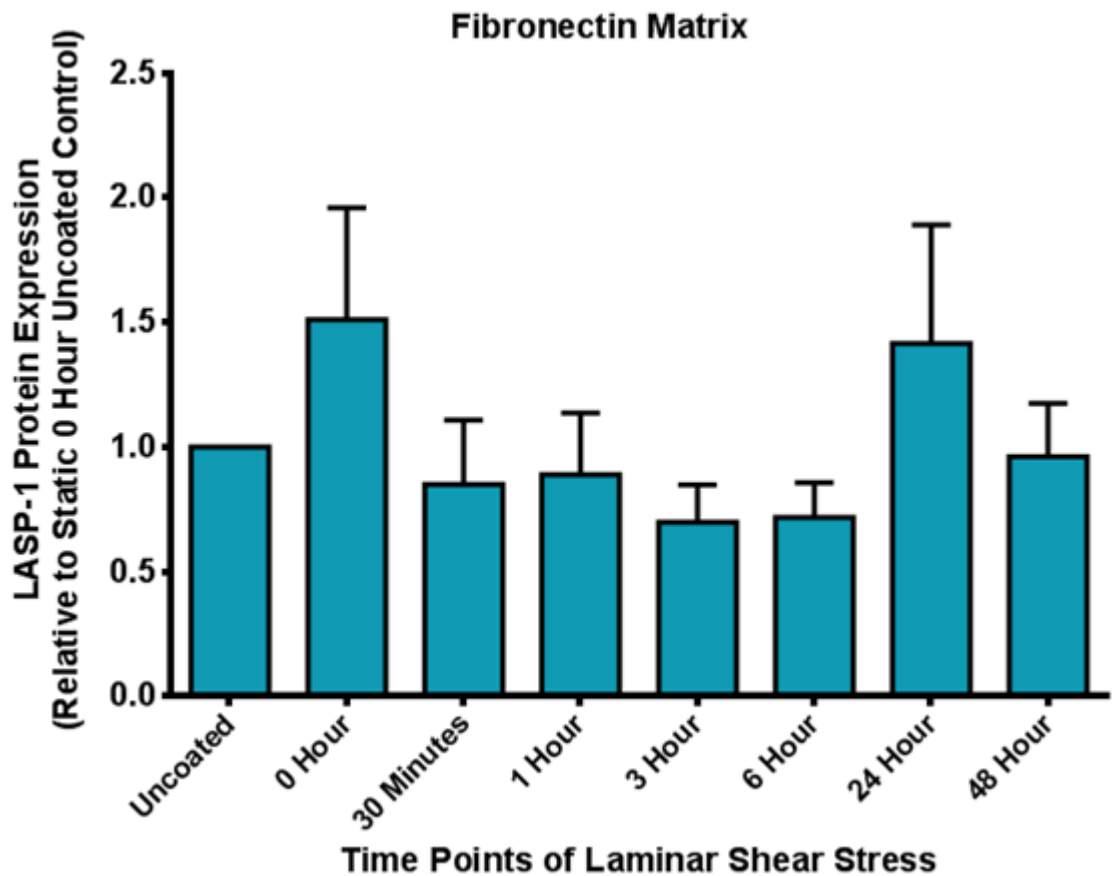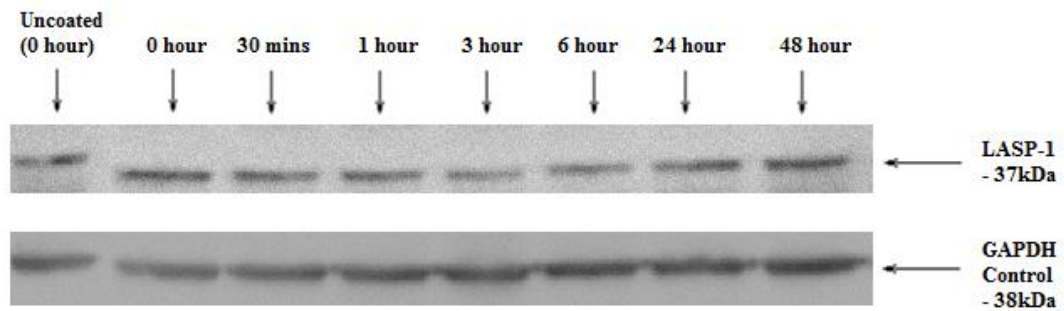
Figure 4.7: LASP-1 protein expression in HAECs seeded onto Fibronectin Matrix and Sheared at 10 dynes/cm^2. HAECs were seeded onto a matrix consisting of 10μg/ml fibronectin and allowed to reach confluency. Following this, they were sheared at the listed time points and then blotted for LASP-1. Lysate from regular HAECs was also used as a control to illustrate the effect of the fibronectin matrix alone on the expression of LASP-1. All bands were analysed using ImageJ software. Results are listed relative to the static zero hour control, where cells were seeded onto regular uncoated culture dishes and not subjected to laminar shear stress. Statistical analysis failed to show $p < 0.05$, so a definitive conclusion cannot be deduced.
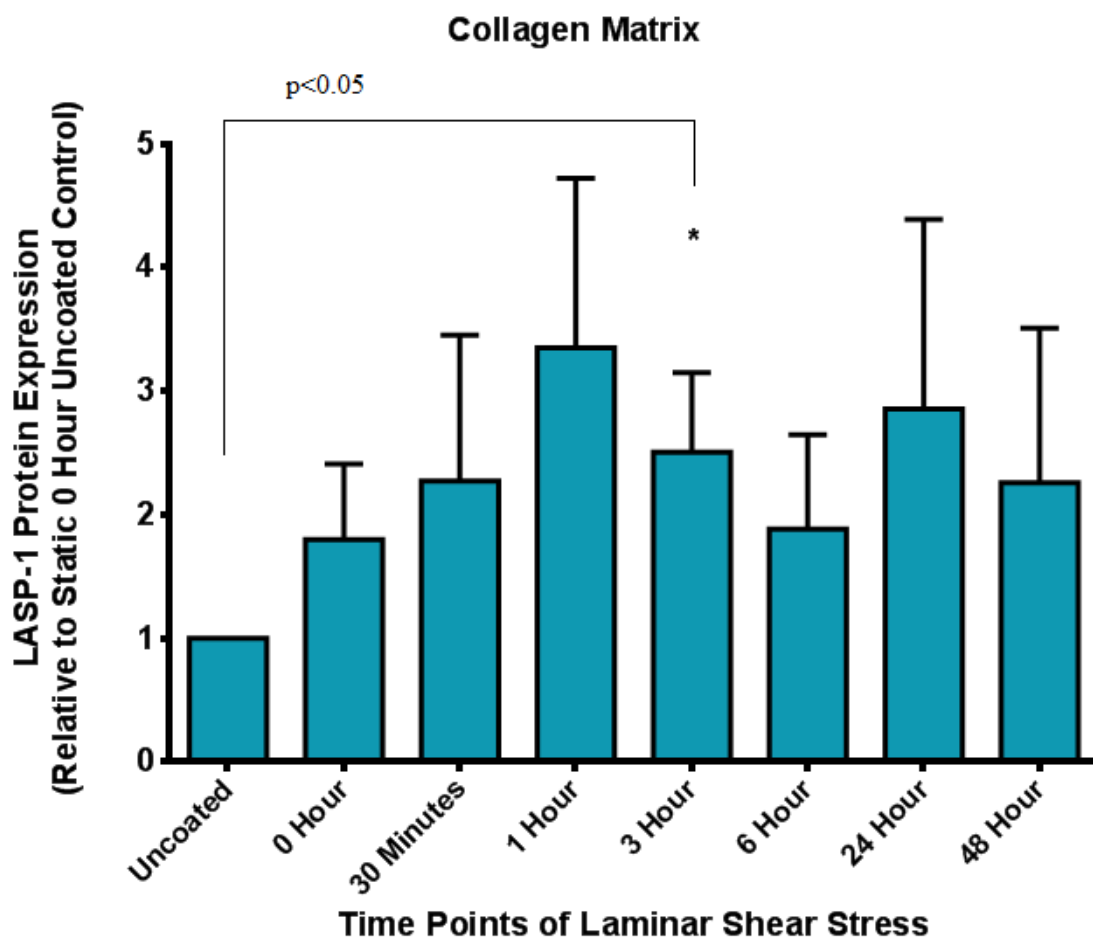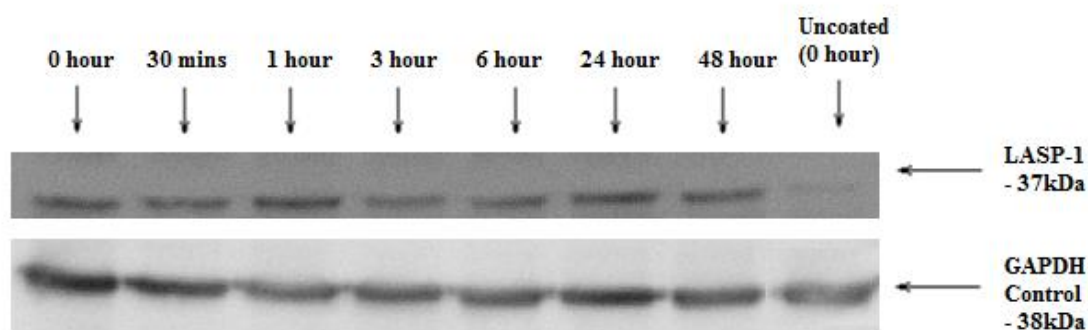
Figure 4.8: LASP-1 protein expression in HAECs seeded onto Collagen Matrix and Sheared at 10 dynes/cm². HAECs were seeded onto a matrix consisting of 20μg/ml Type IV collagen and allowed to reach confluency. Following this, they were sheared at the listed time points and then blotted for LASP-1 Lysate from regular HAECs was also used as a control to illustrate the effect of the collagen matrix alone on the expression of LASP-1. All bands were analysed using ImageJ software. Results are listed relative to the static zero hour control, where cells were seeded onto regular uncoated culture dishes but not subjected to laminar shear stress. *p<0.05. However, some results had too large of a variance in standard error to allow statistical analysis to prove them to be significant changes.

Another result following the immunoprecipitation of Palladin merited further investigation. The Drebrin protein is typically a protein found within the brain, where it plays a role in cell structure and development, but it has been found in other cell types. Recently this protein has been determined to be present within HUVECs (Rehm *et al.*, 2013) so it was hypothesised that the protein should be present within HAECs also. Investigations involving immunoprecipitation showed that the protein was pulled out of HAECs and indeed present in this cell type (Figure 4.9). However, the mass spectrometric analysis did not prove as successful as hoped, in that a result for Drebrin was not returned (Table 4.5). This may be due to the protein being obscured by other, more ubiquitous proteins within the eluted protein complex. Some of the results from the mass spectrometric analysis did show a shared number of proteins with Palladin and LASP-1. Proteins such as Vimentin, or Myosin Light Chain 12A were shown to be shared among the three proteins of interest. When investigating the Vimentin and Myosin proteins in Figure 4.2, it is shown how these proteins are part of the same network, with them being connected to Palladin, Drebrin and LASP-1 via different actin and myosin isoforms. The immunoprecipitated Drebrin sample also returned results for other actin-binding proteins in Table 4.5. Such proteins include Galectin or Calmodulin, the roles of which are discussed later in this chapter.

To prove the presence of Drebrin within HAECs, immunofluorescence experiments were also performed, results of which are demonstrated in Figure 4.10. Drebrin is confirmed within HAECs, where it can be observed localising to stress fibres (SF), but appears depleted in the nucleus (N). Notably, strong clusters of Drebrin appear at the edges of the cells. Images are provided with or without a Phalloidin actin stain, or with and without a DAPI nuclear stain. A more detailed image at 200X was obtained with Figure 4.10 (iii) illustrating a clearer picture of Drebrin localising to the stress fibres.
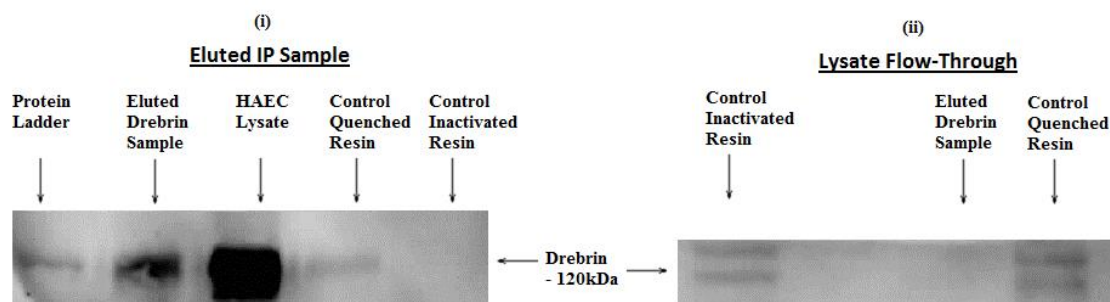
Figure 4.9: Validation of Immunoprecipitated Drebrin with Western Blotting techniques. The Drebrin sample immunoprecipitated from HAECs was analysed on a Western Blot along with the eluted samples from the control IP columns – one with the activated binding resin having being quenched, and one with an inactivated resin used instead. As shown above, there did not appear to be any immunoprecipitation of the protein to the controls, but a clear band could be seen in the Eluted protein sample. A HAEC lysate was probed on the same band for a separate investigation - care was taken for the sample not to spill into surrounding wells, where it could provide a false positive. As before, lysate flow-through was probed for Drebrin, so to verify the extraction of the protein from the cells. The eluted sample was analysed using Mass Spectrometry.

Table 4.5: List of Proteins observed following Mass Spectrometry of Drebrin Immunoprecipitated from HAECs. This table displays the results seen from a MASCOT™ search, following analysis of the eluted Drebrin sample on a Mass Spectrometer. While a result for Drebrin did not appear, it is certain the protein is present (Figure 4.9) - the signal may be just drowned out by the presence of the more prominent actin-binding proteins. Proteins listed in bold do not appear in Table 4.1.

Key to table headings:
UI = **Unique Identifier,** referring to the primary accession number of the UniProtKB database.
EN = **Entry Name,** refers to the entry name of the UniProtKB entry.
PN = **Protein Name**.
Pro = **Probability for peptides.** A lower number means a higher probability of a match.
SF = **Score Final.** A value of observed vs. theoretical peptide fragment mass spectrum.
P = **Peptides,** i.e. the total number of peptide matches.

UI	EN	PN	Pro	SF	P
P08670	VIME_HUMAN	Vimentin	6.66E-15	3.55	4
P60709	**ACTB_HUMAN**	**Actin, Cytoplasmic 1**	1.73E-12	2.86	3
P09382	**LEG_HUMAN**	**Galectin-1**	5.47E-12	0.99	1
P04406	**G3P_HUMAN**	**Glyceraldehyde-4-phosphate dehydrogenase**	8.42E-12	0.98	1
Q71U36	TBA1A_HUMAN	Tubulin alpha-1A chain	1.84E-11	1.94	2
P06733	**ENOA_HUMAN**	**Alpha-enolase**	5.88E-11	1.84	2
P21333	**FLNA_HUMAN**	**Filamin-A**	3.15E-10	0.96	1
P02768	**ALBU_HUMAN**	**Serum Albumin**	5.80E-10	3.52	4
P62736	ACTA_HUMAN	Actin, aortic smooth muscle	2.16E-09	5.68	6
P62158	**CALM_HUMAN**	**Calmodulin**	1.22E-08	0.96	1
P19105	ML12A_HUMAN	Myosin regulatory light chain 12A	1.98E-08	1.88	2

(i)
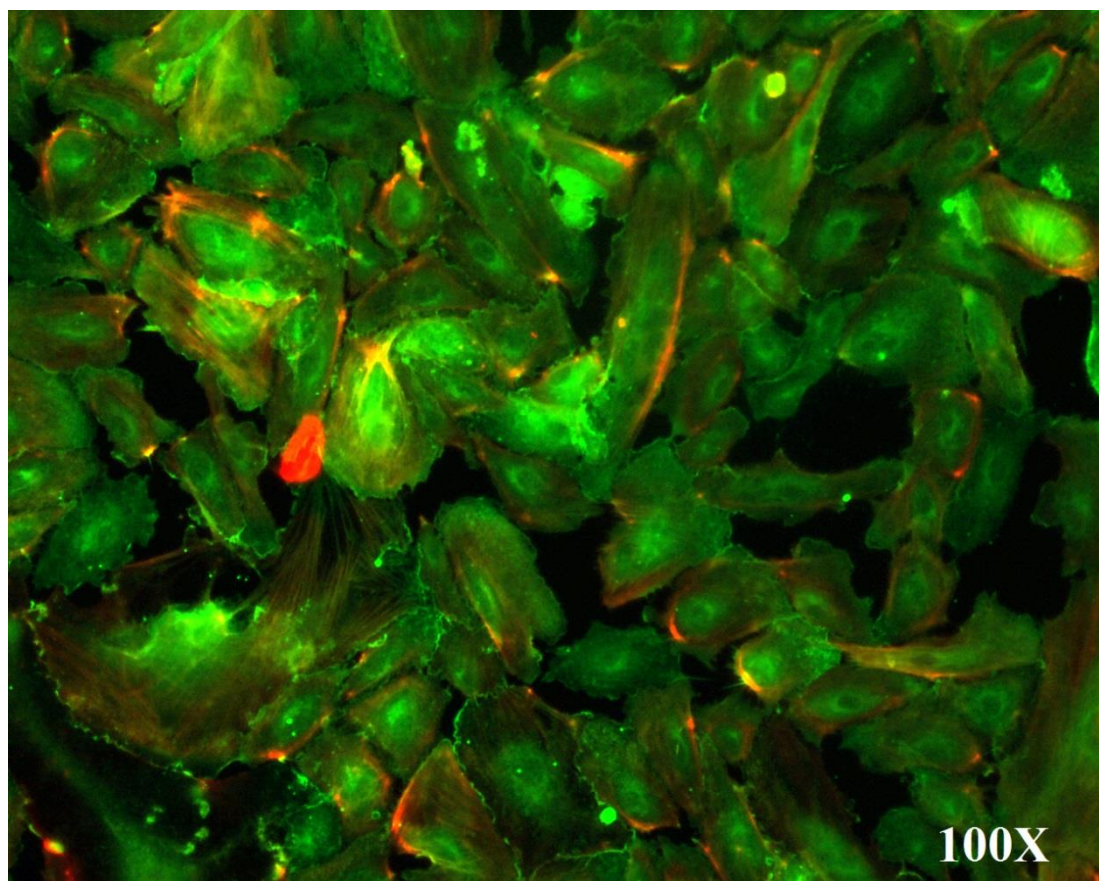
(ii)
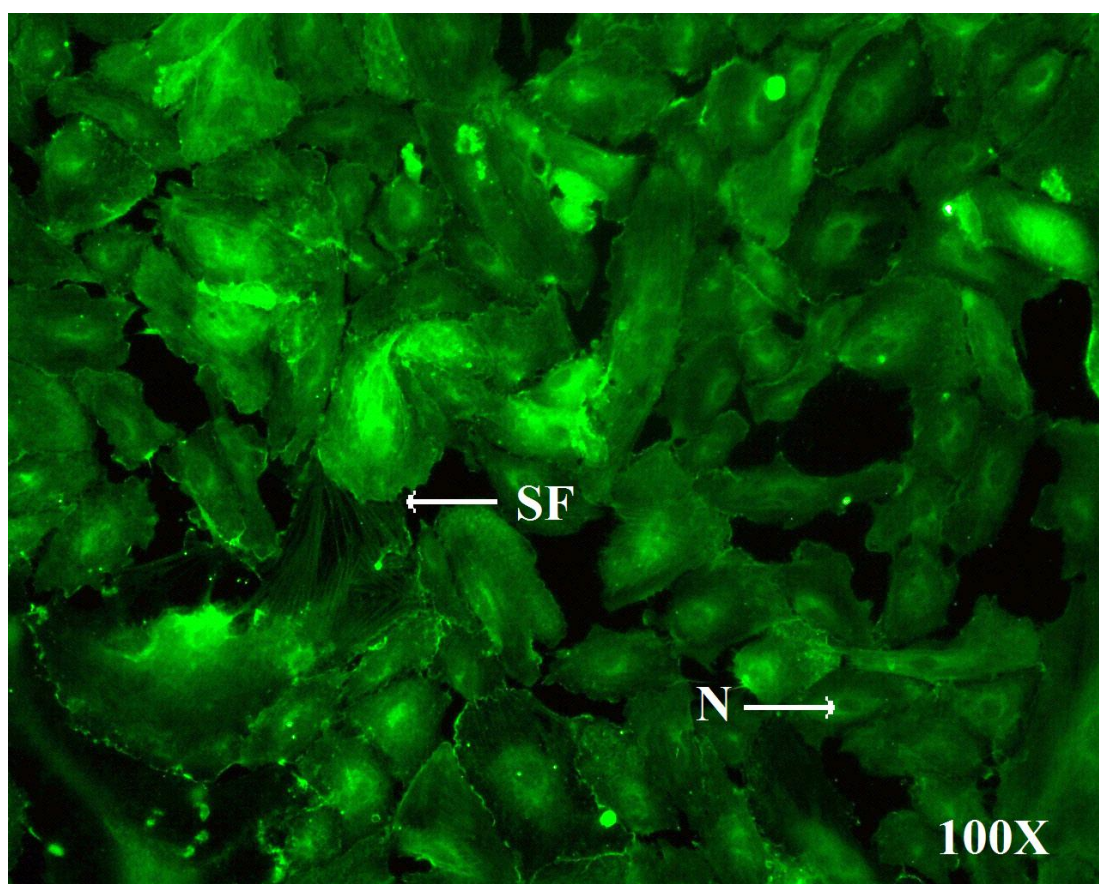
(iii)
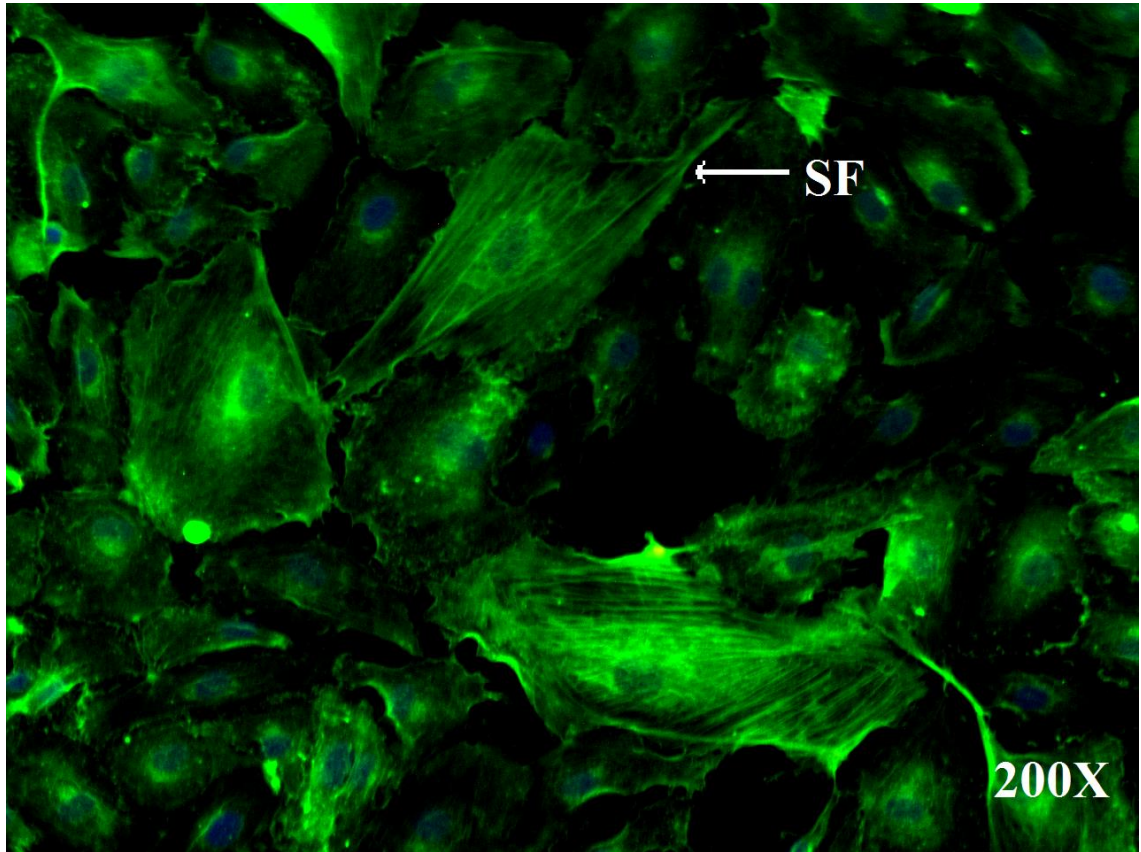
Figure 4.10: Immunofluorescence imaging of Drebrin in static HAECs. In Figure 4.10 (i), HAECs are stained with just Phalloidin (a red actin stain) and an AlexaFluor-488 conjugate that binds with the Drebrin antibody (Green). These cells are viewed at 100x magnification. The cells in Figure 4.10 (ii) are prepared without the Phalloidin actin stain, so as to allow better viewing of Drebrin in the cells. Drebrin can be observed localising to stress fibres (SF), but appears less present in the nucleus (N). Figure 4.10 (iii) shows the cells with a nuclear stain (DAPI) and stained with the Drebrin-AlexaFluor-488 conjugate stain. It is also under a higher definition and at a closer magnification (200x). Notably, strong clusters of Drebrin appear at the edges of the cells.

Drebrin has been proven to be an actin-binding protein (Gordón-Alonso *et al.*, 2013; Worth *et al.*, 2013; Mikati *et al.*, 2013). Since Drebrin was here shown to localise along stress fibres (Figure 4.10), it was hypothesised that it may also be haemodynamic and therefore it follows a similar expression model to LASP-1 and Palladin when cells are subjected to LSS. Results of post-shear lysates probed for Drebrin are shown in Figure 4.11 show that this may not be the case. This graph appears to follow a contrasting pattern as that seen in Figure 3.10 and Figure 4.5, where a post-shear increase of protein was displayed for Palladin and LASP-1, respectively. Drebrin is initially downregulated post-shear. A significant decline is observed within the first 3 hours of LSS, with the amount of Drebrin protein roughly halving. There appears to be a slight increase at 6 hours, but this still stays below the baseline static expression. Drebrin expression is then seen to decline again from 24-48 hours.

The potential signalling pathways of Drebrin were investigated using extracellular matrices, similarly to how they were investigated in Palladin and LASP-1 expression previously. Since Drebrin was downregulated in regular cells after shear stress, it was thought that the protein may follow that pattern here.

Cells cultured on a fibrinogen matrix were first investigated to observe their post-shear expression (Figure 4.12). When comparing the static cells on a regular culture dish against cells on the matrix, there appears to be a slight matrix-induced increase; similarly to how the other proteins were upregulated by virtue of cell-matrix contact. However, this increase does not appear as elevated as with the other previously investigated proteins. LSS appears to induce downregulation here though, with Drebrin expression declining within the first hour post-shear. At 3-24 hours, Drebrin has been shown to be upregulated again, to such a degree that is greater than that expressed in static cells. This upregulation remains steady up to 48 hours, where it begins to decline again. However, it should be noted that these results failed to prove to be significant, meaning that this may not be wholly representative of Drebrin expression on a fibrinogen matrix.

Figure 4.13 appears to show contact with the fibronectin matrix causes an initial downregulation of protein in the cell. Similar downregulation was observed with Palladin (Figure 3.19) where protein was downregulated but still expressed the same pattern of post-shear expression, albeit repressed to a degree. A similar observance is made with Drebrin expression in Figure 4.13. Immediately following LSS, Drebrin is

further downregulated, where for 3 hours expression reaches a plateau – being downregulated, but barely changing in relative expression levels. With regular LSS (Figure 4.11), Drebrin was shown to plateau at these time points also, before increasing at 6 hours. This increase at 6 hours is seen with the fibronectin-seeded cells. Drebrin expression increases up to 24 hours, before declining at 48 hours. This expression is greater than the static cells on the matrix, but less than the static cells on an uncoated matrix.

Finally, the expression of Drebrin in contact with the collagen matrix was investigated in Figure 4.14. Comparing the expression between static cells cultured on an uncoated vs. a coated culture dish shows that collagen appears to promote Drebrin expression, with a three-fold increase observed in cells on collagen compared to those on a regular dish. Following LSS, the expression declines, where by at 1-3 hours it is reduced to lower than the static cells without the collagen matrix. The expression increases at 6 hours, but declines again from 24-48 hours, with all these time points showing lower expression than that of static cells cultured on collagen. Notably, these results failed to prove significant so a definitive result cannot be determined.
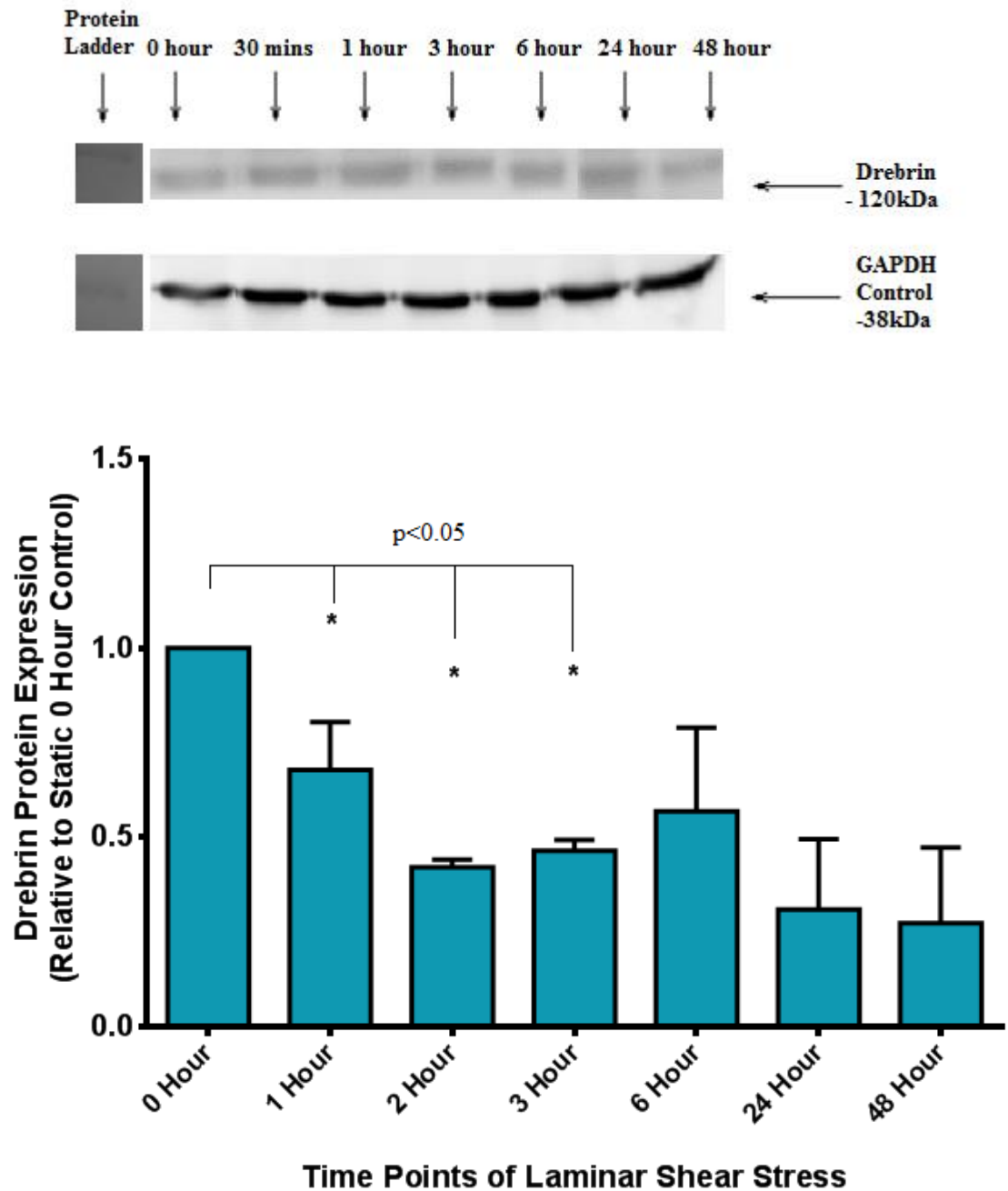
Figure 4.11: Drebrin protein expression in HAECs subjected to Laminar Shear Stress at 10 dynes/cm². Following Western Blotting of sheared HAEC lysates, the blot was probed with antibodies for Drebrin and GAPDH (as a control) and analysed using ImageJ Densitometric quantification software. The values given for intensity of each Drebrin band is given here, following normalisation against the GAPDH control Western Blotting bands, and are expressed in comparison to the baseline zero hour shear. *p<0.05.
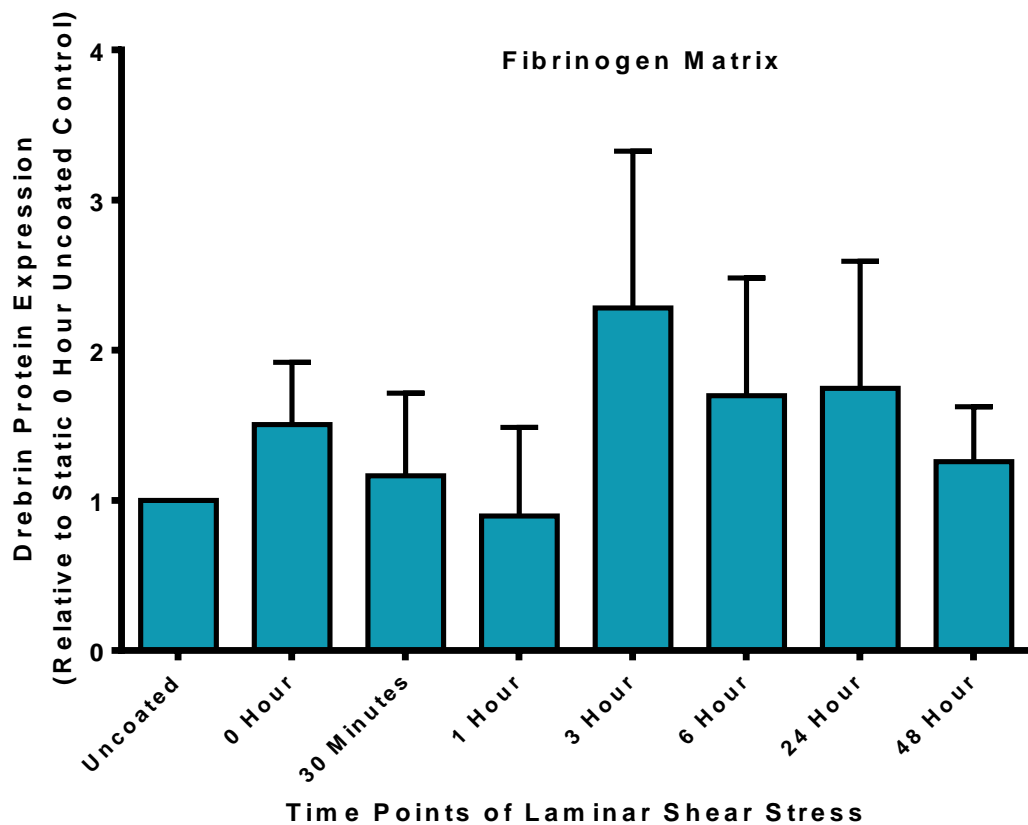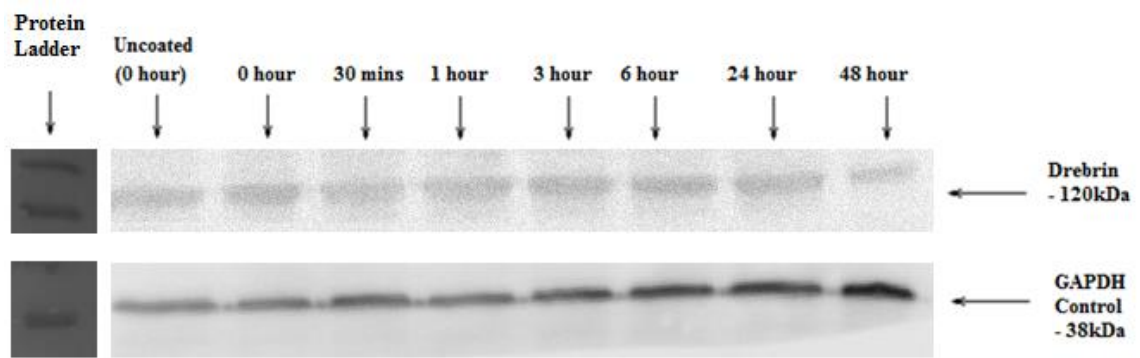
Figure 4.12: Drebrin protein expression in HAECs seeded onto Fibrinogen Matrix and Sheared at 10 dynes/cm^2. HAECs were seeded onto a matrix consisting of 10μg/ml fibrinogen and allowed to reach confluency. Following this, they were sheared at the listed time points and then blotted for Drebrin. Lysate from cells that were seeded onto a regular culture dish surface was also used as a control to illustrate the effect of the fibrinogen matrix on the expression of Drebrin. Western Blots were analysed using ImageJ software. Results are listed relative to the static zero hour control, where cells were seeded onto regular uncoated culture dishes and not subjected to LSS. Statistical analysis indicated p>0.05 – results are not significant.
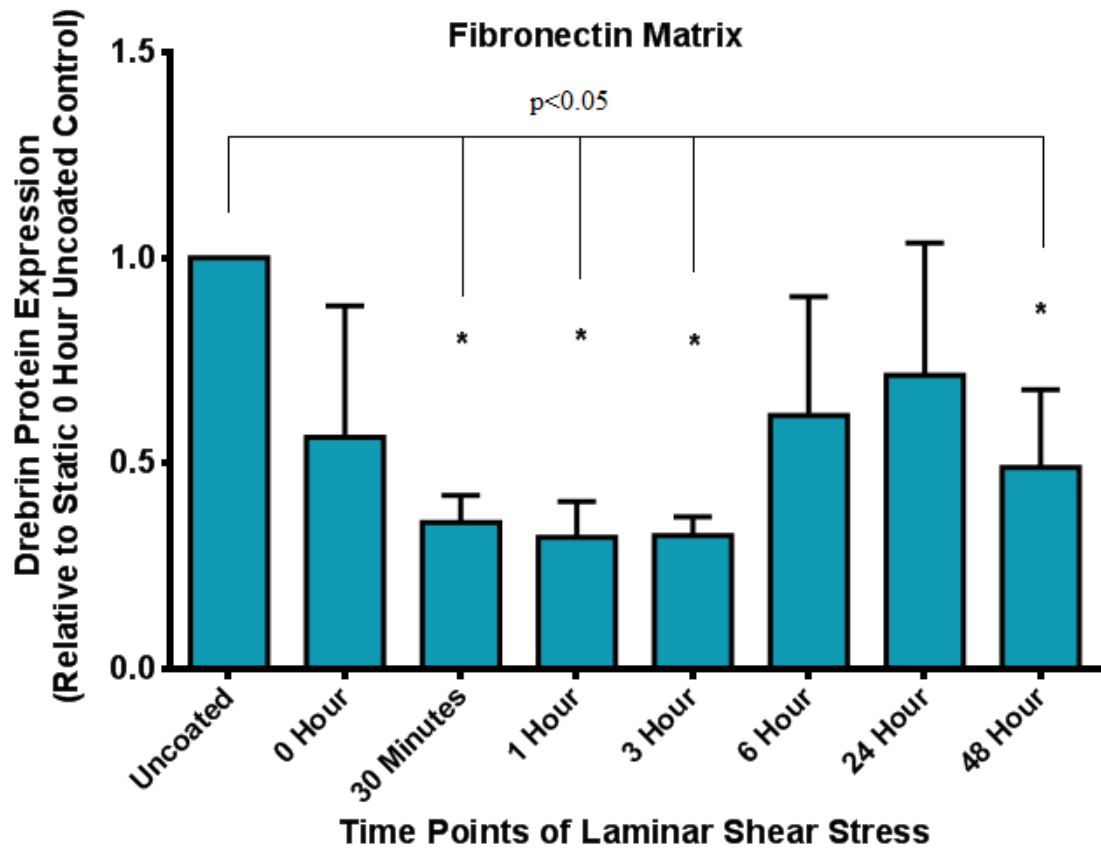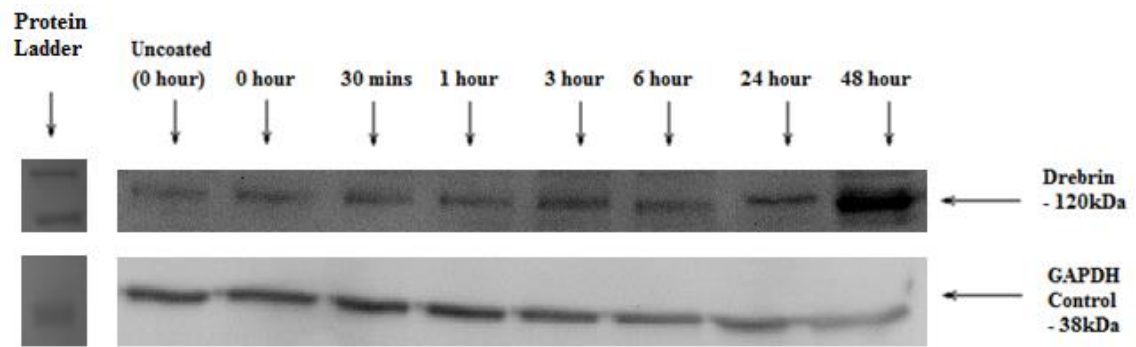
Figure 4.13: Drebrin protein expression in HAECs seeded onto Fibronectin Matrix and Sheared at 10 dynes/cm^2. HAECs were seeded onto a matrix consisting of 10μg/ml fibronectin and allowed to reach confluency. Following this, they were sheared at the listed time points and then blotted for Drebrin. Lysate from cells that were seeded onto a regular culture dish surface was also used as a control to illustrate the effect of the fibronectin matrix on the expression of Drebrin in cells. Western Blots were analysed using ImageJ software. Results are listed relative to the static zero hour control, where cells were seeded onto regular uncoated culture dishes and not subjected to LSS.*p<0.05.
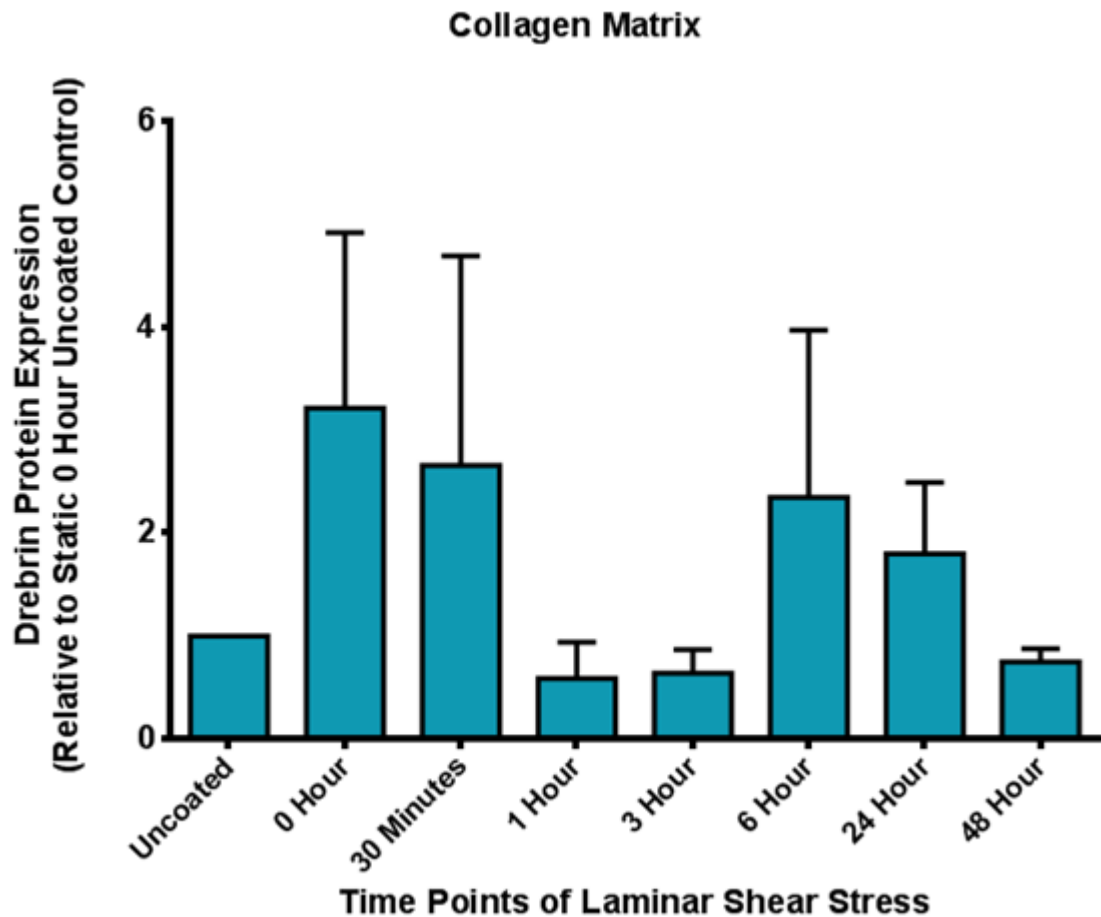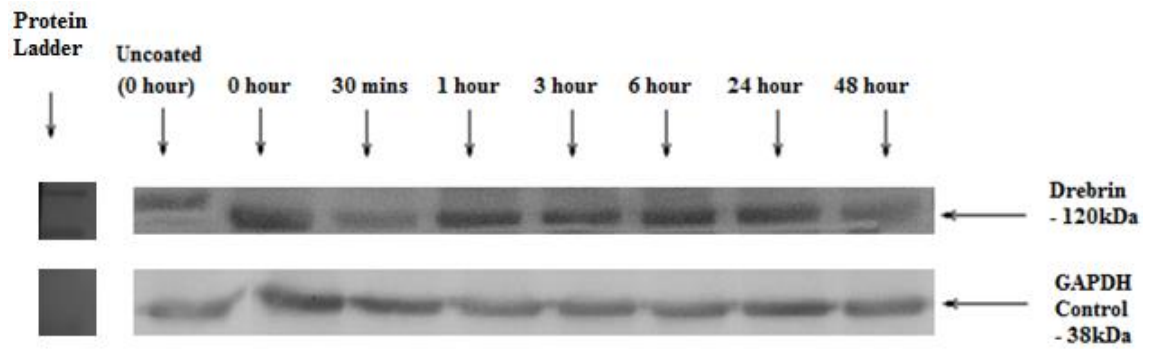
Figure 4.14: Drebrin protein expression in HAECs seeded onto Collagen Matrix and Sheared at 10 dynes/cm^2. HAECs were seeded onto a matrix consisting of 20µg/ml Type IV collagen and allowed to reach confluency. Following this, they were sheared at the listed time points and then blotted for Drebrin. Lysate from cells that were seeded onto a regular culture dish surface was also used as a control to illustrate the effect of the collagen matrix on the expression of Drebrin in cells. Western Blots were analysed using ImageJ software. Results are listed relative to the static zero hour control, where cells were seeded onto regular uncoated culture dishes and not subjected to LSS. Statistical analysis failed to show $p<0.05$, so a definitive conclusion cannot be deduced.

4.3: DISCUSSION

Following on from the characterisation of Palladin in HAECs in Chapter 3, and the observation of its upregulation in response to haemodynamic stimuli, immunoprecipitation experiments were performed in order to analyse Palladin using mass spectrometric analysis. Table 4.1 shows that Palladin is one of the results returned, proving that the immunoprecipitation was successful. Through pulling out Palladin, the interacting protein complex was also extracted, and the proteins within this complex were able to be also identified. Protein-glutamine gamma-glutamyltransferase 2, an important protein cross–linking catalyst was identified, indicating that protein binding was occurring. Two results – LASP-1 and Drebrin – were identified as potential proteins within the Palladin complex. Their role within the vasculature, with regards to response to haemodynamic forces (laminar shear stress), was further investigated.

While Palladin appears to show a low number of peptides (3) compared to proteins such as myosin (27), this is due to the ubiquitous nature of the other proteins in comparison to Palladin. Palladin has been proven to be present in the cells, but the amount present is dwarfed by that of major proteins such as myosins or actins in the cell. Some of the results in Table 4.1 list isoforms of actin, or actin like proteins. Because Palladin is involved in binding to actin, these results are expected. Most of the other proteins listed in Table 4.1 are also actin-binding in nature. Many results are also for various isoforms of Myosin. Myosins are proteins highly involved in cell motility. Actin and myosin, along with other various actin-binding proteins, form stress fibre bundles that apply tension between adhesive structures on the plasma membrane (Bershadsky *et al.*, 2006). These adhesive structures are used in cell-cell or cell-matrix adhesion, and can be modified through various manipulations of the filaments bound to them. As Palladin plays a role in cell migration, it associates with Myosin in this regard. The Ig domains of Palladin may provide rigidity for the Myosin proteins and help separate the structural components during reorganization in the cell (Mykkänen *et al.*, 2001; Otey *et al.*, 2009).

Also listed in Table 4.1 is Vimentin, an intermediate filament protein. Intermediate filaments, along with tubulin based microtubules and actin based microfilaments, comprise the cytoskeleton. Vimentin plays an important role then in maintaining cell integrity and adhesion (Tsuruta and Jones, 2003). Since Vimentin is one of the cytoskeletal control proteins used for proteocellular fractionation (Figure 3.14), it is unsurprising that it can be observed and identified in the proteomic screening. The

protein itself can be suitable as a normalising control in the fractionation experiments as it may not bind directly to Palladin, instead linking via a secondary protein such as Ezrin or α-actinin. Figure 4.2 later maps out these protein connections, demonstrating how Palladin and Vimentin are not directly linked. Another result of the Mass Spectrometric data, Desmin, is an intermediate filament protein as well. It is more commonly seen in muscle cells, but it can also found in endothelial cells, where it plays a similar role (Costa *et al.*, 2004). Multiple isoforms of a further protein listed – Tubulin - appear to associate with Palladin. This is an important protein as it polymerises into long filaments that form microtubules – another major component of the cytoskeleton which also play a huge role in transporting of molecules in the cell (Craddock *et al.*, 2012). Further strengthening the association of this complex to microtubule function is the cytoskeleton-associated protein (CKAP4) which is also listed in Table 4.1. CKAP4 is believed to be a protein involved in mediating the anchoring of the endoplasmic reticulum to microtubules. These proteins confirm that Palladin is part of a network of structural proteins within HAECs.

However, following LSS, the cells undergo a change in structure. As they do so, different proteins are utilised and alternative protein binding occurs in order to remodel the cell (Li *et al.*, 2005). By performing immunoprecipitation of HAECs after different time points of shear, the proteins can be visualised. Through a cross-comparison of Mass Spectrometry data, it was hypothesised that a variety of proteins can be observed to be uniquely expressed alongside Palladin at each time point of LSS.

At 30 minutes post-shear, Prothymosin-α appears to associate with Palladin. This protein, while usually observed to be overexpressed under hypoxic conditions, is also suggested to be related to cell proliferation (Roland *et al.*, 2003). Annexin A2 is a calcium-dependent phospholipid-binding protein which aids in organization of intracellular proteins to the extracellular domain. As the cells begin to shear, the membrane is disrupted and increased microparticle release occurs (discussed later in Chapter 5). Another form of Annexin, Annexin V, has already been discussed regarding its use in microparticle detection methods (Chapter 1). Annexin A2 also plays a role in cell motility and linkage of membrane proteins to the actin cytoskeleton. It would make sense that such a protein would be upregulated as an immediate response to stress. MVP – Major Vault Protein – is also presented as a protein result in Table 4.2. This protein is required for vault structure. Vaults are multi-subunit structures that may act as scaffolds for signal transduction proteins (Kolli *et al.*, 2004). MVP has been observed to be a

dominant PTEN binding protein (Yu *et al.*, 2002). As discussed in Chapter 1, PTEN serves as a negative component of the PI3-K / Akt signalling pathway, suggesting a potential link. Interestingly, there is also expression of Non-receptor tyrosine-protein kinase TNK1. This is a protein with tumour suppressor properties, which means it is capable of downregulating cell growth. It perhaps works as a preventative measure to keep cells in check as they restructure.

By 3 hours the cells are more remodelled. Here a variety of other proteins are uniquely expressed. Some are alternative isoforms of proteins already expressed (e.g. Tubulin α-4-A, or α-Actin 1). One result, barrier-to-autointegration factor, is a highly expressed protein which acts in bridging DNA. At this time point, *PALLD* gene expression peaks (Figure 3.9). Therefore it is possible that the barrier-to-autointegration factor is upregulated as the cells continue their remodelling and Palladin gene expression increases. Many of the other results - various histones, speckle type POZ protein, FUS protein, Ribonucleoprotein U, or translocases can be categorized as being normally observed in regular protein synthesis.

Results of the MASCOT™ analysis at this time point show a variety of histones present. Histones are highly alkaline proteins found in the nucleus which package DNA into chromatin and order it into structural nucleosome subunits. These subunits can compact into higher order structures to affect gene expression. The nucleosomes are composed of DNA wrapped in histone octamers (composed of two H2A, H2B, H3, and H4) and are connected by a linker DNA, which associates with histone H1 to form heterochromatin, which has many functions including gene regulation and chromosome integrity (Yan *et al.*, 2010). Methylation and/or hyper-activation of the histones have been implicated in epigenetic modification (Vo and Millis, 2012; Phillips, 2008). Histone phosphorylation is additionally involved in the transcriptional control of gene expression. Furthermore, histone deacetylase enzymes exist within the cell, and are responsible for regulation of the chromatin structure and function. Evidence suggests that these enzymes are involved in shear-mediated gene expression and function in endothelial cells (Chiu and Chien, 2011). Histone H4 in particular (observed in Table 4.2) is strongly associated with transcriptional activation when hyperacetylated (Matouk and Marsden, 2008) suggesting that it may significantly affect Palladin expression.

Laminar shear stress elicits both global and gene-specific histone modification changes in cultured endothelial cells (Illi *et al.*, 2003). Many of the histone modifications are

known to play functional roles in transcription (Yan *et al.*, 2010). It is proposed that the combination of posttranslational histone modifications encode regulatory information interpretable by the cell. Cellular dysfunction initiated by disease and increased shear stress is believed to be associated with increased epigenetic modification (Aird, 2007). As these cells are subjected to LSS, there appears to be an increase in the presence of histones, indicating that they are involved in the modification of the cell function in response to shear, and also interacting with the Palladin protein complex.

Another interacting protein, observed in Table 4.2, is for Galectin-1. This isoform appears later in Table 4.5, where it is shown to be part of the Drebrin protein complex. The protein possesses a variety of functions. It is known to be upregulated in activated endothelial cells (Upreti *et al.*, 2013). This upregulation stimulates both endothelial cell proliferation and cell migration. It may be that as the cells are re-organising in response to sustained shear, that they are utilising different pathways in order to remodel. Nuclease-sensitive element-binding protein 1 is seen to also stimulate proliferation and migration. The EH domain-containing protein 2 and C9orf174 protein are observed to be within the cell membrane. It is likely that these proteins are utilized in cell proliferation also, or else they could also play a role in the release of microparticles from the cell at this time.

At 6 hours, many previously listed proteins are observed to bind to the Palladin complex. Two new proteins are observed at this time point however. The collagen α-1 (VIII) chain is observed to be upregulated during injury (Gerth *et al.*, 2007). This may be upregulated as the cells adjust to chronic shear conditions. CDC42 plays a role in the extension and maintenance of the formation of filopodia (Gauthier-Campbell *et al.*, 2004). These structures are rich in actin, so the association of Palladin to this protein could be a further sign that the cells are undergoing a different form of remodelling after 6 hours, one which up regulates Palladin.

Finally, following 24 hours of shear stress, the cells have restructured and now express different proteins as they react to chronic shear stress. There are multiple Palladin-associate proteins that are exclusive to this time point. Again, many of them are simply various histones, RNA binding proteins or alternative isoforms of actin. However some of the protein results show different function. Cysteine-rich protein 2 (CRIP2) is a protein highly expressed within the vasculature (Zhang *et al.*, 2005). Like LASP-1, it contains a LIM domain. The LIM domain is found within a variety of proteins which

have may different functions, including being a component of adhesion plaques and the actin cytoskeleton (Li et al., 2012b). The protein may be utilised here in response to the chronic shear stress. Another protein that appears to associate with Palladin under chronic shear is Cofilin, a filamentous actin-binding protein responsible for regulation of actin cytoskeleton dynamics. It plays an important role in organization of the cytoskeleton and the regulation of cell morphology, especially as it has actin depolymerisation abilities (Bai *et al.*, 2011).

At 24 hours of shear the cells are fully adapted to chronic shear stress. It is possible they now have less of a need for Palladin and remodelling of the cells, hence the association of actin depolymerisation proteins. Many of the other protein results (Putative RNA-binding protein 3, Plasminogen-activator inhibitor-1 RNA-binding protein, Eukaryotic translation initiation factor 3 subunit A proline and glutamine rich splicing factor, and Terminal uridylyltransferase 4) all play a role in stabilizing mRNA, and capping expression levels. The rest of the proteins play similar minor roles in DNA and tRNA binding.

Many of the proteins listed in the static HAEC analysis were compared on a database to provide an image of how they proteins exist alongside one another. The STRING® version 9.0 database is an online database of known and predicted protein interactions. The proteins were inputted into the database in order to generate a diagram showing the known links and interactions between one another. These interactions displayed are derived from four integrated sources of data: Genomic Context (a comparative approach between two proteins), High-throughput Experiments, (Conserved) Co-expression and Previous Existing Knowledge (i.e. published results). The database then assigns a confidence score for the protein interactions. This score is obtained by comparing the associations against the results from another database (KEGG database) and the results are presented as a visual map between pathways.

The software was used with particular regard to investigating two other proteins of interest – LASP-1 and Drebrin. Figure 4.2 details some of the interactions between these proteins and Palladin. Palladin (*PALLD*) and LASP-1 show a direct interaction, whereas Palladin and Drebrin (*DBN*1) appear to interact via the Ezrin and/or α-actinin proteins. It should be noted that some protein interactions are not always physical interactions. Two proteins may be linked through genetic interaction or being part of a metabolic pathway (Szklarczyk *et al.*, 2011). Because of this, the fundamental unit

stored in STRING® is the 'functional association', i.e. the specific and biologically meaningful functional connection between two proteins. It is this association which is documented by STRING®. As Figure 4.2 highlights, there are some cytoskeletal proteins which show an overlap in associations. Ezrin and α-actinin 2 not only interact with each other, but also with Palladin and Drebrin. LASP-1, which binds to Palladin, shows interactions with β-Actin − another protein that interacts with Ezrin, which in turn associates with Palladin.

The proteins listed are not the only ones to associate with these proteins. Other proteins exist with more tenuous connections between these ones listed. For instance, Vasodilator-stimulated phosphoprotein (VASP) has a VCAM-1 mediated association with Ezrin (Barreiro *et al.*, 2002), while still being associated with Palladin (Boukhelifa *et al.*, 2004) and LASP-1 (Keicher *et al.*, 2004). VASP furthermore displays a zyxin-mediated interaction α-actinin 1 (Rottner *et al.*, 2001), a protein also known to bind with Palladin (Beck *et al.*, 2011). The proteins are part of a network where they are all connected either with one another, or through a degree of separation. Alteration of one protein homeostasis can therefore have a knock-on effect on a large part of its network.

Figure 4.2.1 shows Western Blotting experiments that indicate the link between Palladin and (i) LASP-1 and (ii) Drebrin. Immunoprecipitated Palladin is probed with antibodies for these two proteins and show resulting bands for the respective protein targets. This illustrates how both LASP-1 and Drebrin are part of the Palladin protein complex. Presence of LASP-1 appears stronger than Drebrin, highlighting that Drebrin may be less closely associated to Palladin. Notably the 90kDa isoform of Palladin is not present; LASP-1 is known to bind to the other isoforms (Rachlin and Otey, 2006).

Further investigation followed in investigating LASP-1 itself using mass spectrometric methods. By investigating the LASP-1 binding partners and comparing the results to those of Palladin, an overlap of other shared proteins could be observed, and other proteins specific to LASP-1 binding could be determined. Comparing the results of Table 4.4 against those of Table 4.1 showed that Reticulon-4 and Caveolin are the only LASP-1 associating proteins different to those associating with Palladin (and which is not simply an isoform of another protein listed). Reticulon-4 is a simple membrane protein involved in intracellular transport (Yang and Strittmatter, 2007). Meanwhile, Caveolin is thought to act as a scaffolding protein within the membranes of caveolae - small plasma membrane infoldings found in endothelial cells (Cohen *et al.*, 2003). It has

been hypothesised that the compartmentalisation of certain signalling molecules into caveolar membranes can allow for a faster and more efficient coupling of activated receptors to more than one effector system (Patel *et al.*, 2008). Such molecules may be transported by Reticulon-4, demonstrating why it appeared as a result. Caveolin also regulates NO signalling through inhibition of eNOS (Minshall *et al.*, 2003). The protein furthermore plays a role in cell migration (Nohata *et al.*, 2011). LASP-1 appears to have some sort of exclusive interaction with Caveolin that Palladin or Drebrin do not have. This may be due to some sort of role in signalling that LASP-1 displays. It is thought that both LASP-1 and uPAR are both part of the PI3-K signalling pathway (Salvi *et al.*, 2009). uPAR plays a role in such as cell migration, cell cycle regulation and cell adhesion. Caveolin, along with vitronectin and integrins, is needed by uPAR to initiate intracellular signalling. The connection between these two proteins may be via this signalling pathway.

Following on from the observance of LASP-1 in HAECs, expression of the protein was investigated under LSS conditions. The presence of the protein within HAECs is confirmed in Figure 4.4. While the expression appearing to reduce in the nucleus, this result may be the localisation of the protein out from the nucleus to the edge of the cells as they adhere to the glass slide. LASP-1 expression was quantified using Western Blotting methods. This method also helped to observe the post-shear changes in expression better. It was hypothesised that since Palladin is a protein which shows an increase in expression immediately following shear, that the associated LASP-1 protein would follow the same expression patterns.

Figure 4.5 illustrates how LASP-1 indeed is immediately upregulated following shear. This upregulation is similar to that of Figure 3.10, where the expression of Palladin also increases 1 hour post-shear. This appears to again be a part of the inflammatory response of the cells as they go from a static to haemodynamic state. Figure 4.5 appears to continue along a similar trend, whereby protein expression rapidly increases for the first hour, but then slowly declines and peaks again at hour 6 before being downregulated. This pattern of expression is indicative of LASP-1 being haemodynamically regulated in a similar manner to that of Palladin. This is likely due to LASP-1 facilitating actin re-organisation following shear stress. The binding of LASP-1 to actin stress fibres is mediated through its interaction with Palladin that binds to the SH3 domain of LASP-1. The actin-binding domains of LASP-1 itself mediate a direct interaction between LASP-1 and actin at the cell membrane extensions. It is understood

that LASP-1 and Palladin have an important role in working together. Without Palladin, there is a loss of LASP-1 at actin stress fibres and redirection to focal contacts without changing actin filaments (Rachlin and Otey, 2006). Again, when subjected to chronic haemodynamic forces, the expression of LASP-1 slowly decreases over time. Some of this protein is exported through microparticle release (discussed in Chapter 5), while some is likely downregulated as the cells adapt to the forces and the cytoskeleton restructures.

The expression of LASP-1 was also investigated in cells that were sheared after seeding onto ECMs. As before, this was performed in order to understand their integrin-mediated signalling pathways and to gain a better understanding of how the protein functions within an *in vivo* setting. Comparative results for all proteins are summarized in Table 4.6.

The effect of fibrinogen on post-shear expression levels of LASP-1 is first illustrated in Figure 4.6. It appears that expression significantly increases when cells are in contact with a matrix. However when the cells are subjected to laminar shear stress, there is a slight decrease in LASP-1 expression, which doesn't appear to change much over increased time points of shear. It is likely that seeding the cells onto fibrinogen causes some integrin inhibition, preventing the signal that normally causes post-shear upregulation of LASP-1. Alternatively, the integrins engaged by fibrinogen may not elicit the necessary response for upregulation. This is similar to the expression pattern seen with Palladin in Figure 3.17. In both figures, expression levels are still higher than that of the uncoated sample, suggesting there is some event occurring whereby expression is promoted as a result of interactions with the matrix, which at the same time inhibits a response to haemodynamic force.

When investigating LASP-1 expression under shear conditions after seeding cells on a fibronectin matrix (Figure 4.7), there is a different expression trend. While expression is upregulated when cells are cultured on the matrix, LASP-1 expression slowly decreases following immediate shear. A slight peak is seen at 24 hours, not unlike that seen at 6 hours with cells on an uncoated culture dish. The pattern suggests some signalling event that prevents the inflammatory response and delays the chronic response. Protein kinase Cα is shown to be activated on fibronectin, where it mediates suppression of the α2β1 integrin (Orr *et al.*, 2006). Such an integrin may be responsible for LASP-1 signalling here. However, initial protein expression still remains slightly higher when compared to

the uncoated sample. Again this could be some sort of matrix mediated stimulation of LASP-1 expression. When this figure is compared to Palladin expression under the same conditions (Figure 3.19), the pattern of expression is different. LASP-1 expression doesn't sharply decrease at 48 hours; however this could be attributed to the delayed response to chronic stress. LASP-1 is downregulated within 3 hours, whereas Palladin is upregulated. This suggests that the two proteins could in fact be affected by different signalling methods. Also of note is that LASP-1 expression is higher in coated samples as opposed to uncoated samples, whereas the opposite applies for Palladin. It appears that fibronectin may have opposing effects on the proteins; initiating an upregulation of LASP-1, but also the downregulation of Palladin. At the same time this stops LASP-1 from responding to LSS, but allows Palladin to follow the normal profile it displays following shear (Figure 3.10). An explanation may be that Palladin and LASP-1 take over each other's functions if one protein is prevented from being expressed. It must be pointed out that the statistical analysis failed to show $p<0.05$, so patterns of LASP-1 expression may not be affected to such a degree by the fibronectin matrix. However, the possible alternative patterns in two closely-linked proteins deserve further investigation in future work.

Lastly, the expression of LASP-1 on a collagen matrix (Figure 4.8) showed a different result in comparison to the pattern of expression on uncoated cells (seen in Figure 4.5). Up to 1 hour post-shear on a collagen matrix, LASP-1 expression appears to increase, indicative of an inflammatory response. This expression starts to decrease where, with the exception of a slight increase at 24 hours, stays in a declining trend. The 24 hour slight increase is reminiscent of that seen in the expression pattern of the fibronectin seeded cells; however it is not as sharp a peak, suggesting that collagen is less inhibitive of protein synthesis. When comparing this figure to Palladin expression under the same conditions (Figure 3.21), again a difference between the two proteins is seen. LASP-1 shows a change in expression when seeded on collagen; however Palladin doesn't register a change until 48 hours, where it drops sharply. Similarly to how comparison of the two proteins on a fibronectin matrix shows different results, it is probable that there are different matrix-related signalling pathways influencing the two proteins in different ways. Here though, it allows for LASP-1 to be expressed in response to shear, while preventing a Palladin response. As the shear and matrix-induced cell spreading is a Rac GTPase mediated response, the interaction of the cell with the matrix may stimulate a pathway that LASP-1 is a member of, but Palladin is not. The precise mechanisms

involved in this specific protein signalling merits further investigation to characterise them in full detail.

The developmentally regulated brain protein (Drebrin) was investigated also following its observation in Mass Spectrometric analysis of immunoprecipitated Palladin protein. Again, by investigating the Drebrin binding proteins and comparing the results to the binding partners of Palladin, it was hoped that a list of their shared proteins could be observed. The E2 isoform of Drebrin is involved in remodelling of the actin cytoskeleton and in formation of cell processes. Overexpression of Drebrin in different cell types induces formations of long actin filament-rich cell processes (Keon *et al.*, 2000). As seen in Table 4.5, when performing an immunoprecipitation of Drebrin itself, some proteins appeared which also appeared alongside Palladin (Table 4.1) and LASP-1 (Table 4.4). These proteins (Tubulin α-1A chain, Actin and Vimentin) help give an insight into how Palladin, LASP-1 and Drebrin can all be a part of the same network of proteins.

Some proteins were pulled out along with Drebrin which appeared unique to Table 4.5. Many of these proteins are just different isoforms of proteins already observed (e.g. Cytoplasmic Actin 1) but some of alternative proteins were observed. Galectin-1 is a highly conserved protein that plays a role in modulating cell-cell and cell-matrix interactions, as well as migration and adhesion (Camby *et al.*, 2006; Elola *et al.*, 2007). It has been shown that it also facilitates increased adhesion of cells to the ECM via cross-linking integrins on the cell surface with the functional groups of other ECM components (Sanchez-Ruderisch *et al.*, 2011). Activation of cells results in increased expression of Galectin-1, which in turn leads to the translocation of protein to the outer membrane. Drebrin is suggested to interact with gap junctions in cell-cell contact zones in response to extracellular signals (Butkevich *et al.*, 2004) so it is possible Drebrin and Galectin-1 interact at the outer membrane. Cementing this hypothesis is the observation of Filamin-A in the results. It anchors transmembrane proteins to the actin cytoskeleton, while working as a scaffold for signalling proteins within the cytoplasm (Yue *et al.*, 2013). Furthermore, protein kinases dependent on Calmodulin – another result from the mass spectrometric analysis - are observed to play a role in the regulation of the cell barrier function (Borbiev *et al.*, 2000). Calmodulin itself is used as a binding site for Caveolin-1 (seen in the LASP-1 immunoprecipitation) for inhibition of endothelial Nitric Oxide Synthase (Davignon and Ganz, 2004). Immunofluorescence imaging of Drebrin in HAECs (Figure 4.10) appears to show the larger clusters of protein near the

membrane edges. Drebrin is known to be most plentiful at junctional plaques (Peitsch *et al.*, 1999; Rehm *et al.*, 2013) so it is expected that these clusters would be closer to the edge of the cells.

The actin-binding Drebrin was investigated under the same LSS conditions as before with the other proteins. It was initially thought that Drebrin may follow a similar post-shear expression pattern as Palladin or LASP-1. Figure 4.11 shows the response of Drebrin in HAECs to similar time-points of LSS on regular uncoated cell culture dishes. The bands for Drebrin appear weaker – suggesting that Drebrin is scarcer in HAECs than other proteins. The protein notably had a lower number of peptides when extracted as part of the Palladin protein complex (Table 4.1), suggesting it may not be as ubiquitous within the cell. Drebrin expression unusually decreases immediately following LSS. This is in contrast to the previous investigations of Palladin and LASP-1, which both showed an increase of protein immediately following shear stress. Drebrin expression showing a slight increase at 3-6 hours is reminiscent of the pattern seen in the other proteins however. This is suggestive that the change in morphology at 6 hours shear causes an increase of many of the cytoskeletal proteins, even in ones such as Drebrin which were steadily being downregulated**.**

The production of Drebrin may reduce as a result of actin remodelling post-shear. It is possible though that there may be some sort of regulatory effect with Drebrin, where it is downregulated as Palladin and LASP-1 are upregulated. Drebrin has been seen to act against α-actinin – an actin-binding cytoskeletal protein, where it is observed inhibiting the actin-binding and cross-linking activity of both α-actinin and tropomyosin (Ishikawa and Kohama, 2007; Li *et al.*, 2011; Ishikawa *et al.*, 1994). As stated, α-actinin itself has a known association with Palladin (Rachlin and Otey, 2006), so it is possible that some sort of competition occurs via the protein interactions here. Since Palladin knockout mice result in embryonic lethality and Drebrin is developmentally regulated, the early growth phase of the cells may be when this competition of the proteins occurs. Further investigation into the precise protein interactions at different growth phases could provide interesting results.

The expression of Drebrin following LSS on extracellular matrices was also investigated in an effort to understand the signalling pathways involved in the protein's expression. Figure 4.12 shows how Drebrin still decreases following LSS of cells on a fibrinogen matrix, albeit at a slower decline. The same upturn in protein expression at 3-

6 hours is seen here, before declining. Notably, when compared to the static control sample where cells were grown on an uncoated culture dish, expression levels are elevated, and subsequently stay higher than the control, despite the shear induced downregulation. The graph is similar to the expression of Palladin in Figure 3.17. In both figures, protein expression reduces following shear, while still remaining elevated compared to cells without the fibrinogen matrix. While it is expected that downregulation of Drebrin occurs because of shear stress, the matrix-related upregulation may be due to the increasing cell migration induced by fibrinogen. It must be noted that these results did not prove to be statistically significant, so this cannot be stated for certain.

While fibrinogen appears to stimulate an upregulation of Drebrin, Figure 4.13 shows how Drebrin is severely downregulated when cells are seeded onto fibronectin. There is a significant decrease in Drebrin expression between the matrix-seeded samples when compared to the control cells on an uncoated matrix. When compared against the investigation of Palladin on a fibronectin matrix (Figure 3.19), a similar matrix-induced inhibition of protein expression can be seen. It is an interesting result considering fibronectin aids cell migration, and there did not seem to be any inhibition of LASP-1 when comparing coated and uncoated culture dishes (in Figure 4.7). It could be that fibronectin selectively inhibits some cytoskeletal proteins, but not others in the same network. As mentioned earlier, certain protein kinases such as PKCα are activated on fibronectin, where it mediates suppression of the α2β1 integrin (Orr *et al.*, 2006) so such inhibition may be affecting the Drebrin expression here. The change in expression as a result of shear stress on this matrix in Figure 4.13 appears negligible though. There is a slight decrease within the first 3 hours of LSS, which is then followed by an increase at 6-24 hours before dropping again. These results follow a similar pattern as seen in cells without a matrix (Figure 4.11). Therefore if fibronectin does inhibit protein, it is more likely through signalling mechanisms affecting cell-matrix interactions, and less likely through the cell-cell interactions that result from shear stress induced remodelling.

Figure 4.14 shows that Drebrin inhibition does not appear to occur with collagen. Here, protein expression is elevated in samples seeded on a collagen matrix compared to the sample on a regular cell culture dish. This matrix-assisted increase of expression is similar to that seen occuring with Palladin (Figure 3.21) and LASP-1 (Figure 4.8), highlighting how collagen plays a role in the increase of cytoskeletal protein expression. From observing the pattern of Drebrin expression in the shear time points of Figure

4.14, it appears to follow the regular pattern where expression decreases steadily, with a small upturn between 6-24 hours as the cells adapt to chronic shear, before beginning to decrease again at 48 hours. It seems that collagen doesn't have much of an effect on the shear pattern in Drebrin. However, statistical analysis failed to show $p < 0.05$, so a definitive conclusion cannot be deduced.

Interestingly, the matrix doesn't affect the shear-related expression pattern of LASP-1 either, but does affect the Palladin expression in an inhibitory manner. This comparative study highlights how these three proteins can be differently affected by the extracellular matrices, even though they all remain part of the same protein network in the vasculature. It suggests that while they are all part of this network, they can be mediated by different signaling pathways, and subsequently can be affected differently by haemodynamic forces.

Table 4.6: Expression patterns of proteins of interest following Cell-Matrix interactions and subsequent Laminar Shear Stress. This table compares the results found from Chapter 3 (Figures 3.10, 3.16-3.21) for Palladin; and from this chapter for LASP-1 (Figures 4.5-4.8) and Drebrin (Figures 4.11-4.14), summarising how they are regulated during LSS when grown on different extracellular matrices.

	Palladin	**LASP-1**	**Drebrin**
No Matrix	Immediate increase with shear Decreases at 3 hours Peaking at 6-24 hours Decreases at 48 hours	Immediate increase with shear Decreases at 3 hours Peaking at 6 hours Decreases at 24-48 hours	Immediate decrease with shear Slight increase at 3-6 hours, still below baseline Decreases at 24-48 hours
Fibrinogen	Promoted expression Immediate decrease with shear Increases to near-baseline levels at 3-24 hours Decreases at 48 hours	Promoted expression Slight reduction in expression, but no major expressional change at 0-48 hours	Promoted expression Immediate decrease with shear Increases above baseline levels at 3-24 hours Decreases at 24-48 hours
Fibronectin	Inhibited expression Immediate increase with shear Declines at 3 hours before peaking at 6-24 hours Decreases at 48 hours	Promoted expression Immediate decrease with shear Increases to near-baseline levels at 24 hours Decreases at 48 hours	Reduced expression Immediate decrease with shear Slight increase at 6-24 hours, not much above baseline Decreases at 48 hours
Collagen	Promoted expression Shear has no effect on expression at 0-24 hours Decreases at 48 hours	Promoted expression Immediate increase until 1 hour Declines at 3-6 hours before increasing slightly at 24 hours Decreases at 48 hours	Promoted expression Immediate decrease with shear Slight increase at 3-6 hours, but still below baseline Decreases at 48 hours

CHAPTER FIVE

FUNCTIONAL ROLE OF

PALLADIN: CELL MIGRATION

AND ENDOTHELIAL

MICROPARTICLE RELEASE

5.1: INTRODUCTION

The actin cytoskeleton plays pivotal roles for many fundamental processes such as cell structure and migration. Such processes are facilitated by a dynamic remodelling of the actin cytoskeleton, which itself is regulated by various actin-binding proteins, one of which is Palladin (Asano *et al.*, 2011). Having investigated the response of this protein to haemodynamic force, where it was seen to restructure the cytoskeleton, the functional role of Palladin was investigated in more detail. There is strong evidence suggesting that Palladin plays a role in cell migration: it appears to have a conserved function in cell and tissue remodelling in response to injury; with a strong correlation existing between high levels of Palladin expression and increased cell migration (Goicoechea *et al.*, 2008; Jin *et al.*, 2007). The production of a genetically modified Palladin knock-out mouse was reported to result in embryonic lethality, due to defects of cranial neural tube closure and herniation of vital organs (Luo *et al.*, 2005). Palladin was shown to be expressed in the cranial neural folds of the wild-type embryos. The closure of these folds requires the active migration of the cells, suggesting that the closure defect of Palladin-null embryos was caused by the disturbance of cell migration. Suppression of the protein in fibroblasts and carcinoma cell lines has also been documented to result in the disruption of the cytoskeleton (Goicoechea *et al.*, 2009; Parast and Otey, 2000). Furthermore, knockdown of Palladin in vascular Smooth Muscle Cells results in the decrease and disorder of stress fibres associated with the diminished F-actin to G-actin ratio (Goicoechea *et al.*, 2006; Jin *et al.*, 2011).

However, there have been very few studies observing the effects of a similar knockdown of Palladin in vascular endothelial cells, or even observations of the role of Palladin in endothelial cell migration. It was hypothesised that knockdown of Palladin in endothelial cells should noticeably affect HAEC migration as it did with other vascular cell types. This was therefore investigated in this chapter, with the employing of siRNA knockdown of Palladin in HAECs, followed by the subjecting of these cells to a scratch wound assay. It was theorised that cells transfected with siRNA would display a reduced migratory profile over the observed time course. Through a cross-comparison with non-transfected cells in the same assay, this experiment can demonstrate how Palladin plays a role in facilitating the migration of HAECs, coupled with how the repression or deletion of this protein may affect migration. Further investigations on knocked-down cells and the effect Palladin has on cell migration used the

xCELLigence™ system, which records the real-time migratory patterns of these cells. To determine the role of Palladin on cell migration following haemodynamic force, the siRNA-transfected cells were subjected to cyclic strain before being analysed with the system.

It has already been demonstrated that Palladin displays a biphasic response to mechanical stimuli, playing a role in structural reorganisation of the cells as they adapt to haemodynamic forces. Chapter 3 has illustrated that immediately following LSS or cyclic strain there is an increase in Palladin expression, likely due to an inflammatory response in the cells. This spike in expression is relatively short-lived however; by 3 hours of sustained strain or shear the levels have peaked and start to decline. The levels increase at 6 hours (likely due to the cells adapting to chronic haemodynamic forces), but they end up declining further again by 48 hours. While the protein may be simply catabolised in these instances, a hypothesis for the reduction in expression levels was that the protein may be exported from the cells via Endothelial Microparticle release. This hypothesis of microparticle release could also explain why there is a massive reduction of Palladin documented within the cell membrane following LSS (Figure 3.12), as membrane bound protein is readily exported from the cell. Much of this chapter therefore focuses on investigating the release of Palladin via Endothelial Microparticles shed from HAECs.

While cyclic strain can initiate microparticle release (Vion *et al.*, 2013), the primary focus of the investigation of microparticles is given to those induced by shear stress. The reasoning for this is that firstly, a greater volume of these shear-induced microparticles are released from cells than strain-induced, owing to the flow vs. pulse effect of stimulating disruption of the membrane and subsequent particle release. Secondly, there is a vast difference in the content of each type of induced microparticle, since different agonists can result in different particles from a single cell type (vanWijk *et al.*, 2003). With regard to the observations of Palladin in strain-induced EMPs, results displayed here show that Palladin is absent from this subsection of microparticles (Figure 5.3), indicating that there may be a different signalling method involved in the release of protein from the cells.

Microparticles that are released from the cell have been shown to contain various mRNAs, miRNAs or proteins (Diehl *et al.,* 2012; Diamant *et al.*, 2004). Recent data indicates that microRNAs (miRNAs) in endothelial cells can play an essential role in

shear stress-regulated responses (Vion *et al.*, 2013). Shear stress can induce miRNAs that inhibit mediators of oxidative stress and inflammation while promoting those involved in maintaining vascular homeostasis (Marin *et al.*, 2013). The release of such signalling molecules via EMP shedding can seriously alter cell fate and function. As the EMPs are released from cells, they are free to travel downstream and transfer such mRNA, miRNA and also proteins to other cells, affecting their state as a result. Experiments were performed whereby HAECs were incubated with conditioned media i.e. cell media which was taken from a previously sheared plate of cells and therefore, contain a large volume of EMPs. By adding these EMPs to new static cells, it was thought that an observation could be made of Palladin expression in HAECs being altered by an influx of shear-induced microparticles through specific signalling pathways.

In an additional method to characterise how signalling methods are involved in microparticle release, the release of shear-induced EMPs from cells cultured on ECMs was also investigated. As detailed in Chapter 3, nonpermissive matrices such as collagen may interfere with integrin signalling (Orr *et al.*, 2006) and appear to affect Palladin expression in HAECs. Collagen can alter endothelial cell function following shear stress (Kemeny *et al.,* 2011), so it is possible that it may also have an effect on the activation of the cell membrane and subsequent particle release. The permissive matrices – fibrinogen and fibronectin – are also investigated for shear-induced microparticles. Since these matrix proteins are observed to increase in response to elevated shear stress, it was hypothesised that they may also influence the increased EMP release which also occurs as a result of elevated shear. As these matrices have already been shown to affect protein expression in the cell via interactions with integrins, they were investigated to observe if they affected EMP-facilitated protein release in the same way.

Most of the microparticles used in these experiments were obtained after extracting them from harvested cell media. However, the presence of Palladin in EMPs extracted from human blood post-exercise was also investigated, to highlight the presence within an *in vivo* environment as well as an *in vitro* one. Exercise increases shear stress in vessels, which in turn increases microparticle number (Tinken *et al.*, 2010). Blood was obtained after subjects were subjected to exercise, following the methods of Chapter 2.2.2.4. Through investigation of EMPs obtained from these blood samples, a clearer

understanding of the *in vivo* expulsion of Palladin from cells within the vasculature could be obtained.

Finally, this chapter further investigates the presence of the two other actin-binding proteins, LASP-1 and Drebrin, within shear-induced EMPs. Chapter 4 showed that these two actin-binding proteins play different roles within the vasculature while appearing to exist in the same network as Palladin. LASP-1 is a structural protein which appears to regulate actin cytoskeleton organisation at the edges of cells (Lin *et al.*, 2004), whereas Drebrin appears to be involved in actin cytoskeleton remodelling and in the formation of cell processes. Having observed how LASP-1 follows a similar post-shear pattern of expression as Palladin, whereby it increases expression, then decreases at later time points, it was hypothesised that it may also follow a similar pattern of release via microparticles. The Drebrin protein showed an alternative post-shear expression pattern; whereby it immediately became downregulated. Shear-released EMPs were probed for Drebrin to determine if there was protein also released via this mechanism. By doing so, it could be shown if downregulation of Drebrin was a result of release from the cells, or else active repression of the protein within the cell itself.

5.1.1 Study Aims

The work performed out in this chapter firstly sets out to determine the functional role of the Palladin protein with regards to cell migration in endothelial cells. Secondly, the work also investigates the release of Palladin via Endothelial Microparticle release. Therefore the overall aims of this chapter include:

- To observe the cell migratory patterns of cells where Palladin has been knocked down, and to determine the protein function in cell migration.

- To investigate the release of Palladin within EMPs after the subjecting of HAECs to the haemodynamic forces of cyclic strain and laminar shear stress.

- Determining the change in Palladin expression when incubating regular HAECs with conditioned cell media containing elevated volumes of EMPs.

- Investigation of the release of Palladin protein via EMPs released from interactions of the cells with permissive and nonpermissive extracellular matrices following laminar shear.

- Observing the release of Palladin via Endothelial Microparticles taken from human blood samples post-exercise.

- Characterisation of the related actin-binding proteins – LASP-1 and Drebrin in shear-induced EMPs.

5.2: RESULTS

The first experiment demonstrated here shows the imaging of static HAECs which were transfected with a Palladin-specific siRNA and subjected to a scratch wound assay as described in Chapter 2.2.4.2. Controls were also prepared - either transfected with scrambled siRNA, or else non-transfected cells. Cells were photographed for a number of time points up until 6 hours (after this point, cells cannot be differentiated between migrating and proliferating). The measured distance between each set of cells is measured in size of pixels across the image - to show the rate of migration between samples as the wound closed over. Within 1 hour post scratch, the cells transfected with Palladin siRNA have barely closed, while the scrambled and the non-transfected have already lost roughly 25% of the space between cells. The scrambled siRNA transfected cells appear to migrate slightly slower than the non-transfected. This divide between the two controls is more prominent at 3 hours. Here, the scratch wound in the non-transfected cells is roughly 1/3 of the size it was at 0 hours. Meanwhile the distance in the scrambled cells is around half the size it was immediately post-wound. The cells transfected with Palladin siRNA are migrating also, but they are much slower to migrate than the control cells. At 3 hours, they have the same distance as the scrambled cells did at 1 hour. This slowdown in migration is confirmed when the cells are imaged at 6 hours. Here, the Palladin siRNA cells have migrated only 50% of the distance created by the wound at 0 hours. Both sets of the control cells at the same time point have migrated fully across the initial wound.

The measured distances between cells is quantified in Figure 5.1.1, showing the relative migration pattern between the three groups of cells. This highlights how the Palladin siRNA transfected cells demonstrate less migration. Figure 5.1.2 shows Western Blotting of HAECs transfected with Palladin siRNA performed against control lysate samples to prove the knockdown of protein. Lysate was also obtained from cells transfected with a GFP-tagged Palladin plasmid and it was used here as a secondary positive control (as well as demonstrating relative over-expression of Palladin). As shown by the absence of protein bands, knockdown of Palladin was achieved with both 25nM and 50nM of siRNA. The lower amount was used for subsequent experiments.

Palladin siRNA	Scrambled siRNA	Non-transfected

(0 hours post scratch wound)

87 px   86 px   76 px

(1 hour post scratch wound)

84 px   66 px   57 px

(3 hours post scratch wound)

67 px   45 px   30 px

(6 hours post scratch wound)

44 px   Cells Fully Migrated   Cells Fullly Migrated
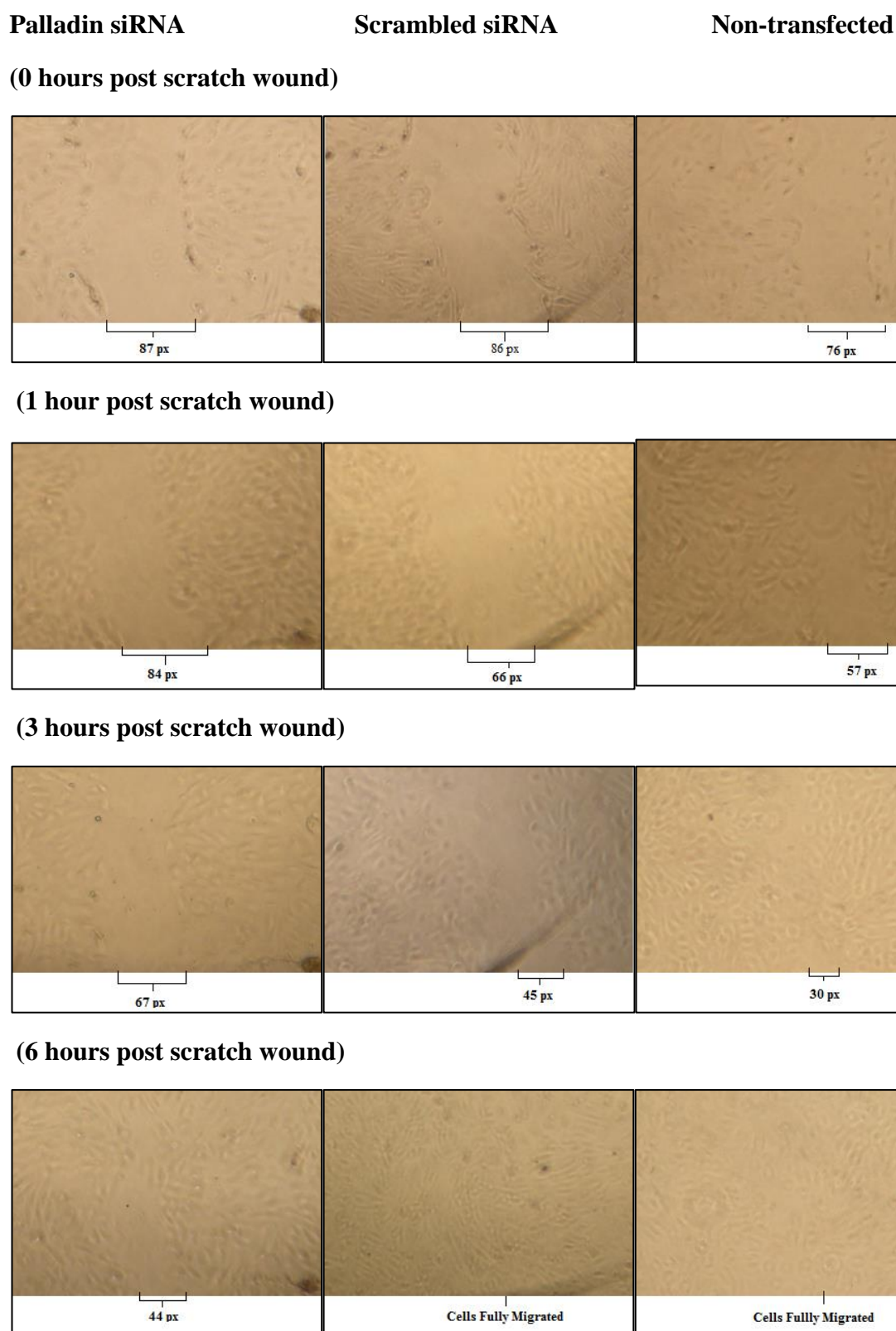
Figure 5.1: Cell Migration following Scratch Wound Assay in HAECs subjected to siRNA-mediated knockdown of Palladin. HAECs transfected with either: Palladin siRNA, scrambled siRNA or non-transfected, were allowed to adhere to the culture dish. Optimisation proved that knockdown was first seen to occur at 30 hours post-transfection. At this time point, a 1mm in diameter line of cells was scraped away. Cells were imaged at the time points listed. Diameter between the cells in the images was measured and is expressed in length of pixels (px). All images are taken at 100X magnification.
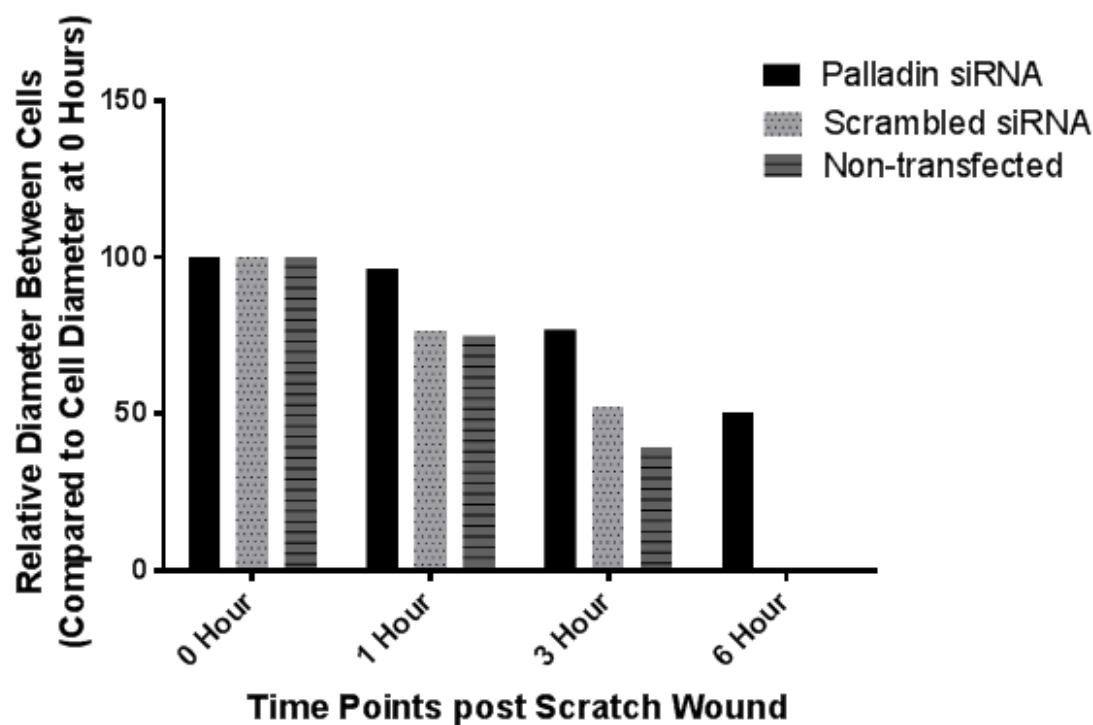
Figure 5.1.1: Expression of Cell Migration in Palladin Knockdown HAECs vs. Control HAECs. The diameter of the scratch wound from each image from Figure 5.1 was calculated and is expressed here relative to the diameter observed in the 0 Hour (immediately post-scratch wound) cell migration images. Relative diameter is expressed in this graph, indicating how much of a distance there was between cells at each time point post scratch wound. In Scrambled siRNA cells and Non-transfected HAECs, cells had fully migrated across the wound at 6 hours. As such, they were then recorded as zero in the above graph.
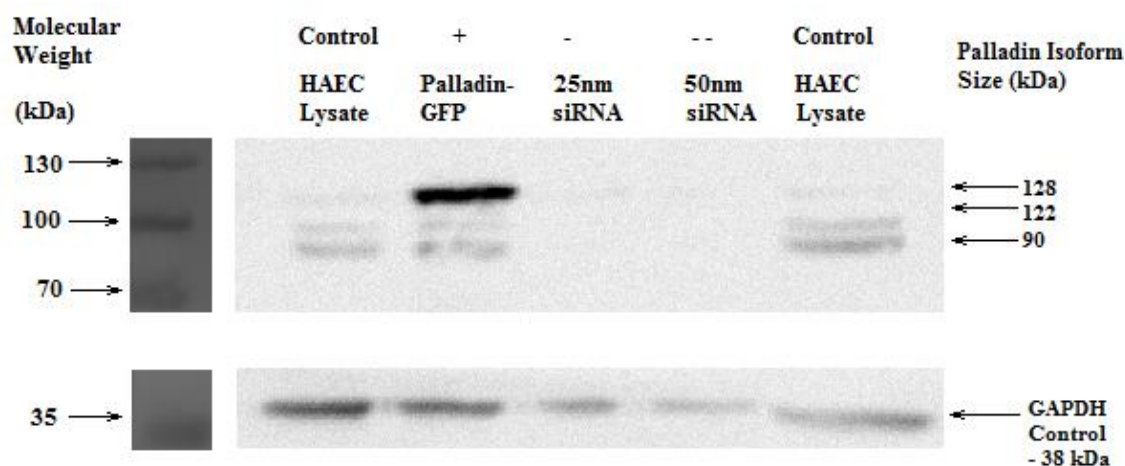
Figure 5.1.2: Optimisation of siRNA-mediated knockdown of Palladin. This figure demonstrates the efficacy of siRNA knockdown of Palladin. Regular HAEC lysate was analysed via Western Blot methods as described previously. At 30 hours post-transfection, cells transfected with siRNA were also lysed and analysed. The sample designated '+' was lysate obtained from cells transfected with a GFP-tagged Palladin plasmid. It was used here as a secondary positive control and to also show over-expression of Palladin compared to the other lysates. The sample designated '-' is representative of lysate taken from HAECs transfected with 25nM of siRNA. The double negative '--' sample represents HAECs transfected with 50nM of siRNA. As observed, both achieved knockdown, so 25nM was employed for cell migration experiments.

Transfected cells were also assayed using the xCELLigence™ system, a novel method that allows monitoring of cell migration and adhesion real-time without any labelling. The system works by measuring the electrical impedance across the integrated micro-electrodes at the base of specialised cell culture plates (Ke *et al.,* 2011). The impedance is measured using a dimensionless parameter called the Cell Index (CI) which is derived from the relative change in electrical impedance. The CI is characteristically set at zero when cells are absent or not-adhered to the electrodes. Under the same physiological conditions, when more cells are attached (from adhesion or migration), the impedance is larger, leading to increased CI value. Additionally, change in a cell status, such as cell morphology, or cell viability will lead to a change in CI. Change in CI is represented as the slope of the curves calculated over a two hour time frame. This time frame was picked as initial results showed the greatest changes in impedance occurring up to this time point.

Knocked-down cells were analysed for cell migration. Cells were transfected as before, with the relevant controls. In an effort to understand the role of Palladin in cell migration following haemodynamic stimulation, cells transfected with Palladin siRNA were subjected to 3 hours of cyclic strain post-transfection. This time point was determined to be the optimum time to observe changes in cell morphology. These cells were all then seeded in triplicate into the CIM plate, as described in Chapter 2.2.4.3. Results are displayed in Figure 5.2 (i) where the events have been graphed at each 5 minute recording of impedance. As a negative control, some wells of the CIM plate contained standard cell media (Red). Results appear to show that differences in impedance events are very miniscule, owing to the closeness of the curves. The slope of the migration curve for each sample was calculated using the RTCA 1.2 Software and results are shown in Figure 5.2 (ii). This indicates the degree of migration that each set of treated cells are experiencing. Results indicate that strained non-transfected cells (with the lowest slope) unusually experience the least migration. They are followed by scrambled siRNA cells and then Palladin siRNA cells. Migration is faster in strained knockdown cells than static. This indicates that the strain induces migration further on cells lacking in Palladin.

(i)
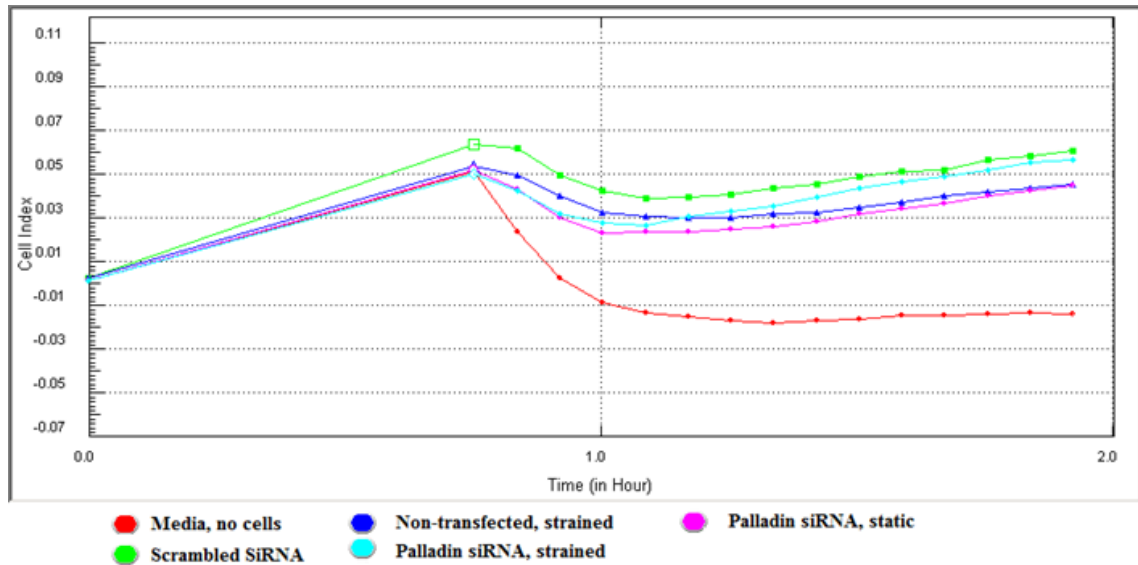
(ii)
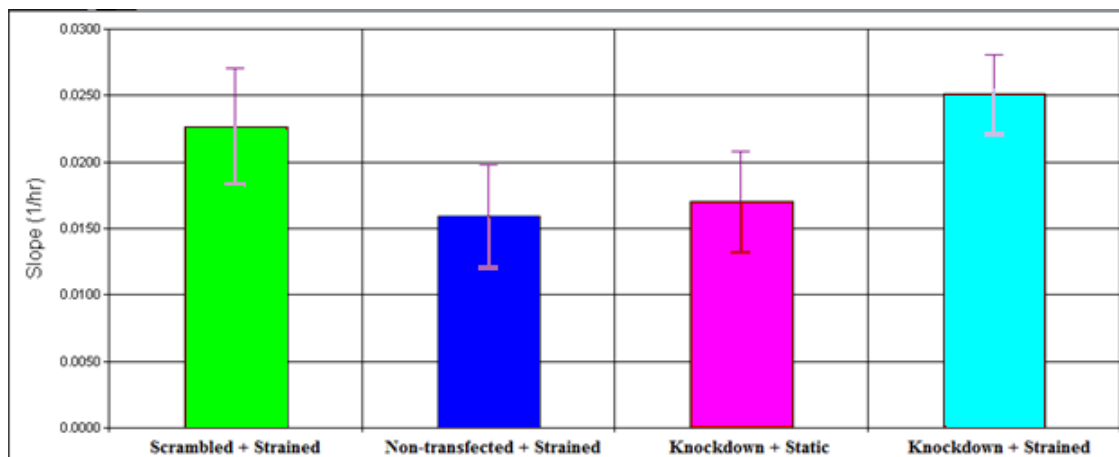
Figure 5.2: xCELLigence™ Assay of Cell Migration in Palladin Knockdown Cells. HAECs were transfected as per previous methods. Cells were also subjected to cyclic strain at 10% for 3 hours. A control knockdown sample, where cells were transfected with Palladin siRNA and not strained is also provided. Cells were seeded in triplicate on an xCELLigence™ CIM plate for assaying of migration. The recorded CI results for the first two hours are presented here in Figure 5.2 (i). Two hours was determined to be an optimum time to observe immediate cellular events before cells started to proliferate, affecting results. Empty wells on the plate were filled with media to provide a negative control. The recorded impedance for this baseline is highlighted in red. The slope of the migration curve for each sample was calculated using the RTCA 1.2 Software, with results shown in Figure 5.2 (ii). The increase in the slope is indicative of an increase in cellular migration. Results are representative of three independent experiments. Statistical analysis failed to show $P<0.05$.

The effect of haemodynamic force on the release of endothelial microparticles is next demonstrated. Figure 5.3 illustrates the Western Blot analysis of EMPs released after a number of time points of cyclic strain at both (i) physiological and (ii) pathological levels. Whole cell lysates are probed on the same blot as a positive control. As shown below, only the lysates returned showed bands. This indicates that Palladin is absent in the EMPs that are released following either types of cyclic strain. Because of this, subsequent microparticle experiments focused exclusively on shear-induced EMPs.

(i)
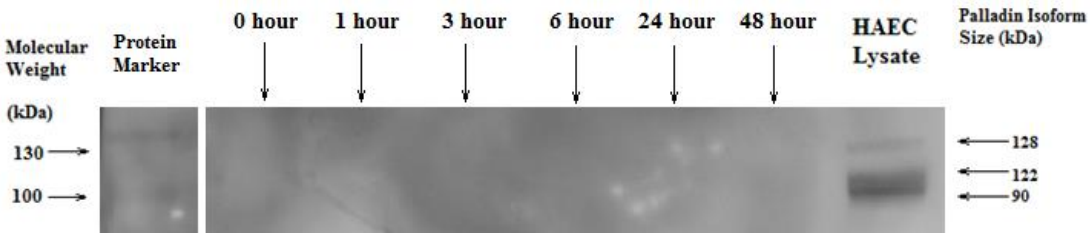
(ii)
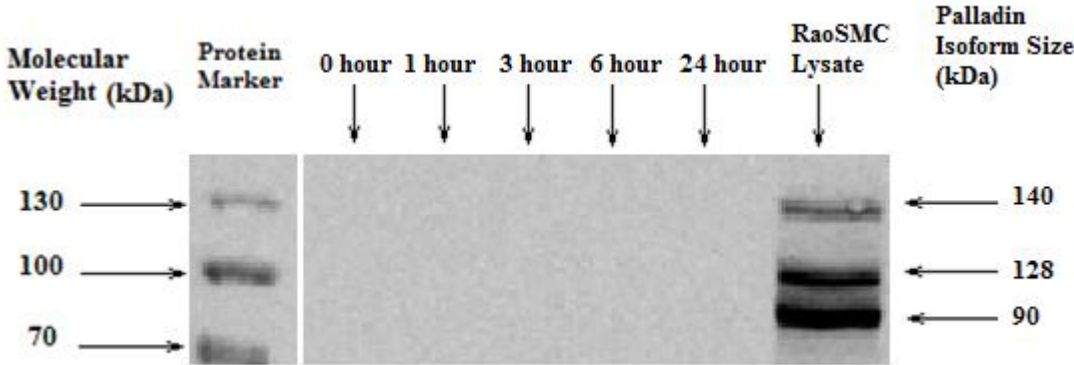
Figure 5.3: Investigation of Palladin within Cyclic Strain-derived Endothelial Microparticles. Following time points of cyclic strain of (i) 5% physiological and (ii) 10% pathological strain, microparticles were extracted from harvested cell, using the methods described in Chapter 2.2.2.3. Cell lysate was loaded into the same gel, and is displayed here as a positive control. Ponceau S staining of the membrane and Coomassie Blue staining of the gel post transfer (not shown) showed that microparticles completely transferred across to the membrane during the process.

Endothelial microparticles were obtained from cells subjected to 24 hours of LSS as well as static cells. Both sets were assayed using an APC-conjugated antibody for VCAM-1 (Vascular cell adhesion molecule 1, also known as CD106). VCAM-1 is a noted endothelial cell marker, so this was used to indicate that the microparticles obtained following shear stress were endothelial in nature. Samples were prepared as described in Chapter 2.2.3.1 and analysed using the Millipore® Guava system. The illustrated results (Figure 5.4) show that a small amount of APC-positive microparticles are recorded in the sheared sample, which are not present in the control static sample. The result confirms that a number of microparticles are released from cells post-shear are indeed endothelial in origin.

.
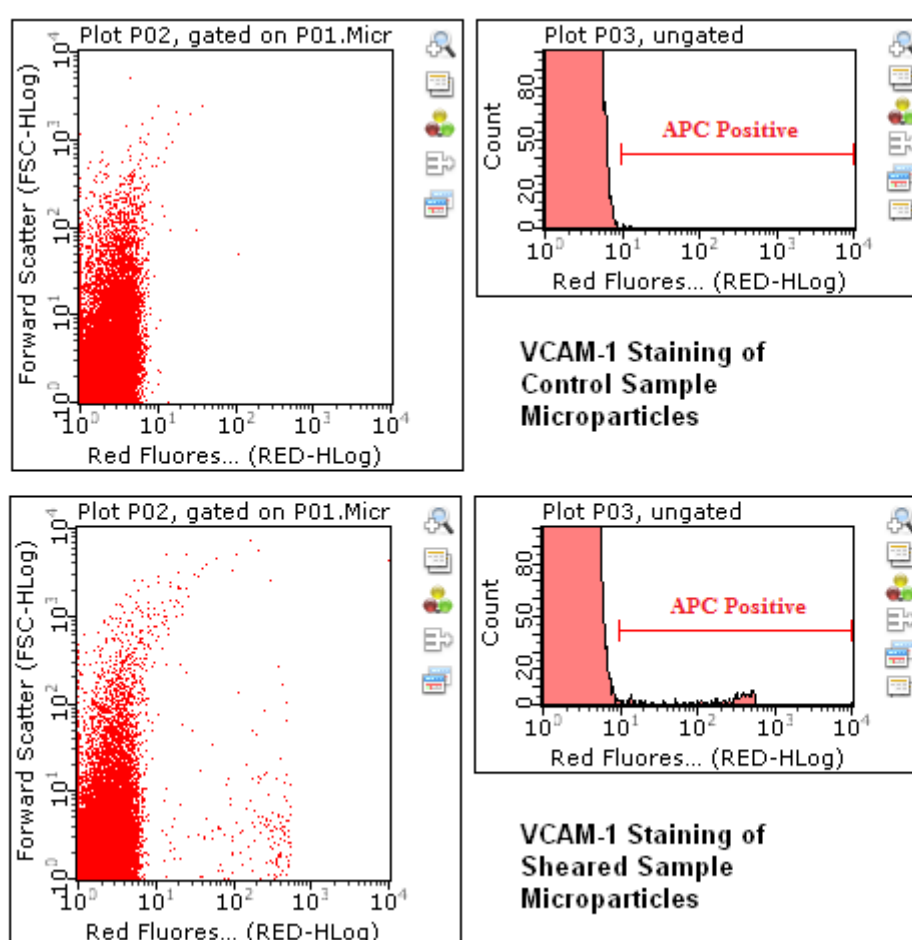
Figure 5.4: Characterisation of Shear-derived Endothelial Microparticles through FACS analysis. Microparticles obtained from cells subjected to 24 hours of LSS were analysed using the Millipore® Guava system. The microparticles were probed using an APC-conjugated antibody for VCAM-1, a noted endothelial cell marker, so this was used to indicate that the microparticles observed were endothelial in nature.

Having determined that shear-induced microparticles are indeed endothelial in origin, experiments were repeated to extract them from sheared cell media. Results had shown that Palladin expression in whole cells increased immediately within the first hour post-shear, before declining at 3 hours (Figure 3.10). A second peak is seen then at 6 hours, but this declines after later time points. It was hypothesised that this decline in protein could be explained by the release of protein through EMPs. To confirm this theory, the microparticles were themselves probed for Palladin using Western Blotting methods, results of which are shown in Figure 5.5. As observed, Palladin is almost absent within EMPs from static cells. The protein bands appear to increase in intensity following increased shear time points. One isoform, either 122kDa or 128kDa in size, is observed to become more prominent at 1 hour than the 90kDa isoform. However it declines in intensity by 6-24 hours. Densitometric analysis of the 90kDa isoform shows that there is a significant amount of Palladin released at 6 hours, where expression reaches a peak. A slight decline in expression is observed at 24 hours, but protein remains significantly more expressed at this time.

Figure 5.5.1 compares the relative expression of Palladin in whole cells (as determined in Figure 3.10) with the expression in microparticles (as shown in Figure 5.5). As shown, within the first hour of LSS, the relative protein expression within the microparticles follows the same pattern as protein expression from whole cells. There are differences between the two sets of data from 3-24 hours. Here, there is a higher relative-to-baseline expression of Palladin within the EMPs. This experiment confirms that there is a higher release of Palladin from HAECs at longer time points of LSS.
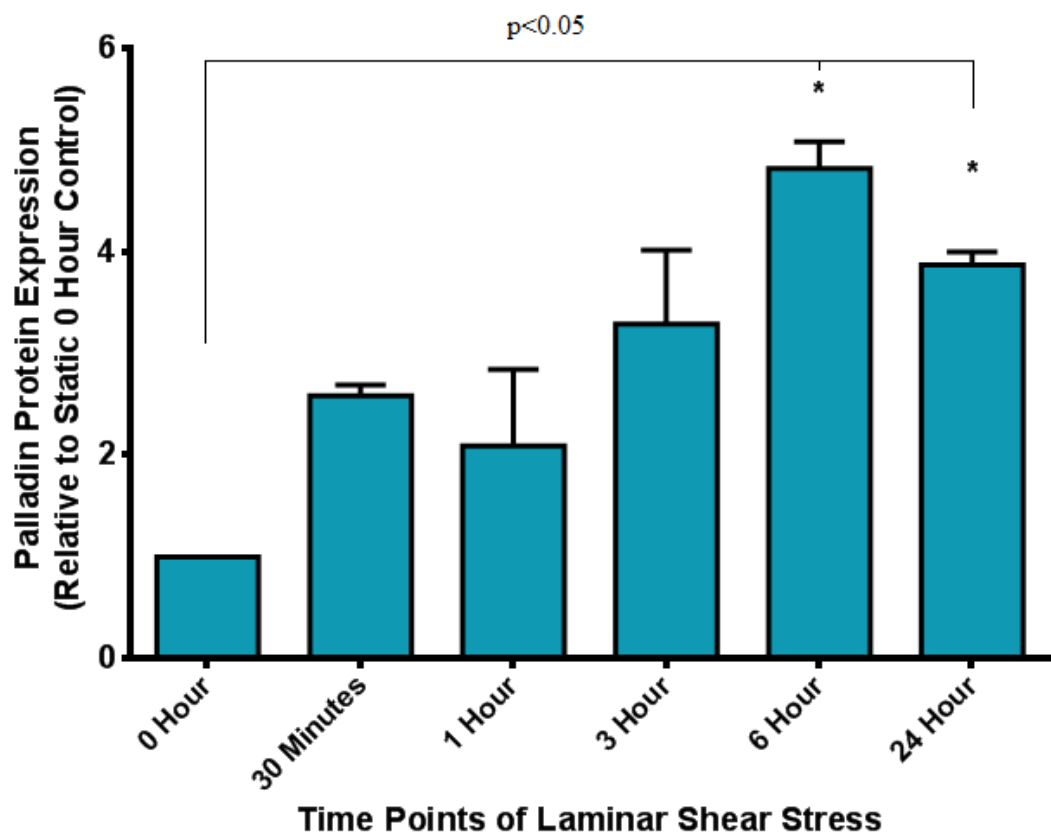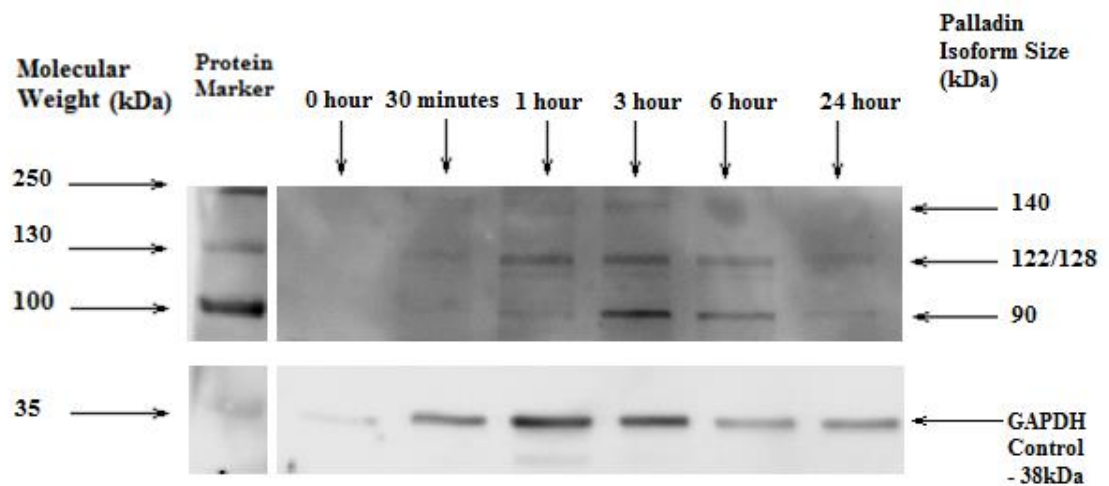
Figure 5.5: Observation of Palladin release in Shear-induced Endothelial Microparticles from HAEC media samples. Microparticles obtained from cells subjected to different time points of shear were probed for Palladin using Western Blot methods. GAPDH was used as a control marker, and microparticles were extracted from equal volumes of cell media. The blot was analysed using ImageJ densitometric quantification software. The values given for intensity of each 90kDa sized Palladin band is given here, following normalisation against the GAPDH control protein bands, and are expressed in comparison to the microparticle release at the baseline zero hour shear. *$p<0.05$.
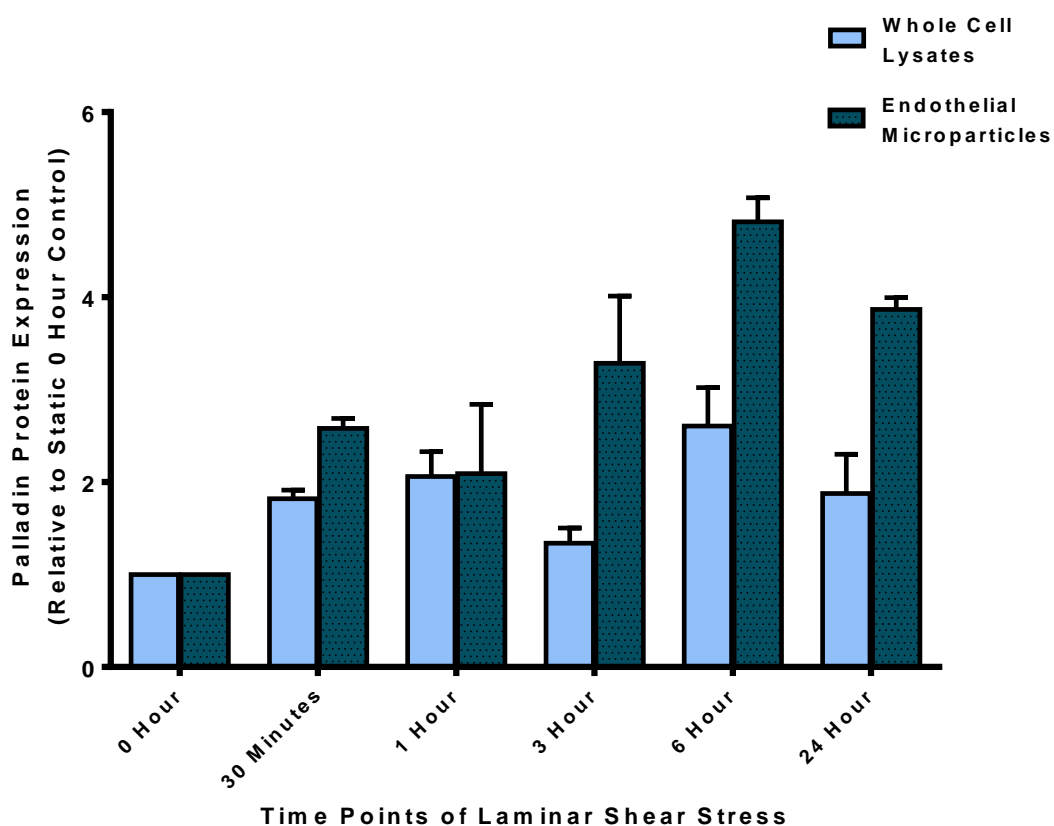
Figure 5.5.1: Comparative trends of Palladin protein expression in HAECs subjected to Laminar Shear Stress vs. Palladin protein expression in Shear-induced Endothelial Microparticles. Here, the data from Figure 3.10– Palladin expression in whole cell lysates of cells subjected to shear – is compared to the similar expression of Palladin in shear-induced Endothelial Microparticles from Figure 5.5. Whole cell lysates are designated by the light blue columns, while Endothelial Microparticles are designated by the dark blue columns. The values given for intensity of each 90kDa sized Palladin band is given here, following normalisation against the GAPDH control Western Blotting bands, and are expressed in comparison to the relevant protein expression at the baseline zero hour shear.

The experiments confirmed that Palladin was released in larger amounts from HAECs that had been subjected to LSS. An experiment was devised with the intentions of investigating the effects that these microparticles may have on Palladin expression in healthy cells. Cells were incubated with conditioned cell media – either completely fresh new media (designated as Static 0 hour), media that was already on static cells for 24 hours prior (Static 24 hour), or else the media that was on cells sheared for 24 hours (Sheared 24 hour) which would contain a larger number of Endothelial Microparticles. All three plates were incubated as normal for an additional 24 hours, before the media was harvested and the cells were lysed. Figure 5.6 here displays the expression of Palladin observed with the HAECs following incubation with these different media samples. As shown, the incubation had negligible effects on expression in cells incubated with either the fresh media or media obtained from static cells. However, there was a significant decline in Palladin expression with cells that were incubated with media taken from previously sheared cells. Palladin expression is roughly half that of the static control cell lysate.

When these experiments were performed, the media was retained following the second incubation with new cells. EMPs were subsequently extracted and probed via Western Blotting methods for Palladin, to observe if there was any Palladin present in these microparticles at post-incubation. Figure 5.6.1 demonstrates that there are strong bands present in the microparticles extracted from the sheared media sample. The two other samples – static 0 hours and static 24 hours – show only miniscule amounts of Palladin. This demonstrates that the previous sample was indeed incubated with EMPs containing Palladin, while also illustrating that there is very little protein released from cells that remain static.
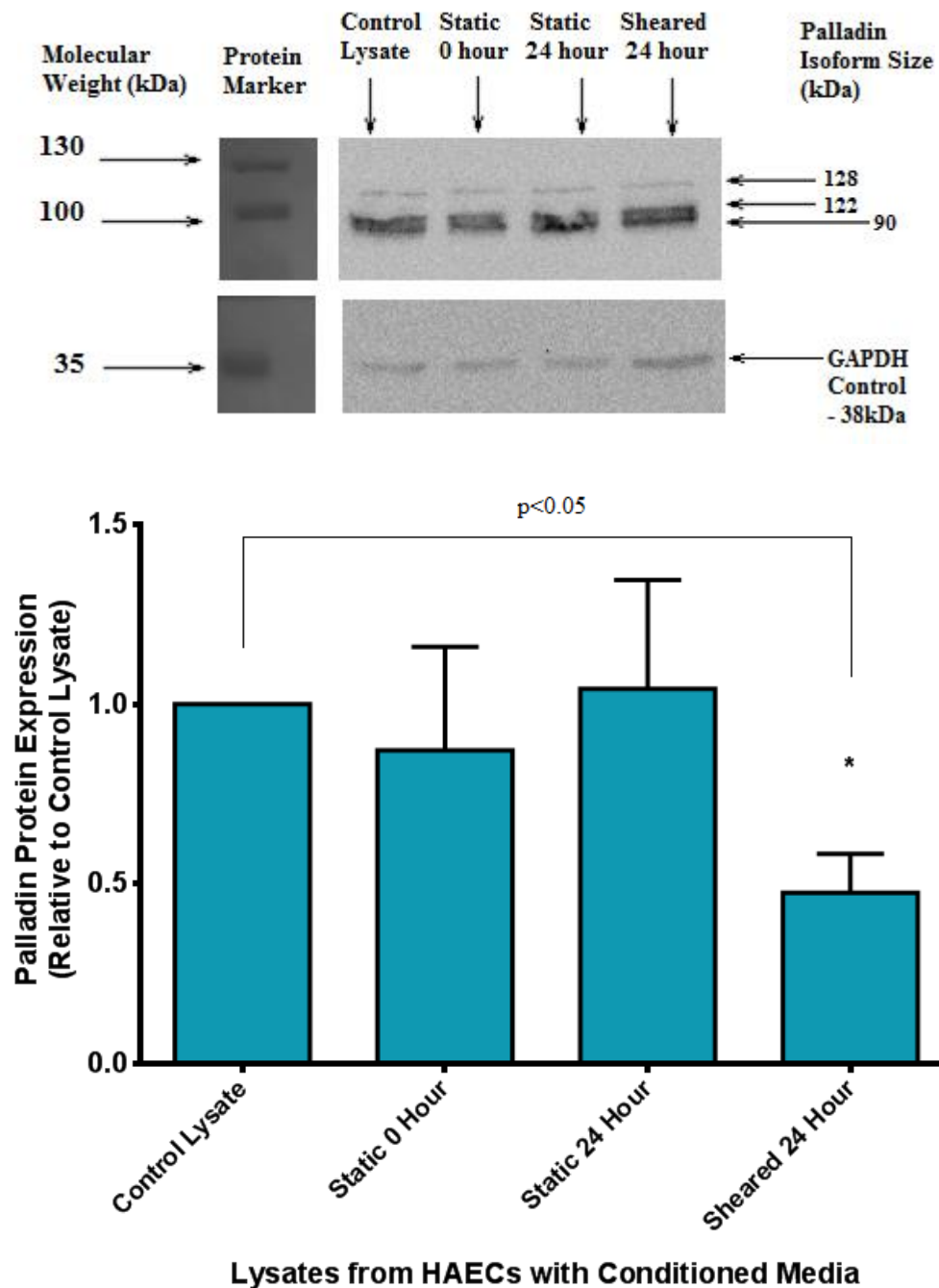
Figure 5.6: Expression of Palladin in HAECs incubated with conditioned Static vs. Sheared media samples. Figure 5.6 here displays the expression of Palladin observed with the HAECs following incubation with different media samples - fresh new media (Static 0 hour), media incubated with static cells for 24 hours prior (Static 24 hour), or else media from cells sheared for 24 hours (Sheared 24 hour). HAEC lysate from static cells was also analysed to use as a comparative control. GAPDH is used as a control to ensure equal loading of protein. The Western Blot was analysed using ImageJ densitometric quantification software. The values given for intensity of each Palladin band is given here, following normalisation against the GAPDH control Western Blotting bands, and are expressed in comparison to the baseline zero hour shear. *p<0.05.
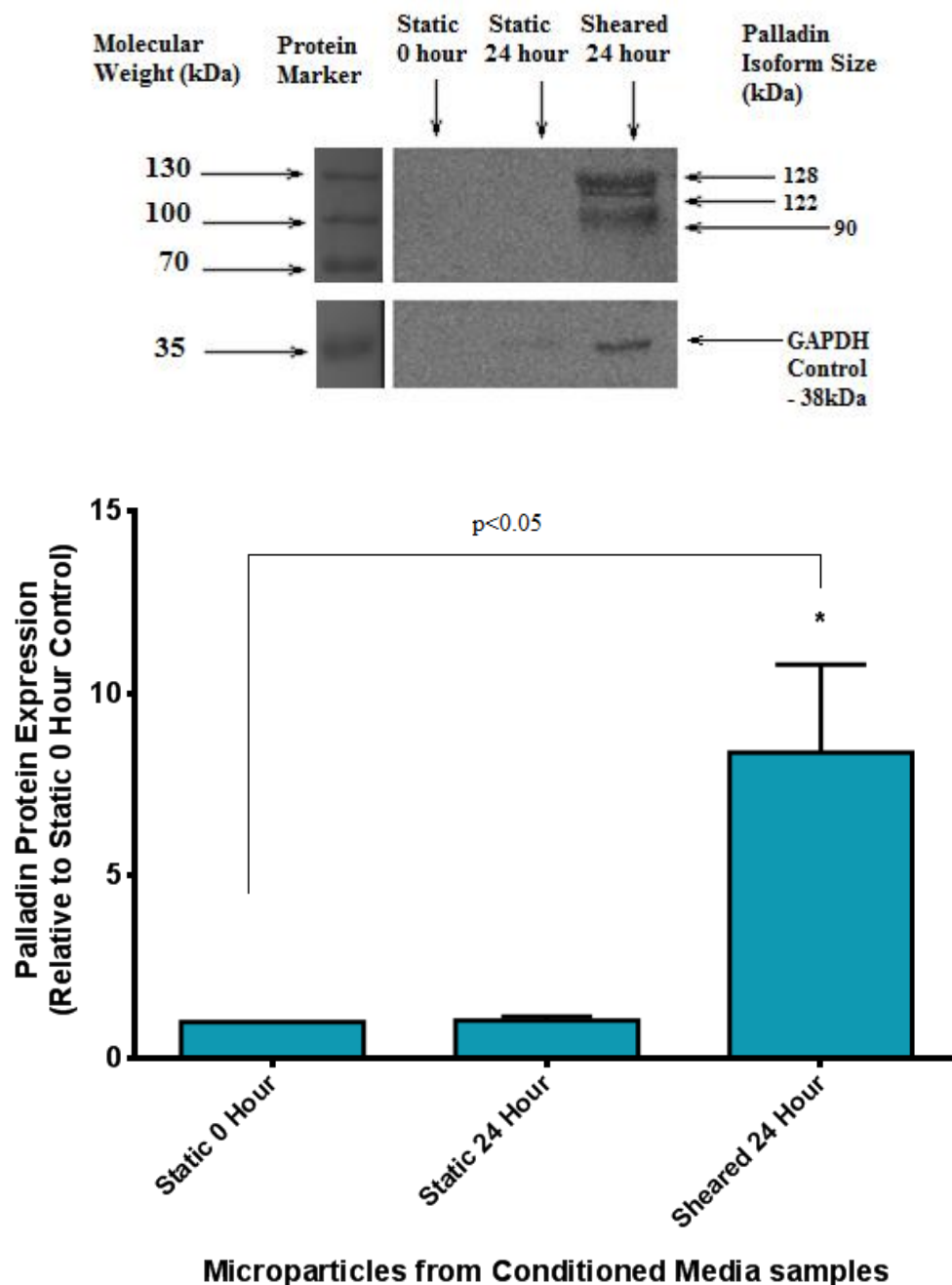
Figure 5.6.1: Observation of Palladin release from Endothelial Microparticles extracted from conditioned cell media post-incubation with HAECs. Following the aforementioned 24 hour incubation with the cells, the different conditioned cell media samples used in the experiments – Static 0 hour, Static 24 hour, and Sheared 24 hour - were harvested and Endothelial Microparticles were extracted from equal volumes of the media as per previously described methods. The microparticles were subsequently probed for Palladin, with GAPDH used as a control. The Western Blot was analysed using ImageJ densitometric quantification software. The values given for intensity of each Palladin band is given here, following normalisation against the GAPDH control Western Blotting bands, and are expressed in comparison to the baseline zero hour shear. *$p<0.05$.

The shear induced release of EMPs was investigated in greater detail, with the investigation of Palladin in cells cultured on extracellular matrices. As detailed in Chapter 3, these cells were sheared and the presence of Palladin within the whole cells was investigated. The sheared media was also retained, with microparticles being extracted from the samples. These microparticles were assayed for Palladin using Western Blotting methods.

Figure 5.7 first demonstrates Palladin expression following cells that were cultured on a fibrinogen matrix. While bands for the GAPDH control are visible at all of the time points and increase in intensity, there is only Palladin observed at 24 hours post-shear. None of the other earlier time points demonstrate a release of Palladin through EMPs. The protein released is also a clearly smaller amount than that present in the whole cell lysate control.

Unusually, this lack of expression is observed within the microparticles extracted from cells on other cell matrices. Figure 5.8 illustrates the expression in microparticles from cells cultured on a fibronectin matrix and then sheared. Here, similarly to Figure 5.7, there is a lack of Palladin expression until 24 hours, where a faint band is finally visible. Again, this is miniscule compared to that of the whole cell lysate control sample.

The microparticles extracted from cells cultured on Type IV collagen also fail to show any early expression of Palladin (Figure 5.9). A band is visible at 24 hours, but this is very faint also. This is in stark contrast to the control cell lysate, or the GAPDH control – both of which demonstrate very strong bands for protein. The reasoning for this active repression of release of Palladin in EMPs from cells on these matrices is discussed in Chapter 5.3.
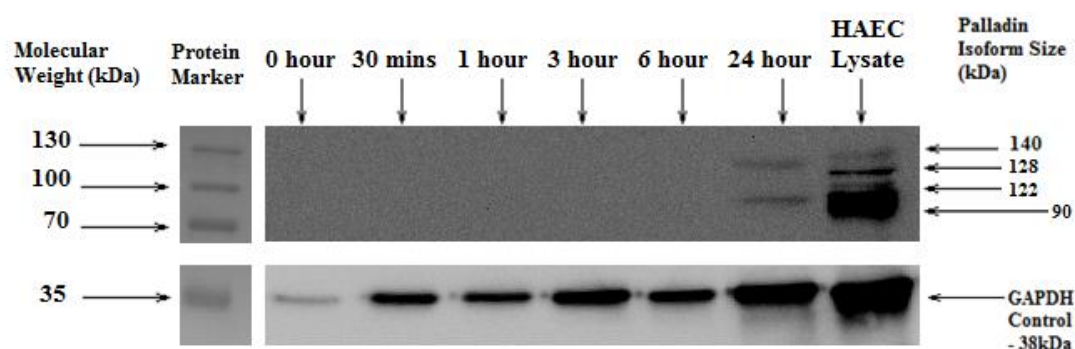
Figure 5.7: Observation of Palladin release from Shear-induced Endothelial Microparticles derived from HAECs seeded onto a Fibrinogen Matrix and Sheared at 10 dynes/cm^2. HAECs were cultured on dishes coated with 10μg/ml fibrinogen. Upon reaching confluency, the cells were subjected to LSS for different time points. Endothelial Microparticles were subsequently extracted from the cell media and then probed for Palladin using Western Blot methods. GAPDH was used as a control marker, and equal volumes of cell media were used for microparticle extraction. HAEC whole cell lysate was also probed on the Western Blot, to use as a positive control.
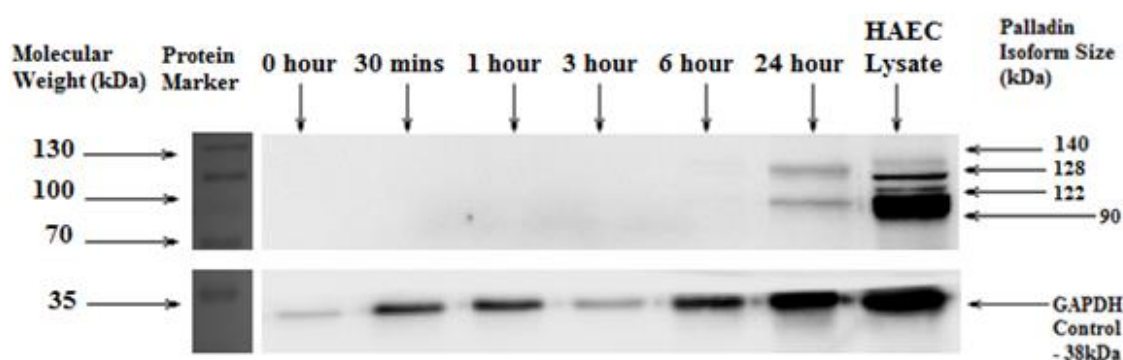
Figure 5.8: Observation of Palladin release from Shear-induced Endothelial Microparticles derived from HAECs seeded onto a Fibronectin Matrix and Sheared at 10 dynes/cm². HAECs were cultured on dishes coated with 10μg/ml fibronectin. Upon reaching confluency, the cells were subjected to LSS for different time points. Endothelial Microparticles were subsequently extracted from the cell media and then probed for Palladin using Western Blot methods. GAPDH was used as a control marker, and equal volumes of cell media were used for microparticle extraction. HAEC whole cell lysate was also probed on the Western Blot, to use as a positive control.
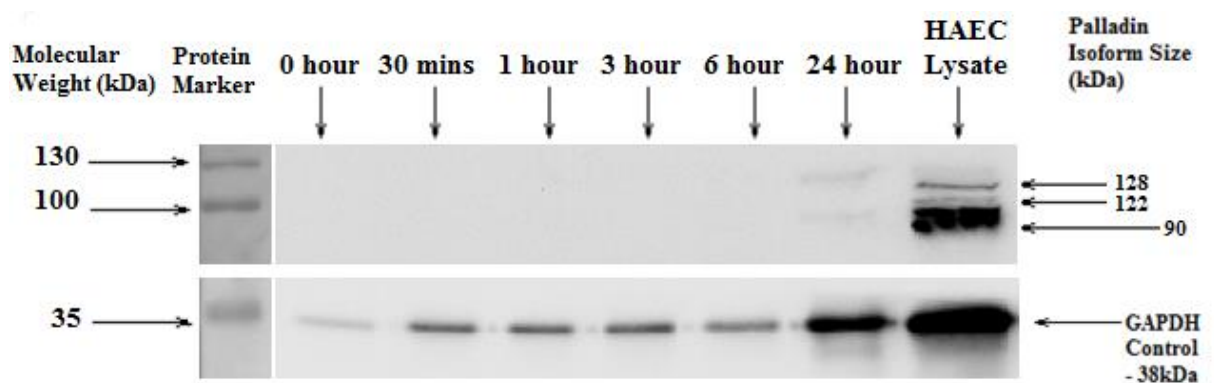
Figure 5.9: Observation of Palladin release from Shear-induced Endothelial Microparticles derived from HAECs seeded onto a Collagen Matrix and Sheared at 10 dynes/cm^2. HAECs were cultured on dishes coated with 20μg/ml Type IV collagen. Upon reaching confluency, the cells were subjected to LSS for different time points. Endothelial Microparticles were subsequently extracted from the cell media and then probed for Palladin using Western Blot methods. GAPDH was used as a control marker, and equal volumes of cell media were used for microparticle extraction. HAEC whole cell lysate was also probed on the Western Blot, to use as a positive control.

The results from investigating the release of microparticles on cells in contact with extracellular matrices showed an apparent repression of Palladin in EMPs, with only miniscule amounts of protein present. A better model of *in vivo* release of Palladin in shear-induced EMPs is demonstrated with Figure 5.10. Here, plasma was extracted (as described in Chapter 2.2.2.4) from subjects post-exercise and the EMPs were extracted, as were the exosomes – a smaller class of particle. Probing these samples on a Western Blot indicated that Palladin was indeed present in an *in vivo* model, with an elevation in protein in samples taken post-exercise compared to samples from a relaxed state. There appeared to be a selective localisation of the Palladin isoforms to different particle subsets – the 90kDa and 128kDa isoforms were visible in the microparticles, whereas the 43kDa isoform remained exclusive to the exosomes. In samples obtained from the relaxed state, this 43kDa isoform was visible in the exosomes also. However the 90kDa and 128kDa isoforms were absent in the corresponding microparticle sample.
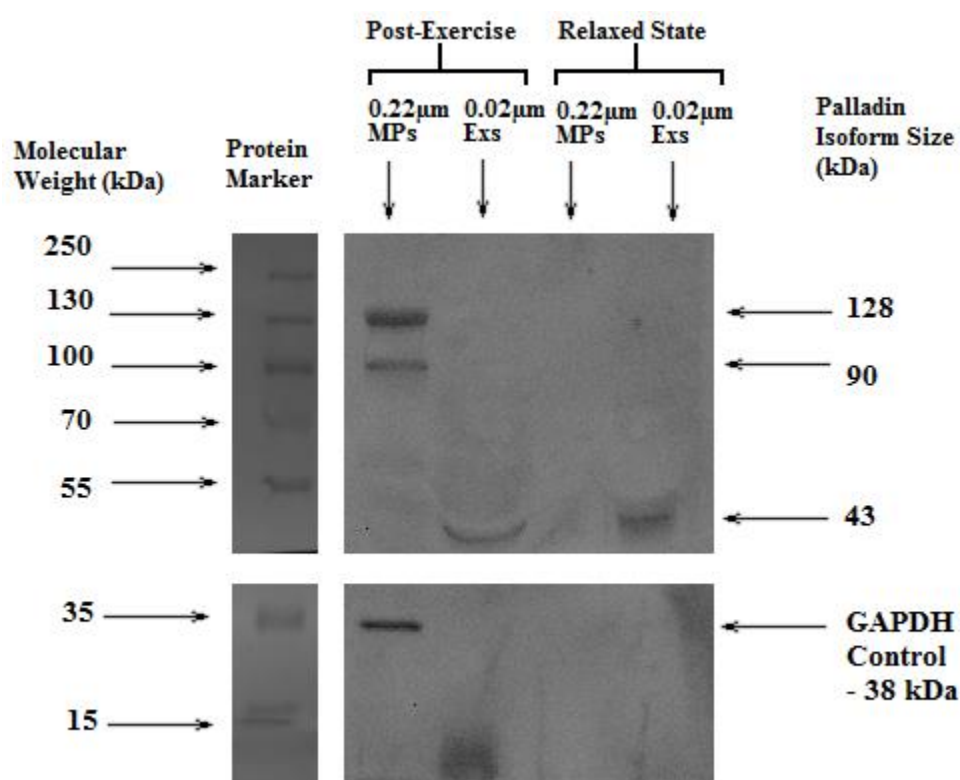
Figure 5.10: Observation of Palladin release in Shear-induced Endothelial Microparticles and Exosomes from Healthy Blood Plasma Samples. Equal volumes of blood were drawn from a healthy male immediately following active exercise – quantified as reaching 15-20 on the Borg Scale (Borg, 1982). Samples were also taken from the subject at a relaxed state (6-7 on the Borg Scale). The Endothelial Microparticles (MPs) and Exosomes (Exs) extracted from the plasma are presented here after probing on a Western Blot for Palladin. GAPDH was used as a control.

Palladin has been shown to be expressed in shear-induced EMPs, shedding light on the mechanisms of protein release from the cell post-shear. The two other proteins of interest in this thesis – LASP-1 and Drebrin – were investigated to observe how they are released within EMPs also. Given that Palladin is released from the cells as a coping mechanism to cope with excess protein, it was hypothesised that the same may happen with LASP-1. Since Drebrin is shown to decrease immediately following shear, it was thought that some of this protein may be exported from cells via an endothelial microparticle release mechanism.

LASP-1 was initially shown to increase in whole cells post-shear. In Figure 5.11, the expression of LASP-1 in microparticles shows that following LSS, the amount of LASP-1 appears to decline. Western Blot protein bands are visible in the initial time points, but they appear to fade. Densitometric analysis shows that LASP-1 release in EMPs is significantly deplete within the first 3 hours of shear. An increase in LASP-1 release is seen at 6 hours, but this declines again at 24 hours. Comparing the expression of LASP-1 in whole cells to the expression in EMPs (Figure 5.11.1) shows that the release of protein in microparticles appears to follow the pattern of the expression in whole cells; however the expression in EMPs is relatively lower than that of the whole cell lysates.

Drebrin is investigated in release of microparticles also. Figure 5.12 demonstrates that there is a significant increase in the amount of protein released from the microparticles. Protein bands appear much more prominent in microparticle samples than that of the bands illustrated in Figure 4.11. Densitometric analysis of the blot in this figure highlights how there is a steady increase of Drebrin released within the EMPs for the first 6 hours post-shear. At 24 hours, there is a decline in the amount of protein expressed, although this remains elevated compared to the static baseline expression. A comparative figure is provided (Figure 5.12.1) to show post-shear expression of Drebrin in both microparticles and whole cell lysates. Here, the relative expression of protein within the EMPs greatly outweighs that of the whole cell lysates. For the first 6 hours, expression in EMPs increases as expression in lysates decreases. At 24 hours, the expression in lysates decreases further, but so does the expression in microparticles.
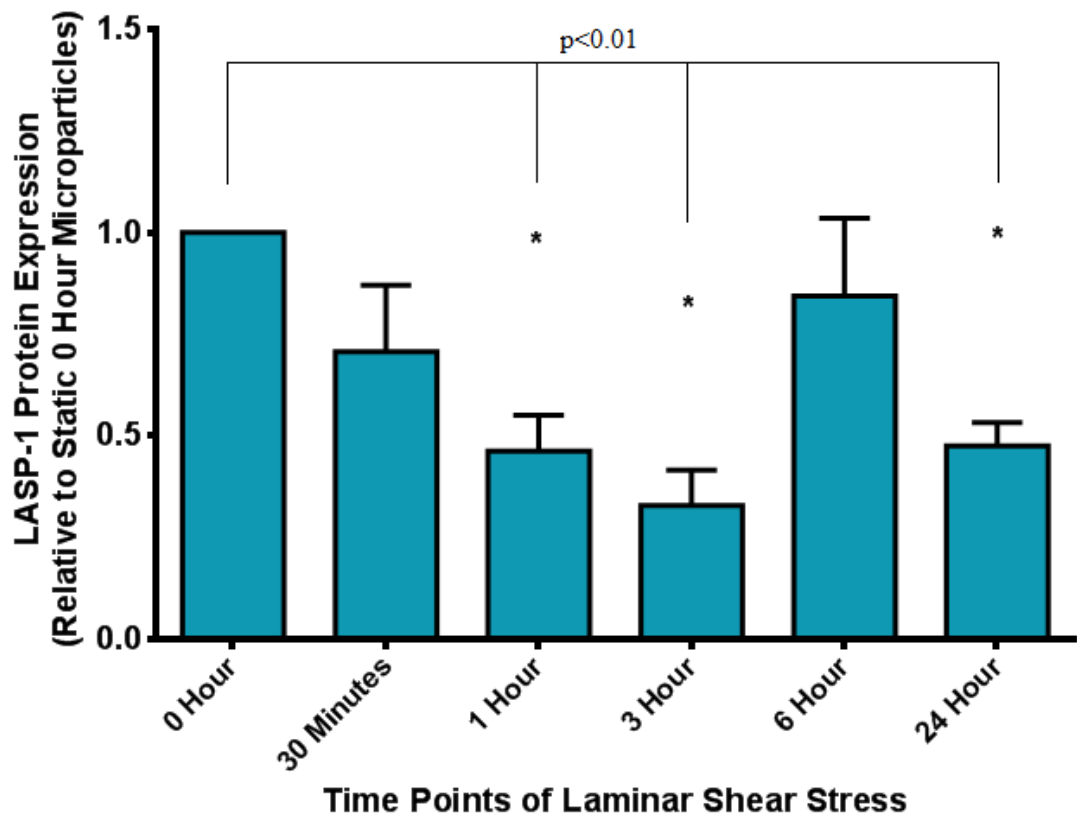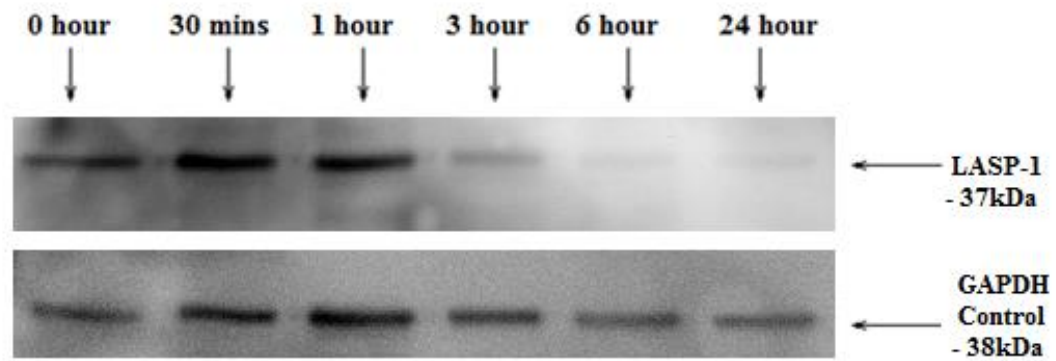
Figure 5.11: Observation of LASP-1 release in Shear-induced Endothelial Microparticles from HAEC media samples. Microparticles were extracted from the media of HAECs that were subjected to time points of LSS at 10 dynes/cm^2. Following this, they were analysed on a Western Blot and probed for LASP-1. Blots were stripped and probed again for GAPDH for use as an endogenous control. Following probing, the bands were analysed using ImageJ densitometric quantification software. The values given for intensity of each LASP-1 band is given here, following normalisation against the GAPDH control Western Blotting bands, and are expressed in comparison to expression in the zero hour static cells. *p<0.01.
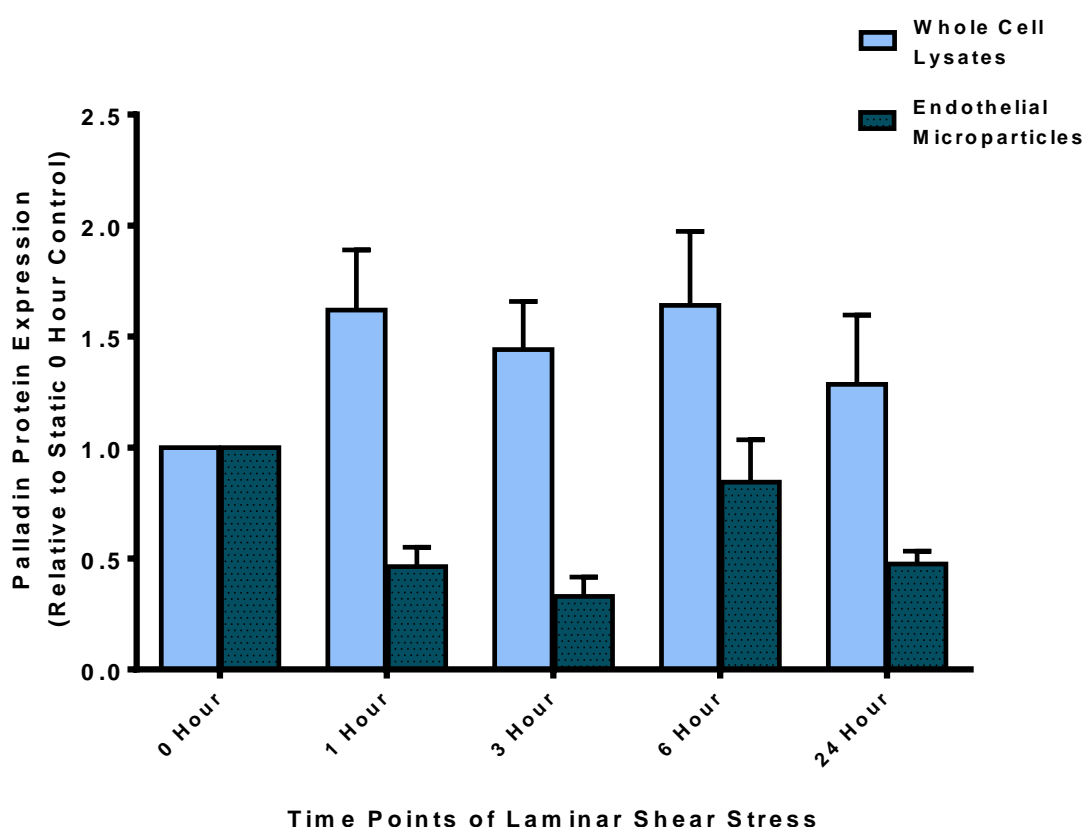
Figure 5.11.1: Comparative trends of LASP-1 protein expression in HAECs subjected to Laminar Shear Stress vs. LASP-1 protein expression in Shear-induced Endothelial Microparticles. Here, the data from Figure 4.6 - LASP-1 expression in whole cell lysates of sheared cells – is compared to the similar expression of LASP-1 in shear-induced Endothelial Microparticles from Figure 5.11. Whole cell lysates are designated by the light blue columns, while Endothelial Microparticles are designated by the dark blue columns. The values given for intensity of each LASP-1 band is given here, following normalisation against the GAPDH control Western Blotting bands, and are expressed in comparison to the relevant protein expression at the baseline zero hour shear.
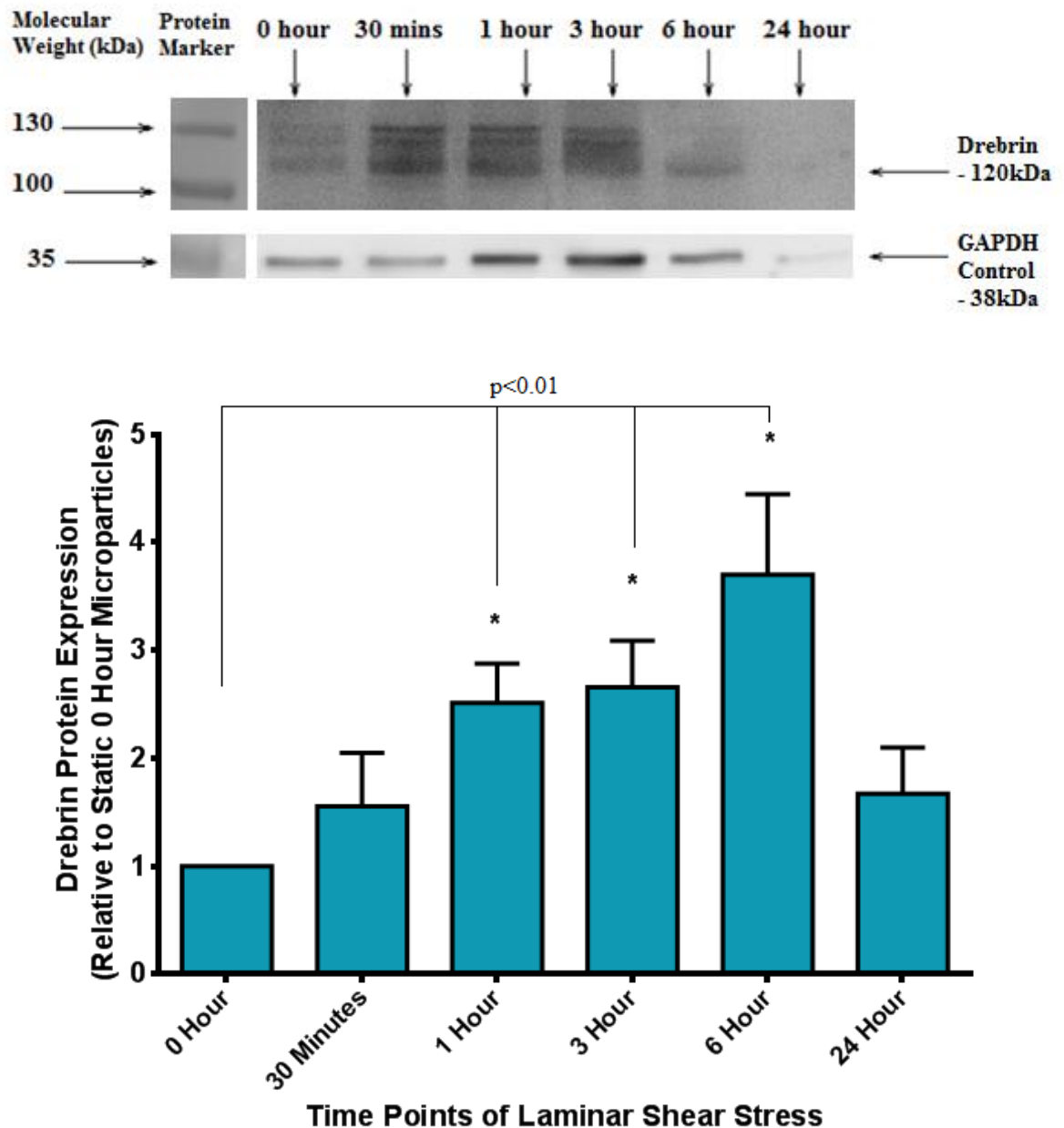
Figure 5.12: Observation of Drebrin release in Shear-induced Endothelial Microparticles from HAEC media samples. HAECs were subjected to time points of LSS at 10 dynes/cm^2, with EMPs being extracted from the cell media post-shear. Following this, they were analysed on a Western Blot and probed for Drebrin. GAPDH was also probed as an endogenous control. The blot was analysed using ImageJ densitometric quantification software. The values given for intensity of each Drebrin protein band is given here, following normalisation against the GAPDH control protein bands, and are expressed in comparison to expression in the zero hour static cells. *p<0.01.
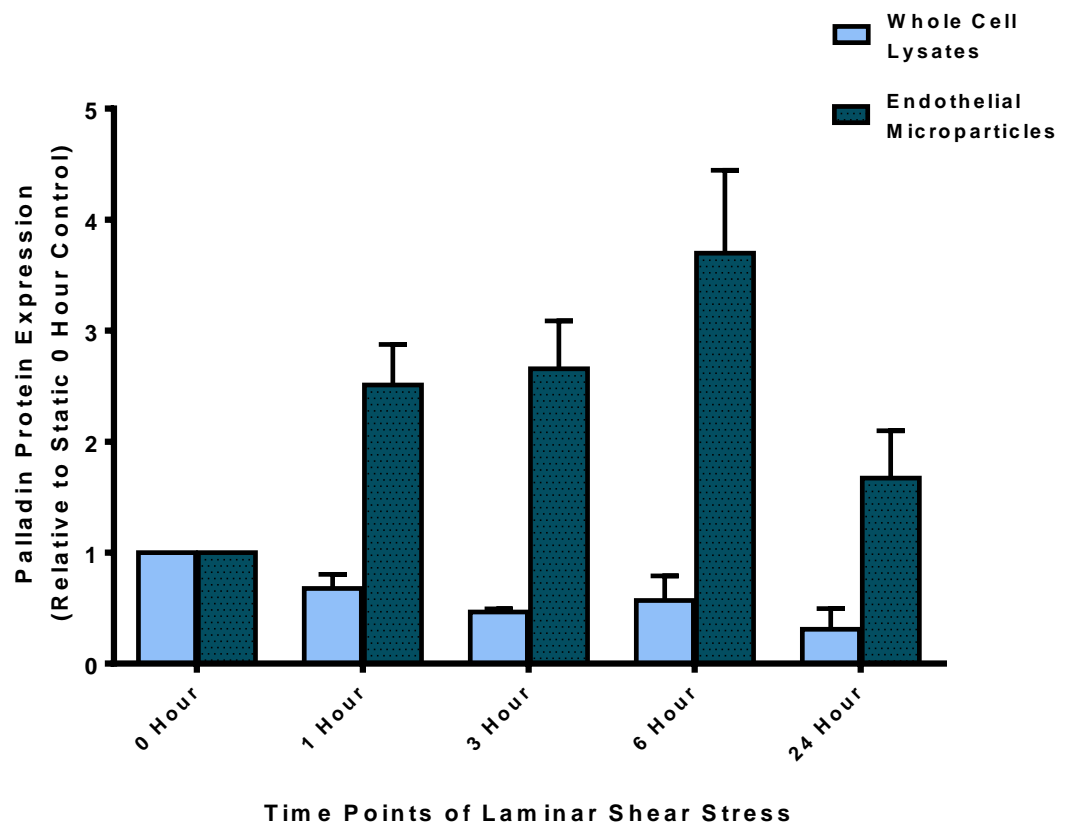
Figure 5.12.1: Comparative trends of Drebrin protein expression in HAECs subjected to Laminar Shear Stress vs. Drebrin protein expression in Shear-induced Endothelial Microparticles. Here, the data from Figure 4.11 - Drebrin expression in whole cell lysates of cells subjected to LSS – is compared to the similar expression of Drebrin in shear-induced Endothelial Microparticles from Figure 5.12. Whole cell lysates are designated by the light blue columns, while EMPs are designated by the dark blue columns. The values given for intensity of each Drebrin band is given here, following normalisation against the GAPDH control Western Blotting bands, and are expressed in comparison to the relevant protein expression at the baseline zero hour shear.

5.3: DISCUSSION

Palladin is a protein with many functional roles, one of which has been observed to be its involvement in cellular remodelling in response to injury. The protein has been observed to be upregulated in different cell types along wound edges (Boukhelifa *et al.*, 2003). In vascular smooth muscle, Palladin has been seen to play a role in cell motility and contractility (Goicoechea *et al.*, 2006). The closing of wounds typically requires an increased contractility and motility to bring the edges together and fill the wound; suggesting that Palladin is likely an essential protein for these processes.

It is thought that the knockdown of Palladin in other cell types results in disruption in cell migration, caused by the depolymerisation of filamentous actin and disarrangement of stress fibres (Jin *et al.*, 2009; Brentnall *et al.*, 2012). Knockdown of Palladin in *in vitro* models has also been observed to result in the loss of LASP-1 from stress fibres in cells (Rachlin and Otey, 2006), highlighting how it is part of a functional network (as documented in Chapter 4). The silencing of Palladin appears to have a negative downstream effect on some of the related proteins in this manner. Palladin silencing was investigated before in an *in vivo* setting, with knockout mice being developed. However, the phenotype of these mice was embryonic lethality at about 15-16 days (Luo *et al.*, 2005), which further highlights the importance of Palladin within the cell.

While literature has discussed the protein knockdown in various cell types resulting in decreases in migratory patterns (Goicoechea *et al.*, 2009; Otey *et al.*, 2009), studies on the effects of Palladin knockdown on endothelial cell migration have yet to be reported. It was hypothesised that knocking down of Palladin in HAECs would result in a decrease of cell migration. Figure 5.1 displays the results of a scratch wound assay on HAECs transfected with Palladin siRNA. For use as comparative controls, an equal number of cells either (i) transfected with scrambled siRNA or else (ii) non-transfected, were both seeded onto culture dishes at the same time and subjected to the same scratch wound assay. Palladin knockdown efficiency is quantified in Figure 5.1.2, where Western Blot methods showed knockdown of protein within the cells.

Within the first hour post-scratch, the non-transfected control cells are already migrating across the wound. By 3 hours, these same cells have almost completely formed a monolayer, one which is fully evident by 6 hours. In comparison, the transfected cells (both Palladin siRNA and scrambled) are slower to migrate across the wound area. Cells transfected with Palladin siRNA do not show much migration within the first 3

hours of investigation. At 6 hours, some migration has occurred, but a monolayer phenotype has yet to be achieved. In comparison, the scrambled siRNA transfected cells at first appear to follow a similar pattern, showing slower migration at 1 hour post-scratch wound compared to the non-transfected cells. However, at 3 hours the cells appear to have migrated further than the Palladin siRNA knockdown cells, and are closer to achieving the same phenotype as the non-transfected cells. At 6 hours, they have completely formed a monolayer. When this measured and expressed in a graphed format (Figure 5.1.1), the decrease in migration in Palladin siRNA-transfected cells over the time points is more noticeable. Morphologically, control and knockdown cells also looked similar throughout the time course.

The results appear to indicate that there is a general delay in migration when comparing transfected cells to the non-transfected cells. This is likely due to the reduction in stability of the transfected cells, owing to the microporation process and the insertion of foreign molecules (siRNA) into the cell. Despite this, the cells are still viable, and capable of cell migration, albeit at a slower rate. At 3 hours following the scratch wound, all the cells appear to show movement; however the Palladin siRNA transfected cells appear the slowest to migrate when compared to the other sets of cells. This illustrates how Palladin is an important protein for cell migration, since knockdown has a delayed effect on the cell movement across the wound. Six hours post-scratch wound appears to be the point at which cells migrate regardless of knockdown, demonstrating that there is only a small window of time to observe post-knockdown effects before cell proliferation occurs, making the migration of cells tougher to determine.

Initial experiments were performed with similarly transfected cells using the novel xCELLigence™ system. The cells were strained to investigate the effect of haemodynamic force on cells lacking in Palladin. The silicon membrane of the BioFlex plates means it is harder to image cells for using in a wound healing assay; hence the xCELLigence™ system was used. Strain increases cell migration (Von Offenberg Sweeney *et al.*, 2005), and it is shown in Figure 5.2 that migration increases in cells where Palladin is knocked down compared to the non-transfected cells. However, the rate of migration appears elevated after general transfection (the scrambled siRNA cells show elevated migration also) suggesting that this rise may be due to the transfection process causing the cells to alter in morphology and migrate quicker. There is a small increase in knocked-down cells that were strained versus those that were static, indicating that the removal of Palladin followed by haemodynamic force affects cell

migration. However, statistical analysis failed to show a significant change, so a conclusion based on this study cannot be reached.

A possible reason for the removal of Palladin resulting in increased migration post-strain may be that the role of Palladin in cell migration could be compensated by a different protein. This could also explain the delay in cell migration in the scratch wound assay occurring instead of a complete halt. It indicates that the cell could have a functional overlap mechanism for proteins involved in migration. While some proteins show a decline when Palladin is knocked down (e.g. LASP-1), there are other proteins in the same network that may be able to take over the role of Palladin (Goicoechea *et al.*, 2009). Palladin expression appears to be tightly controlled to allow for transitions from non-motile to motile phenotypes. If it is tightly controlled in such a manner, then there may be other proteins that exist to compensate for its loss in the cell. The strong binding interaction between Palladin and its binding partners (e.g. α-actinin), coupled with their high degree of co-localization in cells and tissues, suggest that these proteins may have a shared function in motility and adhesion.

An alternative reason for the short time frame for observing knockdown could also be on account of the excretion of the siRNA from the cells themselves, and subsequent normalisation of Palladin expression once again. As shown earlier, cells possess a method of exporting protein, RNA and miRNA out through microparticles; it is not unreasonable to think that the transfected siRNA can be exported in the same way. The cell membrane is already in a fragile state post-transfection, which in theory would make microparticle release easier. The fact that Palladin is a vitally important protein for cell development and function suggests that the microparticle excretion hypothesis may be likely.

Endothelial Microparticles vary in size, phospholipid and protein composition. They promote coagulation, have a pro-inflammatory effect and affect vascular function. These processes are all involved in the pathogenesis of cardiovascular disease and it is suggested that microparticles may play also a role in the pathogenesis of CVDs. As discussed in Chapter 1, they may also show potential use as a biomarker for the disease state, potentially being used as a quantitative method of detecting CVD symptoms (Viera *et al.*, 2012). EMPs are also known to be elevated in severe hypertension and other conditions associated with endothelial injury (Diamant *et al.*, 2004). As well as

endothelial function, some haemodynamic force has an effect on stimulation of microparticle release.

Shear stress modulates the integrity and permeability of endothelial cells, largely through its effects on intercellular junctional proteins such as connexins and VE-Cadherin. These proteins are used as unique antigenic signatures that can differentiate the endothelial microparticles from other microparticles (Dignat-George and Boulanger, 2011). Notably, these proteins can be upregulated in response to increased blood flow (Marin *et al.*, 2013), not unlike how Chapter 3 showed the same upregulation occurring with Palladin. Shear stress may also elicit mechanotransduction pathways to induce or silence the transcription of miRNAs along with their parental genes (Wang *et al.*, 2010). Despite an apparent lack of data on shear stress regulation of the junctional proteins through miRNAs, both connexins and VE-Cadherin are shown to be targeted by miRNAs (Muramatsu *et al.*, 2013; Li *et al.*, 2012) and therefore may contribute to the shear stress-regulated endothelial permeability, which in turn allows for increase of microparticle release.

This release of microparticles is one which is induced differently by different signals (Shai and Varon, 2011). In particular, there appears to be a difference in the EMPs released through cyclic strain and from LSS. Figure 5.3 illustrates the probing of Palladin within cyclic strain-induced EMPs. Western Blots were used instead of ELISA methods for cost reasons and for easier comparison to protein expression from the whole cell lysates used in Chapter 3. Notably, with both (i) 5% physiological and (ii) 10% pathological strain, there is an absence of Palladin. While bands appear for the positive control lysates, there is no protein detected in any of the microparticle samples released at any time point, from either 5% or 10% strain. There are reasons for this peculiar result. Firstly, there are only a relatively smaller volume of EMPs released from cells following cyclic strain when compared to those released from shear stress, due to the flow vs. pulse effect of stimulating membrane disruption and particle release (Brodsky *et al.*, 2004). Cells are more prone to release microparticles when the flow causes a friction across the membrane, as opposed to the repetitive pulsing of blood (or media) pushing into the cells. Because of the reduction in microparticle number, it would follow that there is a reduction of levels of Palladin being released too.

Secondly, since LSS and cyclic strain have a different effect on microparticle number, there may be differential regulation of what gets exported through the released

microparticles, depending on type of haemodynamic force. Different agonists have been shown to result in the release of different particles subsets from a single cell type (vanWijk *et al.*, 2003); shear and strain may affect release in a similar way. There may also be different signalling methods (such as miRNA) prohibiting the release of Palladin from strain-induced microparticles while allowing release in shear-induced microparticles, but this is something that merits future investigation. We have shown that there is a localisation of Palladin to different areas of the cell following LSS (Figure 3.14.1); it is likely that there is a similar localisation following cyclic strain, one which relocates the protein away from the membrane and reduces the chance of release through strain-induced microparticles. A similar relocalisation mechanism is suggested later on HAECs sheared on extracellular matrices

Because Palladin appears to be absent from strain-induced microparticles, which themselves also appeared in lower numbers, the rest of the studies were based on microparticles released due to shear stress. Figure 5.4 characterises these shear-induced particles as being endothelial in nature, having being subjected to FACS analysis using VCAM-1 as an endothelial specific marker. There are a number of VCAM-1 particles present, confirming the particle type. Figure 5.5 subsequently demonstrates the presence of Palladin in EMPs following time points of laminar shear. It appears that the amount of the 90-kDa isoform of Palladin protein released within the microparticles increases in a steady trend following the conditions of shear stress, significantly peaking at 6 hours – the same time point of peak protein expression in whole cell lysates (Figure 3.10), demonstrating that as Palladin is upregulated in the cell, protein is exported from the cell at the same time.

Figure 5.5.1 illustrates how, for the first 3 hours of LSS, the relative protein expression within the microparticles follows the same pattern as protein expression from whole cells. This pattern is suggestive that following the inflammatory response, HAECs compensate for excess protein production through microparticle secretion. However, the relative levels of protein expression become disparate between the two sets of data at 6-24 hours, showing higher expression of Palladin within microparticles. As the cells adapt to chronic shear stress, the cells begin remodelling further, resulting in an increase of Palladin, but also destabilisation of the membrane as the cell morphologically changes. This destabilisation can result in an increase of EMP release, which results in the elevated Palladin levels. The 24 hour time point shows a slight reduction in microparticles, suggesting that the cells may have a phagocytic mechanism for cells to

internalise surrounding microparticles and the protein found within (Terrisse *et al.*, 2010). Also of note is the apparent expression of the other isoforms of Palladin appearing in the microparticles. Figure 5.5 demonstrates that either the 122kDa or 128kDa isoform appears to be present in EMPs at 1-6 hours. This is an interesting occurrence; it appears that there may be a selective mechanism in the cells to release Palladin isoforms at different time points of shear, while retaining others. The selective release of Palladin is observed later in Figure 5.10 when Palladin is investigated in microparticles from plasma samples.

The effect of the internalisation of EMPs on HAECs was investigated first however. Endothelial cells with high levels of microparticles *in vitro* have been already observed to play an inhibitory effect on cell growth and function (Mezentsev *et al.*, 2005; Taraboletti *et al.*, 2002). Having observed this, an experiment was designed where cell media containing shear-induced EMPs would be added to new, static plates of HAECs (Figure 5.6). It was performed to investigate if these extra EMPs may have an inhibitory effect on Palladin production, or if the extra Palladin in the EMPs create overexpression of protein in the cells. Lysates from static HAECs, HAECs cultured in new media and HAECs cultured with 24 hour-old media from other static cells were also assayed. The addition of either fresh or 24 hour-old media to static HAECs does not appear to significantly affect the expression of Palladin. This is expected, as the HAECs remain static the whole time, without any haemodynamic force stimulating an increase of Palladin expression. In HAECs cultured with media from 24-hour sheared cells (containing a large volume of EMPs), the expression level of Palladin significantly decreases.

Curiously, when the media from these cells is assayed in Figure 5.6.1, the level of Palladin-containing EMPs outside of the cell remains high – indicating that the protein is not re-absorbed into the cells. It appears that the addition of EMPs to HAECs causes Palladin downregulation; even though these microparticles themselves contain Palladin and could be absorbed, they don't increase the protein level within the cell, and may in fact reduce it. A reasoning for this may be that the cells identify they are surrounded by a massive supply of Palladin, and therefore are signalled (Likely through RNA or miRNA transfer) to halt production of protein, resulting in a downregulation of endogenous levels in the static cells (Mause, 2010). Microparticles are observed to carry a specific subset of cellular mRNA or miRNA, not just a random sample (Mause and Weber, 2010). Therefore it may be that this may be a specialised signal that the cell

actively secretes from microparticles, to initiate downregulation of Palladin in neighbouring cells. The mechanisms for this selectivity still remain to be characterised, but it is suggested that the "packaging" of microparticles with specific RNA depends on the activating stimulus and that the transferred levels of RNA are regulated by specific nucleases in the recipient cell (Yuan *et al.*, 2009). As discussed earlier in Chapter 1, the elevated levels of microparticles released can be a result of endothelial dysfunction, but also worsen the said dysfunction (Brodsky *et al.*, 2004). This downregulation of Palladin appears to be a further example of how elevated microparticle levels may be detrimental for endothelial cell morphology.

It should be noted that this media may contain other factors apart from microparticles which may affect protein expression. It must be considered that the signalling that influences Palladin expression may occur from other substances, such as vWF or other cytokines and chemokines which are released post-shear (Urschel *et al.*, 2012). For now we cannot conclusively prove the effects of microparticles on protein expression in neighbouring cells, but this provides the groundwork for future investigation.

The signalling effects involved in Palladin expression were investigated further, through observation of protein within shear-induced EMPs released from HAECs cultured on extracellular matrices: fibrinogen, fibronectin or collagen. Figure 5.7 first demonstrates the expression of Palladin in EMPs when cells are seeded on the permissive fibrinogen matrix and subjected to time points of LSS. Palladin expression appears to be halted for the first set of time points, with faint bands only appearing at 24 hours. When observing the protein expression of the whole cells (Figure 3.17) expression of Palladin stays relatively steady until there is a decrease in protein from 24-48 hours, suggesting that the reduction in protein at that time is likely due to it being exported through EMPs. It appears that the fibrinogen matrix has an effect on the cells where it promotes Palladin upregulation, but also retains the protein within the cell, most likely to utilise in cell adhesion and migration as the HAECs adapt to the matrix and subsequent shear stress. Fibrinogen binding to the receptors of endothelial cells appears to activate MAP kinase signalling, which then triggers alterations in protein transport within the cell (Patibandla *et al.*, 2010). It is conceivable that Palladin may be transferred towards the base of the cell, in order to adhere the cells better to the ECM, and help the cells migrate better across this matrix; therefore keeping the protein away from the apical membrane, where it could be lost through microparticle release. When the cells have completely adapted

to chronic shear by 24 hours i.e. stopped migrating, it is only then that they start exporting Palladin through microparticles.

This pattern of retaining Palladin within the cell is observed again when the cells are seeded on a fibronectin matrix – as demonstrated in Figure 5.8. Here, Palladin is once again retained within the cells and is only exported following an extended period of shear stress. Protein expression from whole cells (Figure 3.19) is shown reducing slightly from 3-6 hours - explaining the slight presence of bands in the 6 hour time point of Figure 5.8 - before significantly decreasing at 24-48 hours of shear stress, where the Palladin protein is firmly exported from the cells. The $\alpha5\beta1$ integrin is initially present in focal adhesions formed on a fibronectin substrate, but unless the fibronectin is immobilized it may cause formation of exaggerated $\alpha5\beta1$-containing focal adhesions (Katz *et al.*, 2000). The increase of $\alpha5\beta1$ may result in repression of Palladin. The expression of Palladin within cells was observed in Figure 3.19 to be inhibited on the permissive fibronectin matrix compared against an uncoated matrix; however this did not appear to affect the microparticle release in a significantly different way. Since Palladin expression would be muted in whole cells because of interactions with the ECM, it follows that the protein would be retained within cells for an extended period as the cells needed it to help remodel in response to the subsequent shear stress.

When observing Palladin expression of whole cells seeded onto the nonpermissive collagen matrix (Figure 3.21), the protein expression appeared to be sustained for the first 24 hours, before it started to reduce. As observed in Figure 5.9, Palladin is not exported from the cells via EMPs until the 24 hour time point of LSS. It was already suggested that, while the collagen matrix causes total upregulation of Palladin from just seeding cells onto the matrix, it also blocks the signal for Palladin upregulation following shear stress. Here, Figure 5.9 seems to indicate that growing the cells on the matrix also blocks the release of Palladin from the cells until they have completely adapted to chronic shear. Collagen is seen to increase cell adhesion (Kemeny *et al.*, 2013); this theoretically may cause Palladin to localise from one area of the cell to another (such as from the membrane to the cytoskeleton) to aid cell adhesion, indicating why the protein is not released from the cell. As discussed in Chapter 3, the ECMs can also enhance cell migration, so by 24-48 hours the cells have finished remodelling and do not require Palladin in such quantities. Figures 5.7-5.9 jointly appear to confirm that the protein is retained by the cells up to this time point before it is exported via EMP release. ECMs have also been shown to cause adhesion of microparticles to the basal

matrix, indicating that a small number of particles themselves may have been retained (Keuren *et al.*, 2007).

While these matrices help to better characterise the release of EMPs, they are still only an *in vitro* model. It must be noted that the increasing densitometric values of Palladin within EMPs may be due to the simple accumulation of microparticles in media. In regular conditions in the vasculature, the blood which creates shear stress would inherently move over further distances through the aorta, carrying the released endothelial microparticles with it as it moves through the vessels. An *in vivo* observation of the EMPs was then sought. Microparticles are observed in the blood of healthy individuals but can elevate from shear stress (Vion *et al.*, 2013). In Figure 5.10, the probing for Palladin within EMPs and exosomes extracted from blood is demonstrated. Equal volumes of blood were drawn from a young and healthy patient immediately following active exercise – quantified as reaching 15-20 on the Borg Scale (Borg, 1982). Samples were also taken from the same person at a relaxed state (6-7 on the Borg Scale). Samples were pre-spun; doing so separated the plasma (which contains EMPs) from platelets and blood cells. Plasma was subjected to the extraction methods detailed in Chapter 2.2.2.4, allowing for the separate collection of both microparticles and exosomes, which were probed on a Western Blot. As observed in Figure 5.10, there was a strikingly different pattern of expression than that observed with endothelial cells – namely that out of all the isoforms observed in endothelial cells, only the 90kDa and 122kDa isoforms appeared in microparticles, with the 43kDa isoform appearing in exosomes. This is similar to the release of different isoforms at different time points of shear that was observed in Figure 5.5. Alternative gene splicing has been observed to happen following exercise (Tonevitsky *et al.*, 2009), so it may be that the *PALLD* gene undergoes such splicing into different isoforms under exercise induced stress. These shear-induced microparticles are also reduced in a relaxed state, resulting in there being less Palladin observed. In the resting state, only the 43kDa isoform is seen, indicating that Palladin is upregulated following the increased shear stress that arises from exercise. This helps confirms that Palladin is upregulated following haemodynamic stimulation in an *in vivo* environment, following the characterisation of the response of Palladin to haemodynamic force in *in vitro* models in Chapter 3.

Also of note is that the 43kDa isoform only shows in the smaller exosomes, whereas the 90 and 122kDa isoforms appear in the slightly larger microparticles. This may be an isoform specific response of the cells as they re-structure under shear conditions, with

specific isoforms having individualised functions. The smaller isoform may be differently regulated and only export via exosomes, as opposed to the other isoforms appearing in microparticles. As microparticles play an important role in inflammation (Martínez *et al.*, 2005) and Palladin itself is shown to have many isoform specific functions (Goicoechea *et al.*, 2010), a further research area may be observing the specific functions in endothelial microparticles. Unusually, GAPDH fails to register a result with exosomes. It might simply be that the GAPDH is lost through the filtration process, but it is something which may require future investigation.

The presence of two other actin-binding proteins within shear-induced EMPs is also illustrated in this chapter. LASP-1 and Drebrin are two proteins that appear to show a link to Palladin within HAECs (as discussed in Chapter 4). Here in this chapter, their release in EMPs following time points of LSS is presented. Figure 5.11 first shows the expression of LASP-1 in shear-induced EMPs. LASP-1 is a protein known to bind with Palladin, but here it appears to follow a differential expression pattern, with the volume of microparticles containing LASP-1 generally decreasing under shear. This occurs despite an upregulation of LASP-1 within whole cell lysates following laminar shear (Figure 5.11.1). The patterns of regulation in both EMPs and whole cell lysates appear to follow a similar trend, suggesting that the amount of particles lost post-shear is directly related to the production of protein within the cell.

It already has been demonstrated that Palladin knockdown leads to loss of LASP-1 at actin stress fibres (Rachlin and Otey, 2006). This raises a question as to why LASP-1 decreases in EMPs when a binding partner increases. The reasoning for this occurrence may be that LASP-1 is simply more conserved than Palladin within the cells following shear. The LASP-1 protein is highly conserved (Grunewald and Butt, 2008), and has other functions with regards to the remodelling of endothelial cells under shear stress; therefore the cell may be retaining LASP-1 while exporting Palladin. Having observed that isoform specific cleavage of Palladin can occur when the protein is released in microparticles (Figure 5.10) it is possible that cleavage is also responsible for the separation of the two proteins, allowing for LASP-1 to remain within the cell while Palladin is exported. However further investigation into the interactions of LASP-1 and Palladin in MPs may be required to understand the signalling effect that causes this to happen.

The second actin-binding protein of interest, Drebrin, and its presence within EMPs was illustrated in Figure 5.12. Drebrin appears to be steadily expressed in the microparticles of sheared cells, increasing over the first 6 hours, before declining at 24 hours. This decline at 24 hours may be due to reabsorption of the protein within the cells or else the breakdown of microparticles. This result is noticeably different from the patterns seen in Palladin or LASP-1 expression in similar experiments. In whole cells the Drebrin protein is downregulated in response to shear. The increasing expression within EMPs observed here in Figure 5.12 suggests that the reduction in whole cells could be caused by the protein being exported through microparticles. Figure 5.12.1 highlights the expression of protein in EMPs compared against the protein expression of whole cell lysates (Figure 4.11). A correlation in results is seen; as relative amounts of protein decrease in the whole cell, they increase in the microparticles.

There may be some sort of signalling method occurring that stimulates Drebrin to be exported from the cells immediately in response to LSS. Chapter 4 has already discussed the possibility of Palladin upregulation resulting in the downregulation of Drebrin. Such signalling pathways may also be the reason for the expulsion of the protein through EMPs. In both EMPs and protein, expression drops by 24 hours, signifying that Drebrin may be downregulated entirely within the cells in response to chronic shear stress. Since it is a developmentally regulated protein (Majoul *et al.*, 2007; Ishikawa *et al.*, 1994), and the cells are fully remodelled by this time point, it follows that less protein is produced, hence there is less protein exported via EMPs.

In conclusion, the release of protein – Palladin, LASP-1 and Drebrin - through EMPs has been documented here, explaining why there were declines in protein expression in whole cells subjected to shear stress (Chapter 3). Analysis of *in vivo* samples indicates that isoforms of Palladin can be selectively released in different types of particles, showing that they may have specialised functions. The results also indicate that Palladin localises to different sides of the cell (basal instead of apical) in response to extracellular matrices, which affect the protein function and its release through EMPs. We have documented some of the functions of Palladin in cells, showing that absence of Palladin can have an inhibitory effect on cell migration, but notably that the cell eventually compensates for the loss of protein. This compensation may include the synthesis of the otherwise exported Drebrin protein, which appears to be in competition with the Palladin protein, showing an alternative expression pattern to Palladin.

CONCLUSIONS AND FUTURE WORK

This thesis examined the actin cytoskeletal adaptor protein Palladin and exhibited its presence within the vasculature. Palladin is a known actin-binding protein (Dixon *et al.*, 2008), having been observed in structures containing actin filament bundles (Parast and Otey, 2000). Expression is altered by the haemodynamic forces of the vascular system, which include cyclic strain and laminar shear stress and result in a change within actin dynamics (Kris *et al.*, 2008). We have shown for the first time that these forces cause Palladin to be upregulated immediately in Human Aortic Endothelial Cells, at both the gene transcription and proteomic levels. This apparent inflammatory response occurs as the cells change from a static to a haemodynamically stimulated state. Notably, the protein expression increases rapidly – Palladin protein is upregulated just as quick as the *PALLD* gene. The upregulation of the LASP-1 binding partner protein also follows a similar pattern (Figure 4.6). This immediate increase of protein suggests that there may some mechanism by which the already-existing endogenous RNA present in static cells is immediately stimulated into transcribing protein as soon as the cell is subjected to force.

Several studies have demonstrated that microRNAs (miRNAs) play important roles not only in cardiovascular development, but also in cardiovascular disease, the types of which are characterised by an aberrant cell function (Zhang, 2008). It is possible that the stimulatory signal that causes upregulation of Palladin may be microRNA based, with mechanosensitive microRNA controlling both the transcription and translation of the endogenous protein-coding RNAs. The transcription factors which normally regulate gene and protein expression (by either activating or inhibiting transcription) function primarily within the nucleus, requiring a direct interaction with DNA (Thiel *et al.*, 2004). The miRNAs may act upon the target RNAs within the cytoplasm, affecting their function, and initiating an earlier protein response (Tuccoli *et al.*, 2006). It has been demonstrated that the application of haemodynamic force can regulate the expression of microRNAs in endothelial cells, for example miR-19b and miR-23b – both of which are involved in the flow mediated regulation of endothelial cell growth and function (Qin *et al.,* 2010; Wang *et al.,* 2010). Other microRNAs such as miR-126 and miR-296 have also been indicated in playing a role in the regulation of cell migration (Wu *et al.,* 2009; Würdinger *et al.,* 2008). In particular, the knockdown of miR-126 in *in vivo* models has resulted in the loss of vascular integrity and haemorrhage during embryonic development, similarly to how knockout of Palladin may also cause embryonic lethality. As already stated in Chapter 1, mir-126 has also been observed within apoptotic bodies

(Zernecke *et al.*, 2009) and potentially could be found within microparticles, as is Palladin following shear stress. Of course, it is more speculative than definitive to say that mir-126 and Palladin expression therefore are linked, but it would be a microRNA target that would be worth investigating with future microarray analysis. As a single gene may be regulated by multiple microRNAs, further in depth studies would be required to analyse the precise interactions between the microRNAs and Palladin following mechanical stimulation.

It should also be noted that an increase of microRNA commonly results in actually repressing protein expression (Baek *et al.*, 2008; Selbach *et al.*, 2008), which hints that Palladin could perhaps be increasing in expression at another proteins expense. Drebrin may be such a protein, having been observed within the same networks as Palladin (Table 4.1) and in this thesis, having been found to be downregulated in response to shear stress (Figure 4.11), unlike Palladin or LASP-1 which are upregulated. Drebrin has been previously shown to inhibit the actin-binding activity of α-actinin (Mikati *et al.,* 2013; Ishikawa *et al.,* 1994), and as α-actinin itself associates with Palladin (Rachlin and Otey 2006), they appear to be linked via a potential interaction here. As mentioned, knocking out of Palladin displays an embryonically lethal phenotype, and since Drebrin is developmentally regulated, it hints that their interaction in cells could mainly occur within the early growth phase, such as during cellular remodelling. The expressional changes of these proteins were shown here when the HAECs remodel in response to haemodynamic force; further cementing this argument. If the Drebrin protein is indeed being downregulated, a hypothesis is that Drebrin may in fact be actively repressed by mechanosensitive microRNAs.

Considering that miR-126 may then play a role in Palladin expression, it therefore may in fact be inhibitory of Drebrin. It has been shown that when particles containing this microRNA were transferred into endothelial cells, they resulted in the production of the anti-inflammatory CXCL12 chemokine (Pérez-Martínez *et al.*, 2010). The abundance of miR-126-mediated CXCL12 subsequently enhanced CXCR4-mediated functions, such as recruitment of other cells. This CXCR4 chemokine is notably essential for cell migration and inflammation (Müller, *et al.*, 2001). CXCR4 signalling induces a rapid increase in the affinity and mobility of adhesion molecules, including the integrin LFA-1, which interacts with the shear-responsive ICAM-1 protein (Kinashi, 2005). Of particular note is that Drebrin is seen to co-localise with the CXCR4 receptor. Knockdown of Drebrin in cells has been shown to result in a redistribution of CXCR4

and inhibits actin polymerization in immune synapses (Pérez-Martínez *et al.*, 2010). It may very well be that the microRNA miR-126 mediates the downstream regulation of Drebrin, alterations of which may result in the sudden upregulation of Palladin (and to an extent, LASP-1). Experiments on microRNA analysis of cells with Drebrin or Palladin knockdown and subjected to haemodynamic forces would further characterise this potential link between the proteins. If a microRNA screening of both Drebrin and Palladin was performed, a comparison of the results could be performed to observe any overlapping microRNAs involved in the expression of the proteins. By doing so, it could potentially narrow the list of target miRNAs involved in regulating the proteins.

When the cells are subjected to longer time points of cyclic strain, protein expression appears to decrease, indicative of Palladin being responsible for the initial remodelling of the cell in response to force. However, when cells are subjected to time points of laminar shear stress, we have shown that there is an increase in expression at 6-24 hours where the protein is upregulated a second time. It is proposed that this upregulation of Palladin occurs as the cells further adapt to chronic shear stress. At this time point Palladin is required for further function e.g. binding actin for cellular remodelling. This expression may be more traditional, resulting from the *PALLD* gene synthesis of new protein. It is a curiosity then that there is not a similar 6 hour spike in protein expression as the cells remodel to chronic cyclic strain, especially considering how strain-induced *PALLD* gene expression appears to be on the increase (Figure 3.4.2).

It must be considered though that, under cyclic strain, the cell is required to contract and decrease in size in response to the transmural force periodically stretching and relaxing it. In contrast, under shear stress, elongation and spreading of the cell have been documented to be the responses of this parallel force acting only across its luminal surface. Since cell contraction and cell spreading are differentially mediated (cell contraction is a Rho GTPase mediated response and cell spreading is a Rac GTPase mediated response) the interaction of the cell with extended time points of one bio-mechanical force may simply be stimulating a pathway that Palladin may not be a member of, hence the different expression patterns (Nakamura, 2013; Coleman and Olson, 2002).

Based on the understanding of how pathological strain conditions elicit a higher protein expression than physiological strain, and also how strain and shear differently affect the protein expression, an area of future research may be the characterisation of Palladin

expression under pathological shear conditions and non-uniform laminar shear stress. Non-uniform laminar shear stress occurs *in vivo* at branching bifurcation sites and at other regions of disturbed blood flow in vessels. Experimentally, non-uniform LSS can be achieved by spatially varying flow rates. In more complex experiments, it can be used for studying cells and cellular signalling when the cells are exposed to areas of strongly varying shear stress. The different types of shear stress have different effects on endothelial cells (Kadohama *et al.*, 2007) so it would prove interesting to observe how this affects Palladin expression.

The IBIDI® flow System is a novel perfused flow system for subjecting endothelial cells to higher levels of shear stress through use of specialised Y-shaped Ibidi® μ-slides (Figure 6.1). These slides are designed to mimic the bifurcation of blood vessels. The system itself works by using controlled air pressure to continuously flow media over the cell surface in the smaller area of these μ-slides, allowing for a higher level of shear (20 dynes/cm^2). This pressure can be controlled to subject the cells to low shear also (2 dynes/cm^2). Using this system to observe Palladin, LASP-1 and Drebrin expression levels under the alternate shear levels should prove to show further results.

Under the higher shear stress, we hypothesise that expression of Palladin may be rapidly increased even further. While HAECs in regions of high laminar shear have a quiescent, anti-inflammatory phenotype, they also must align in the direction of flow. This alignment would require the reorganisation of actin as the cell remodelling takes place. Such a reorganisation would necessitate actin-binding proteins such as LASP-1 or Palladin. Endothelial cells in regions of disturbed flow however, have also shown an activated, pro-inflammatory phenotype with poor cell alignment, oxidative stress and expression of inflammatory genes. If Palladin and LASP-1 upregulation is in fact an inflammatory response, then the proteins may be upregulated in this cell phenotype too. Also of interest may be the observation of Drebrin expression following high rates of shear stress. Since the Drebrin protein is significantly downregulated when the cell is subjected to regular LSS (Figure 4.11), it likely could be downregulated with other shear levels also. A future noteworthy area of research would be the investigation of Palladin, LASP-1 and Drebrin expression following these models of altered shear stress.
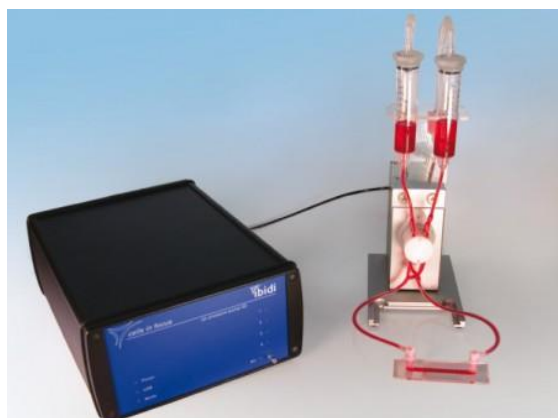
(A)   **(B)**
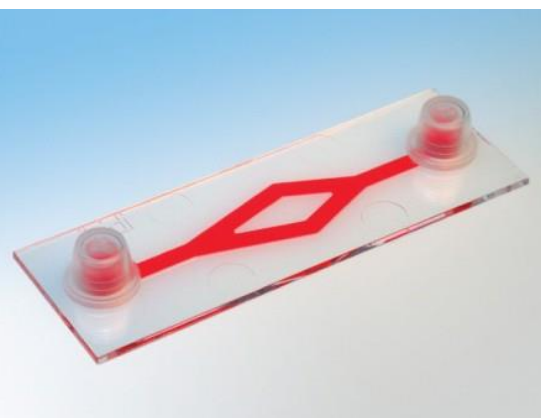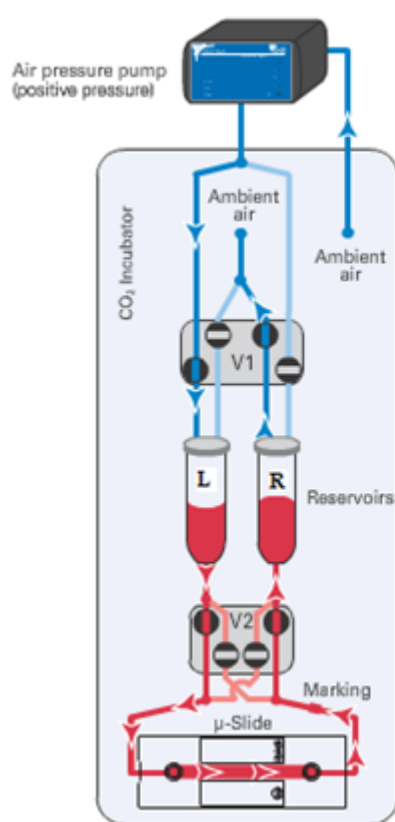
(C)   **(D)**
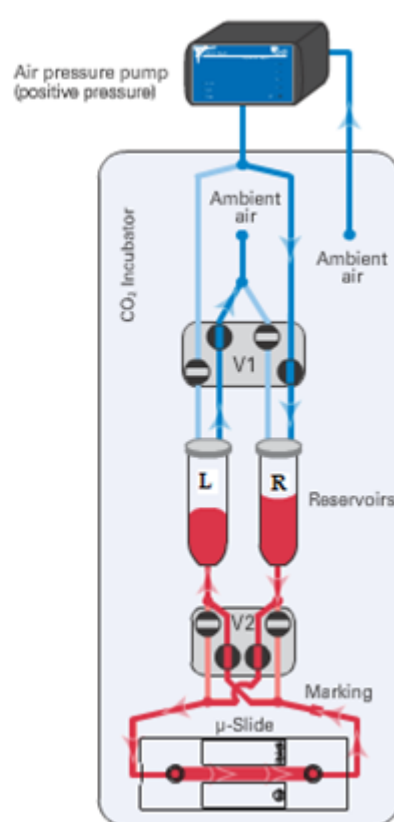
Figure 6.1: The Ibidi® Flow System. Figure 6.1 (A) shows the setup of the Ibidi ® system itself, designed for shear of cells. Figure 6.1 (B) displays the Y-shaped slides used. Media is pumped from one reservoir to the other, flowing over the cells and generating shear stress, and mimicking flow at bifurcations in blood vessels. To avoid wasting media, it gets pumped back and forth between reservoir L and reservoir R through switching of the four-fold valve V1. In Figure 6.1(C), the pressured air is guided to reservoir L, with reservoir R connected to the ambient air pressure. In the second state – Figure 6.1 (D) this is the other way around. The switching between these two states generates a flow of medium between the reservoirs while ensuring they do not run dry. In order to keep the flow unidirectional, a fluidic rectifier pinch valve V2 is placed between the reservoirs and the slide. This valve clamps off two branches of the perfusion set while leaving the other two open. The synchronous manner in which these valves open and close ensure the flow stays in one direction.

Chapter 3 documented the localisation of Palladin to different areas of the cell following the different time points of LSS. Although Palladin was originally described as a cytoplasmic F-actin-binding protein, multiple studies have shown that it can also partially localize to the nucleus in certain cell lines (Goicoechea *et al.*, 2008; Niedenberger *et al.*, 2013), where it can bind transcriptional regulators and influence patterns of gene expression (Jin *et al.*, 2010). It has been illustrated here that Palladin undergoes a major relocation in sheared HAECs as they change morphology (Figure 3.14.1). Protein expression within the cytosol and the nucleus slowly increase following shear – as hypothesised since there is an increase in gene transcription and translation regularly observed. It may also be binding transcriptional regulators and influence patterns of gene expression. The more noticeable change in localisation occurs within the membrane, which massively decreases in Palladin, and the cytoskeleton which increases in protein. The movement of Palladin towards the cytoskeleton is understandable, given that the cell is undergoing structural remodelling at these time points, necessitating the need for actin-binding proteins such as Palladin (or LASP-1) to facilitate organisation.

An examination of the Drebrin and LASP-1 localisation in HAECs following LSS would also prove interesting. LASP-1 is an actin and membrane associated protein and functions as a cytoskeletal scaffold. It and Palladin have been seen to localise in actin rich lamellipodia, highlighting its role in actin cytoskeleton organisation (Chew *et al.*, 2002; Lin *et al*., 2004). LASP-1 has previously been observed to localise to the peripheral edge of non-motile cells. Subsequent exposure to migration-stimulating growth factors causes a rapid localisation to the focal adhesions, followed by a later localisation towards the membrane ruffles. It is expected that its localisation patterns following shear stress may follow that of Palladin. Localisation towards the membrane may account for the increase in LASP-1 within microparticles that is observed at 6 hours post shear (Figure 5.11). Drebrin has already been observed to redistribute to the membrane upon the establishment of cell-cell contacts (Li *et al.*, 2011; Peitsch *et al.*, 1999). Drebrin has also been noted to associate with the actin filaments located at adherens junctions in regular endothelial cells (Rehm *et al.*, 2013; Keon *et al.*, 2000). It is probable that following the subjecting of HAECs to haemodynamic forces, this localisation of Drebrin may change. While Drebrin was characterised before in endothelial cells (Rehm *et al.*, 2013), it had not been shown until now to be responsive to mechanical forces in HAECs.

The patterns of Palladin expression following haemodynamic force, and the alternative localisation in response to LSS, all suggest that there may be some epigenetic regulation of protein expression. Epigenetic pathways have received increasing attention in embryonic development and cellular differentiation. However, it is only in recent times that these pathways have been explored in vascular endothelial cells (Matouk and Marsden, 2008). Epigenetics refers to chromatin-based mechanisms important in the regulation of gene expression, which do not involve changes to the sequence of the DNA (Bird, 2007). These include DNA methylation, histone density and posttranslational modifications, and RNA-based mechanisms. With epigenetic regulation, DNA is observed to be part of a DNA-protein complex. The fundamental repeating unit of this complex, termed chromatin, is the nucleosome comprising a group of core histone proteins which are intertwined with DNA. Each nucleosome comprises 2 molecules of H2A, H2B, H3, and H4 (Matouk and Marsden, 2008). Laminar shear stress elicits both global and gene-specific histone modification changes in cultured endothelial cells (Illi *et al.*, 2003). Having performed immunoprecipitation of Palladin following different shear time points (Table 4.2), many results post-shear stress indicated that histones were involved within the Palladin network. It is quite possible that the histone regulation plays a major function within Palladin expression. Alternatively, Palladin may play a role in the remodelling of chromatin. Using Chromatin Immunoprecipitation (ChIP) combined with further quantitative qRT-PCR, a future area of research is to investigate histone posttranslational modifications and how they may affect the expression of Palladin, and to an extent, LASP-1 and Drebrin.

While a majority of the Palladin protein may be utilised within the cytoskeletal remodelling, it appear that was still a large amount lost from the membrane. Our hypothesis to account for this massive loss in membrane protein was that Palladin was released via Endothelial Microparticles (EMPs). The data for shear-induced microparticle release from HAECs (Figure 5.5) indicated that there was a steady stream of Palladin released via these vesicles. The membrane loses some of its integrity in its remodelling phase, resulting in an increased number of EMPs to be released, which generally leads to an increase in the amount of protein lost. Interestingly, it is suggested that these particles carry other signals such as RNA or microRNA (Diehl *et al.,* 2012; Vion *et al.,* 2013), indicating that they may pass signals to other cells which change protein expression.

The release of microparticles from HAECs was investigated in detail within Chapter 5, in order to further understand how Palladin, LASP-1 and Drebrin function within the whole cell. An interesting result was the disparate expression of LASP-1 and Palladin release from EMPs. As expected, protein was released from both. However, LASP-1 appears to decrease in expression within the EMPs, as opposed to Palladin which generally increases. This is an indication that the two proteins may not be as closely linked as first thought. It should be expected that they differ in some manner regarding their role within the vasculature. This alternative expression in microparticles may shed light on how they differ. LASP-1 is ostensibly retained within the cell following LSS, serving further functions that Palladin does not. The highly conserved LASP-1 protein evidently has other functions with regards to the remodelling of endothelial cells under shear stress (Grunewald and Butt, 2008).

Also of note was the release of Drebrin through microparticles. The protein is observed to be decreased when cells are sheared. But it is also observed that there is a steady increase of protein release through EMPs (Figure 5.12). If Drebrin is in fact inhibitory of Palladin, then it may be that Drebrin is not so much downregulated in response to shear, more that it is released through microparticles. The loss in this protein from the cell may allow the upregulation of Palladin then as a result. Notably this Drebrin microparticle level drops at 24 hours, which suggests that the protein may be reabsorbed into the cell. We see that Drebrin expression within the cell stays level at this time instead of reducing further (Figure 4.11), but the expression of Palladin also starts reducing (Figure 3.10). It may be that Drebrin works here as a sort of inhibitory mechanism if reabsorbed back into the cell. Further investigation into the interactions of Drebrin, LASP-1 and Palladin and their different release mechanisms through EMPs may be required to understand the signalling effect that causes this to happen.

The signalling effects involved in Palladin expression within whole cells was investigated in this thesis, through use of cell-matrix interactions. Interactions with different endothelial matrices via distinct receptors can trigger distinct cellular responses (Geiger and Yamada, 2011). By culturing cells on different matrices, we observed distinct expression levels of protein following LSS. Protein release from the matrix-seeded cells via shear-induced microparticle release was also analysed. In HAECs sheared on regular culture dishes, the Palladin expression levels in whole cells decline after 3 hours (Figure 3.10), typified by an increase in the amount of microparticle-bound Palladin being released from the cells (Figure 5.5.1). This method

of release – derived from shear-induced remodelling and the loss of cellular integrity – appears to change when cells are in contact with ECMs, with Palladin protein retained in the cell until 24 hours post-shear, suggesting that some signalling method occurs that causes Palladin to be utilised within the cell for a newer function.

When first looking at the protein response to the fibrinogen matrix, we observe that interactions with the matrix cause an immediate upregulation in the expression of Palladin. As the static cells are allowed to adhere to a fibrinogen matrix, the expression of Palladin is greatly increased, compared to cells adhering at the same time to a regular culture dish. Increased fibrinogen content in the vasculature leads to increased binding to its endothelial receptors, such as the α5β1 integrin (Plow *et al.*, 2000) – which itself increases in response to LSS (Urbich *et al.*, 2000). Increased fibrinogen also results in the increased formation of filamentous actin (Tyagi *et al.*, 2008). This increase in actin results from the cell spreading across the matrix, stiffening the cells and retracting some actin filaments. Since the cell undergoes such a remodelling, it requires the rapid upregulation of Palladin, which may be brought on through some stimulatory, possibly integrin based signal. Curiously, fibrinogen has been characterised as increasing cellular permeability (Tyagi *et al.*, 2008) which would suggest that there would be an increase of Palladin release from the microparticles, since the cell loses its integrity. However, while microparticle content may increase, the release of Palladin through these particles does not, appearing to be instead retained for further purposes. It has been suggested that fibrinogen binding to its endothelial receptors may activate MAP kinase signalling, triggering alterations in the cellular transport mechanism (Patibandla *et al.*, 2010). This may be a mechanism which Palladin is localised through, preventing its release through the microparticles. We have already seen that Palladin is localised to different areas following LSS (Figure 3.14.1). The expression of Palladin following LSS when the cells are in contact with fibrinogen has a different pattern. Palladin appears downregulated following immediate shear, but still stays more prevalent than expression in an uncoated matrix. The expression only increases past the static baseline levels at 24 hours of LSS (Figure 3.17) but then drops sharply at 48 hours – the point at which protein begins to be exported from the cell (Figure 5.7). This suggests to us that the protein is retained within the cells post-shear. It is likely that the localisation patterns within HAECs are different as a result of cell-matrix contact. Since Palladin does not appear within early time points to be released via EMPs, it may therefore be retained within the membrane, or alternatively increase in localisation towards the cytoskeleton. This localisation of

protein may occur as the protein moves to different areas of the cell itself; relocating from the apical side of the cell towards the basal side instead. Integrins located on the basal side of the membrane can recognise and bind the different components of the basement membrane ECMs. There, they link a chain of actin-binding proteins (Yurchenco *et al.*, 2011) which may include Palladin, illustrating why there is an upregulation of protein, but lack of release through microparticles.

The actin-binding proteins they link may also include LASP-1 or Drebrin. In contact with fibrinogen, the (normally upregulated) protein is observed to decrease following LSS. In comparison, the (normally downregulated) Drebrin appears upregulated when in contact with fibrinogen. This upregulation of Drebrin again could account for the downregulation of the other proteins – it may be that Drebrin is increased because of microRNA signalling and integrin signalling pathways initiated by the fibrinogen matrix. Interestingly though, the protein expression pattern of Drebrin appears close to the regular pattern when cells are initially seeded on fibronectin (although it does increase after 6 hours), indicating that if there is such a specific signal that causes a Drebrin increase, it may be influenced more by the fibrinogen matrix.

A retention of Palladin is seen though when the cells are seeded onto a fibronectin matrix (Figure 3.19). Fibronectin and certain polypeptide regions of this adhesive glycoprotein mediate cell attachment and spreading on various substrates. Here, the post-shear expression is similar to the normal expression observed within cells on an uncoated culture dish. However, this expression appears inhibited to a degree. Comparison with the static uncoated cells showed that fibronectin drastically reduced the levels of Palladin observed within the cells. This suggests that fibronectin may have inhibitory qualities on protein expression. Notably LASP-1 expression is also withheld because of cell-matrix contact (Figure 4.7). As stated in Chapter 3, the $\alpha 5 \beta 1$ integrin is initially present in focal adhesions formed on a fibronectin substrate, along with $\alpha v \beta 3$, but is lost from these adhesions unless the fibronectin is immobilized, in which case it forms exaggerated $\alpha 5 \beta 1$-containing focal adhesions (Katz *et al.*, 2000). It may be that the increase of $\alpha 5 \beta 1$ may affect Palladin and LASP-1 in a repressive manner. The $\alpha 5 \beta 1$ and $\alpha V \beta 3$ integrins binding to fibronectin specifically activate the transcription factor NF-κB (Orr *et al.*, 2005). Flow-induced NF-κB activation is downstream of conformational activation of integrins, resulting in new integrin binding to the subendothelial extracellular matrix and subsequent signalling mechanisms occurring. These signalling mechanisms may be repressing the expression of Palladin and LASP-1

instead. NF-κB triggers inflammatory gene expression in the endothelium in response to the onset of flow or disturbed flow. This lends more weight to the alternative hypothesis that Palladin is in competition with another protein (i.e. Drebrin) which may be upregulated instead by the activation of NF-κB. Importantly, there is little fibronectin or fibrinogen beneath the endothelium in most of the vasculature, but these proteins are found at sites of disturbed flow *in vivo* (Orr *et al.*, 2006). This indicates that it may not be accurate to compare the patterns of expression to the one seen on regular uncoated cells following LSS. Investigating the protein expression following high shear using Ibidi® slides may provide a better comparison with the expression on these matrices.

Collagen also affects the expression of Palladin, but differently – while protein is upregulated compared to growth on an uncoated matrix, it appears to halt shear-induced expression of the protein. Cells on collagen are observed to inhibit the α5β1 and αVβ3 integrins (Orr *et al.*, 2006). The inhibition of these integrins, which as hypothesised may halt the expression of Palladin, could theoretically cancel out Palladin inhibition - leaving protein expression levels to remain level as the time points of shear continue, as observed in Figure 3.21. Downstream flow-induced NF-κB activation, which may also play a role in repression, is prevented from the activation of the integrins. Notably, this appeared to also inhibit the release of Palladin through microparticles in these cells too. The protein appears to be more conserved and halted from being released in this manner. Given that post-shear expression remains stable, this might be expected. It is evident that there is some mechanism which keeps Palladin from leaving the cell when the cell-matrix interactions are occurring.

Collagen increases cell adhesion (Kemeny *et al.*, 2013); which could cause Palladin to localise from one area of the cell to another (such as from the membrane to the cytoskeleton) in order to increase cell adhesion. Such relocation may explain why there initially is no Palladin in the shear-induced microparticles. At 24 hours the protein is finally released through EMPs. At this time point, cells should be fully adhered and fully realigned in response to shear stress, which would mean Palladin is no longer required for adhering of cells, hence the release of some protein through microparticles.

Strangely, the seeding of HAECs onto collagen didn't appear to alter the expression patterns of LASP-1 and Drebrin (Figures 4.8 and 4.14 respectively). If anything, the culturing of the cells on these matrices made protein expression patterns more exaggerated – LASP-1 is upregulated to a higher degree while Drebrin is downregulated

more. If the cells on collagen inhibit the α5β1 and αVβ3 integrins, then perhaps that means that these integrins play a role in increasing Drebrin expression and also repressing LASP-1 expression. It is an aspect of the research which needs definite assays to be performed before a conclusive result can be determined, but it is something which further investigations can build on.

These studies demonstrate that Palladin does play a significant role in cell and ECM interaction, as does LASP-1 and Drebrin. Cellular behaviours related to this cell-matrix interaction, such as cell adhesion and cell migration, can be compromised by the disruption of Palladin. The impaired cell adhesion and spreading may result from a disorganized actin cytoskeleton and decreased expression of specific integrin proteins. Further cell migration and cell adhesion assays will also needed to be performed on Palladin and its related proteins to characterise these interactions further. This study can be performed using cells with Palladin knocked down using gene-specific siRNA. Initial results show that Palladin knockout affects cell migration, slowing it down (Figure 5.1); however this is from an observational assay. Use of the xCELLigence™ system with knockdowns and regular cells illustrated migration events in real-time. Initial experiments have investigated adhesion of the knocked-down cells on ECMs, results of which are attached in the Appendix. The cells with Palladin knockdown can also be utilised in order to study the interactions with LASP-1 and Drebrin, observing these protein functions when Palladin is not present. Determining further how the cells function without Palladin when subjected to haemodynamic forces should provide a further insight into the role of Palladin under mechanical stimulation.

The investigation of Endothelial Microparticles is a relatively new area of research that has started yielding results. In this report, we have demonstrated how Palladin is present in microparticles released from shear stress, but not cyclic strain. Further characterisation of these particles could be performed using FACS analysis, generating a proper characterisation of Palladin in EMPs, in both *in vitro* and *in vivo* models. More research on blood samples, taken from different time points following exercise, differently healthy subjects, or at a resting rate, merit probing for Palladin, with special regards to the apparent isoform specific localisation to smaller exosomes. While we speculate that this alternative localisation of isoforms may depend on different functions of the isoforms in the vasculature, a precise characterisation should prove to yield some interesting results.

Immunoprecipitation data for Palladin has led to research on two other interesting actin-binding proteins: LASP-1 and Drebrin. While some work has been performed already in our laboratory on LASP-1, Drebrin is a newly examined protein. Furthermore there hasn't been much investigation into their presence in microparticles within the *in vivo* blood samples following exercise. Investigation of the response of these proteins following other haemodynamic force (LSS has been performed, but not oscillatory shear or cyclic strain) using Western Blotting, Immunofluorescence, Proteocellular Fractionation and qRT-PCR could provide a new area of research. Furthermore, if determining the response of these proteins to Palladin siRNA knockdown yields some results, it would be interesting to try observe what happens following LASP-1 or Drebrin knockdowns, and to see if the proteins are upregulated or downregulated in response. Considering how Drebrin seems to act in a different way to Palladin and LASP-1 following LSS, we have theorised that there may be some inhibitory effect occurring, with α-actinin potentially having a role in this effect. Knockout models of Drebrin especially could confirm the competition between it and Palladin. Immunoprecipitation results here showed that both Palladin and Drebrin bind to Galectin, so this protein could also be part of the complex. The Co-IP results also suggested that Palladin, LASP-1 and Drebrin all share an interaction with Vimentin and the α-1A chain of Tubulin. Investigation of these proteins through various methods such as immunoprecipitation, immunofluorescence or even Yeast-2-hybrid analysis could help further determine the protein-protein interactions that appear to be occurring.

While we could observe Palladin within *in vivo* models, a final aspect of Palladin expression that may also prove fruitful is the observation of this protein within other *in vitro* cell models. While a brief characterisation of the expression within HaoSMCs under cyclic strain was provided, it may be worth investigating this cell type and others in greater detail. Characterisation of the proteins within embryonic cell types for instance could show different results, especially as Drebrin is a developmentally regulated protein and Palladin plays a major role in embryonic development; their pathways and interactions may be different than in the adult form. Considering that Palladin has this connection with Drebrin – a protein which is largely observed within the brain, research may also branch into the characterisation of these proteins within the microvasculature. LASP-1 is also highly expressed in the central nervous system where it is prominently expressed in the cortex, hippocampus, and cerebellum and is densely concentrated at the postsynaptic membrane of dendritic spines. With regard to the

endothelial cells lining the blood vessels of the brain, interactions between the proteins would be quite interesting to characterise.

Further to this avenue of research involving the brain, one of the major problems with drug delivery mechanisms in the brain is the blood-brain barrier (BBB) preventing the crossing over of other molecules. Investigations of the proteins here showed they were released through microparticles and exosomes, which are capable of travelling through the vessel to other cells. Alvarez-Erviti *et al.,* (2011) demonstrated a novel method of using exosomes in a therapeutic manner. Using encapsulation by exosomes, they were able to transport siRNA across the BBB. The exosome surface protein LAMP2b was used to display a targeting peptide which ensured binding to the nicotinic acetylcholine receptor on neurons and the vascular endothelium of the BBB. The method showed up to 60% knockdown of target RNA and protein, with little or no toxicity, demonstrating the efficiency of using microvesicles in a therapeutic setting. By harnessing the capabilities of these particles, perhaps in the future they might be utilised as a future method of bypassing this selectively restrictive barrier. Having already shown they can carry other signals, they might one day be used in the area of targeted therapeutics and theranostics.

6.1   SUMMARY OF FUTURE AREAS OF RESEARCH

This thesis documented the role of the actin-binding cytoskeletal protein Palladin and its response to haemodynamic forces within the vasculature, as well as investigating potential protein interactions it may have. However, there are still many areas of this research that merit future work. They include:

- Investigation of the microRNA pathways involved within the upregulation of Palladin following haemodynamic force. Focus may be given on mir-126 and its potential links to Palladin.

- Further research on the microRNA pathways involved in the interactions of Palladin with LASP-1 and Drebrin; particularly into how the Drebrin protein is downregulated following haemodynamic forces, possibly through competition between the proteins to bind to actin.

- Use of Drebrin knockdown models to observe effects on Palladin and LASP-1 expression. Similarly, using LASP-1 knockdown models to observe the effects on expression of other proteins.

- Characterisation of the expression of Palladin, LASP-1 and Drebrin when subjected to pathological shear stress rates (>20 dynes/cm^2) through the use of the Ibidi® shear system. Also, the investigation of the protein expression at bifurcations of cells using the Y-shaped Ibidi® μ-slides. Techniques such as Western Blotting, Immunofluorescence, Proteocellular Fractionation or qRT-PCR can be used to characterise this. ELISA methods may also be used to characterise expression.

- Using ChIP assays to investigate histone posttranslational modifications across the *PALLD* gene, as well as the modifications of LASP-1 and Drebrin, coupled with the cellular localisation of these proteins in response to haemodynamic forces.

- Further cell adhesion assays to be performed, through the use of siRNA knockdown cells, and the xCELLigence™ system to monitor migration and adhesion events in real-time. Particular regard will be given to observation on knockdown cells subjected to cyclic strain, shear stress, and knockdown cells cultured on the passive and permissive extracellular matrices.

- Further research into the release of Palladin through microparticles from *in vivo* models. Drebrin and LASP-1 may also be investigated within *in vivo* samples. Transfer of these proteins via microparticles may also be studied.

- Determination of the precise integrin signalling pathways involved within the shear-induced expression of the Palladin, LASP-1 and Drebrin proteins. Coupled with this, the interactions of these proteins within these pathways may be understood further.

- Characterisation of these proteins and their potential interactions within other cell types: HaoSMCs, HBMVECs and embryonic stem cells.

- Potential use of Endothelial Microparticles or Exosomes as delivery vesicles for protein, microRNA signals or as drug delivery mechanisms for therapeutic uses.

BIBLIOGRAPHY

Abedin, M., King, N. (2010). Diverse evolutionary paths to cell adhesion. *Trends Cell Biol.* Dec;20(12):734-42.

Abid-Hussein, M.N., Böing, A.N., Sturk, A., Hau, C.M., Nieuwland, R. (2007). Inhibition of microparticle release triggers endothelial cell apoptosis and detachment. *Thromb Haemost.* 98:1096–110.

Abu Shah, E., Keren, K.. (2013). Mechanical forces and feedbacks in cell motility. *Curr Opin Cell Biol.* Oct;25(5):550-7.

Aird, W.C. (2007). Phenotypic heterogeneity of the endothelium: I. Structure, function, and mechanisms. *Circ Res.* Feb 2;100(2):158-73.

Aird, W.C. (2011). Discovery of the cardiovascular system: from Galen to William Harvey. *J Thromb Haemost.* Jul;9 Suppl 1:118-29.

Alvarez-Erviti, L., Seow, Y., Yin, H., Betts, C., Lakhal, S., Wood, M.J. (2011). Delivery of siRNA to the mouse brain by systemic injection of targeted exosomes. *Nat Biotechnol.* Apr;29(4):341-5.

Anderson, B.R., Bogomolovas, J., Labeit, S., Granzier, H. (2013). Single molecule force spectroscopy on titin implicates immunoglobulin domainstability as a cardiac disease mechanism. *J Biol Chem.* Feb 22;288(8):5303-15.

Ando, J., Yamamoto, K. (2011). Effects of shear stress and stretch on endothelial function. *Antioxid Redox Signal.* Sep 1;15(5):1389-403.

Andriantsitohaina, R., Gaceb, A., Vergori, L., Martínez, M.C. (2012). Microparticles as regulators of cardiovascular inflammation. *Trends Cardiovasc Med.* May;22(4):88-92.

Asano, E., Maeda, M., Hasegawa, H., Ito, S., Hyodo, T., Yuan, H., Takahashi, M., Hamaguchi, M., Senga, T. (2011) Role of Palladin Phosphorylation by Extracellular Signal-Regulated Kinase in Cell Migration. *PLoS ONE* 6(12):e29338.

Avraham R, and Yarden Y. (2012). Regulation of signalling by microRNAs. *Biochem Soc Trans.* Feb;40(1):26-30.

Azevedo, L.C. (2012). Microparticles and Exosomes: Are They Part of Important Pathways in Sepsis Pathophysiology?, Severe Sepsis and Septic Shock - Understanding a Serious Killer, Ricardo Fernandez (Ed.), ISBN: 978-953-307-950-9, InTech,

Bai, S.W., Herrera-Abreu, M.T., Rohn, J.L., Racine, V., Tajadura, V., Suryavanshi, N., Bechtel, S., Wiemann, S., Baum, B., Ridley, A.J. (2011). Identification and characterization of a set of conserved and new regulators of cytoskeletal organization, cell morphology and migration. *BMC Biol.* Aug;11;9:54.

Baek, D., Villén, J., Shin, C., Camargo, F.D., Gygi, S.P., Bartel, D.P. (2008).The impact of microRNAs on protein output. *Nature.* Sep;4;455(7209):64-71.

Balbarini, A., Barsotti, M.C., Di Stefano, R., Leone, A., Santoni, T. (2007). Circulating endothelial progenitor cells characterization, function and relationship with cardiovascular risk factors. *Curr Pharm Des*.;13(16):1699-713.

Bandres, E., Bitarte, N., Arias, F., Agorreta, J., Fortes, P., Agirre, X., Zarate, R., Diaz-Gonzalez, J.A., Ramirez, N., Sola, J.J., Jimenez, P., Rodriguez, J., Garcia-Foncillas, J. (2009). microRNA-451 regulates macrophage migration inhibitory factor production and proliferation of gastrointestinal cancer cells. *Clin Cancer Res.* 2009 Apr;1;15(7):2281-90.

Bang, M.L., Mudry, R.E., McElhinny, A.S., Trombitás, K., Geach, A.J., Yamasaki, R., Sorimachi, H., Granzier, H., Gregorio, C.C., Labeit, S. (2001). Myopalladin, a novel 145-kilodalton sarcomeric protein with multiple roles in Z-disc and I-band protein assemblies. *J Cell Biol.* Apr;16;153(2):413-27.

Barclay, A.N. (2003). Membrane proteins with immunoglobulin-like domains--a master superfamily of interaction molecules. *Semin Immunol.* Aug;15(4):215-23.

Barczyk, M., Carracedo, S. and Gullberg, D. (2010). Integrins. *Cell and Tissue Research,* 339(1), pp.269-280.

Barreiro, O., Yanez-Mo, M., Serrador, J.M., Montoya, M.C., Vicente-Manzanares, M., Tejedor, R., Furthmayr, H., Sanchez-Madrid, F. (2002). Dynamic interaction of VCAM-1 and ICAM-1 with moesin and ezrin in a novel endothelial docking structure for adherent leukocytes. *J Cell Biol.* Jun 24;157(7):1233-45.

Beck, M.R., Otey, C.A., and Campbell, S.L. (2011).Structural characterization of the interactions between palladin and α-actinin. *J Mol Biol.* Oct 28;413(3):712-25.

Beck, M.R., Dixon, R.D., Goicoechea, S.M., Murphy, G.S., Brungardt, J.G., Beam, M.T., Srinath, P., Patel, J., Mohiuddin, J., Otey, C.A., Campbell, S.L. (2013). Structure and function of palladin's actin-binding domain. *J Mol Biol. Sep* 23;425(18):3325-37.

Bernal-Mizrachi, L., Jy, W., Jimenez, J.J., Pastor, J., Mauro, L.M., Horstman, L.L., de Marchena, E., Ahn, Y.S. (2003). High levels of circulating endothelial microparticles in patients with acute coronary syndromes. *Am Heart J.* Jun;145(6):962-70.

Berrier, A.L. and Yamada, K.M. (2007). Cell-matrix adhesion. *J Cell Physiol* 213, 565-73.

Bershadsky, A.D., Ballestrem, C., Carramusa, L., Zilberman, Y., Gilquin, B., Khochbin, S., Alexandrova, A.Y., Verkhovsky, A.B., Shemesh, T., Kozlov, M.M. (2006). Assembly and mechanosensory function of focal adhesions: experiments and models. *Eur J Cell Biol* 85, 165-73.

Bird, A. (2007). Perceptions of epigenetics. *Nature.* 447: 396–398.

Birukov, K.G. (2009). Cyclic stretch, reactive oxygen species, and vascular remodeling. *Antioxid Redox Signal.*Jul;11(7):1651-67.

Borbiev, T., Verin, A.D., Shi, S., Liu, F., Garcia, J.G. (2001). Regulation of endothelial cell barrier function by calcium/calmodulin-dependent protein kinase II. *Am J Physiol Lung Cell Mol Physiol*. May;280(5):L983-90.

Borisy, G.G. and Svitkina, T.M. (2000). Actin machinery: pushing the envelope. *Curr Opin Cell Biol* 12, 104-12.

Borg, G.A. (1982). Psychophysical bases of perceived exertion. *Medicine and Science in Sports and Exercise*. 14:377-381.

Bouaouina, M., Jani, K., Long, J.Y., Czerniecki, S., Morse, E.M., Ellis, S.J., Tanentzapf, G., Schöck, F., Calderwood, D.A. (2012). Zasp regulates integrin activation. (2012). *J Cell Sci.* Dec;1;125(Pt 23):5647-57.

Boukhelifa, M., Parast, M.M., Bear, J.E., Gertler, F.B. and Otey, C.A. (2004). Palladin is a novel binding partner for Ena/VASP family members. *Cell Motil Cytoskeleton* 58,17-29.

Boukhelifa, M., Rachlin, A., Parast, M.M., Moza, M., Johansson, T., Carpen, O., Karlsson, R., Otey, C.A. (2005). The proline-rich protein palladin binds directly to profilin. *FEBS J.* 273:26–33.

Boukhelifa, M., Moza, M., Johansson, T., Rachlin, A., Parast, M., Huttelmaier, S., Roy, P., Jockusch, B.M., Carpen, O., Karlsson, R., Otey, C.A. (2006). The proline-rich protein palladin is a binding partner for profilin. *FEBS J.* Jan;273(1):26-33.

Boulanger, C.M., Amabile, N., Guérin, A.P., Pannier, B., Leroyer, A.S., Mallat, C.N., Tedgui, A., London, G.M. (2007). In vivo shear stress determines circulating levels of endothelial microparticles in end-stage renal disease. *Hypertension.* Apr;49(4):902-8.

Boulanger, C.M., Scoazec, A., Ebrahimian, T., Henry P., Mathieu, E., Tedgui, A., Mallat, Z. (2001). Circulating microparticles from patients with myocardial infarction cause endothelial dysfunction. *Circulation* 104: 2649–2652.

Brentnall, T.A., Lai, L.A., Coleman, J., Bronner, M.P., Pan, S., Chen, R. (2012) Arousal of Cancer-Associated Stroma: Overexpression of Palladin Activates Fibroblasts to Promote Tumor Invasion. *PLoS ONE* 7(1): e30219.

Brodsky, S.V., Zhang, F., Nasjletti, A., Goligorsky, M.S. (2004). Endothelium-derived microparticles impair endothelial function in vitro. *Am J Physiol Heart Circ Physiol.* May;286(5):H1910-5.

Brunton, V.G., MacPherson, I.R. and Frame, M.C. (2004). Cell adhesion receptors, tyrosine kinases and actin modulators: a complex three-way circuitry. *Biochim. Biophys. Acta* 1692, 121-144.

Bucciarelli, P., Martinelli, I., Artoni, A., Passamonti, S.M., Previtali, E., Merati, G., Tripodi, A., Mannucci, P.M. (2012). Circulating microparticles and risk of venous thromboembolism. *Thromb Res*. May;129(5):591-7.

Buccione, R., Orth, J.D. and McNiven, M.A. (2004). Foot and mouth: podosomes, invadopodia and circular dorsal ruffles. *Nat. Rev. Mol. Cell Biol.* 5, 647-657.

Bundey, R.A. (2007). Endothelial cell mechanosensitivity. Focus on "Cyclic Strain and motion control produce opposite oxidative responses in two human endothelial cell types". *Am J Physiol Cell Physiol.* Jul;293(1):C33-4.

Burger, D., Montezano, A.C., Nishigaki, N., He, Y., Carter, A., Touyz, R.M. (2011). Endothelial microparticle formation by angiotensin II is mediated via Ang II receptor type I/NADPH oxidase/ Rho kinase pathways targeted to lipid rafts. *Arterioscler Thromb Vasc Biol.* Aug;31(8):1898-907.

Burnier, L., Fontana, P., Kwak, B.R., Angelillo-Scherrer, A. (2009) Cell-derived microparticles in haemostasis and vascular medicine. *Thromb. Haemost.*; 101: 439–451.

Butkevich, E., Hulsmann, S., Wenzel, D., Shirao, T., Duden, R., Majoul, I. (2004) Drebrin stabilizes connexin-43 and links gap junctions to the sub-membrane cytoskeleton. *Curr Biol* 14:650–658.

Calderwood, D.A., Tai, V., Di Paolo, G., De Camilli, P., Ginsberg, M.H. (2004). Competition for talin results in trans-dominant inhibition of integrin activation. *J Biol Chem.* Jul 9;279(28):28889-95.

Camby, I., Le Mercier, M., Lefranc, F., Kiss, R. (2006). Galectin-1: a small protein with major functions. *Glycobiology.* Nov;16(11):137R-157R.

Camussi, G., Deregibus, M.C., Bruno, S., Cantaluppi, V., Biancone, L. (2010). Exosomes/microvesicles as a mechanism of cell-to-cell communication. *Kidney Int.* Nov;78(9):838-48.

Canel, M., Serrels, A., Frame, M.C., Brunton, V.G. (2013). E-cadherin-integrin crosstalk in cancer invasion and metastasis. *J Cell Sci.* Jan 15;126(Pt 2):393-401.

Cecchi, E., Giglioli, C., Valente, S., Lazzeri, C., Gensini, G.F., Abbate, R., Mannini, L. (2011). Role of hemodynamic shear stress in cardiovascular disease. *Atherosclerosis.* Feb;214(2):249-56.

Celermajer, D.S., Chow, C.K., Marijon, E., Anstey, N.M., Woo, K.S. (2012). Cardiovascular disease in the developing world: prevalences, patterns, and the potential of early disease detection. *J Am Coll Cardiol.* Oct 2;60(14):1207-16.

Chan, M.W., Hinz, B., McCulloch, C.A. (2010). Mechanical induction of gene expression in connective tissue cells. *Methods Cell Biol.* 98:178-205.

Chang, L. and Goldman, R.D. (2004). Intermediate filaments mediate cytoskeletal crosstalk. *Nat Rev Mol Cell Biol.* Aug;5(8):601-13.

Chew, C.S., Parente, J.A Jr, Chen, X., Chaponnier, C., Cameron, R.S. (2000). The LIM and SH3 domain-containing protein, lasp-1, may link the cAMP signaling pathway with dynamicmembrane restructuring activities in ion transporting epithelia. *Cell Sci.* Jun;113 (Pt 11):2035-45.

Chew, C.S., Chen, X., Parente, J.A. Jr., Tarrer, S., Okamoto, C., Qin, H.Y. (2002). Lasp-1 binds to non-muscle F-actin in vitro and is localized within multiple sites of dynamic actin assembly in vivo. *J Cell Sci* 115, 4787-99.

Chew, C.S., Okamoto, C.T., Chen, X., Thomas, R. (2005). Drebrin E2 is differentially expressed and phosphorylated in parietal cells in the gastric mucosa. *Am J Physiol Gastrointest Liver Physiol.* Aug;289(2):G320-31.

Chew, C.S., Chen, X., Bollag, R.J., Isales, C., Ding, K.H., Zhang, H. (2008). Targeted disruption of the Lasp-1 gene is linked to increases in histamine-stimulated gastric HCl secretion. *Am J Physiol Gastrointest Liver Physiol.* Jul;295(1):G37-G44.

Chien, S. (2007). Mechanotransduction and endothelial cell homeostasis: the wisdom of the cell. *Am J Physiol Heart Circ Physiol.* Mar;292(3):H1209-24.

Chien, S., Li, S. and Shyy, Y.J. (1998). Effects of mechanical forces on signal transduction and gene expression in endothelial cells. *Hypertension* 31, 162-9.

Chironi, G.N., Boulanger, C.M., Simon, A., Dignat-George, F., Freyssinet, J.M., Tedgui, A. (2009). Endothelial microparticles in diseases. *Cell Tissue Res.* Jan;335(1):143-51.

Chiu, J.J, and Chien, S. (2011) Effects of Disturbed Flow on Vascular Endothelium: Pathophysiological Basis and Clinical Perspectives. *Physiol Rev* vol.91 no.1 327-387.

Cho, J.A., Lee, Y.S., Kim, S.H., Ko, J.K., Kim, C.W. (2009). MHC independent antitumor immune responses induced by Hsp70-enriched exosomes generate tumor regression in murine models. *Cancer Lett*. 275(2):256–265

Choi, C.K., Helmke, B.P. (2008). Short-Term Shear Stress Induces Rapid Actin Dynamics in Living Endothelial Cells. *Mol Cell Biomech.* Jan 1;5(4):247-258.

Cicha, I., Goppelt-Struebe, M., Yilmaz, A., Daniel, W.G., Garlichs, C.D. (2008). Endothelial dysfunction and monocyte recruitment in cells exposed to non-uniform shear stress. *Clin Hemorheol Microcirc.* 39(1-4):113-9.

Ciobanasu., C., Faivre, B. Le Clainche, C. (2012) Actin dynamics associated with focal adhesions. *Int J Cell Biol.* 2012:941292

Clayton, A., Court, J., Navabi, H., Adams, M., Mason, M.D., Hobot, J.A., Newman, G.R., Jasani, B. (2001). Analysis of antigen presenting cell derived exosomes, based on immuno-magnetic isolation and flow cytometry. *J Immunol Methods.* Jan;1;247(1-2):163-74.

Cohen, A.W., Combs, T.P., Scherer, P.E., Lisanti, M.P. (2003). Role of caveolin and caveolae in insulin signaling and diabetes. *Am J Physiol Endocrinol Metab.* Dec;285(6):E1151-60

Coleman, M.L., Olson, M.F. (2002). Rho GTPase signalling pathways in the morphological changes associated with apoptosis. *Cell Death Differ.* May;9(5):493-504.

Collins, N., Cummins, P., Colgan, O., Ferguson, G., Birney, Y., Murphy, R., Meade, G. and Cahill, P. (2005). Cyclic Strain-mediated regulation of vascular endothelial occludin and ZO-1: Influence on intercellular tight junction assembly and function. *Arteriosclerosis, Thrombosis, and Vascular Biology*, 26pp.62-68.

Costa, M.L., Escaleira, R., Cataldo, A., Oliveira, F., Mermelstein, C.S. (2004). Desmin: molecular interactions and putative functions of the muscle intermediate filament protein. *Braz J Med Biol Res.* Dec;37(12):1819-30.

Cooper, J.A. and Schafer, D.A. (2000). Control of actin assembly and disassembly at filament ends. *Curr Opin Cell Biol* 12, 97-103.

Craddock, T.J., Tuszynski, J.A., Hameroff, S. (2012). Cytoskeletal signaling: is memory encoded in microtubule lattices by CaMKII phosphorylation? *PLoS Comput Biol.*;8(3):e1002421.

Croft, D.R., Coleman, M.L., Li, S., Robertson, D., Sullivan, T., Stewart, C.L., Olson, M.F. (2005). Actin-myosin-based contraction is responsible for apoptotic nuclear disintegration. *J Cell Biol.* Jan;17;168(2):245-55.

Cummins, P.M., von Offenberg Sweeney, N., Killeen, M.T., Birney, Y.A., Redmond, E.M., Cahill, P.A. (2007). Cyclic Strain-mediated matrix metalloproteinase regulation within the vascular endothelium: a force to be reckoned with. *Am J Physiol Heart Circ Physiol.* Jan;292(1):H28-42.

Danen, E.H., Yamada, K.M. (2001). Fibronectin, integrins, and growth control. *J Cell Physiol.* Oct;189(1):1-13.

Davignon, J. and Ganz, P. (2004) Role of endothelial dysfunction in atherosclerosis. *Circulation.* Jun;15;109(23 Suppl 1):III27-32.

Davis, G.E., and Senger, D.R. (2005). Endothelial extracellular matrix: Biosynthesis, remodeling, and functions during vascular morphogenesis and neovessel stabilization. *Circ. Res.* 97, 1093–1107.

Deanfield, J.E., Halcox, J.P., Rabelink, T.J. (2007). Endothelial function and dysfunction: testing and clinical relevance. *Circulation.* Mar 13;115(10):1285-95.

DeCaterina, R., and Libby, P. (2007) *Endothelial Dysfunctions and Vascular Disease.* Blackwell Publishing, Massachusetts.

Decleva, E., Dri, P., Menegazzi, R., Busetto, S., Cramer, R. (2002). Evidence that TNF-induced respiratory burst of adherent PMN is mediated by integrin alpha(L)beta(2). *J Leukoc Biol.*Oct;72(4):718-26.

del Pozo, M.A., Price, L.S., Alderson, N.B., Ren, X.D., Schwartz, M.A. (2000). Adhesion to the extracellular matrix regulates the coupling of the small GTPase Rac to its effector PAK. *EMBO J* 19,2008-14.

Delva, E., Tucker, D.K., Kowalczyk, A.P. (2009). The desmosome. *Cold Spring Harb Perspect Biol.* Aug;1(2):a002543.

Diamant, M., Tushuizen, M.E., Sturk, A., Nieuwland, R. (2004). Cellular microparticles: new players in the field of vascular disease? *Eur J Clin Invest.* Jun;34(6):392-401.

Diehl, P., Fricke, A., Sander, L., Stamm, J., Bassler, N., Htun, N., Ziemann, M., Helbing, T., El-Osta, A., Jowett, J.B., Peter, K. (2012). Microparticles: major transport vehicles for distinct microRNAs in circulation. *Cardiovasc Res.* Mar;15;93(4):633-44.

Dignat-George, F. (2008) Microparticles in vascular diseases. *Thrombosis Research;* 122:55–59.

Dignat-George, F. and Boulanger, C.M. (2011). The many faces of endothelial microparticles. *Arterioscler Thromb Vasc Biol.* Jan;31(1):27-33

Dimmeler, S., and Zeiher, A.M. (1999). Nitric oxide-an endothelial cell survival factor. *Cell Death Differ.* Oct;6(10):964-8.

Dimmeler, S., and Zeiher, A.M. (2000). Reactive oxygen species and vascular cell apoptosis in response to angiotensin II and pro-atherosclerotic factors. *Regul Pept.* Jun 30;90(1-3):19-25.

Distler, J.H., Akhmetshina, A., Dees, C., Jüngel, A., Stürzl, M., Gay, S., Pisetsky, D.S., Schett, G., Distler, O. (2011). Induction of apoptosis in circulating angiogenic cells by microparticles. Arthritis Rheum. Jul;63(7):2067-77.

Dixon, R.D., Arneman, D.K., Rachlin, A.S., Sundaresan, N.R., Costello, M.J., Campbell, S.L., Otey, C.A. (2008) Palladin is an actin cross-linking protein that uses immunoglobulin-like domains to bind filamentous actin. *J Biol Chem.* Mar;7;283(10):6222-31.

Donato, D.M., Ryzhova, L.M., Meenderink, L.M., Kaverina, I., Hanks, S.K. (2010). Dynamics and mechanism of p130Cas localization to focal adhesions. *J Biol Chem.* 2010 Jul 2;285(27):20769-79.

Dominguez, R. (2004). Actin-binding proteins--a unifying hypothesis. *Trends Biochem Sci.* Nov;29(11):572-8.

Elola, M.T., Wolfenstein-Todel, C., Troncoso, M.F., Vasta, G.R., Rabinovich, G.A. (2007). Galectins: matricellular glycan-binding proteins linking cell adhesion, migration, and survival. *Cell Mol Life Sci.* Jul;64(13):1679-700.

Endemann, D.H. and Schiffrin, E.L. (2004). Endothelial Dysfunction. *J Am Soc Nephrol.* Aug;15(8):1983-92.

Esper, R.J., Nordaby, R.A., Vilarino, J.O., Paragano, A., Cacharron, J.L. Machado, R.A. (2006) Endothelial dysfunction: a comprehensive appraisal. *Cardiovasc Diabetol* 5, 4.

Estrada, R., Giridharan, G.A., Nguyen, M.D., Prabhu, S.D., Sethu, P. (2011). Microfluidic endothelial cell culture model to replicate disturbed flow conditions seen in atherosclerosissusceptible regions. *Biomicrofluidics.* Sep;5(3):32006-3200611.

Even-Ram, S., Doyle, A.D., Conti, M.A., Matsumoto, K., Adelstein, R.S., Yamada, K.M. (2007). Myosin IIA regulates cell motility and actomyosin-microtubule crosstalk. *Nat Cell Biol.* Mar;9(3):299-309.

Fox, S.I. (1993). Human physiology 4th edition, Brown Publishers.

Fitzgerald, T.N., Shepherd, B.R., Asada, H., Teso, D., Muto, A., Fancher, T., Pimiento, J.M., Maloney, S.P., Dardik, A.J. (2008). Laminar shear stress stimulates vascular smooth muscle cell apoptosis via the Akt pathway. *Cell Physiol.* Aug;216(2):389-95.

Fleming, I. (2010). Molecular mechanisms underlying the activation of eNOS. *Pflugers Arch.* May;459(6):793-806.

Fleming, I., Fisslthaler, B., Dixit, M., Busse, R. (2005). Role of PECAM-1 in the shear-stress-induced activation of Akt and the endothelial nitric oxide synthase (eNOS) in endothelial cells. *Journal of Cell Science,* 118(18), pp.4103-4111.

Frietsch, J.J., Grunewald, T.G., Jasper, S., Kammerer, U., Herterich, S., Kapp, M., Honig, A., Butt, E. (2010). Nuclear localisation of LASP-1 correlates with poor long-term survival in female breast cancer. *Br J Cancer.* May 25;102(11):1645/-53.

Furman, C., Sieminski, A.L., Kwiatkowski, A.V., Rubinson, D.A., Vasile, E., Bronson, R.T., Fassler, R., Gertler, F.B. (2007). Ena/VASP is required for endothelial barrier function in vivo. *J Cell Biol* 179, 761-75.

Gareus, R., Kotsaki, E., Xanthoulea, S., van der Made, I., Gijbels, M.J., Kardakaris, R., Polykratis, A., Kollias, G., de Winther, M.P., Pasparakis, M. (2008). Endothelial cell-specific NF-kappaB inhibition protects mice from atherosclerosis. *Cell Metab.* Nov;8(5):372-83

Gauthier-Campbell, C., Bredt, D.S., Murphy, T.H, El-Husseini, Ael-D. (2004). Regulation of dendritic branching and filopodia formation in hippocampal neurons by specific acylated protein motifs. *Mol Biol Cell.* May;15(5):2205-17.

Gavard, J., Lambert, M., Grosheva, I., Marthiens, V., Irinopoulou, T., Riou, J. F., Bershadsky, A. and Mege, R. M. (2004). Lamellipodium extension and cadherin adhesion: two cell responses to cadherin activation relying on distinct signalling pathways. *J Cell Sci* 117, 257-70.

Gaziano, T., Reddy, K.S., Paccaud, F., Horton, S., Chaturvedi, V. (2006). Cardiovascular Disease. In: Jamison DT, Breman JG, Measham AR, Alleyne G, Claeson M, Evans DB, Jha P, Mills A, Musgorve P, editors. Disease Control Priorities in Developing Countries. 2nd edition. Washington (DC): World Bank; 2006. Ch33.

Geiger, B. and Yamada, K.M. (2011). Molecular architecture and function of matrix adhesions. *Cold Spring Harb Perspect Biol.* May 1;3(5).

Gelderman, M.P. and Simak, J. (2008). Flow cytometric analysis of cell membrane microparticles. *Methods Mol Biol* 2008; 484: 79–93.

Genové, E., Shen, C., Zhang, S., Semino, C.E. (2005). The effect of functionalized self-assembling peptide scaffolds on human aortic endothelial cell function. *Biomaterials.* Jun;26(16):3341-51.

Gerth, J., Cohen, C.D., Hopfer, U., Lindenmeyer, M.T., Sommer, M., Grone, H.J., Wolf, G. (2007). Collagen type VIII expression in human diabetic nephropathy. *Eur. J. Clin. Invest.* 37:767-773.

Giannotti, G., and Landmesser, U. (2007) Endothelial dysfunction as an early sign of atherosclerosis. *Herz.* Oct;32(7):568-72.

Gimbrone, M.A, García-Cardena, G. (2012).Vascular endothelium, hemodynamics, and the pathobiology of atherosclerosis. *Cardiovasc Pathol.* Jan-Feb;22(1):9-15.

Go, A.S., Mozaffarian, D., Roger, V.L., *et al.,* on behalf of the American Heart Association Statistics Committee and Stroke Statistics Subcommittee. (2013). Heart Disease and Stroke Statistics--2014 Update: A Report From the American Heart Association. *Circulation.* Dec 18.

Godsel, L.M., Hobbs, R.P., Green, K.J. (2008). Intermediate filament assembly: dynamics to disease. *Trends Cell Biol.*Jan;18(1):28-37.

Goicoechea, S.M., Arneman, D., Disanza, A., Garcia-Mata, R., Scita, G., Otey, C.A. (2006). Palladin binds to Eps8 and enhances the formation of dorsal ruffles and podosomes in vascular smooth muscle cells. *J Cell Sci.* Aug;15;119(Pt 16):3316-24.

Goicoechea, S.M., Arneman, D., Otey, C.A. (2008). The role of palladin in actin organization and cell motility. *Eur J Cell Biol.* Sep;87(8-9):517-25.

Goicoechea, S.M., Bednarski, B., García-Mata, R., Prentice-Dunn, H., Kim, H.J., Otey, C.A. (2009). Palladin contributes to invasive motility in human breast cancer cells. *Oncogene.* Jan;29;28(4):587-98.

Goicoechea, S.M., Bednarski, B., Stack, C., Cowan, D.W., Volmar, K., Thorne, L., Cukierman, E., Rustgi, A.K., Brentnall, T., Hwang, R.F., McCulloch, C.A., Yeh, J.J., Bentrem, D.J., Hochwald, S.N, Hingorani, S.R., Kim, H.J., Otey, C.A. (2010). Isoform-specific upregulation of palladin in human and murine pancreas tumors. *PLoS One*. Apr;26;5(4):e10347.

Gonzalez, A.M., Bhattacharya, R., deHart, G.W., Jones, J.C. (2010). Transdominant regulation of integrin function: mechanisms of crosstalk. *Cell Signal.* Apr;22(4):578-83.

Gordón-Alonso, M., Rocha-Perugini, V., Álvarez, S., Ursa, Á., Izquierdo-Useros, N., Martinez-Picado, J., Muñoz-Fernández, M.A., Sánchez-Madrid, F. (2013). Actin-binding protein drebrin regulates HIV-1-triggered actin polymerization and viral infection. *J Biol Chem.* Sep 27;288(39):28382-97.

Gospodarowicz, D., Delgado, D., and Vlodavsky, I. (1980). Permissive effect of the extracellular matrix on cell proliferation in vitro. *Proc Natl Acad Sci USA.* Jul;77(7):4094-8.

Green, D.J., O'Driscoll, G., Joyner, M.J., Cable, N.T. (2008). Exercise and cardiovascular risk reduction: time to update the rationale for exercise? *J Appl Physiol* 105:766-768.

Grinnell, K. and Harrington, E. (2012). Interplay between FAK, PKCδ, and p190RhoGAP in the Regulation of Endothelial Barrier Function. *Microvascular Research,* Jan;83(1):12-21.

Grintsevich, E.E., Galkin, V.E., Orlova, A., Ytterberg, A.J., Mikati, M.M., Kudryashov, D.S., Loo, J.A., Egelman, E.H., Reisler, E. (2010). Mapping of drebrin binding site on F-actin. *J Mol Biol.* May;14;398(4):542-54.

Grooman, B., Fujiwara, I., Otey, C., Upadhyaya, A. (2012) Morphology and Viscoelasticity of Actin Networks Formed with the Mutually Interacting Crosslinkers: Palladin and Alpha-actinin. *PLoS ONE* 7(8): e42773.

Grunewald, T.G. and Butt, E. (2008). The LIM and SH3 domain protein family: structural proteins or signal transducers or both? *Mol Cancer.* Apr;17;7:31.

Grunewald, T.G., Kammerer, U., Schulze, E., Schindler, D., Honig, A., Zimmer, M., Butt, E. (2006). Silencing of LASP-1 influences zyxin localization, inhibits proliferation and reduces migration in breast cancer cells. *Exp Cell Res* 312, 974-82.

Grunewald, T.G., Kammerer, U., Winkler, C., Schindler, D., Sickmann, A., Honig, A., Butt, E. (2007A). Overexpression of LASP-1 mediates migration and proliferation of human ovarian cancer cells and influences zyxin localisation. *Br J Cancer* 96, 296-305.

Grunewald, T.G., Kammerer, U., Kapp, M., Eck, M., Dietl, J., Butt, E., Honig, A. (2007B). Nuclear localization and cytosolic overexpression of LASP-1 correlates with tumor size and nodal-positivity of human breast carcinoma. *BMC Cancer.* Oct;23;7:198.

Grützner, A., Garcia-Manyes, S., Kötter, S., Badilla, C.L., Fernandez, J.M., Linke, W.A. (2009). Modulation of titin-based stiffness by disulfide bonding in the cardiac titin N2-B unique sequence. *Biophys J.* Aug 5;97(3):825-34.

Gunst, S.J., Zhang, W. (2008). Actin cytoskeletal dynamics in smooth muscle: a new paradigm for the regulation of smooth muscle contraction. *Am J Physiol Cell Physiol.* Sep;295(3):C576-87.

Haas, T.L., Lloyd, P.G., Yang, H.T., Terjung, R.L. (2012). Exercise training and peripheral arterial disease. *Compr Physiol.* Oct;2(4):2933-3017.

Hadi, H.A., Carr, C.S. and Al Suwaldi, J. (2005). Endothelial Dysfunction: cardiovascular risk factors, therapy and outcome. *Vascular Health and Risk Management* 1(3) 183–198.

Hahn, C. and Schwartz, M.A. (2008). The role of cellular adaptation to mechanical forces in atherosclerosis. *Arterioscler Thromb Vasc Biol.* Dec;28(12):2101-7.

Hahn, C. and Schwartz, M.A. (2009). Mechanotransduction in vascular physiology and atherogenesis. *Nat Rev Mol Cell Biol* 10,53-62.

Harburger, D. and Calderwood, D. (2009). Integrin signalling at a glance. *Journal of Cell Science,* 122(2),pp.159-193.

Harrison, D. G., Widder, J., Grumbach, I., Chen, W., Weber, M., Searles, C. (2006). Endothelial mechanotransduction, nitric oxide and vascular inflammation. *J Intern Med,* 259,351-63.

Heikkinen, O., Permi, P., Koskela, H., Carpén, O., Ylänne, J., Kilpeläinen, I. (2009). Solution structure of the first immunoglobulin domain of human Myotilin. *J Biomol NMR*. Jun;44(2):107-12.

Hellénius, M.L., de Faire, U., Berglund, B., Hamsten, A., Krakau, I. (1993). Diet and exercise are equally effective in reducing risk for cardiovascular disease. Results of a randomized controlled study in men with slightly to moderately raised cardiovascular risk factors. *Atherosclerosis.*1031:31-91.

Henderson-Jackson, E.B., Helm, J., Strosberg, J., Nasir, N.A., Yeatman, T.J., Kvols, L.K., Coppola, D., Nasir, A. (2011). Palladin is a marker of liver metastasis in primary pancreatic endocrine carcinomas. *Anticancer Res.* Sep;31(9):2957-62.

Hinz, B. (2007). Formation and function of the myofibroblast during tissue repair. *J. Invest. Dermatol.*127:526–537.

Hirata, H., Tatsumi, H. and Sokabe, M. (2008). Mechanical forces facilitate actin polymerization at focal adhesions in a zyxin-dependent manner. *J Cell Sci* 121,2795-804.

Hirase, T., Node, K. (2012). Endothelial dysfunction as a cellular mechanism for vascular failure. *Am J Physiol Heart Circ Physiol.* Feb 1;302(3):H499-505.

Hoffman, L.M., Jensen, C.C., Kloeker, S., Wang, C.L., Yoshigi, M. and Beckerle, M.C. (2006). Genetic ablation of zyxin causes Mena/VASP mislocalization, increased motility, and deficits in actin remodeling. *J Cell Biol* 172, 771-82.

Hohenester, E., Yurchenco, P.D. (2013).Laminins in basement membrane assembly. *Cell Adh Migr*. Jan-Feb;7(1):56-63.

Holtom, E., Usherwood, J.R., Macey, M.G., Lawson, C. (2012). Microparticle formation after co-culture of human whole blood and umbilical artery in a novel in vitro model of flow. *Cytometry A*. May;81(5):390-9.

Horstman, L.L., Jy, W., Jimenez, J.J., Ahn, Y.S. (2004) Endothelial microparticles as markers of endothelial dysfunction. *Front Biosci.* May;1;9:1118-35.

Hossain, M., Qadri, S.M., Liu, L. (2012). Inhibition of nitric oxide synthesis enhances leukocyte rolling and adhesion in human microvasculature. *J Inflamm (Lond).* Jul 19;9(1):28.

Hotulainen, P. and Lappalainen, P. (2006). Stress fibers are generated by two distinct actin assembly mechanisms in motile cells. *J Cell Biol* 173, 383-94.

Hoyer, F.F., Nickenig, G., Werner, N. (2010). Microparticles: messenger of biological information. *J Cell Mol Med.* Sep;14(9):2250-6

Hu, Y.L., Haga, J.H., Miao, H., Wang, Y., Li, Y.S., Chien, S. (2006). Roles of microfilaments and microtubules in paxillin dynamics. *Biochem Biophys Res Commun* 348,1463-71.

Huveneers, S., Truong, H., Fässler, R., Sonnenberg, A., Danen, E.H. (2008). Binding of soluble fibronectin to integrin alpha5 beta1 - link to focal adhesion redistribution and contractile shape. *J Cell Sci*. Aug 1;121(Pt 15):2452-62.

Hynes, R.O. (1999). Cell adhesion: old and new questions. *Trends Cell Biol* 9, M33-7.

Hynes, R.O. (2002). Integrins: bidirectional, allosteric signaling machines. *Cell* 110, 673-87.

Illi, B., Nanni, S., Scopece, A., Farsetti, A., Biglioli, P., Capogrossi, M.C., Gaetano, C. (2003). Shear stress-mediated chromatin remodeling provides molecular basis for flow-dependent regulation of gene expression. *Circ Res* 93: 155–161.

Imberti, B., Morigi, M., Zoja, C., Angioletti, S., Abbate, M., Remuzzi, A., Remuzzi, G. (2000). Shear stress-induced cytoskeleton rearrangement mediates NF-kappaB-dependent endothelial expression of ICAM-1. *Microvascular Research*, 60(2), pp.182-188.

Insall, R. and Machesky, L. (2001). Cytoskeleton. Encyclopedia of Life Sciences. John Wiley & Sons, Ltd: Chichester.

Ishikawa, R., Kohama, K. (2007). Actin-binding proteins in nerve cell growth cones. *J Pharmacol Sci.* 2007 Sep;105(1):6-11.

Ishikawa, R., Hayashi, K., Shirao, T., Xue, Y., Takagi, T., Sasaki, Y., Kohama, K. (1994). Drebrin, a development-associated brain protein from rat embryo, causes the dissociation of tropomyosin from actin filaments. *J Biol Chem.* Nov;25;269(47):29928-33.

Ishikawa, R., Katoh, K., Takahashi, A., Xie, C., Oseki, K., Watanabe, M., Igarashi, M., Nakamura, A., Kohama, K. (2007). Drebrin attenuates the interaction between actin and myosin-V. *Biochem Biophys Res Commun.* Jul 27;359(2):398-401.

Jalali, S., del Pozo, M.A., Chen, K., Miao, H., Li, Y., Schwartz, M.A., Shyy, J.Y., Chien, S. (2001). Integrin-mediated mechanotransduction requires its dynamic interaction with specific extracellular matrix (ECM) ligands. *Proc. Natl. Acad. Sci. USA*.98:1042–1046.

Jin, M., Tanaka, S., Sekino, Y., Ren, Y., Yamazaki, H., Kawai-Hirai, R., Kojima, N., Shirao, T. (2002). A novel, brain-speciWc mouse drebrin: cDNA cloning, chromosomal mapping, genomic structure, expression, and functional characterization. *Genomics* 79:686–692.

Jin, L., Kern, M.J., Otey, C.A., Wamhoff, B.R., Somlyo, A.V. (2007). Angiotensin II, focal adhesion kinase, and PRX1 enhance smooth muscle expression of lipoma preferred partner and its newly identified binding partner palladin to promote cell migration. *Circ. Res.*100:817–825.

Jin, L., Hastings, N.E., Blackman, B.R., Somlyo, A.V. (2009). Mechanical properties of the extracellular matrix alter expression of smooth muscle protein LPP and its partner Palladin; relationship to early atherosclerosis and vascular injury. *J Muscle Res Cell Motil* 30,41-55.

Jin, L., Gan, Q., Zieba, B.J., Goicoechea, S.M., Owens, G.K., Otey, C.A., Somlyo, A.V. (2010). The actin associated protein palladin is important for the early smooth muscle cell differentiation. *PLoS One*. Sep 22;5(9):e12823.

Jin, L. (2011). The actin associated protein palladin in smooth muscle and in the development of diseases of the cardiovasculature and in cancer. *J Muscle Res Cell Motil.* Aug;32(1):7-17.

Johnson, B.D., Mather, K.J., Wallace, J.P. (2011). Mechanotransduction of shear in the endothelium: basic studies and clinical implications. *Vasc Med.* Oct;16(5):365-77.

Joshi, R., Jan, S., Wu, Y., MacMahon, S. (2008). Global Inequalities in Access to Cardiovascular Health Care: Our Greatest Challenge. *J.Am.Coll.Cardiol.,*52,23,1817-1825.

Kadohama, T., Nishimura, K., Hoshino, Y., Sasajima, T., Sumpio, B.E. (2007). Effects of different types of fluid shear stress on endothelial cell proliferation and survival. *J Cell Physiol.* Jul;212(1):244-51.

Kalluri, R. (2003). Basement membranes: structure, assembly and role in tumor angiogenesis. *Nat Rev Cancer.* 3:422–433.

Katritsis, D., Kaiktsis, L., Chaniotis, A., Pantos, J., Efstathopoulos, P., Marmarelis, V. (2007). Wall shear stress: theoretical considerations and methods of measurement. *Prog Cardiovasc Dis.* Mar-Apr;49(5):307-29.

Katsumi, A., Orr, A.W., Tzima, E., Schwartz, M.A. (2004). Integrins in mechanotransduction. *J Biol Chem.* Mar 26;279(13):12001-4.

Katz, B.Z., Zamir, E., Bershadsky, A., Kam, Z., Yamada, K.M., Geiger, B. (2000). Physical state of the extracellular matrix regulates the structure and molecular composition of cell-matrix adhesions. *Mol Biol Cell* 11:1047–1060.

Ke, N., Wang, X., Xu, X., Abassi, Y.A. (2011). The xCELLigence system for real-time and label-free monitoring of cell viability. *Methods Mol Biol.* 740:33-43.

Keicher, C., Gambaryan, S., Schulze, E., Marcus, K., Meyer, H.E., Butt, E. (2004). Phosphorylation of mouse LASP-1 on threonine 156 by cAMP- and cGMP-dependent protein kinase. *Biochem Biophys Res Commun.* Nov 5;324(1):308-16.

Keller, S., Sanderson, M.P., Stoeck, A., Altevogt, P. (2006) Exosomes:From biogenesis and secretion to biological function. *Immunol Lett.* Nov;15;107(2):102-8.

Kelly, B.B. (2010). Promoting Cardiovascular Health in the Developing World: A Critical Challenge to Achieve Global Health. Washington, D.C: National Academies Press. ISBN 0-309-14774-3

Kemeny, S.F., Figueroa, D.S., Andrews, A.M., Barbee, K.A., Clyne, A.M. (2011). Glycated collagen alters endothelial cell actin alignment and nitric oxide release in response to fluid shear stress. *J Biomech.* Jul;7;44(10):1927-35.

Kemeny, S.F., Cicalese, S., Figueroa, D.S., Clyne, A.M. (2013). Glycated collagen and altered glucose increase endothelial cell adhesion strength. *J Cell Physiol.* Aug;228(8):1727-36.

Kempe, S., Kestler, H., Lasar, A., Wirth, T. (2005). NF-kappaB controls the global pro-inflammatory response in endothelial cells: evidence for the regulation of a pro-atherogenic program. *Nucleic Acids Res.* Sep;21;33(16):5308-19.

Keon, B.H., Jedrzejewski, P.T., Paul, D.L., Goodenough, D.A. (2000). Isoform specific expression of the neuronal F-actin-binding protein, drebrin, in specialized cells of stomach and kidney epithelia. *J Cell Sci.* Jan;113 Pt 2:325-36.

Kesner, B.A., Ding, F., Temple, B.R., Dokholyan, N.V. (2010). N-terminal strands of filamin Ig domains act as a conformational switch under biological forces. *Proteins.* Jan;78(1):12-24.

Keuren, J.F., Magdeleyns, E.J., Govers-Riemslag, J.W., Lindhout, T., Curvers, J. (2006). Effects of storage-induced platelet microparticles on the initiation and propagation phase of blood coagulation. *Br J Haematol.* Aug;134(3):307-13.

Keuren, J.F, Magdeleyns, E.J., Bennaghmouch, A., Bevers, E.M., Curvers, J., Lindhout, T. (2007). Microparticles adhere to collagen type I, fibrinogen, von Willebrand factor and surface immobilised platelets at physiological shear rates. *Br J Haematol.* Aug;138(4):527-33.

Kim, J.A., Cho, K., Shin, M.S., Lee, W.G., Jung, N., Chung, C., Chang, J.K. (2008). A novel electroporation method using a capillary and wire-type electrode. *Biosens Bioelectron.* Apr;15;23(9):1353-60.

Kinashi, T. (2005). Intracellular signalling controlling integrin activation in lymphocytes. *Nat. Rev. Immunol.* 5, 546-559.

Klaavuniemi, T., Kelloniemi, A., Ylänne, J. (2004). The ZASP-like motif in actinin-associated LIM protein is required for interaction with the alpha-actinin rod and for targeting to the muscle Z-line. *J Biol Chem.* Jun 18;279(25):26402-10.

Koenig, A., Mueller, C., Hasel, C., Adler, G., Menke, A. (2006). Collagen type I induces disruption of E-cadherin-mediated cell-cell contacts and promotes proliferation of pancreatic carcinoma cells. *Cancer Res* 66, 4662-71.

Kolli, S., Zito, C.I., Mossink, M.H., Wiemer, E.A., Bennett, A.M. (2004). The major vault protein is a novel substrate for the tyrosine phosphatase SHP-2 and scaffold protein in epidermal growth factor signaling. *J Biol Chem.* Jul;9;279(28):29374-85.

Krause, M., Dent, E.W., Bear, J.E., Loureiro, J.J., Gertler, F.B. (2003). Ena/VASP proteins: regulators of the actin cytoskeleton and cell migration. *Annu Rev Cell Dev Biol* 19, 541-64.

Kreplak, L. and Fudge, D. (2007). Biomechanical properties of intermediate filaments: from tissues to single filaments and back. *Bioessays* Jan;29(1):26-35.

Kumar, V., Abbas, A.K., Fausto, N., Aster, J. (2009). Robbins & Cotran Pathologic Basis of Disease, Professional Edition, 8th ed. pg 46-47.

Lai, C.F., Bai, S., Uthgenannt, B.A., Halstead, L.R., McLoughlin, P., Schafer, B.W., Chu, P.H., Chen, J., Otey, C.A., Cao, X., Cheng, S.L. (2006). Four and half lim protein 2 (FHL2) stimulates osteoblast differentiation. *J. Bone Miner*. Res. 21, 17-28.

Laplace, E. (1899). A new forceps for intestinal anastomosis. *Annals of Surgery*, 29(3), pp.297-305.

Laughlin, M.H., Bowles, D.K., Duncker, D.J. (2012). The coronary circulation in exercise training. *Am J Physiol Heart Circ Physiol.* Jan 1;302(1):H10-23.

Lehoux, S., Castier, Y. and Tedgui, A. (2006). Molecular mechanisms of the vascular responses to haemodynamic forces. *J Intern Med* 259, 381-92.

Lewis, B.P., Shih, I., Jones-Rhoades, M.W., Bartel, D.P., Burge, C.B. (2003). Prediction of mammalian microRNA targets. *Cell,* 115, pp. 787–798.

Li, B., Zhuang, L. and Trueb, B. (2004). Zyxin interacts with the SH3 domains of the cytoskeletal proteins LIM-nebulette and Lasp-1. *J Biol Chem* 279, 20401-10.

Li, M.W., Xiao, X., Mruk, D.D., Lam, Y.L., Lee, W.M., Lui, W.Y., Bonanomi, M., Silvestrini, B., Cheng, C.Y. (2011). Actin-binding protein drebrin E is involved in junction dynamics during spermatogenesis. *Spermatogenesis.* Apr;1(2):123-136.

Li, X., Pan, J.H., Song, B., Xiong, E.Q., Chen, Z.W., Zhou, Z.S., Su, Y.P. (2012).Suppression of CX43 expression by miR-20a in the progression of human prostate cancer. *Cancer Biol Ther.* Aug;13(10):890-8.

Li, A., Ponten, F., dos Remedios, C.G. (2012b). The interactome of LIM domain proteins: the contributions of LIM domain proteins to heart failure and heart development. *Proteomics.* Jan;12(2):203-25.

Li, Y., Haga, J.H. and Chien, S. (2005). Molecular basis of the effects of shear stress on vascular endothelial cells. *Journal of Biomechanics*, 38(10), pp.1949-1971.

Liliensiek, S.J., Nealey, P. and Murphy, C.J. (2009). Characterization of endothelial basement membrane nanotopography in rhesus macaque as a guide for vessel tissue engineering. *Tissue Eng Part A*. Sep;15(9):2643-51.

Lin, Y.H., Park, Z.Y., Lin, D., Brahmbhatt, A.A., Rio, M.C., Yates, J.R., 3rd, Klemke, R.L. (2004). Regulation of cell migration and survival by focal adhesion targeting of Lasp-1. *J Cell Biol* 165, 421-32.

Linder, S. (2007). The matrix corroded: podosomes and invadopodia in extracellular matrix degradation. *Trends Cell Biol.* Mar;17(3):107-17.

Linder, S. and Aepfelbacher, M. (2003) Podosomes: adhesion hot-spots of invasive cells. *Trends Cell Biol.* Jul;13(7):376-85

Ling, Z.L., Combes, V., Grau, G.E., King, N.J. (2011). Microparticles as immune regulators in infectious disease - an opinion. *Front Immunol.* 2:67.

Liu, X.S., Luo, H.J., Yang, H., Wang, L., Kong, H., Jin, Y.E., Wang, F., Gu, M.M., Chen, Z., Lu, Z.Y., Wang, Z.G. (2007). Palladin regulates cell and extracellular matrix interaction through maintaining normal actin cytoskeleton architecture and stabilizing beta1-integrin. *J Cell Biochem.* Apr;1;100(5):1288-300.

Liu, F., Bardhan, K., Yang, D., Thangaraju, M., Ganapathy, V., Waller, J.L., Liles, G.B., Lee, J.R., Liu, K. (2012). NF-κB directly regulates Fas transcription to modulate Fas-mediated apoptosis and tumor suppression. *J Biol Chem.* Jul;20;287(30):25530-40.

Liu, H.B., Zhang, J., Xin, S.Y., Liu, C., Wang, C.Y., Zhao, D., Zhang, Z.R. (2013). Mechanosensitive properties in the endothelium and their roles in the regulation of endothelial function. *J Cardiovasc Pharmacol.* Jun;61(6):461-70.

Lodish, H., Berk, A., Zipursky, S.L. (2000). Molecular Cell Biology. 4th edition. New York: W. H. Freeman. Section 22.3, Collagen: The Fibrous Proteins of the Matrix.

Lord, M. (2011). Cytoskeletal regulation: sorting out stress fibers with tropomyosin. *Curr Biol.* Apr;12;21(7):R255-7.

Luo, H., Liu, X., Wang, F., Huang, Q., Shen, S., Wang, L., Xu, G., Sun, X., Kong, H., Gu, M., Chen, S., Chen, Z., Wang, Z. (2005). Disruption of palladin results in neural tube closure defects in mice. *Mol Cell Neurosci.* Aug;29(4):507-15.

Lu, P., Takai, K., Weaver, V.M., Werb, Z. (2011). Extracellular matrix degradation and remodeling in development and disease. *Cold Spring Harb Perspect Biol.* Dec 1;3(12).

Lusis, A.J. (2000). Atherosclerosis. *Nature* 407, 233-41.

Lyle, K.S., Corleto, J.A., Wittmann, T. (2012). Microtubule dynamics regulation contributes to endothelial morphogenesis. *Bioarchitecture.* Nov;1;2(6).

Maeda, M., Asano, E., Ito, D., Ito, S., Hasegawa, Y., Hamaguchi, M., Senga, T. (2009). Characterization of interaction between CLP36 and palladin. *FEBS J.*May;276(10):2775-85.

Majoul, I., Shirao, T., Sekino, Y., Duden, R. (2007). Many faces of drebrin: from building dendritic spines and stabilizing gap junctions to shaping neurite-like cell processes. *Histochem Cell Biol*. Apr;127(4):355-61.

Marin, T., Gongol, B., Chen, Z., Woo, B., Subramaniam, S., Chien, S., Shyy, J.Y. (2013). Mechanosensitive microRNAs-role in endothelial responses to shear stress and redox state. *Free Radic Biol Med*. May;30.

Martin, S., Tesse, A., Hugel, B., Martínez, M.C., Morel, O., Freyssinet, J.M., Andriantsitohaina, R. (2004). Shed membrane particles from T lymphocytes impair endothelial function and regulate endothelial protein expression. *Circulation.* 2004 Apr;6;109(13):1653-9.

Martínez, M.C., Tesse, A., Zobairi, F., Andriantsitohaina, R. (2005). Shed membrane microparticles from circulating and vascular cells in regulating vascular function. *Am J Physiol Heart Circ Physiol*. Mar;288(3):H1004-9.

Martínez, M.C. and Andriantsitohaina, R. (2011). Microparticles in angiogenesis: therapeutic potential. *Circ Res.* Jun;24;109(1):110-9.

Mallat, Z., Benamer, H., Hugel, B., Benessiano, J., Steg, P.G., Freyssinet, J.M., Tedgui, A. (2000). Elevated levels of shed membrane microparticles with procoagulant potential in the peripheral circulating blood of patients with acute coronary syndromes. *Circulation.* Feb;29;101(8):841-3.

Mammoto, A., Sasaki, T., Asakura, T., Hotta, I, Imamura, H., Takahashi, K., Matsuura, Y., Shirao, T., Takai, Y. (1998). Interactions of drebrin and gephyrin with profilin. *Biochem Biophys Res Commun.* Feb;4;243(1):86-9.

Matouk, C.C. and Marsden, P.A. (2008). Epigenetic regulation of vascular endothelial gene expression. *Circ Res.*Apr;25;102(8):873-87.

Mause, S.F. and Weber, C. (2010). Microparticles: protagonists of a novel communication network for intercellular information exchange. *Circ Res.* Oct9;107(9):1047-57.

Mause, S.F., Ritzel, E., Liehn, E.A., Hristov, M., Bidzhekov, K., Müller-Newen, G., Soehnlein, O., Weber, C. (2010). Platelet microparticles enhance the vasoregenerative potential of angiogenic early outgrowth cells after vascular injury. *Circulation* 122:495–506.

Mayr, M., Grainger, D., Mayr, U., Leroyer, A.S., Leseche, G., Sidibe, A., Herbin, O., Yin, X., Gomes, A., Madhu, B., Griffiths, J.R., Xu, Q., Tedgui, A., Boulanger, C.M. (2009). Proteomics, metabolomics, and immunomics on microparticles derived from human atherosclerotic plaques. *Circ Cardiovasc Genet.* Aug;2(4):379-88.

Mazzag, B.M., Tamaresis, J.S., Barakat, A.I. (2003) A Model for Shear Stress Sensing and Transmission in Vascular Endothelial Cells. *Biophys J.* June; 84(6): 4087–4101.

Mehta, D. and Malik, A.B. (2006). Signaling mechanisms regulating endothelial permeability. *Physiol Rev* 86, 279-367.

Mezentsev, A., Merks, R.M., O'Riordan, E., Chen, J., Mendelev, N., Goligorsky, M.S., Brodsky, S.V. (2005). Endothelial microparticles affect angiogenesis in vitro: role of oxidative stress. *Am J Physiol Heart Circ Physiol.* Sep;289(3):H1106-14.

Mikati, M.A., Grintsevich, E.E., Reisler, E. (2013). Drebrin-induced stabilization of actin filaments. *J Biol Chem.*Jul 5;288(27):19926-38.

Mikirova, N., Casciari, J., Hunninghake, R., Riordan, N. (2011). Increased Level of Circulating Endothelial Microparticles and Cardiovascular Risk Factors. *J Clinic Experiment Cardiol* 2:131.

Minshall, R.D., Sessa, W.C., Stan, R.V., Anderson, R.G., Malik, A.B. (2003). Caveolin regulation of endothelial function. *Am J Physiol Lung Cell Mol Physiol.*Dec;285(6):L1179-83.

Mokkapati, S., Fleger-Weckmann, A., Bechtel, M., Koch, M., Breitkreutz, D., Mayer, U., Smyth, N., Nischt, R. (2011). Basement membrane deposition of nidogen 1 but not nidogen 2 requires the nidogen binding module of the laminin gamma1 chain. *J Biol Chem.* 2011 Jan 21;286(3):1911-8.

Mosesson, M.W. (2005). Fibrinogen and fibrin structure and functions. *J Thromb Haemost.* Aug;3(8):1894-904.

Mostefai, H.A., Agouni, A., Carusio, N., Mastronardi, M.L., Heymes, C., Henrion, D., Andriantsitohaina, R., Martinez, M.C. (2008). Phosphatidylinositol 3-kinase and xanthine oxidase regulate nitric oxide and reactive oxygen species productions by apoptotic lymphocyte microparticles in endothelial cells. *J Immunol.* Apr;1;180(7):5028-35.

Müller, A., Homey, B., Soto, H., Ge, N., Catron, D., Buchanan, M.E., McClanahan, T., Murphy, E., Yuan, W., Wagner, S.N., Barrera, J.L., Mohar, A., Verástegui, E., Zlotnik, A. (2001). Involvement of chemokine receptors in breast cancer metastasis. *Nature.*Mar;1;410(6824):50-6.

Münzel, T., Sinning, C., Post, F., Warnholtz, A., Schulz, E. (2008). Pathophysiology, diagnosis and prognostic implications of endothelial dysfunction. *Ann Med.* ;40(3):180-96.

Muralidharan-Chari, V., Clancy, J.W., Sedgwick, A., D'Souza-Schorey, C. (2010). Microvesicles: mediators of extracellular communication during cancer progression. *J Cell Sci.* May;15;123(Pt 10):1603-11.

Muramatsu, F., Kidoya, H., Naito, H., Sakimoto, S., Takakura, N. (2013). microRNA-125b inhibits tube formation of blood vessels through translational suppression of VE-cadherin. *Oncogene.* Jan 24;32(4):414-21.

Mykkänen, O.M., Gronholm, M., Rönty, M., Lalowski, M., Salmikangas, P., Suila, H., Carpen, O. (2001). Characterization of human palladin, a microfilament-associated protein. *Mol Biol Cell* 12, 3060-73.

Nakagawa, H., Terasaki, A.G., Suzuki, H., Ohashi, K., Miyamoto, S. (2006). Short-term retention of actin filament binding proteins on lamellipodial actin bundles. *FEBS Lett* 580, 3223-8.

Nakamura, F. (2013). FilGAP and its close relatives: a mediator of Rho-Rac antagonism that regulates cell morphology and migration. *Biochem J.* Jul 1;453(1):17-25.

Nakamura, Y., Sagara, T., Seki, K., Hirano, S., Nishida, T. (2003). Permissive effect of fibronectin on collagen gel contraction mediated by bovine trabecular meshwork cells. *Invest Ophthalmol Vis Sci.* Oct;44(10):4331-6.

Neisch, A.L., Fehon, R.G. (2011). Ezrin, Radixin and Moesin: key regulators of membrane-cortex interactions and signaling. *Curr Opin Cell Biol.* Aug;23(4):377-82.

Nichols, M., Townsend, N., Scarborough, P., Rayner, M. (2013). European Cardiovascular Disease Statistics 4th edition 2012: EuroHeart II. Eur Heart J. Oct;34(39):3007.

Niedenberger, B.A., Chappell, V.K., Kaye, E.P., Renegar, R.H., Geyer, C.B. (2013). Nuclear localization of the actin regulatory protein Palladin in sertoli cells. *Mol Reprod Dev.*May;80(5):403-13.

Nguyen, M., Arkell, J. and Jackson, C.J. (1998). Active and tissue inhibitor of matrix metalloproteinase-free gelatinase B accumulates within human microvascular endothelial vesicles. *J Biol Chem* 273:5400–5404.

Nohata, N., Hanazawa, T., Kikkawa, N., Mutallip, M., Fujimura, L., Yoshino, H., Kawakami, K., Chiyomaru, T., Enokida, H., Nakagawa, M., Okamoto, Y., Seki, N. (2011). Caveolin-1 mediates tumor cell migration and invasion and its regulation by miR-133a in head and neck squamous cell carcinoma. *Int J Oncol.*Jan;38(1):209-17.

Nolte'Hoen, E., van der Vlist, E.J., Aalberts, M., Mertens, H.C., Bosch, B.J., Bartelink, W., Mastrobattista, E., van Gaal, E.V., Stoorvogel, W., Arkesteijn, G.J., Wauben, M.H. (2011). Quantitative and qualitative flow cytometric analysis of nanosized cell-derived membrane vesicles. *Nanomedicine.* Jul;8(5):712-20.

Nomura, S., Ozaki, Y. and Ikeda, Y. (2008). Function and role of microparticles in various clinical settings. *Thromb Res.*123(1):8-23.

Noria, S., Xu, F., McCue, S., Jones, M., Gotlieb, A.I., Langille, B.L. (2004). Assembly and reorientation of stress fibers drives morphological changes to endothelial cells exposed to shear stress. *Am J Pathol* 164,1211-23.

Oberleithner, H., Riethmüller, C., Schillers, H., MacGregor, G., De Wardener, H., Hausberg, M. (2007). Plasma sodium stiffens vascular endothelium and reduces nitric oxide release. *Proceedings of the National Academy of Sciences U.S.A.*104(41), pp.16281-16286.

Obi, S., Yamamoto, K., Shimizu, N., Kumagaya, S., Masumura, T., Sokabe, T., Asahara, T., Ando, J. (2009). Fluid shear stress induces arterial differentiation of endothelial progenitor cells. *J Appl Physiol.* Jan;106(1):203-11.

Orr, A.W., Sanders, J.M., Bevard, M., Coleman, E., Sarembock, I.J.,Schwartz, M.A. (2005). The subendothelial extracellular matrix modulates NFκB activation by flow: a potential role in atherosclerosis. *J Cell Biol,*169,191-202.

Orr, A.W., Ginsberg, M.H., Shattil, S.J., Deckmyn, H., Schwartz, M.A. (2006). Matrix-specific suppression of integrin activation in shear stress signaling. *Mol Biol Cell.* Nov;17(11):4686-97.

Orr, A.W., Helmke, B.P., Blackman, B.R., Schwartz, M.A. (2006b). Mechanisms of mechanotransduction. *Dev Cell.* Jan;10(1):11-20.

Orr, A.W., Stockton, R., Simmers, M.B., Sanders, J.M., Sarembock, I.J., Blackman, B.R., Schwartz, M.A. (2007). Matrix-specific p21-activated kinase activation regulates vascular permeability in atherogenesis. *J Cell Biol.* Feb;26;176(5):719-27.

Osborn, E.A., Rabodzey, A., Dewey, Jr. C.F., Hartwig, J.H. (2006). Endothelial actin cytoskeleton remodeling during mechanostimulation with fluid shear stress. *Am J Physiol Cell Physiol* 290,C444-52.

Otey, C.A. and Carpen, O. (2004). Alpha-actinin revisited: a fresh look at an old player. *Cell Motil Cytoskeleton.*Jun;58(2):104-11.

Otey, C.A, Rachlin, A., Moza, M., Arneman, D., Carpen, O. (2005). The palladin/myotilin/myopalladin family of actin-associated scaffolds. Int Rev Cytol. 246:31-58.

Otey, C.A., Dixon, R., Stack, C., Goicoechea, S.M. (2009). Cytoplasmic Ig-domain proteins: cytoskeletal regulators with a role in human disease. *Cell Motil Cytoskeleton.* Aug;66(8):618-34.

Pankov, R., Yamada, K.M. (2002). Fibronectin at a glance. *J Cell Sci* 115:3861–3863.

Parast, M.M. and Otey, C.A. (2000). Characterization of palladin, a novel protein localized to stress fibers and cell adhesions. *J Cell Biol.* Aug;7;150(3):643-56.

Pasyk, K.A. and Jakobczak, B.A. (2004). Vascular endothelium: recent advances. *Eur J Dermatol.* Jul-Aug;14(4):209-13.

Patel, H.H., Murray, F., Insel, P.A. (2008). Caveolae as organizers of pharmacologically relevant signal transduction molecules. *Annu Rev Pharmacol Toxicol.*;48:359-91

Patibandla, P.K., Tyagi, N., Dean, W.L., Tyagi, S.C., Roberts, A.M., Lominadze, D. (2009). Fibrinogen induces alterations of endothelial cell tight junction proteins. *J Cell Physiol.* Oct;221(1):195-203.

Pellegrin, S. and Mellor, H. (2007). Actin stress fibres. *J Cell Sci* 120,3491-9.

Peitsch, W.K., Grund, C., Kuhn, C., Schnölzer, M., Spring, H., Schmelz, M., Franke, W.W. (1999). Drebrin is a widespread actin-associating protein enriched at junctional plaques, defining a specific microfilament anchorage system in polar epithelial cells. *Eur J Cell Biol.* Nov;78(11):767-78.

Peitsch, W.K., Hofmann, I., Prätzel, S., Grund, C., Kuhn, C., Moll, I., Langbein, L., Franke, W.W. (2001). Drebrin particles: components in the ensemble of proteins regulating actin dynamics of lamellipodia and filopodia. *Eur J Cell Biol.*Sep;80(9):567-79.

Peitsch, W.K., Hofmann, I., Endlich, N., Prätzel, S., Kuhn, C., Spring, H., Gröne, H.J., Kriz, W., Franke, W.W. (2003). Cell biological and biochemical characterization of drebrin complexes in mesangial cells and podocytes of renal glomeruli. *J Am Soc Nephrol*. Jun;14(6):1452-63.

Peitsch, W.K., Hofmann, I., Bulkescher, J., Hergt, M., Spring, H., Bleyl, U., Goerdt, S., Franke, W.W. (2005). Drebrin, an actin-binding, cell-type characteristic protein: induction and localization in epithelial skin tumors and cultured keratinocytes. *J Invest Dermatol.* Oct;125(4):761-74.

Pérez-Martínez, M., Gordón-Alonso, M., Cabrero, J.R., Barrero-Villar, M., Rey, M., Mittelbrunn, M., Lamana, A., Morlino, G., Calabia, C., Yamazaki, H., Shirao, T., Vázquez, J., González-Amaro, R., Veiga, E., Sánchez-Madrid, F. (2010). F-actin-binding protein drebrin regulates CXCR4 recruitment to the immune synapse. *J Cell Sci*.Apr;1;123(Pt 7):1160-70.

Pericleous, C., Giles, I., Rahman, A. (2009). Are endothelial microparticles potential markers of vascular dysfunction in the antiphospholipid syndrome? *Lupus*. Jul;18(8):671-5.

Petzold, T., Orr, A.W., Hahn, C., Jhaveri, K.A., Parsons, J.T., Schwartz, M.A. (2009). Focal adhesion kinase modulates activation of NF-kappaB by flow in endothelial cells. *Am J Physiol Cell Physiol*.Oct;297(4):C814-22.

Philippova, M., Suter, Y., Toggweiler, S., Schoenenberger, A.W., Joshi, M.B., Kyriakakis, E., Erne, P., Resink, T.J. (2011). T-cadherin is present on endothelial microparticles and is elevated in plasma in early atherosclerosis. *Eur Heart J*. Mar;32(6):760-71.

Phillips, T. (2008). The role of methylation in gene expression. *Nature Education* 1(1):116.

Plow, E., Haas, T., Zhang, L., Loftus, J., Smith, J. (2000). Ligand binding to integrins. *J Biol Chem*.275:21785–21788.

Pogue-Geile, K.L., Chen, R., Bronner, M.P., Crnogorac-Jurcevic, T., Moyes, K.W., Dowen, S., Otey, C.A., Crispin, D.A., George, R.D., Whitcomb, D.C., Brentnall, T.A. (2006). Palladin mutation causes familial pancreatic cancer and suggests a new cancer mechanism. *PLoS Med*. Dec;3(12):e516.

Preston, R.A., Jy, W., Jimenez, J.J., Mauro, L.M., Horstman, L.L., Valle, M., Aime, G., Ahn, Y.S. (2003). Effects of severe hypertension on endothelial and platelet microparticles. *Hypertension* Feb;41(2):211-7.

Price, C.J. and Brindle, N.P. (2000). Vasodilator-stimulated phosphoprotein is involved in stress-fiber and membrane ruffle formation in endothelial cells. *Arterioscler Thromb Vasc Biol*.Sep;20(9):2051-6.

Puklin-Faucher, E., Sheetz, M.P. (2009). The mechanical integrin cycle. *J Cell Sci.* Jan 15;122(Pt 2):179-86.

Qi, Y.X., Qu, M.J., Yan, Z.Q., Zhao, D., Jiang, X.H., Shen, B.R., Jiang, Z.L. (2010). Cyclic Strain modulates migration and proliferation of vascular smooth muscle cells via Rho-GDIalpha, Rac1, and p38 pathway. *J Cell Biochem.* Apr;1;109(5):906-14.

Qin, X., Wang, X., Wang, Y., Tang, Z., Cui, Q., Xi, J., Li, Y.S., Chien, S., Wang, N. (2010). MicroRNA-19a mediates the suppressive effect of laminar flow on cyclin D1 expression in human umbilical vein endothelial cells.*Proc Natl Acad Sci USA*;107: 3240–3244.

Rachlin, A.S. and Otey, C.A. (2006). Identification of palladin isoforms and characterization of an isoform-specific interaction between Lasp-1 and palladin. *J Cell Sci* 119,995-1004.

Rehm, K., Panzer, L., van Vliet, V., Genot, E., Linder, S. (2013). Drebrin preserves endothelial integrity by stabilizing nectin at adherens junctions. *J Cell Sci.* Jun;7.

Reich, C.F. and Pisetsky, D.S. (2009). The content of DNA and RNA in microparticles released by Jurkat and HL-60 cells undergoing in vitro apoptosis. *Exp Cell Res.* Mar;10;315(5):760-8.

Reriani, M.K., Lerman, L.O., Lerman A. (2010). Endothelial function as a functional expression of cardiovascular risk factors. *Biomark Med.* Jun;4(3):351-60.

Resnick, N., Yahav H., Shay-Salit A., Shushy M., Schubert S., Zilberman L.C., Wofovitz, E. (2003). Fluid shear stress and the vascular endothelium: for better and for worse. *Prog Biophys Mol Biol,*81(3): p.177-99.

Robert, S., Lacroix, R., Poncelet, P., Harhouri, K., Bouriche, T., Judicone, C., Wischhusen, J., Arnaud, L., Dignat-George, F. (2012). High-sensitivity flow cytometry provides access to standardized measurement of small-size microparticles-- brief report. *Arterioscler Thromb Vasc Biol.*Apr;32(4):1054-8.

Rojas, A., Figueroa, H., Re, L., Morales, M.A. (2006). Oxidative stress at the vascular wall. Mechanistic and pharmacological aspects. *Arch Med Res.*May;37(4):436-48.

Roland, I., Minet, E., Ernest, I., Pascal, T., Michel, G., Remacle, J., Michiels, C. (2000). Identification of hypoxia-responsive messengers expressed in human microvascular endothelial cells using differential display RT-PCR. *Eur J Biochem.*Jun;267(12):3567-74.

Romer, L.H., Birukov, K.G., Garcia, J.G. (2006). Focal adhesions: paradigm for a signaling nexus. *Circ Res.*Mar 17;98(5):606-16.

Rönty, M., Taivainen, A., Moza, M., Otey, C.A., Carpen, O. (2004). Molecular analysis of the interaction between palladin and alpha-actinin. *FEBS Lett* 566, 30-4.

Rönty, M.J., Leivonen, S.K., Hinz, B., Rachlin, A., Otey, C.A., Kähäri, V.M., Carpén, O.M. (2006). Isoform-specific regulation of the actin-organizing protein palladin during TGF-beta1-induced myofibroblast differentiation. *J Invest Dermatol.* 2006 Nov;126(11):2387-96.

Rönty, M., Taivainen, A., Heiska, L., Otey, C., Ehler, E., Song, W.K., Carpen, O. (2007). Palladin interacts with SH3 domains of SPIN90 and Src and is required for Src-induced cytoskeletal remodeling. *Exp Cell Res.* Jul;15;313(12):2575-85.

Rottner, K., Krause, M., Gimona, M., Small, J.V., Wehland, J. (2001). Zyxin is not colocalized with vasodilator-stimulated phosphoprotein (VASP) at lamellipodial tips and exhibits different dynamics to vinculin, paxillin, and VASP in focal adhesions. *Mol Biol Cell.* Oct;12(10):3103-13.

Rybarczyk, B.J., Lawrence, S.O., Simpson-Haidaris, P.J. (2003). Matrix-fibrinogen enhances wound closure by increasing both cell proliferation and migration. *Blood.* Dec 1;102(12):4035-43.

Safar, M.E., Nilsson, P.M., Blacher, J., Mimran, A. (2012). Pulse pressure, arterial stiffness, and end-organ damage. *Curr Hypertens Rep.* Aug;14(4):339-44.

Salameh, A., Dhein, S. (2013). Effects of mechanical forces and stretch on intercellular gap junction coupling. *Biochim Biophys Acta.* Jan;1828(1):147-56.

Salvi, A., Bongarzone, I., Miccichè, F., Arici, B., Barlati, S., De Petro, G. (2009). Proteomic identification of LASP-1 down-regulation after RNAi urokinase silencing in human hepatocellular carcinoma cells. *Neoplasia.* Feb;11(2):207-19.

Sanchez-Ruderisch, H., Detjen, K.M., Welzel, M., André, S., Fischer, C., Gabius, H.J., Rosewicz, S. (2011). Galectin-1 sensitizes carcinoma cells to anoikis via the fibronectin receptor α5β1-integrin. *Cell Death Differ.* May;18(5):806-16.

Sapet, C., Simoncini, S., Loriod, B., Puthier, D., Sampol, J., Nguyen, C., Dignat-George, F., Anfosso, F. (2006). Thrombin-induced endothelial microparticle generation: identification of a novel pathway involving ROCK-II activation by caspase-2.*Blood*.2006;108:1868 –1876.

Sasaki, N., Toyoda, M. (2013). Glycoconjugates and Related Molecules in Human Vascular Endothelial Cells. *Int J Vasc Med.* 963596.

Schaper, W. (2009). Collateral circulation: past and present. *Basic Research in Cardiology*, 104(1), pp.5-21.

Schirenbeck, A., Arasada, R., Bretschneider, T., Stradal, T.E., Schleicher, M., Faix, J. (2006). The bundling activity of vasodilator-stimulated phosphoprotein is required for filopodium formation. *Proc Natl Acad Sci U S A.* May 16;103(20):7694-9.

Schwartz, M.A. and DeSimone, D.W. (2008). Cell adhesion receptors in mechanotransduction. *Curr Opin Cell Biol* 20,551-6.

Seeger, F.H., Blessing, E., Gu, L., Bornhold, R., Denger, S, Kreuzer, J. (2002). Fibrinogen induces chemotactic activity in endothelial cells. *Acta Physiologica Scandinavica,*176:109–115.

Sekula, M., Janawa, G., Stankiewicz, E., Stępień, E. (2011). Endothelial microparticle formation in moderate concentrations of homocysteine and methionine in vitro. *Cell Mol Biol Lett.*Mar;16(1):69-78.

Selbach, M., Schwanhäusser, B., Thierfelder, N., Fang, Z., Khanin, R., Rajewsky, N. (2008). Widespread changes in protein synthesis induced by microRNAs. *Nature*.Sep;4;455(7209):58-63.

Shai, E., Varon, D. (2011). Development, cell differentiation, angiogenesis--microparticles and their roles in angiogenesis. *Arterioscler Thromb Vasc Biol.* Jan;31(1):10-4.

Sharma, S., Grintsevich, E.E., Hsueh, C., Reisler, E., Gimzewski, J.K. (2012). Molecular cooperativity of drebrin1-300 binding and structural remodeling of F-actin. *Biophys J.*Jul;18;103(2):275-83.

Shattil, S.J., Kim, C. and Ginsberg, M. (2010). The final steps of integrin activation: the end game.*Nature Reviews Molecular Cell Biology,*11(4),pp.288-300.

Shirao, T., Hayashi, K., Ishikawa, R., Isa, K., Asada, H., Ikeda, K., Uyemura, K. (1994). Formation of thick, curving bundles of actin by drebrin A expressed in fibroblasts. *Exp Cell Res.*Nov;215(1):145-53.

Shyy, J. and Chien, S. (2002). Role of integrins in endothelial mechanosensing of shear stress. *Circulation Research,*91(9),pp.769-775.

Siljander, P.R. (2011). Platelet-derived microparticles - an updated perspective. *Thromb Res.*Jan;127.Suppl2:S30-3

Simak, J. and Gelderman, M.P. (2006). Cell membrane microparticles in blood and blood products: potentially pathogenic agents and diagnostic markers. *Transfus Med Rev.*Jan;20(1):1-26.

Skog, J., Würdinger, T., van Rijn, S., Meijer, D.H., Gainche, L., Sena-Esteves, M., Curry, W.T. Jr., Carter, B.S., Krichevsky, A.M., Breakefield, X.O. (2008). Glioblastoma microvesicles transport RNA and proteins that promote tumour growth and provide diagnostic biomarkers. *Nat Cell Biol.*Dec;10(12):1470-6.

Small, E.M., O'Rourke, J.R., Moresi, V., Sutherland, L.B., McAnally, J., Gerard, R.D., Richardson, J.A., Olson, E.N. (2010). Regulation of PI3-kinase/Akt signaling by muscle-enriched microRNA-486. *Proc Natl Acad Sci USA.*Mar;2;107(9):4218-23.

Stec, J.J., Silbershatz, H., Tofler, G.H., Matheney, T.H., Sutherland, P., Lipinska, I., Massaro, J.M., Wilson, P.F., Muller, J.E., D'Agostino, R.B. Sr. (2000). Association of fibrinogen with cardiovascular risk factors and cardiovascular disease in the Framingham Offspring Population. *Circulation.* Oct 3;102(14):1634-8.

Steward, R.L. Jr, Cheng, C.M., Ye, J.D., Bellin, R.M., LeDuc P.R. (2011). Mechanical stretch and shear flow induced reorganization and recruitment of fibronectin in fibroblasts. *Sci Rep.* 2011;1:147.

Stölting, M., Wiesner, C., van Vliet, V., Butt, E., Pavenstädt, H., Linder, S., Kremerskothen, J. (2012). Lasp-1 regulates podosome function. *PLoS One.*;7(4):e35340.

Suehiro, K., Gailit, J., Plow, E.F. (1997). Fibrinogen is a ligand for integrin alpha5beta1 on endothelial cells. *J Biol Chem.*Feb 21;272(8):5360-6.

Sumpio, B.E., Riley, J.T., Dardik, A. (2002). Cells in Focus: Endothelial Cell. *Int J Biochem Cell Biol.* Dec;34(12):1508-12.

Suwaidi, J.A., Hamasaki, S., Higano, S.T., Nishimura, R.A., Holmes, D.R. Jr, Lerman, A. (2000). Long-term follow-up of patients with mild coronary artery disease and endothelial dysfunction. *Circulation.* Mar 7;101(9):948-54.

Szklarczyk, D., Franceschini, A., Kuhn, M., Simonovic, M., Roth, A., Minguez, P., Doerks, T., Stark, M., Muller, J., Bork, P., Jensen, L.J., von Mering, C. (2011). The STRING database in 2011:functional interaction networks of proteins, globally integrated and scored. *Nucleic Acids Res.* 2011 Jan;39:D561-8.

Tan, A., De La Peña, H. and Seifalian, A.M. (2010). The application of exosomes as a nanoscale cancer vaccine. *Int J Nanomedicine.* Nov;10;5:889-900.

Tang, R., Kong, F., Hu, L., You, H., Zhang, P., Du, W., Zheng, K. (2012). Role of hepatitis B virus X protein in regulating LIM and SH3 protein 1 (LASP-1) expression to mediate proliferation and migration of hepatoma cells. *Virol J.*Aug;16;9:163.

Tanjore, H., Kalluri, R. (2006). The role of type IV collagen and basement membranes in cancer progression and metastasis. *Am J Pathol.* 2006 Mar;168(3):715-7.

Tao, G., Kotick, J.D., Lincoln, J. (2012). Heart valve development, maintenance, and disease: the role of endothelial cells. *Curr Top Dev Biol.* 100:203-32.

Taraboletti, G., D'Ascenzo, S., Borsotti, P., Giavazzi, R., Pavan, A., Dolo, V. (2002). Shedding of the matrix metalloproteinases MMP-2, MMP-9, and MT1-MMP as membrane vesicle-associated components by endothelial cells. *Am J Pathol.*160:673–680.

Terakawa, Y., Agnihotri, S., Golbourn, B., Nadi, M., Sabha, N., Smith, C.A., Croul, S.E., Rutka, J.T. (2013). The role of drebrin in glioma migration and invasion. *Exp Cell Res.*Feb;15;319(4):517-28.

Terasaki, A.G., Suzuki, H., Nishioka, T., Matsuzawa, E., Katsuki, M., Nakagawa, H., Miyamoto, S., Ohashi, K. (2004). A novel LIM and SH3 protein (lasp-2) highly expressing in chicken brain. *Biochem Biophys Res Commun* 313,48-54.

Terrisse, A.D., Puech, N., Allart, S., Gourdy, P., Xuereb, J.M., Payrastre, B., Sié, P. (2010). Internalization of microparticles by endothelial cells promotes platelet/endothelial cell interaction under flow. *J Thromb Haemost.*Dec;8(12):2810-9.

Théry, C., Boussac, M., Véron, P., Ricciardi-Castagnoli, P., Raposo, G., Garin, J., Amigorena, S. (2001). Proteomic analysis of dendritic cell-derived exosomes: a secreted subcellular compartment distinct from apoptotic vesicles.*J Immunol.*Jun;15;166(12):7309-18.

Théry, C., Zitvogel, L., Amigorena, S. (2002) Exosomes: composition, biogenesis and function. *Nature Reviews Immunology* Vol.2,No.8,(August),pp.569–579.

Thiel, G., Lietz, M., Hohl, M. (2004). How mammalian transcriptional repressors work. *Eur J Biochem* 271:2855 62.

Thompson, R.F. and Langford, G.M. (2002). Myosin superfamily evolutionary history. *Anat Rec.*Nov 1;268(3):276-89.

Thorin, E. and Thorin-Trescases, N. (2009). Vascular endothelial ageing, heartbeat after heartbeat. *Cardiovasc Res.*Oct 1;84(1):24-32..

Tinken, T.M., Thijssen, D.H.J., Hopkins, N., Dawson, E.A., Cable, N.T., Green, D.J. (2010). Shear stress mediates endothelial adaptations to exercise training in humans. *Hypertension*; 55: 312–318.

Tirnauer, J.S., Bierer, B.E. (2000). EB1 proteins regulate microtubule dynamics, cell polarity, and chromosome stability. *J Cell Biol.* May 15;149(4):761-6.

Toda, M., Shirao, T., Minoshima, S., Shimizu, N., Toya, S., Uyemura, K. (1993). Molecular cloning of cDNA encoding human drebrin E and chromosomal mapping of its gene. *Biochem Biophys Res Commun.*Oct;15;196(1):468-72.

316

Tojkander, S., Gateva, G., Lappalainen P. (2012). Actin stress fibers--assembly, dynamics and biological roles. *J Cell Sci.* Apr 15;125(Pt 8):1855-64.

Tomasetto, C., Moog-Lutz, C., Regnier, C.H., Schreiber, V., Basset, P., Rio, M.C. (1995). Lasp-1 (MLN 50) defines a new LIM protein subfamily characterized by the association of LIM and SH3 domains.*FEBS Lett* 373,245-9.

Tonevitsky, E.A., Trushkin, E.V., Shkurnikov, M.U., Akimov, E.B., Sakharov, D.A. (2009). Changed profile of splicing regulator genes expression in response to exercise. *Bull Exp Biol Med.* Jun;147(6):733-6.

Tousoulis, D., Papageorgiou, N., Androulakis, E., Briasoulis, A., Antoniades, C., Stefanadis, C. (2011). Fibrinogen and cardiovascular disease: genetics and biomarkers. *Blood Rev.*Nov;25(6):239-45.

Trusolino, L., Cavassa, S., Angelini, P., Andó, M., Bertotti, A., Comoglio, P.M., Boccaccio, C. (2000). HGF/scatter factor selectively promotes cell invasion by increasing integrin avidity. *FASEB J.*Aug;14(11):1629-40.

Tuccoli, A., Poliseno, L., Rainaldi, G. (2006). miRNAs regulate miRNAs: coordinated transcriptional and post-transcriptional regulation. *Cell Cycle.*Nov 1;5(21):2473-6.

Turner, D.P., Findlay, V.J., Kirven, A.D., Moussa, O., Watson, D.K. (2008). Global gene expression analysis identifies PDEF transcriptional networks regulating cell migration during cancer progression. *Mol Biol Cell.*19:3745–3757.

Tushuizen, M.E., Diamant, M., Sturk, A., Nieuwland, R. (2011). Cell-derived microparticles in the pathogenesis of cardiovascular disease: friend or foe? *Arteriosclerosis Thrombosis and Vascular Biology.* Vol.31, No.1, (January), pp.4-9.

Tyagi, N., Roberts, A., Dean, W., Tyagi, S., Lominadze, D. (2008). Fibrinogen induces endothelial cell permeability. *Mol Cell Biochem.*307:13–22.

Tzima, E., del Pozo, M.A., Shattil, S.J., Chien, S., Schwartz, M.A. (2001). Activation of integrins in endothelial cells by fluid shear stress mediates Rho-dependent cytoskeletal alignment. *EMBO J* 20, 4639-47.

Untergasser, A., Cutcutache, I., Koressaar, T., Ye, J., Faircloth, B.C., Remm, M., Rozen, S.G. (2012). Primer3--new capabilities and interfaces. *Nucleic Acids Res.* Aug;40(15):e115.

Upreti, M., Jamshidi-Parsian, A., Apana, S., Berridge, M., Fologea, D.A., Koonce, N.A., Henry, R.L., Griffin, R.J. (2013). Radiation-induced galectin-1 by endothelial cells: a promising molecular target for preferential drug delivery to the tumor vasculature. *J Mol Med (Berl).* Apr;91(4):497-506.

Urbich, C., Walter, D.H., Zeiher, A.M., Dimmeler, S. (2000). Laminar shear stress upregulates integrin expression: role in endothelial cell adhesion and apoptosis. *Circ Res.*Oct;13;87(8):683-9.

Urbich, C., Dernbach, E., Reissner, A., Vasa, M., Zeiher, A.M., Dimmeler, S. (2002).Shear stress-induced endothelial cell migration involves integrin signaling via the fibronectin receptor subunits alpha(5) and beta(1). *Arterioscler Thromb Vasc Biol.*Jan;22(1):69-75.

Urschel, K., Cicha, I., Daniel, W.G., Garlichs, C.D. (2012). Shear stress patterns affect the secreted chemokine profile in endothelial cells. Clin Hemorheol Microcirc. 2012;50(1-2):143-52.

VanDommelen, S.M., Vader, P., Lakhal, S., Kooijmans, S.A., van Solinge, W.W., Wood, M.J., Schiffelers, R.M. (2012). Microvesicles and exosomes: Opportunities for cell-derived membrane vesicles in drug delivery. *J Control Release.*Jul;20;161(2):635-44

VanSchravendijk, M.R., Handunnetti, S.M., Barnwell, J.W., Howard, R.J. (1992). Normal human erythrocytes express CD36, an adhesion molecule of monocytes, platelets, and endothelial cells. *Blood.*Oct;15;80(8):2105-14.

VanWijk, M.J., VanBavel, E., Sturk, A., Nieuwland, R. (2003). Microparticles in cardiovascular diseases. *Cardiovasc Res.*Aug;1;59(2):277-87.

Varon, C., Tatin, F., Moreau, V., Van Obberghen-Schilling, E., Fernandez-Sauze, S., Reuzeau, E., Kramer, I., Génot, E. (2006). Transforming growth factor beta induces rosettes of podosomes in primary aortic endothelial cells. *Mol Cell Biol.*May;26(9):3582-94.

Vasioukhin, V., Bauer, C., Yin, M. and Fuchs, E. (2000). Directed actin polymerization is the driving force for epithelial cell-cell adhesion. *Cell* 100, 209-19.

Versari, D., Daghini, E., Virdis, A., Ghiadoni, L., Taddei, S. (2009). Endothelial dysfunction as a target for prevention of cardiovascular disease. *Diabetes Care.*Nov;32 Suppl 2:S314-21.

Viera, A.J., Mooberry, M., Key, N.S. (2012). Microparticles in cardiovascular disease pathophysiology and outcomes. *J Am Soc Hypertens.*Jul-Aug;6(4):243-52.

Vince, R.V., Chrismas, B., Midgley, A.W., McNaughton, L.R., Madden, L.A. (2009). Hypoxia mediated release of endothelial microparticles and increased association of S100A12 with circulating neutrophils. Oxid Med Cell Longev.Jan-Mar;2(1):2-6.

Vion, A.C., Birukova, A.A., Boulanger, C.M., Birukov, K.G. (2013). Mechanical forces stimulate endothelial microparticle generation via caspase-dependent apoptosis-independent mechanism. *Pulm Circ.*Jan;3(1):95-9.

Virdis, A., Giannarelli, C., Neves, M.F., Taddei, S., Ghiadoni, L. (2010). Cigarette smoking and hypertension. *Curr Pharm Des*. 16(23):2518-25.

Vo, A.T., Millis, R.M. (2012). Epigenetics and breast cancers. *Obstet Gynecol Int.* 2012:602720.

Von Offenberg Sweeney, N., Cummins, P.M., Birney, Y.A., Cullen, J.P., Redmond, E.M., Cahill P.A. (2004). Cyclic strain-mediated regulation of endothelial matrix metalloproteinase-2 expression and activity. *Cardiovasc.* Res. 63:625–634.

Von Offenberg Sweeney, N., Cummins, P., Cotter, E., Fitzpatrick, P., Birney, Y., Redmond, E., Cahill, P. (2005). Cyclic Strain-mediated regulation of vascular endothelial cell migration and tube formation. *Biochemical and Biophysical Research Communications,* 329(2), pp.573-582.

Wall, M.E., Rachlin, A., Otey, C.A., Loboa, E.G. (2007). Human adipose-derived adult stem cells upregulate palladin during osteogenesis and in response to cyclic tensile strain. *Am J Physiol Cell Physiol.*Nov;293(5):C1532-8.

Wang, B., Feng, P., Xiao, Z., Ren, E.C. (2009). LIM and SH3 protein 1 (Lasp1) is a novel p53 transcriptional target involved in hepatocellular carcinoma. *J Hepatol,* 50(3) pp.528–537.

Wang, H.V. and Moser, M. (2008). Comparative expression analysis of the murine palladin isoforms. *Dev Dyn*.Nov;237(11):3342-51.

Wang, K.C., Garmire, L.X., Young, A., Nguyen, P., Trinh, A., Subramaniam, S., Wang, N., Shyy, J.Y., Li, Y.S., Chien, S. (2010). Role of microRNA-23b in flow-regulation of Rb phosphorylation and endothelial cell growth. *Proc Natl Acad Sci U S A*.Feb;16;107(7):3234-9.

Watanabe-Nakayama, T., Saito, M., Machida, S., Kishimoto, K., Afrin, R., Ikai, A. (2013). Requirement of LIM domains for the transient accumulation of paxillin at damaged stress fibres. *Biol Open.* May 23;2(7):667-74.

Wehrle-Haller, B. (2012). Assembly and disassembly of cell matrix adhesions. *Curr Opin Cell Biol.* Oct;24(5):569-81.

Weijers, E.M., van Wijhe, M.H., Joosten, L., Horrevoets, A.J., de Maat, M.P., van Hinsbergh, V.W., Koolwijk, P. (2010). Molecular weight fibrinogen variants alter gene expression and functional characteristics of human endothelial cells. *J Thromb Haemost.* Dec;8(12):2800-9.

Westhoff, M.A., Serrels, B., Fincham, V.J., Frame, M.C., Carragher, N.O. (2004). SRC-mediated phosphorylation of focal adhesion kinase couples actin and adhesion dynamics to survival signaling. *Mol Cell Biol*.Sep;24(18):8113-33.

Whelan, M.C. and Senger, D.R. (2002). Collagen I initiates endothelial cell morphogenesis by inducing actin polymerization through suppression of cyclic AMP and protein kinase *A*.*J Biol Chem*.Jan;3;278(1):327-34.

Wierzbicka-Patynowski, I., Schwarzbauer, J.E. (2003). The ins and outs of fibronectin matrix assembly. *J Cell Sci*. Aug 15;116(Pt 16):3269-76.

Wight, T.N., Potter-Perigo, S. (2011). The extracellular matrix: an active or passive player in fibrosis? *Am J Physiol Gastrointest Liver Physiol.* Dec;301(6):G950-5.

Williams, J.B., Jauch, E.C., Lindsell, C.J., Campos, B. (2007). Endothelial microparticle levels are similar in acute ischemic stroke and stroke mimics due to activation and not apoptosis/necrosis. *Acad Emerg Med.* Aug;14(8):685-90.

Wilson, C.J., Kasper, G., Schütz, M.A., Duda, G.N. (2009). Cyclic strain disrupts endothelial network formation on Matrigel. *Microvasc Res*. Dec;78(3):358-63.

Witke, W. (2004). The role of profilin complexes in cell motility and other cellular processes. *Trends Cell Biol.*Aug;14(8):461-9.

Wojciak-Stothard, B. and Ridley, A.J. (2003). Shear stress–induced endothelial cell polarization is mediated by Rho and Rac but not Cdc42 or PI 3-kinases. *J Cell Biol.* April 28;161(2):429–439.

Wolf, P. (1967). The nature and significance of platelet products in human plasma. *Br. J.Haematol.* 13(3):269-288.

Woolner, S., O'Brien, L.L., Wiese, C., Bement, W.M. (2008). Myosin-10 and actin filaments are essential for mitotic spindle function. *J Cell Biol.* Jul 14;182(1):77-88.

World Health Organization. (2011). World Health Statistics, 2011. Geneva, 2011.

Worth, D.C., Daly, C.N., Geraldo, S., Oozeer, F., Gordon-Weeks, P.R. (2013). Drebrin contains a cryptic F-actin-bundling activity regulated by Cdk5 phosphorylation. *J Cell Biol.* Sep 2;202(5):793-806.

Wu, F., Yang, Z. and Li, G. (2009).Role of specific microRNAs for endothelial function and angiogenesis. *Biochemical and Biophysical Research Communications.* 386;549–553.

Würdinger, T., Tannous, B.A., Saydam, O. (2008). MiR-296 regulates growth factor receptor overexpression in angiogenic endothelial cells. *Cancer Cell* 14;382–393.

Yan, M.S., Matouk, C.C., Marsden, P.A. (2010). Epigenetics of the vascular endothelium. *J Appl Physiol.*Sep;109(3):916-26.

Yang, Y.S., Strittmatter, S.M. (2007). The reticulons: a family of proteins with diverse functions. *Genome Biol.* 8(12):234.

Yockell-Lelièvre, J., Riendeau, V., Gagnon, S.N., Garenc, C., Audette, M. (2009). Efficient transfection of endothelial cells by a double-pulse electroporation method. *DNA Cell Biol*. Nov;28(11):561-6.

Yoshigi, M., Hoffman, L.M., Jensen, C.C., Yost, H.J., Beckerle, M.C. (2005). Mechanical force mobilizes zyxin from focal adhesions to actin filaments and regulates cytoskeletal reinforcement. *J Cell Biol* 171,209-15.

Yu, Z., Fotouhi-Ardakani, N., Wu, L., Maoui, M., Wang, S., Banville, D., Shen, S.H. (2002). PTEN associates with the vault particles in HeLa cells. *J Biol Chem.* Oct;25;277(43):40247-52.

Yuan, A., Farber, E.L., Rapoport, A.L., Tejada, D., Deniskin, R., Akhmedov, N.B., Farber, D.B. (2009). Transfer of microRNAs by embryonic stem cell microvesicles. *PLoS One*;4:e4722.

Yue, J., Huhn, S. and Shen, Z. (2013). Complex roles of filamin-A mediated cytoskeleton network in cancer progression. *Cell Biosci.* Feb 6;3(1):7.

Yurchenco, P.D. (2011). Basement membranes: cell scaffoldings and signaling platforms. *Cold Spring Harb Perspect Biol.* Feb 1;3(2).

Zagura, M., Kals, J., Serg, M., Kampus, P., Zilmer, M., Jakobson, M., Unt, E., Lieberg, J., Eha, J. (2012). Structural and biochemical characteristics of arterial stiffness in patients with atherosclerosis and in healthy subjects. *Hypertens Res.* Oct;35(10):1032-7.

Zaragoza, C., Márquez, S., Saura, M. (2012). Endothelial mechanosensors of shear stress as regulators of atherogenesis. *Curr Opin Lipidol*. Oct;23(5):446-52.

Zernecke, A., Bidzhekov, K., Noels, H., Shagdarsuren, E., Gan, L., Denecke, B., Hristov, M., Köppel, T., Jahantigh, M.N., Lutgens, E., Wang, S., Olson, E.N., Schober, A., Weber, C. (2009). Delivery of microRNA-126 by apoptotic bodies induces CXCL12-dependent vascular protection. Sci Signal.Dec;8;2(100).

Zhang, C. (2008). MicroRNAs: role in cardiovascular biology and disease. *Clin Sci (Lond).*Jun;114(12):699-706.

Zhang, L., Hoffman, J.A. and Ruoslahti, E. (2005). Molecular profiling of heart endothelial cells. *Circulation.*Sep;13;112(11):1601-11.

Zou, L., Cao, S., Kang, N., Huebert, R.C., Shah, V.H. (2012). Fibronectin induces endothelial cell migration through β1 integrin and Src-dependent phosphorylation of fibroblast growth factor receptor-1 at tyrosines 653/654 and 766. *J Biol Chem.* Mar 2;287(10):7190-202.

APPENDIX

A brief study investigating the effects of the knockdown of Palladin on endothelial cell adhesion to extracellular matrices is provided here. As shown, the endothelial cells can be affected by culturing on the ECMs, with protein expression greatly increased. Furthermore, it was suggested in this thesis that Palladin is relocalised in response to the cell-matrix interactions, given that the protein appeared retained in microparticles harvested from sheared cells cultured on these extracellular matrices.

Cells subjected to knockdown were cultured on a variety of ECMs – fibrinogen, fibronectin and collagen. They were again analysed using the xCELLigence™ system, which demonstrated in real time how the knockdown of Palladin affected cells adhering to the ECMs. It was proposed that the retention of Palladin was in part caused by a relocalisation of protein to the basal side of the cell. Such relocalisation subsequently would have a knock on effect on the adhesive capabilities of the cell – increased protein causing increased adhesion. By knocking down the Palladin protein, it was hypothesised that adhesion events would be greatly affected.

Results show that cells knocked down are indeed affected with adhesion appearing to in fact increase in response to knockdown; however the response appears matrix-specific. Results are indicative of one independent experiment, so a definitive conclusion cannot be stated.

Protocol for Cell Adhesion Assay of Transfected siRNA Knockdown Cells

For Palladin knock-down adhesion assays, 6-well plates were prepared and coated as described previously in Chapter 2.2.2.2.1. HAECs were transfected with siRNA, also using the same methods as described previously in Chapter 2.2.4.1, and seeded onto the wells of the 6-well plate. The plates were incubated at 30 hours, which was previously determined to be the optimal time for knockdown. Meanwhile, the wells of a 16-well xCELLigence™ E-plate were also pre-coated in triplicate with a extracellular matrix: fibronectin or fibrinogen at a concentration of 10 µg/ml or Type IV collagen at a concentration of 20 µg/ml. Uncoated wells were also used as a control. The E-plates resemble the CIM-plate, being sealed at the base with a micro-porous membrane containing micro-fabricated gold electrode arrays on the base of the membrane. Each individual well on an E-Plate incorporates a sensor electrode array that allows cells in the well to be monitored and assayed. Plates were covered and then incubated overnight as per the usual methods.

At the 30 hour time point, the wells of the E-plate were aspirated and 100 µl of serum free medium was added into each well. It was important to ensure no air bubbles were introduced and also be careful not to touch the electrodes on the bottom of the well with the tips. This equilibrates the plate to the media. 300 µl of de-ionized water was added to the troughs surrounding the wells which helped humidify the plate. The plate was covered and then incubated at $37^{o}C$ for 30 minutes before it was placed in the plate holder. The E-plate background was then scanned and used to calibrate the software.

During this time, the transfected cells were trypsinised and counted. Upon completion of the E-plates 30 minute incubation and subsequent calibration, 30,000 cells per experimental condition (i.e. culturing on the different matrices) were then added to the appropriately coated well of the E-Plate. This plate was incubated for another 30 minutes at $17\text{-}20^{o}C$ allowing the cells to acclimatise to the media. The plate was covered and then loaded into the plate docking port of the xCELLigence™ system. Initial adhesion of cells was measured at 5 minutes intervals from 0-24 hours. The resulting readings were analysed using the software provided.

(i)
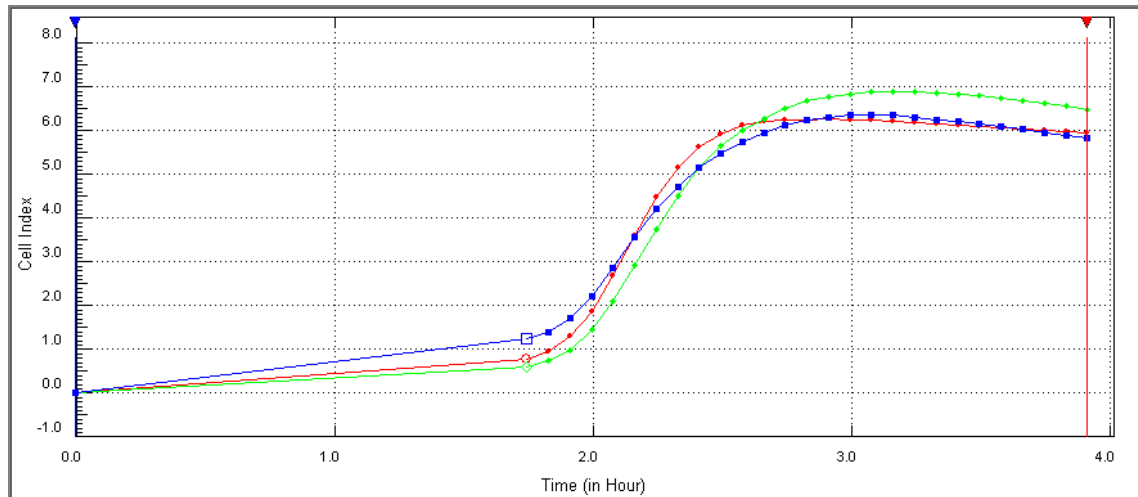
🔴 **Palladin siRNA**
🟢 **Scrambled siRNA**
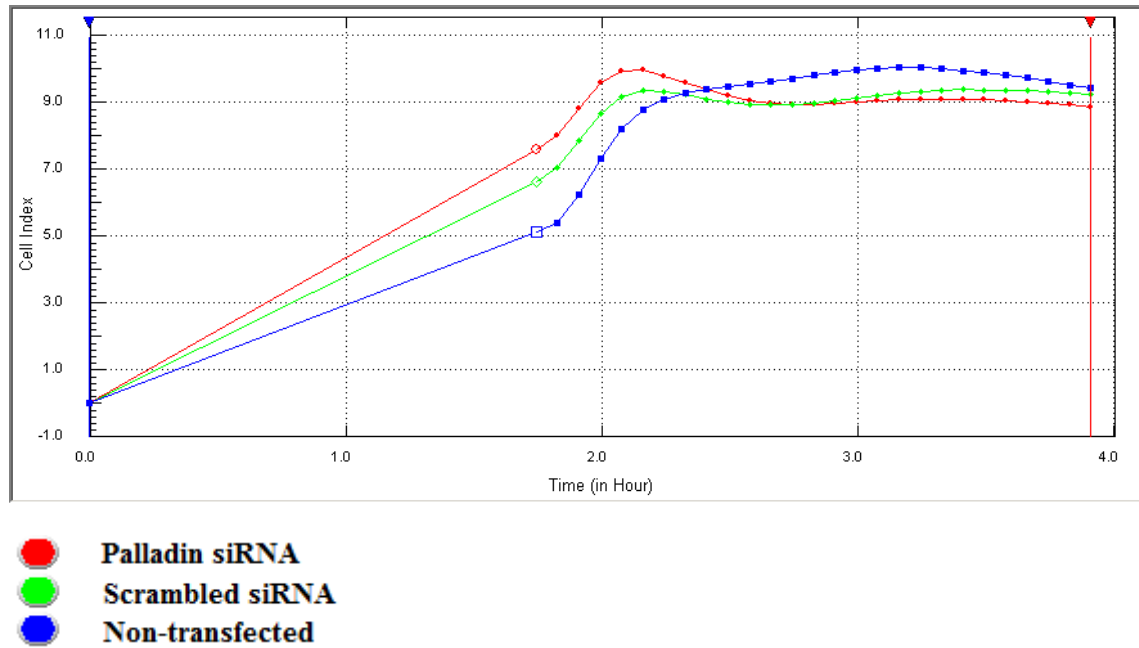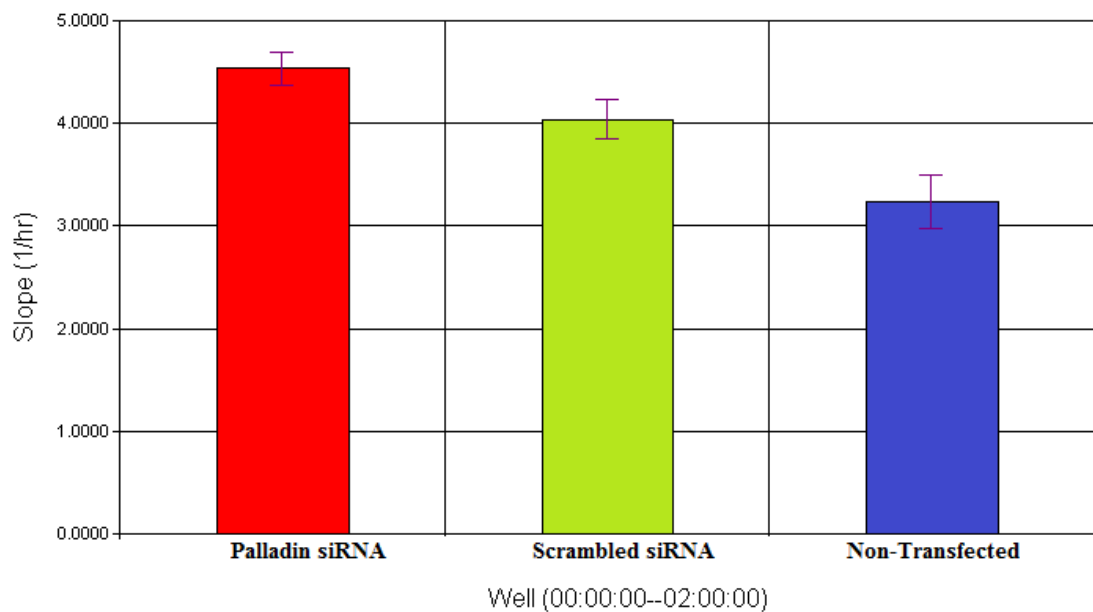🔵 **Non-transfected**

(ii)
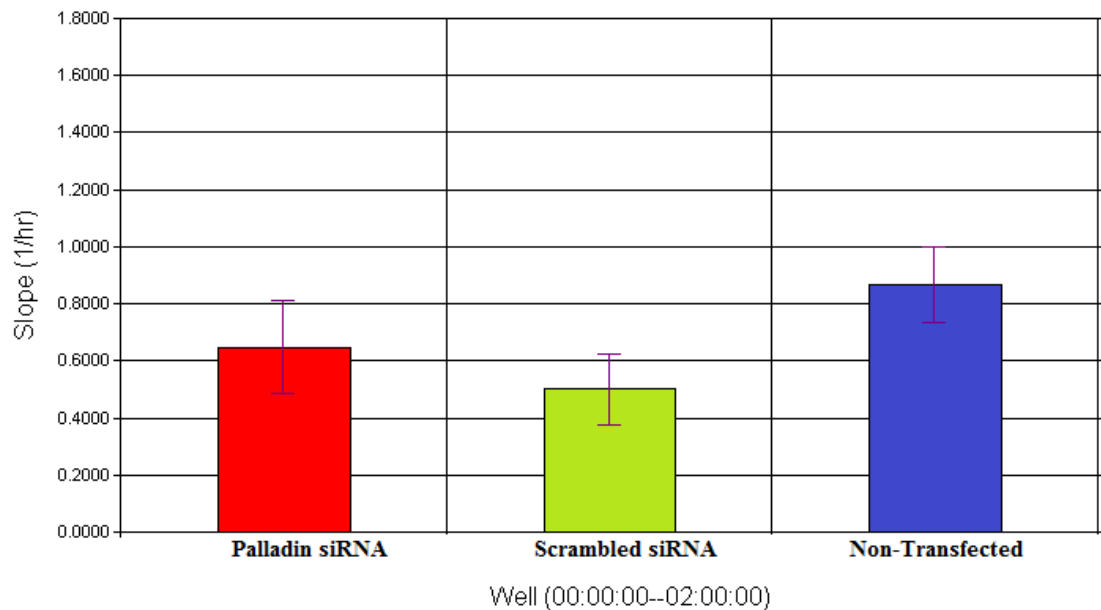
Figure A: xCELLigence™ Assay of Cell Adhesion in Palladin Knockdown Cells Cultured on a Fibrinogen Matrix. HAECs were transfected with Palladin siRNA as per previous methods, and cultured on a fibrinogen matrix. Control samples (scrambled siRNA or non-transfected) were prepared also. These cells were seeded on an xCELLigence™ E-plate for assaying of adhesion as described. The recorded Cell Index results for the first hours of analysis are presented here in Figure A (i). Two hours was determined to be an optimum time to observe immediate cellular events before cells started to proliferate, affecting results. The slope of the adhesion curve for each sample at 2 hours was calculated using the RTCA 1.2 Software, with results shown in Figure A (ii). The increase in size of the slope is indicative of an increase in cellular adhesion.

D

(i)

🔴 **Palladin siRNA**
🟢 **Scrambled siRNA**
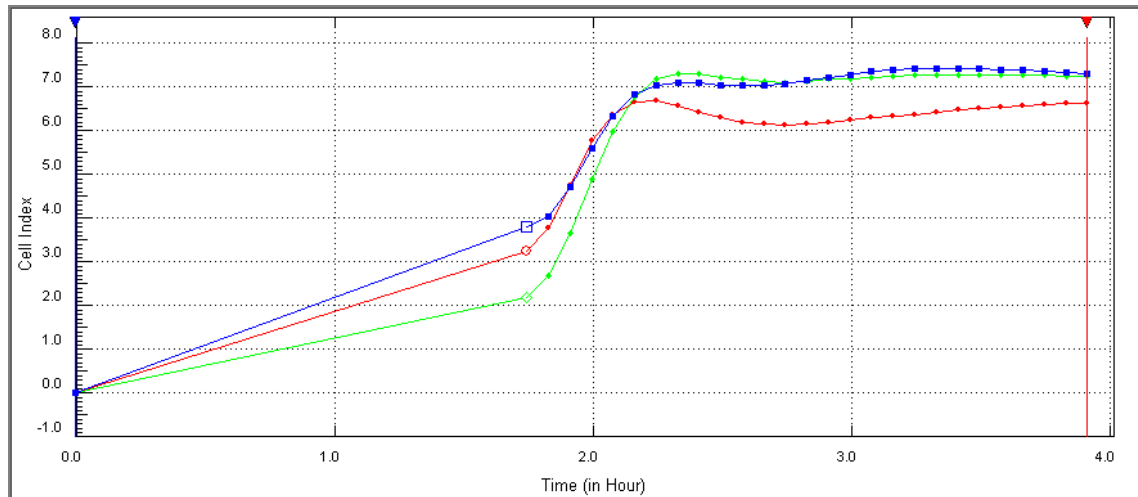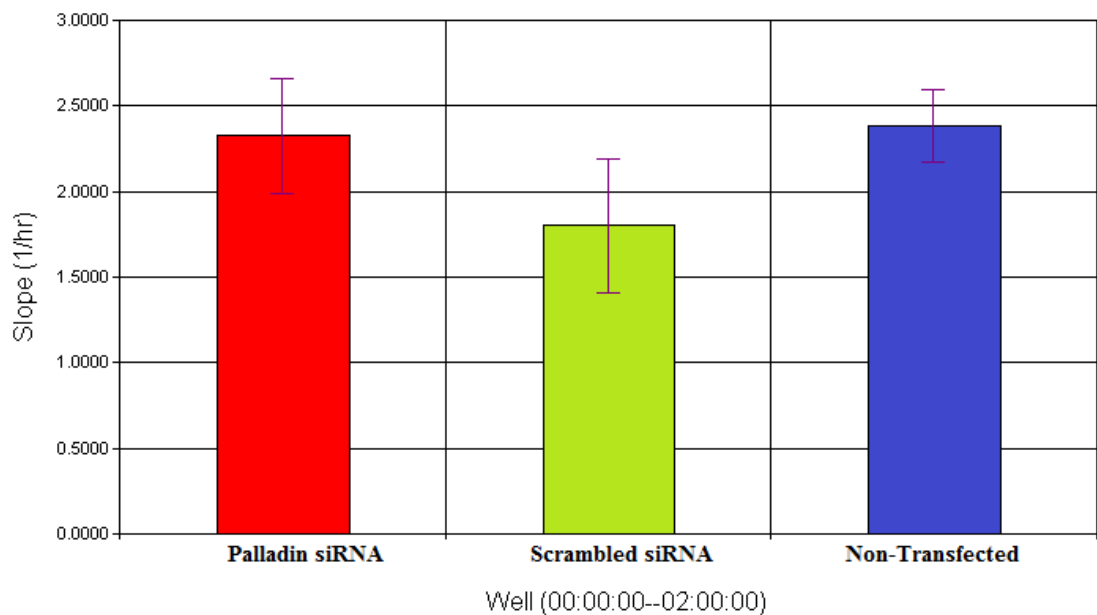🔵 **Non-transfected**

(ii)

Figure B: xCELLigence™ Assay of Cell Adhesion in Palladin Knockdown Cells Cultured on a Fibronectin Matrix. HAECs were transfected with Palladin siRNA as per previous methods, and cultured on a fibronectin matrix. Control samples (scrambled siRNA or non-transfected) were prepared also. These cells were seeded on an xCELLigence™ E-plate for assaying of adhesion as described. The recorded Cell Index results for the first hours of analysis are presented here in Figure B (i). Two hours was determined to be an optimum time to observe immediate cellular events before cells started to proliferate, affecting results. The slope of the adhesion curve for each sample at 2 hours was calculated using the RTCA 1.2 Software, with results shown in Figure B (ii). The increase in size of the slope is indicative of an increase in cellular adhesion.

(i)

(ii)

Figure C: xCELLigence™ Assay of Cell Adhesion in Palladin Knockdown Cells Cultured on a Collagen Matrix. HAECs were transfected with Palladin siRNA as per previous methods, and cultured on a collagen matrix. Control samples (scrambled siRNA or non-transfected) were prepared also. These cells were seeded on an xCELLigence™ E-plate for assaying of adhesion as described. The recorded Cell Index results for the first hours of analysis are presented here in Figure C (i). Two hours was determined to be an optimum time to observe immediate cellular events before cells started to proliferate, affecting results. The slope of the adhesion curve for each sample at 2 hours was calculated using the RTCA 1.2 Software, with results shown in Figure C (ii). The increase in size of the slope is indicative of an increase in cellular adhesion.

F

Figure A first illustrates adhesion of transfected cells to a fibrinogen matrix. The slopes of adhesion indicate that knockdown of Palladin causes cell adhesion to decrease, with a lower slope observed compared to the non-transfected cells. However, the adhesion remains less than that of the scrambled siRNA control, which suggests that the transfection itself of cells causes a reduction in adhesion and that loss of Palladin boosts adhesion on this matrix. We have previously discussed how knockdown of Palladin may possibly result in the compensation of other closely related proteins taking over the role of the protein; this may be further proof of such an occurrence.

Investigation of the knockdown cells on a fibronectin matrix (Figure B) showed a different result. Here, the transfection of cells appears to increase cell adhesion to the matrix, with the scrambled siRNA transfected cells showing greater adhesion than the non-transfected cells. It may be that the fibronectin matrix is able to promote adhesion in the transfected cells. Given that fibronectin can be seen at sites of cell dysfunction, the matrix may function in increasing the adherence of damaged cells – a result which is reflected in the increased adhesion of transfected cells here. Cells transfected with Palladin specific siRNA show an even greater adhesion to the matrix within the first two hours of analysis. Again, this appears suggestive of the loss of Palladin causing compensation from other proteins, which may in turn overcompensate, causing the increased adhesion visualised here.

Finally, Figure C demonstrates the adhesion of knocked-down cells interacting with a collagen matrix. In this figure, the adhesion stayed relatively similar comparing the Palladin siRNA transfected cells with the non-transfected cells. However, these cells showed greater adhesion than the scrambled siRNA cells, indicating that transfection reduced adhesion, but the lack of Palladin resulted in an increase of adhesion back to baseline levels. Collagen is seen to increase cell adhesion (Kemeny et al., 2013); this may cause proteins, such as ones replacing the function of Palladin, to localise from one area of the cell to another (such as from the membrane to the cytoskeleton) to aid adhesion.

In conclusion, it appears that the knockdown of Palladin affects cells, but may be compensated by other proteins within the cell which have a functional overlap with Palladin. This in turn can lead to overcompensation, which increases adhesion in the cell. Figure 5.1 similarly showed that this may occur with regards to migration, albeit at a slower turnover of protein function being taken over by other proteins.